THE Marquardt CORPORATION VAN NUYS, CALIFORNIA

Marquardt Final Report S-545

THREE-AXIS PARAMETERIZATION STUDY ADVANCED LIMIT CYCLE CONTROL TECHNIQUES FOR ATTITUDE CONTROL SYSTEMS

Contract NAS 8-20018

George C. Marshall Space Flight Center

FINAL REPORT

Contract NAS8-20018

Period Covered: June 29, 1965 thru June 10, 1966

THREE-AXIS PARAMETERIZATION STUDY

ADVANCED LIMIT CYCLE CONTROL TECHNIQUES FOR ATTITUDE CONTROL SYSTEMS

Compiled by

D. R. Slagle

The Marquardt Corporation
16555 Saticoy Street
Van Nuys, California

Aerospace Equipment Department

Prepared for

GEORGE C. MARSHALL SPACE FLIGHT CENTER
Huntsville, Alabama

TABLE OF CONTENTS

I. SUMMARY

Initial effort was directed towards investigating analog computer simulation techniques as applied to performing a single axis statistical study of the proposed attitude control techniques. The most important element in this study is the simulation of random errors. Conventional techniques employing a white noise generator in conjunction with sample and hold circuits were tried. Filtering and drift problems were encountered and satisfactory performance could not be obtained. Lack of high speed digital devices prevented use of hybrid simulation techniques which are desirable for this type of study. The analog computer approach was abandoned in favor of a digital computer program to perform a three axis parameterization studies of the important system variables.

The majority of the effort in Task II was devoted to writing the digital computer program. This program is capable of performing the same functions as the program developed in the Phase I study and in addition contains the ability to handle external disturbance torques (both random and predictable as a function of time). The disturbance torques are analyzed by means of discrete interval (grid time) integration. Four different control techniques were analyzed for various types and magnitudes of engine and installation errors and external disturbance torques. Important to the analysis is the application of realistic engine errors and tolerances. This information was derived from data obtained from engine pulse firings at The Marquardt Corporation.

An important consideration requiring investigation is the compensation for slowly changing variables during the course of an extended mission. The philosophy of what these changes are and how they can be handled in the computer simulation are presented. The computer program as written does not allow for changing the important variables on a continuous basis and a series of runs updated and changed for each run are required for this analysis.

A group of ten 450 Newton engine pulse firings was analyzed on a statistical basis both for general information and for use in the digital computer program. These engines reflect typical attitude control engines for manned vehicles. Lack of sufficient data allowed only one impulse size to be analyzed on a statistical basis. Additional information concerning biased and random thrust level errors and installation errors were derived from specification and gross engine performance characteristics.

Curves describing propellant consumption (mean propellant flow rate), statistical quantity (σ) of the flow rate and mean time between firings are presented for the parameterization studies.

II. INTRODUCTION

The problem of maintaining a space vehicle in a desired attitude for long periods of time with a minimum amount of fuel expenditure has been given much attention in the past few years. The Phase I program completed by The Marquardt Corporation, "Optimization Study of Mass Expulsion Attitude Control Systems By Means of Advanced Limit Cycle Techniques", compared the relative merits of five different control techniques when the systems were subjected to selected system errors. This study revealed that the advanced control techniques indeed did improve the overall performance (minimizing fuel consumption) for the type and range of system errors tested. However, this study left certain questions unanswered since it did not include the effects of external disturbance torques or what might be referred to as "sloppy engines." A follow-on program to study the system performance for the changes not considered in the initial program was conducted.

The use of an analog computer as the analytical tool was considered to have advantages over the digital computer for the purpose of this study. With the analog computer the application of external disturbance torques is a relatively simple operation. However, the analog computer has inherent inaccuracies and a study to determine the limitations of the important elements required for the analog circuits was conducted. The random error generation and computer drift and noise characteristics were investigated and it became obvious that with the limited amount of digital logic equipment available, the analog approach could not be followed because of inaccuracies. This conclusion led to the development of a new digital computer program incorporating the desired changes and additions from the Phase I program. This new program has an improved output format as well as the flexibility in applying external distrubance torques. The feature included to allow for external disturbances is a secondary integration where all of the external disturbances (random and predictable) are summed and then applied to the system at discreet intervals referred to in the program as grid time. The grid time can be set at any interval desired so that the overall system performance can be investigated both for short time control systems analysis and long duration mission analysis.

In order to perform a valid error study, a good representation of real engine errors is required. This led to a survey of data for attitude control engines being produced by The Marquardt Corporation. The data obtained from this survey were limited to small pulse width (10 millisec) because of the nature of the engines in a modified pulse frequency modulated control system.

III. DESCRIPTIONS OF CONTROL TECHNIQUES

A program was evolved which encompasses all four of the following control techniques:

A. Simple box limit cycle (fixed impulse delivered when position band on each axis is reached).

B. Diamond error matrix limit cycle.

C. Advanced limit cycle with velocity information (accurate position sensing.)

D. Advanced limit cycle with rate cutoff (extremely accurate rate and position sensing).

The control systems under consideration possess the general block diagram characteristics shown in the following sketch:

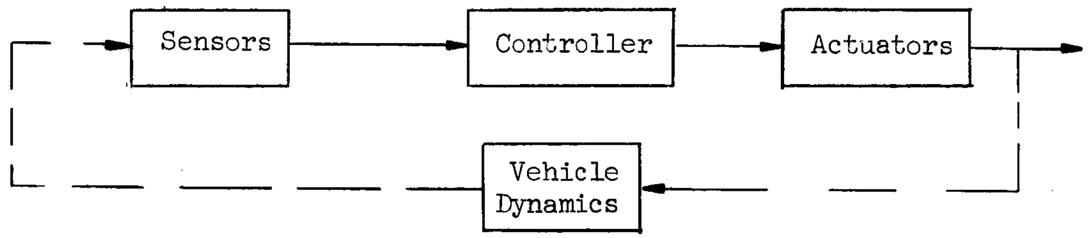

Sketch 1

The controller characteristics for each of the control techniques under consideration are presented in the following discussion.

A. Simple Box Limit Cycle

The most straightforward control mode utilizing this control system is to apply full control torque once the desired accuracy band has been reached. An on-off, single pulse control mode is used. No attempt is made to arrest the angular velocity but merely to limit it to a value which does not exceed that which can be reversed by the application of a minimum impulse bit. Therefore, even under ideal conditions, the vehicle angular position is expected to continually oscillate across the deadband.

In order to determine the theoretical, no-error, mean propellant requirements for this control technique, some insight must be obtained regarding the average pulsing frequency. This is required since the initial rate and disturbance torques are arbitrary in character. Constant vehicle moments of inertia will be assumed and the system dead times, time delays, and pulse widths will be considered negligible compared to the period of oscillation.

If the on-time of the reaction jet is small in comparison with the period, the average off-time of the system per period is:

$$T_s = \frac{2\,\Theta_s}{|\Theta_{s_1}|} + \frac{2\,\Theta_s}{|\Theta_{s_2}|} \qquad (1)$$

where the symbols are defined in Figure 16.

The frequency (f_s) is by definition

$$f_s = \frac{1}{T_s} = \frac{|\dot{\Theta}_{s1}|\ |\dot{\Theta}_{s2}|}{2\,\Theta_s\left(|\dot{\Theta}_{s1}| + |\dot{\Theta}_{s2}|\right)} = \frac{\dot{\Theta}_{s1}\,\Delta\dot{\Theta}_o - \dot{\Theta}_{s1}^{\,2}}{2\,\Theta_s\,\Delta\dot{\Theta}_o} \qquad (2)$$

Where

$$\left|\Delta \dot{\theta}_o\right| = \left|\dot{\theta}_{s_1}\right| + \left|\dot{\theta}_{s_2}\right|$$

Since θ_s is one-half of the total deadband angle and $\Delta\Theta_o$ is determined by the minimum impulse, the frequency is a function of the random variable (θ_{s_1}) as shown in Figure 17. The statistical mean of the frequency can thus be determined as follows:

Assuming the probability density function of $\dot{\theta}_{s_1}$ to be uniformly distributed between 0 and $\Delta\dot{\theta}_o$,

$$P(\dot{\theta}_{s_1}) = \frac{1}{\Delta\dot{\theta}_o} \qquad 0 \leq \dot{\theta}_{s_1} \leq \Delta\dot{\theta}_o \tag{3}$$

The probability density function of the frequency is defined as

$$P(f_s) \triangleq P(\dot{\theta}_{s_1}) \frac{d\,\dot{\theta}_{s_1}}{d\,f_s} \tag{4}$$

$$\frac{d\,f_s}{d\,\dot{\theta}_{s_1}} = \frac{\Delta\dot{\theta}_o - 2\,\dot{\theta}_{s_1}}{\left[2\,\theta_s\right]\left[\Delta\dot{\theta}_o\right]} \tag{5}$$

Therefore

$$P(f_s) = \frac{1}{\Delta\dot{\theta}_o}\left[\frac{2\,\dot{\theta}_s\,\Delta\dot{\theta}_o}{\Delta\dot{\theta}_o - 2\,\dot{\theta}_{s_1}}\right] = \frac{2\,\theta_s}{\Delta\dot{\theta}_o - 2\,\dot{\theta}_{s_1}} \tag{6}$$

The statistical mean of f_s is

$$\overline{f}_s = \int_o^{\Delta\dot{\theta}} f_s\,P(f_s)\,d\,f_s = \int_o^{\Delta\dot{\theta}} \frac{1}{\Delta\dot{\theta}_o}\,\frac{\dot{\theta}_{s_1}\,\Delta\dot{\theta}_o - \dot{\theta}_{s_1}^{\,2}}{2\,\theta_s\,\Delta\dot{\theta}_o}\,d\dot{\theta}_{s_1} \tag{7}$$

Since Equation (7) describes the frequency of oscillation of the vehicle, the pulsing frequency is twice this value, or

$$f_s' = 2 f_s = \frac{\Delta\dot{\theta}_o}{6\,\theta_s} \tag{8}$$

The mean propellant consumption is the propellant-used-per-pulse multiplied by the average pulsing frequency. Thus,

$$\bar{\dot{\omega}}_p = \frac{\omega_p}{2} f_s' \tag{9}$$

Making the proper substitutions,

$$\dot{\omega}_p = \frac{\Delta\dot{\theta}_o\, I}{I_{sp}\, L}\;\frac{\Delta\dot{\theta}_o}{6\,\theta_s} = \frac{\Delta\dot{\theta}_o^{\,2}\, I}{6\, I_{sp}\, L\, \theta_s} \tag{10}$$

Substituting for $\Delta\dot{\theta}_o$, the mean propellant consumption per axis is

$$\bar{\dot{\omega}}_p = \frac{I_T^{\,2}\, L}{3\,\theta_s\, I\, I_{sp}} \tag{11}$$

for four engines (coupled configuration)

or

$$\bar{\dot{\omega}}_p = \frac{I_T^{\,2}\, L}{12\,\theta_s\, I\, I_{sp}} \tag{11a}$$

for two engines (uncoupled configuration)

B. Simple Diamond Error Limit Cycle (Rate Switching Option)

Only the 6-unit configuration is considered applicable to the "Diamond Error Matrix" in this study.

Since two (or more) axes are coupled in the "Diamond Error Matrix", it is designed to have single engine firings to correct for errors in both axes. For example, if a combined error command in (+) yaw and (+) roll has exceeded the diamond error band, the appropriate engine (Engine 53 as shown below) will be fired. In the special cases in which two or three error bands are crossed simultaneously, the computer printout will indicate all engines fired.

The "Diamond Error Matrix" for the yaw-roll axes in the 6-unit configuration is shown in the logic table below. Also shown in this table are the designated engines to be fired for the indicated error signals. The single axis errors are defined as:

$$\text{Yaw} \qquad \lambda_3 = a_1 \theta_Y + b_1 \dot{\theta}_Y \qquad (12)$$

$$\text{Roll} \qquad \lambda_2 = a_2 \theta_R + b_2 \dot{\theta}_R$$

$$\text{Pitch} \qquad \lambda_1 = a_3 \theta_P + b_3 \dot{\theta}_P$$

The equations describing the linear combination of yaw and roll error command band, along with the engine to be fired when this error band is exceeded, are as follows:

Equation	Fire Engine (N)
$\frac{\lambda_3}{\lambda_{3_{max}}} + \frac{\lambda_2}{\lambda_{2_{max}}} - 1 = 0$	53
$\frac{\lambda_3}{\lambda_{3_{max}}} - \frac{\lambda_2}{\lambda_{2_{max}}} - 1 = 0$	63
$\frac{\lambda_3}{\lambda_{3_{max}}} + \frac{\lambda_2}{\lambda_{2_{max}}} + 1 = 0$	54
$\frac{\lambda_3}{\lambda_{3_{max}}} + \frac{\lambda_2}{\lambda_{2_{max}}} - 1 = 0$	64

Associated with these error bands are special or unique cases in which two of the error limit equations intersect. Since these points occur when either the yaw or roll error is zero, a pure "couple" is necessary to drive the system back into its allowable error band which is considered in the present program.

The pitch error deadband in the 6-unit case is a straight deadband and is identical to the previously described simple box system with the exception of the addition of a rate dependent error contribution.

C. Advanced Limit Cycle with Velocity Information

It has been shown that the simple limit cycle method does not include damping. Adding damping to the system is one method by which system improvement can be achieved. The problem of improving the straight limit cycle performance involves defining the means of adding damping to the system. The method of system improvement is to reduce the total system mass and to improve the rocket engine duty cycle. The total system mass includes fixed and expendable components. The fixed mass includes the hardware items and the expendable mass is the propellant.

Mass expenditure is the critical component for long term missions and the criterion for reducing the total system mass will be the minimization of the propellant consumption. The criterion used to improve the rocket engine duty cycle requires the minimization of the number of rocket engine firings and duration of each firing.

The optimization criteria for controller design will therefore be the minimization of the number of pulses and the reduction of propellant consumption. The approach employed in this technique involves the application of two pulses in the correction of any angular deviation. Two pulses are a minimum, since one pulse can effectively null only the rate whereas two pulses are required to also null the position. In order to minimize propellant consumption, the second pulse will be a fixed pulse equal to the minimum impulse bit which the engine can accurately and repeatably produce. The first pulse will then vary depending on the initial entering rate and will establish a fixed rate after the pulse firing. The minimum impulse bit will define this fixed leaving rate of the first pulse. Also, the first impulse bit is not determined since it must be of a magnitude sufficient to null the entering rate and produce a minimum leaving rate which the second pulse can null. This will now be shown.

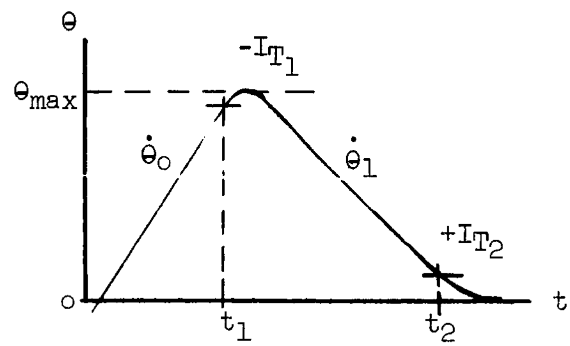

Sketch 2

Where

t_1 = Firing of first pulse

t_2 = Firing of second pulse

$$\ddot{\Theta} = \frac{\sum T_y}{I_y} \tag{12}$$

$$\frac{d\,\dot{\Theta}}{dt} = \frac{\sum T_y}{I_y} \tag{13}$$

$$\Delta\dot{\Theta} = \int_{t_1}^{t} \frac{\sum T_y}{I_y}\, d\,t \tag{14}$$

The analyses are further simplified because the effects of disturbance torques are neglected. The rocket engine thrust cannot be taken as a constant with time even though a constant level is commanded from the controller since the rocket system nonlinearities result in an oscillatory thrust output. This will affect the resulting rate and position versus time which is shown in Equation (14) and expressed as:

$$\Delta\dot{\theta} = \frac{L}{I_y} \int_{t_1}^{t} F\,dt \tag{15}$$

$$\int_{t_1}^{t_1'} F\,dt \triangleq I_{T_1} \tag{16}$$

Where $t_1' - t_1$ = Pulse width

The defining equation for the first pulse case is

$$\dot{\theta}_1 = -\frac{L\,I_{T_1}}{I_{y_1}} + \dot{\theta}_o \tag{17}$$

Where the sign convention is defined in Figure 16.

The defining equation for the second pulse case is

$$\dot{\theta}_2 = \frac{L\,I_{T_2}}{I_{y_2}} + \dot{\theta}_1 \tag{18}$$

which reduces to

$$\dot{\theta}_1 = -\frac{L\,I_{T_2}}{I_{T_2}} \tag{19}$$

since by definition it is desired to null the rate after the second pulse firing ($\dot{\theta}_2 = 0$). Equation (19 fixes the rate after the first pulse firing and Equation (17) now becomes:

$$\frac{L\, I_{T_1}}{I_{y_1}} = \dot{\theta}_o + \frac{L\, I_{T_2}}{I_{y_2}} \tag{20}$$

Since the criterium for minimum propellant consumption dictates that the second pulse should be the minimum impulse bit which the engine can accurately and repeatedly produce, Equation (20) becomes

$$\frac{L\, I_{T_1}}{I_{y_1}} = \dot{\theta}_o + \frac{L\, I_{T_{min}}}{I_{y_2}} \tag{21}$$

A constant moment of inertia between the pulse firings of one control cycle is assumed which dictates that the internal mass and equipment remain relatively fixed during this time period. Therefore, $I_{y_1} = I_{y_2}$ and Equation (21) becomes

$$I_{T_1} = K_1 \dot{\theta}_o + I_{T_{min}} \tag{22}$$

$$K_1 = \frac{I_y}{L}$$

The total stored energy to be expended at each pulse is therefore defined.

The diagram and time derivation presented below illustrate the timing or engine firing criteria.

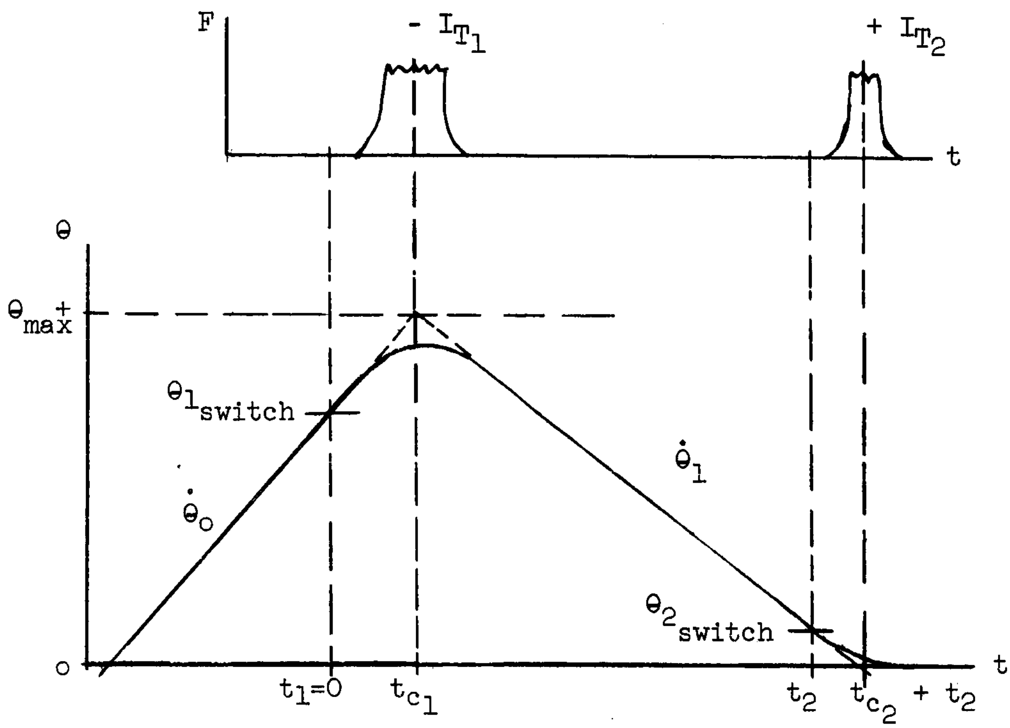

Sketch 3

Where

t_{c_1} and t_{c_2} = The centroid of the individual pulses from electrical signal on time.

t_1 and t_2 = Electrical signal on time.

The θ_1 switch line can be determined as a function of the mission accuracy requirements and initial rate. Once the θ_1 switch line has been selected, the θ_2 switch line can be determined. However, the use of the θ_2 switch line does not lead to a practical system since errors are introduced due to the position sensor threshold. Therefore, the second pulse will be fired as a function of time rather than position. From the Sketch 3 above,

$$\theta^{+}_{max} = \dot{\theta}_1 \left(t_{c_2} + t_2 - t_{c_1}\right) \tag{23}$$

Also

$$\theta^{+}_{max} = \theta_{1_{switch}} + \dot{\theta}_o \, t_{c_1} \tag{24}$$

When $\pm\ \theta^{+}_{max}$ is assumed to represent the mission position accuracy requirements, Equation (24) is used to determine the θ_1 switch line as a function of initial rate and the pulse centeroid. Although θ^{+}_{max} does not represent the actual maximum position reached in the vehicle travel, it does allow a minor degree of conservatism.

The timing of the second pulse firing can now be obtained by combining Equations (23) and (24) as shown below.

$$t_2 = \frac{\theta_{1_{switch}} + \dot{\theta}_o \, t_{c_1}}{\theta_1} + t_{c_1} - t_{c_2} \tag{25}$$

Substituting Equation (19) yields

$$t_2 = \frac{K_1}{I_{T_{min}}} \left(\theta_{1_{switch}} + \dot{\theta}_o \, t_{c_1}\right) + t_{c_1} - t_{c_2} \tag{26}$$

D. Advanced Limit Cycle with Rate Cutoff

This technique is quite similar to control technique 3 discussed above. The difference arises in the fact that the present method assumes an accurate continuous rate sensor. This sensor is used to provide rate information near zero rate to cut off the final pulse phase of the sequence. The impulse delivered after the electrical signal off is such that it will drive the vehicle to zero rate. This method fires the last pulse not as a function of time but rather when the position sensor switches sign (zero angular position). Therefore this system does not have the integrated effects of system errors which plague the other methods. The only gross errors with this method are the error associated with the impulse bit after electrical off signal and the sensor error.

IV. DISCUSSION OF PROGRAM TASKS

A. Task 1 - Analog Computer Simulation

The initial phase of this study program was devoted to investigating the analog computer for use in performing a statistical three-axis study for the four attitude control techniques that indicated promise in the Phase I study program. The advantages of an analog computer analysis for this application are apparent when considering outside disturbance torques, especially for the random type disturbance. This results from the fact that in its standard form, the analog computer employs continuous integration and disturbances of any nature can be injected at point in time. However, it should be noted that the analog computer has inherent inaccuracies associated with it and to insure valid results for this program, some of the conventional integration techniques must be replaced with the more accurate digital techniques. Consequently, the analog computer for this special application is more directed towards a hybrid simulation combining the desirable characteristics of each of the analog and digital computation techniques. The analog approach was then pursued to attempt to satisfy the basic requirements of the study with the available computing equipment.

Specifically, the goals of the Task 1 program were:

1. Develop computer techniques utilizing the analog computer plus limited digital logic.

2. Develop circuits applicable to statistical analysis.

3. Determine accuracy and applicability of single axis simulation so that method of 3 axis parameterization analysis can be evaluated.

4. Investigate tolerance compensation for slowly varying quantities such as decreasing vehicle mass.

5. Investigate effect random or cyclic disturbance torques have on overall performance of the various control techniques.

It should be noted that only a small amount of high speed digital logic equipment was available for use with the analog computer. This limited the simulation to primarily a pure analog study and long run time accuracy was a problem. The circuits considered for simulation of random errors and thrust are shown in Figures 1 and 2 . The simulation of random errors was accomplished through applying random thrust levels in conjunction with the nominal thrust level. The technique utilized in obtaining the random numbers is as follows. The basic elements of this simulation were (1) Elgenco Model 301A Random Noise Generator, and (2) sample and hold circuit built up from analog and digital components. The attitude angle (θ) is continually monitored by the sampling circuit and when the combined characteristics of attitude angle equalling a predetermined reference angle (θ_A) and $\dot{\theta}$ being the same sign as the angle θ, the sampling circuit is triggered for a short period ($\approx$1 millisecond). During this sampling period, the output of the random noise generator is integrated and held. To prevent this circuit from drifting between pulses, thereby indicating a false random value, the noise is sampled just prior to being used. Then following the thrust pulse (after the angular rate has been reversed) the circuit is reset by a direct short of the feedback of the hold circuit to the input. The circuit is then ready for the next random number sample and thrust pulse.

The random number is utilized in the following manner. First, it must be noted that thrust is to be integrated twice to obtain attitude angle. It was originally intended to operate in the same manner as in the digital computer study where total impulse or change in angular rate was simulated and integrated once to obtain attitude angle. However, to properly implement impulse simulation a digital counter, A-D, and D-A converters are necessary. This amount of equipment was not available. Therefore, the analog computer equipment was relied upon to furnish accurate rate and position information.

The results of the Task 1 study program are divided into two areas:

1. Random Error Simulation
2. Long Term Accuracy

The most important requirement of the analog computer simulation is to obtain an accurate representation of random errors. As previously described, this is to be accomplished by sampling the output of a normally distributed random noise generator. The circuit to perform the sampling operation is shown in Figure 1. There are two definite problems associated with this method of obtaining the random errors. These consist of: (1) performing the sampling at a high rate to prevent filtering of the random noise, and (2) preventing the output from drifting during the 'hold' portion of the 'sample and hold' cycle. In either of the aforementioned problem areas the effect is to reduce the distribution configuration both in type (change from Gaussian) and maximum variance (caused by drift towards the mean value of zero). These two problem areas have conflicting solutions. This results from the fact that minimizing filtering requires a small capacitance and minimizing drift requires a large capacitance. This calls for a compromise that can only degrade the randomness of the random noise generator.

Several types and values of capacitors were tried in attempting to find one capacitor that would minimize both filtering and drift. Figure 3 indicates the results of sampling and holding the voltage output of the random noise generator at intervals of one second and holding this voltage for a period of one half second. It should be noted that the output of the Elgenco Model 301A generator has a frequency response flat to 40 cps and the filtering or sampling circuit should be extended to greater than 40 cps. Based on an amplifier input resistance of 1 meg ohm, the feedback capacitor must be less than .004 μfd as a compromise between filtering and drift.

The problems associated with the long term amplifier drift were investigated. It must first be reiterated that adequate digital and/or analog-to-digital and digital-to-analog equipment was not available to apply the most accurate storing and readout techniques. It was therefore necessary to rely on essentially pure analog equipment to satisfy the entire simulation and this is difficult while maintaining the necessary accuracies as required in a statistical study. A series of tests were made on available computer equipment to determine voltage drift that could be expected on computer runs for extended periods. The results of these tests are shown in Figure 4. The length of computer run time required to establish a realistic statistical trend can only be estimated from results of last year's digital computer study. In these studies it was found that approximately 10^6 seconds was sufficient to obtain steady state limit cycles in the majority of the cases tested. Also, in reviewing last year's studies, it was found that the minimum time between pulses for a single axis was approximately 5 seconds (diamond error matrix). Therefore, realistically, the computer time scaling cannot be any greater than approximately 1000:1. For this case the maximum computer run time would be 1000 seconds. Then, as seen in Figure 4, the absolute accumulated error after a period of 1000 seconds could be as high as 5%, based on a hundred volts maximum. Of course this is the maximum value and by repeatedly balancing amplifiers this error could be reduced to some extent. These values are also based on extrapolation of data taken for 300 seconds (or less) run time. The significance of these results is that if the worst case drift integrator was being used as the counter for total fuel consumption, an error of greater than 5% could be indicated for a one million second mission time. However, for the short integration times derived from traversing the limit cycle deadband ($\approx$100 seconds), the computer time (.1 second) would reflect no error due to drift. Therefore, it is concluded that unless a drift-free counter to indicate total fuel consumed during the mission can be obtained, the pure analog simulation is not applicable to the three-axis study from the standpoint of accuracy.

B. Task 2 - Digital Computer Program (also see Appendix A)

The angular position of a vehicle may be resolved into components about three mutually perpendicular axes, called pitch, roll, and yaw axes. These are defined in Figures 18 and 19. A typical graph of the angular position $\theta(i)$, $i = 1, 2, 3$, vs time, is illustrated in Figure 21. This represents a vehicle with a six engine configuration, responding to control philosophy cycle No. 1 (see Table 11). The slope of the graph at any time is $\dot{\theta}(i)$, the angular velocity.

A grid is set up along the time coordinate, with equally spaced intervals $(\Delta t)_g$. The vehicle is acted upon by continuous external torques, possibly brought about by cosmic particles, magnetic fields, and the like. It is assumed that the external torque is applied at the discrete grid times. The change $[\Delta\dot{\theta}(i)]_g$ at the end of any grid interval is computed by assuming constant external torque throughout that interval. The magnitude of this torque is taken equal to that computed at the end of the interval. The difference equation which computes $[\Delta\dot{\theta}(i)]_g$ is given in Appendix 2.

The aim of the control system is to keep the position angle $\theta(i)$ from straying outside the deadband limits $\pm\Delta\theta(i)$, for each axis i (See Figure 21; in that illustration, the three deadband limits $\Delta\theta(i)$ are equal). To accomplish this, appropriate rocket engines (see Tables 11 to 14) are fired, which change the angular velocity $\dot{\theta}(i)$. The increment $[\Delta\dot{\theta}(i)]_e$ brought about by each engine firing is given in Tables 16 and 17.

General Outline of Computations

Knowing the initial values of $\theta(i)$, $\dot{\theta}(i)$, the time TSTART (= 0), and the grid increment $(\Delta t)_g$, we compute the next grid time, TGNEXT:

$$\text{TGNEXT} = \text{TSTART} + (\Delta t)_g$$

Calculate the time T(i) at which an engine pulse is required to correct the motion around axis i. This calculation is based on linear θ - t functions; i.e., external forces are neglected. Tables 11 to 14, in the columns Firing Criteria, outline the computation of each T(i) for the Control Philosophy under consideration.

Set FIR1ST = minimum $\{T(1), T(2), T(3)\}$. FIR1ST is the predicted next firing time, based on constant angular velocity.

We next compute the change $\Delta\dot{\theta}(i)$ in angular acceleration brought about either by engine firings or external forces, depending on whether FIR1ST or TGNEXT, respectively, comes first.

1. Effect of Engine Firings

Determine which engines need to be fixed. This decision is based on the vehicle configuration (6 or 12 engines), the axis for which the engine firing is required, and whether a positive or negative error is involved. In Figures 18 and 19, arrows indicate the direction of positive rotation about each axis. Tables 11 thru 14 define the engines which are fired, as well as the impulse commanded of each.

Having determined which engines are activated, compute the delivered impulse (find the appropriate equation in Table 15 and each increment $[\Delta\dot{\theta}(i)]_e$ in angular acceleration (Tables 16 and 17). Due to the existence of certain random and fixed errors, an engine firing intended to correct motion about one axis will affect rotation around every axis. The random error coefficients $\epsilon_{ijk\alpha}$ which appear in Tables 15, 16 and 17 can be divided into two types: those associated with errors parallel to the center line of the engine (α= 1), and those associated with errors perpendicular to this line (α= 2). The random errors are also broken up into those associated with the minimum impulse (K = 1), and those with the total impulse (K = 2). The former, for example, is concerned with the increasing and decreasing transients of the engine firing. See Appendix 3 for an outline of the computation of $\epsilon_{ijk\alpha}$. The fixed error coefficients $\beta_{ijk\alpha}$ are also discussed in Appendix 3.

2. Effect of External Torques

The procedure for computing $[\Delta\dot{\theta}(i)]_g$, the change in angular velocity due to external torque, is outlined in Appendix 2. Both predictable and random factors are accounted for.

Having computed the increment $\Delta\dot{\theta}$ in angular velocity, we then update the angular motion parameters to the new time, FIR1ST or TGNEXT:

$\theta(i) = \theta(i) + \dot{\theta}(i) * \Delta t$. Δt is time interval

$\dot{\theta}(i) - \dot{\theta}(i) + \Delta\dot{\theta}(i)$

The entire procedure is repeated until a cutoff point (time, number of pulses, or propellant burned) is reached.

At specified time intervals, called TPINCR in the program, the mean time between firings, $\bar{T}$, and a parameter, σ, are printed, for each axis and for the entire system. These terms are defined in Appendix 5.

Piecewise Linear Functions

In Control Philosophy No. 2, a criterion for engine firing is

$$|\lambda_2(t)| + |\lambda_3(t)| = \Delta\Theta$$

Where

$$\lambda_i(t) = a_i\,\Theta_i(t) + b_i\,\dot{\Theta}_i(t)$$

$i = 2, 3$

t = Time variable

$\Delta\Theta$ = Minimum $\{\Delta\Theta(2), \Delta\Theta(3)\}$

Since $\theta(t)$ is linear and $\dot{\theta}(t)$ is constant within a grid interval, $\lambda_i(t)$ are linear. Let $L(t) = |\lambda_2(t)| + |\lambda_3(t)|$.

A typical graph of L(t), which is piecewise linear, is shown in Sketch 4.

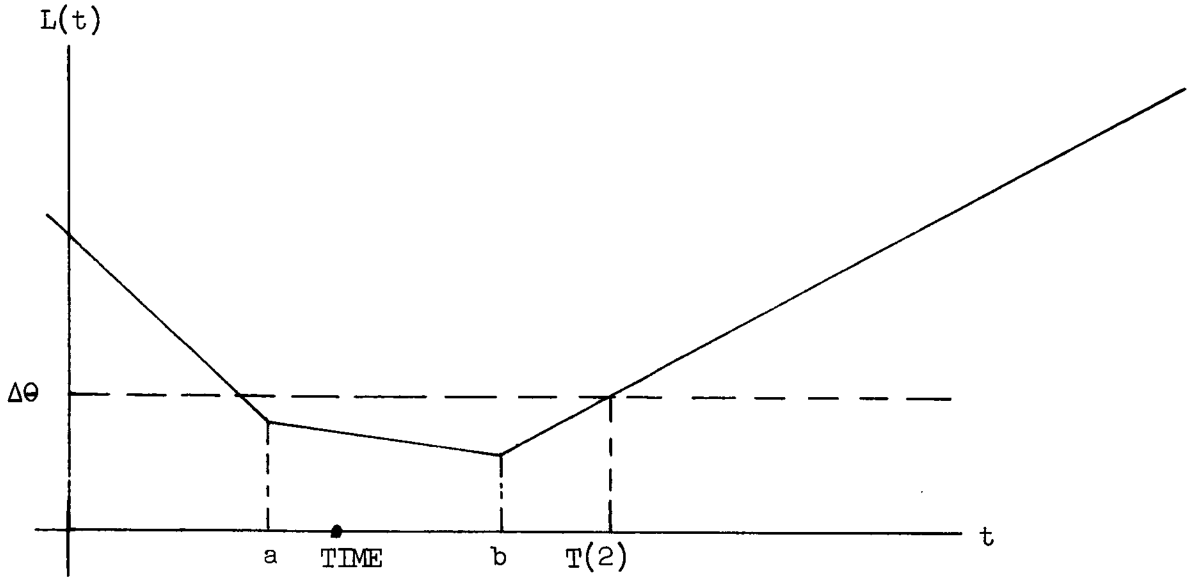

Sketch 4

The time T(2) when engine firings are required is that time when the increasing portion of the function L(t) intersects the line L(t) = $\Delta\theta$. The current time is denoted by TIME.

The nonlinear points a, b of the function are given by:

$$a = \frac{a_2 \dot{\theta} \ast \text{TIME} - \lambda_2}{a_2 \dot{\theta}_2}$$

$$b = \frac{a_3 \dot{\theta}_3 \ast \text{TIME} - \lambda_3}{a_3 \dot{\theta}_3}$$

Where θ_i, $\dot{\theta}_i$ are evaluated at TIME.

C. Task 3 - Investigation of Automatic Tolerance Compensation

The present program does not allow for continuous correction of the important changing variables and only by successive single runs in a piecewise manner can the effect on system performance of the variables be established for a particular configuration. Consequently, the automatic compensation for these changes cannot be adapted to the program.

As an attitude controlled orbiting vehicle progresses through its useful life, numerous changes in its operating parameters may generally be expected. In the case of some of the advanced attitude control methods, the operation of the system logic is sized or "tailored" to the assumedly known values of the critical parameters, so that changes in these values could cause upset to the overall performance.

The two immediate questions which arise in regard to these drifting parameter values are: What is the effect on vehicle performance - and - how may the effect be compensated? If the answer to the first question is favorable, the second may have no need to be asked.

The first question is associated with the prediction of the system behavior, while the second question is associated with the problem of the synthesis of an operational logic. The major portion of the effort expended to date on the current computer program has been directed toward the generation of an answer to the first question, that is: given a certain operational philosophy and a specified set of conditions - how will the system perform? If an answer is produced for the second question, its value is determined by presenting the situation along with any modifications in operational philosophy to the computer.

For the purposes of this investigation, the slowly changing parameter values may be assumed to be limited to engine firing characteristics and variations in vehicle mass and its distribution. For a number of cases, the effects of parameter variations may be evaluated without utilization of additional computer capability. For example, if long term operation causes changes in engine characteristics, these changes may be represented as appropriate bias errors; a capability which the current program already possesses. If due to propellant depletion, the vehicle moments of inertia change and its mass center shifts, the system performance may again be evaluated within the capabilities of the current program. In this case, the errors which would be caused by reason of moment arm changes are introduced to the program by specification of appropriate input values, and errors caused by the reduction of the moments of inertia may be made equivalent to those resulting from increased thrust levels.

The above described methods may often be unwieldy, confusing and prone to error, especially if the effects of these parameter variations are to be investigated widely. In addition, when these methods are employed the computer output represents only steady state running characteristics of the system under the conditions in question. For this reason, the capability to continuously vary moments of inertia would be desirable. This capability would permit a continuous monitor of system performance during its period of deterioration. However, since the moments of inertia may change as functions of several variables, the program changes are considered beyond the scope of the parameterization studies. Currently, the computer regards the initial values of these parameters as constants throughout any individual run. Owing to the large number of variables involved, a similar capability has not been developed for the case of changing engine characteristics. Since in general the greatest sensitivity may be associated with changing moments of inertia, this does not appear to be a serious limitation.

In general, operating difficulties which are introduced into the system because of changing moments of inertia owe their existence to the fact that the system logic is not "aware" of these changes. If some compensation were introduced to the logic so that the values of the system gains would always reflect the current values of these parameters, the dynamics of this compensated system would be essentially the same as that of an ideal uncompensated system. It is therefore clear that since the computer simulates the dynamics of the vehicle, the program is best suited to representing the influence of the uncompensated portion of the system.

D. Task 4 - Compilation of Engine Test Data

Data for ten attitude control engines built by The Marquardt Corporation were obtained for 10 msec pulse widths. These data were arranged in statistical form as shown in Figures 5 thru 14 . It can be seen from these plots that some of the engine samples (Engines 1, 3, 4, 6, 8, 9) approach a Gaussian distribution but the remaining engines do not appear to justify any definite distributional form. There is no specific reason for this and can only be explained as possibly being caused by inadequate number of samples and instrumentation and recording errors. A significant factor derived from these data is the spread of the mean impulse between the ten engines. There is a 35% variation between the highest and lowest mean values of the engines analyzed. This would probably be considered unacceptable if the control technique requires a known value of minimum impulse. However, the repeatability of the pulses for each engine (as indicated by the value of sigma (σ) for each engine) is within 5% with the exception of Engine number 2. Therefore, it is concluded that once an engine has been calibrated and its mean minimum impulse value is known, the control system can be programmed to include the individual engine offsets.

The curve of propellant mass vs. total impulse shown in Figure 15 is also extracted from engine test data. It should be noted that this curve is linear throughout the range indicated and does not become nonlinear until the commanded pulse width is less than 6 millisec (2.64 Newton sec.) The values of sigma for the Gaussian curve fit approximations and were computed by considering 50 pulses of 10 millisec duration (10 millisec on - 100 millisec off) for each engine. The values of sigma were then computed as shown below.

$$\sigma_e = \frac{1}{(N-1)} \sum_{i=1}^{N} \left[I_{T_i}^2 - \frac{(\Sigma I_{T_i})^2}{N} \right]$$

A mean value of sigma as well as a mean value of minimum impulse were computed to indicate the average engine performance.

$$\bar{\sigma}_{engine} = .08362 \text{ Newton-sec}$$

$$\bar{I}_T = 2.231 \text{ Newton-sec}$$

In the case of the Task II digital computer study the actual values of individual engines were used in the simulation. This was considered the most attractive approach since it reflected a real situation where a limited number of engines were available to perform the attitude control job. If a large number of engines were available to choose from, a more consistent or average set of engines would be selected and mean values of impulse and variance would be used.

V. COMPUTER RESULTS

The results of the digital computer three-axis parameterization study are shown graphically in Figures 22 thru 77 for the individual computer runs in the form of:

1. Mean propellant flow rate computed every 1000 sec of mission time by dividing the propellant consumed to that point by the time to that point.

2. Sigma of the mean propellant flow rate which is a statistical indication of the variation of the mean propellant flow rate and is also computed (equation is described in computer analysis) every 1000 sec of mission time. Since the value of sigma is large at the beginning of each run, the first 50,000 sec of run time are blanked out in the plots so that a better indication of sigma is obtained in the later stages of the mission. The computer printout gives a more accurate indication of sigma where some values are reading close to zero on the plots.

3. Mean time between firings which is an indication of the duty cycle for each engine, each axis and the total. It is computed by dividing the time (multiple of 1000 sec) by the number of pulses that have occured to that time.

It is obvious from many of the plots shown in Figures 22 thru 77 that in many cases the system has not settled out from its initial transient. It should be noted here that on an average the runs of 300,000 sec of mission time require approximately 15 minutes of computed run time. Therefore, it was decided to limit the run time to 300,000 sec except in a few instances where 600,000 sec was tried in attempting to achieve a better steady state figure for the propellant flow rate. However, even in these cases the flow rate did not reach what is considered a good statistical steady state level.

Tables 1 thru 5 show the results for the three primary parameter variations made in this study and Tables 7 thru 10 describe the values of random and thrust bias errors for the six-unit configuration.

The vehicle and engine parameters maintained constant for these studies are:

(1) Moments of Inertia

$J_{Pitch} = J_{Yaw} = 4.905 \times 10^6$ KG . M^2

$J_{Roll} = 1.668 \times 10^5$ KG . M^2

(2) Engine Configuration - 6-unit

(3) Lever Arms

$L_1 = 17.2$ meter

$L_2 = 3.55$ meter

(4) Engine

Thrust = 675 Newton

Min Impulse $I_{To} = 20$ Newton sec.

(5) Propellant vs. Total Impulse

(Curve is shown in Figure 15).

(6) Initial Conditions

$\theta_{Roll} = \theta_{Yaw} = \theta_{Pitch} = 0$

$\dot{\theta}_{Roll} = .0001$ deg/sec

$\dot{\theta}_{Pitch} = .001$ deg/sec

$\dot{\theta}_{Yaw} = .01$ deg/sec

(7) Dead Band (same for all three axes)

$\Delta\theta = 1.0$ deg.

(8) Error distributions all Gaussian.

Runs 6 thru 10 were made to describe what were considered real engines from the standpoint of satisfying engine thrust specifications. However, as evidenced by the results, these engines are not accurate enough to consider using advanced limit cycle techniques. Further research into engine data revealed that engines tested were less than the specification requirements by a good amount and the biased errors noted as nominal describe a more realistic set of engines from the standpoint of thrust tolerance and installation errors. It should be pointed out that the specification errors (Runs 6 thru 10) could reflect the errors associated with engines after prolonged cycling and would help to describe performance and, or compensation requirements over the life of an engine.

It is obvious from the results of the thrust biased error study as shown in Table 1, that the advanced limit cycle techniques cannot tolerate biased errors much greater than the nominal errors presented and still maintain a fuel consumption advantage over the simple box limit cycle. Furthermore, the effect on system performance for just one engine with a loose thrust tolerance could be devastating as seen in Table 4. In these comparison runs (6 and 10), the fuel consumption (total system) increases by over 70% in the advanced limit cycle techniques and by only 25% in the box limit cycle and 40% in the diamond error limit cycle when the biased errors for two engines (54, 55) are increased from 5.5% to 16.5% and 2% to 6% respectively. Although this may be a large degradation in engine performance, the fact that one engine in the Yaw-Roll couples can cause the fuel consumption to increase in all four engines is a severe limitation in the advanced limit cycle techniques.

It is also significant that when two engines have loose random errors (as evidenced in Table 5) the effect on fuel consumption is small if not negligible.

The results indicated in Table 2 reveal some interesting results in that the effect of random errors in delivered impulse is quite different for systems with no thrust bias errors and systems with large bias errors. Table 2a shows that:

1. The simple limit cycle control techniques, as would be expected, have slightly increased fuel flow rates for the larger random errors.

2. The advanced techniques show a very substantial increase in fuel consumption also as would be expected.

This trend is reversed for systems with large thrust bias errors as seen in Table 2b. Although the fuel consumption for the engines used in Table 2b is probably excessive, it may be desirable to consider this factor in any future studies where trade-offs in engine performance may be necessary.

Table 3 shows the effect of disturbance torques (cyclic and small random) on fuel consumption. The cyclic disturbance torque used here is considered an aerodynamic torque encountered in an ellyptical earth orbit. It assumes a vehicle nose down configuration where the gravity gradient is small compared to the aerodynamic torque.

The disturbance was assumed to be sinusoidal with a period of 5400 sec in the pitch axis only.

$$H(t) = A + B \sin\ t/5400$$

where for a heavy disturbance

A = .01 Newton-Meter

B = .01 Newton-Meter

and for a light disturbance

A = .0001 Newton Meters

B = .0001 Newton Meters

Also included in these runs were random disturbances with a three sigma value of .0001 Newton-Meters.

As seen in this table the effect on system performance is much greater for the advanced techniques than for the simple limit cycle cases. The cross over point (i.e., the point at which the advanced limit cycle techniques cease to have a fuel consumption advantage over the simple limit cycle techniques) lies between the light and heavy disturbance. Therefore, a thorough knowledge of the mission and expected disturbances is necessary before a desirable control system selection can be made. Another factor of interest in Table 3 is that the total system fuel consumption for the Diamond Error Matrix Limit Cycle (System 2) is improved with the application of external disturbance torques.

A series of nine runs (Systems 1, 3 and 4) were made for a 12-engine configuration utilizing the same basic engine and vehicle parameters and initial angular and rate conditions as used in the 6-engine sensitivity studies. The results of these runs are shown graphically in Figures 69 thru 77 and are summarized in Table 6. The purpose of these runs was threefold.

1. Check out the digital computer program for the 12-engine configuration.
2. Investigate the effect of one engine variable on system propellant consumption.
3. Provide a basis for gross comparison between the 6 and 12-engine configurations.

The effect of biased thrust errors on propellant consumption was selected for parametric variations since it was found to be the most sensitive engine parameter in the 6-engine sensitivity studies. The results of these runs, as shown in Table 6, concur with the trends established for the 6-engine configuration as seen in Table 1 where the propellant flow rates increase rapidly with an increase in thrust bias errors. The absolute value of propellant consumption shown in Tables 1 and 6 cannot be compared directly since the thrust bias errors in the 6-engine configuration were for a specific group of engines with different magnitudes of biased errors and the 12-engine configuration was for biased errors of the same magnitude (0, 1%, 5%) but in selected positive and negative directions.

VI. CONCLUSIONS

From the results of Task I (Analog Computer Simulation) it is concluded that an analog computer without the support of a large amount of digital logic equipment cannot perform the required tasks with the accuracy demanded in the parameterization studies.

The digital computer program developed for the parameterization studies represents a useful tool in evaluating the performance of the four control techniques previously described. It is relatively simple to use and requires a minimum of input parameters so that a knowledge of digital computer program techniques is not a requirement. Once a precise set of engine, vehicle and mission parameters have been selected, this program can serve as an analytical tool to both choose the optimum control system and size the propellant tanks required to complete the mission. The results of this study can only serve as a guide to the trends that could be expected with real engines and further study is required to pin point exact engine and control system requirements.

The presence of external torques has a similar effect on fuel consumption as the biased engine thrust errors. The application of a typical aerodynamic torque found at approximately a 100 mile earth orbit causes nearly the same increase in fuel consumption as does a 1.5% increase in thrust error.

The results of digital computer parameter studies have led to three important conclusions concerning tolerable engine errors.

1. Engine thrust bias errors are of importance in all four of the control techniques investigated but are extremely significant in justifying the use of the advanced techniques. Unless engines with thrust tolerances of less than 1.5% can be selected, the use of the advanced techniques would be questionable.

2. Random errors in delivered impulse are also important in choosing a particular control technique. Values of variance (3 σ) greater than .05 for engine pulse repeatability would certainly reduce if not eliminate the advantage of the advanced techniques.

3. The most important point derived from the engine error sensitivity studies is the effect a single engine with a loose thrust tolerance can have on fuel consumption. A single engine in the yaw-roll couples with a thrust offset of 10% from nominal will increase fuel consumption by as much as 80% as was obtained for System 3. It is concluded that it would be desirable if not necessary) to select a closely matched set of engines for any of the control systems analyzed.

VII. RECOMMENDATIONS

The results of this study have revealed general performance trends of four attitude control techniques when subjected to variations in critical engine characteristics. It is recommended that the digital computer program developed for this study continue to be run to establish more precise performance characteristics for the advanced control techniques as the definition of engines, vehicles and missions are updated and refined.

Another study that is recommended is to investigate the behavior of the advanced control techniques for different shapes of thrust pulses. Depending on the type of propellant valves, injectors and engine configurations, a significant difference in the performance of the advanced control techniques may result. The digital computer program developed is capable of performing this type of study.

The natural eventual follow-on to the parametric studies is to implement hybrid simulations where actual engines would be combined with simulated vehicle and control systems (and, or) breadboard control systems combined with simulated engines and vehicles. These programs are strongly recommended to establish controlled performance in the presence of real component noise, accuracy and dynamic characteristics.

VIII. REFERENCES

1. Englehart, W. C., "Synthesis of a Damped Limit Cycle Reaction Jet Attitude Control System", Master of Science Thesis - UCLA, June 1963.

2. NASA Marshall Space Flight Center Report MTP-ASTR-N-62-14, "A New Concept to Minimize On-Off Jet Fuel Consumption Used for Space Vehicle Attitude Control", Hans F. Kennel and David N. Schultz, 19 December 1962, UNCLASSIFIED.

3. The Marquardt Corporation Memorandum Report 20,115, "Torque Requirements for Satellite Attitude Control", P. Arthur, C. R. Halbach, and W. C. Englehart, March 1963. UNCLASSIFIED

4. The Marquardt Corporation Final Report, "Optimization Study of Mass Expulsion Attitude Control System by Means of Advanced Limit Cycle Techniques, W. C. Englehart, et al, 16 October 1964.

TABLE 1

COMPARISON OF BIAS ERRORS

(Mean Propellant flow rate after 200,000 sec.)
All propellant flow values in (Kg/sec) x 10^6

System	Run	Bias Error *	Random Error **	Engines 53	54	55	63	64	66	Total
1	4-1	0	5%	17.50	17.60	2.45	17.50	17.60	2.40	75.060
	5-1	1.5%		33.00	33.05	2.40	32.05	32.35	2.40	135.290
	6-1	6.5%		40.05	44.15	2.55	41.30	43.20	2.70	160.795
	8-1	15.5%		68.55	66.50	1.75	52.20	58.00	3.70	250.655
2	4-2	0%		23.45	23.55	2.30	23.15	23.25	2.30	97.945
	5-2	1.5%		18.05	18.05	2.05	16.90	17.15	2.05	74.200
	6-2	6.5%		18.55	18.30	2.25	17.80	18.70	2.30	77.915
	8-2	15.5%		25.85	25.05	2.20	27.00	30.05	3.25	113.380
3	4-3	0%		4.05	4.15	0.50	4.05	4.10	0.45	17.335
	5-3	1.5%		11.00	11.00	1.15	10.70	10.80	1.15	45.780
	6-3	6.5%		104.90	105.05	1.60	100.60	100.65	1.80	414.580
	8-3	15.5%		355.35	355.95	5.80	309.65	311.10	9.90	1347.710
4	4-4	0%		2.80	2.80	0.30	2.80	2.80	0.30	11.730
	5-4	1.5%		12.10	12.15	0.70	11.80	11.90	0.70	49.305
	6-4	6.5%		98.10	98.25	1.30	94.00	94.05	1.40	387.030
	8-4	15.5%		268.55	271.60	3.90	234.35	235.00	7.35	1020.580

* Maximum thrust level bias error

** 3-Sigma Value for $\epsilon_{( ) ( ) 12}$

TABLE 2

COMPARISON OF RANDOM ERRORS
(Mean Propellant Flow Rate After 200,000 sec.)
All Propellant Flow Values in (Kg/sec) x 10^6

System	Run	Bias Error *	Random Error **	Engine 53	54	55	63	64	66	Total
1	2-1	0	1.5%	17.15	17.20	2.50	17.15	17.20	2.50	73.770
	4-1	0	5%	17.50	17.60	2.45	17.50	17.60	2.40	75.060
2	2-2	0	1.5%	20.80	20.85	2.40	20.15	20.25	2.40	86.775
	4-2	0	5%	23.45	23.55	2.30	23.15	23.25	2.30	97.945
3	2-3	0	1.5%	0.85	0.85	0.20	0.80	0.90	0.15	3.765
	4-3	0	5%	4.05	4.15	0.50	4.05	4.10	0.45	17.335
4	2-4	0	1.5%	1.15	1.25	0.35	1.20	1.20	0.35	5.470
	4-4	0	5%	2.80	2.80	0.30	2.80	2.80	0.30	11.730

2a.

System	Run	Bias Error *	Random Error **	Engine 53	54	55	63	64	66	Total
1	6-1	6.5%	5%	40.05	44.15	2.55	41.30	43.20	2.70	160.795
	7-1		15%	46.95	46.20	2.65	43.10	45.15	2.55	186.580
2	6-2		5%	18.55	18.30	2.25	17.80	18.70	2.30	77.915
	7-2		15%	20.15	19.90	2.75	19.45	20.35	2.65	85.240
3	6-3		5%	104.90	105.05	1.60	100.60	100.65	1.80	414.580
	7-3		15%	97.25	97.35	3.20	93.15	93.30	2.95	387.160
4	6-4		5%	98.10	98.25	1.30	94.00	94.05	1.40	387.030
	7-4		15%	94.45	94.60	2.90	90.45	90.50	2.70	375.535

2b.

* Maximum thrust level bias error

** 3-sigma value for $\epsilon_{(\,)\,(\,)\,12}$

TABLE 3

COMPARISON OF EXTERNAL TORQUES
(Pitch Axis Only)
(Mean Propellant Consumption After 300,000 sec.)
All Propellant Flow Values in (Kg/sec) x 10^6

System	Run	* Bias Error	** Random Error	External Torques	Engines 55	Engines 66	Total System
1	4-1	1.5%	5%	0	2.17	2.17	78.850
	11-1			Light	2.73	2.73	118.180
	12-1			Heavy	4.43	1.93	134.157
2	4-2			0	2.23	2.23	94.613
	11-2			Light	3.47	3.47	76.123
	12-2			Heavy	4.50	2.03	74.510
3	4-3			0	0.50	0.50	16.860
	11-3			Light	0.73	0.70	17.427
	12-3			Heavy	8.23	6.23	36.577
4	4-4			0	0.33	0.30	12.237
	11-4			Light	0.63	0.60	14.970
	12-4			Heavy	6.90	4.90	27.797

* Maximum thrust level bias error

** 3-Sigma Value for $\epsilon_{()\,()\,12}$

TABLE 4

COMPARISON OF SYSTEMS
FOR TWO ENGINES WITH LARGE BIASED THRUST ERRORS

(Mean propellant consumption after 200,000 sec,
all propellant flow values in (Kg/sec) x 10^6

% Biased Thrust Errors

Run 6	.02	.055	-.02	.065	-.025	.0
Run 10	.02	.165	-.06	.065	-.025	.0

System	Run	Engines 53	54	55	63	64	66	Total
1	6-1	40.05	39.40	2.95	36.75	38.55	3.05	160.795
	10-1	61.40	58.40	1.65	50.50	52.85	2.95	227.760
2	6-2	18.55	18.30	2.25	17.80	18.70	2.30	77.910
	10-2	27.30	25.90	2.65	23.15	24.20	3.15	105.688
3	6-3	104.90	105.05	1.60	100.60	100.65	1.80	414.580
	10-3	184.50	184.40	5.15	160.25	160.00	8.60	702.885
4	6-4	98.10	98.25	1.30	94.00	94.05	1.40	387.030
	10-4	183.10	183.10	3.75	159.00	158.75	7.25	694.875

TABLE 5

COMPARISON OF SYSTEMS

FOR TWO ENGINES WITH LARGE RANDOM IMPULSE ERRORS

(Mean propellant consumption after 200,000 sec - propellant flow values in (Kg/sec) x 10^6)

Run 6 - All engines have 3 Sigma of 5%

Run 9 - Engines 54 and 55 were increased to 3 Sigma of 15%

System	Run	Engine						Total
		53	54	55	63	64	66	
1	6-1	40.05	39.40	2.95	36.75	38.55	3.05	160.795
	9-1	44.90	44.15	2.55	41.30	43.20	2.70	178.795
2	6-2	18.55	18.30	2.25	17.80	18.70	2.30	77.910
	9-2	18.85	18.50	1.95	18.75	19.65	1.95	79.710
3	6-3	104.90	105.05	1.60	100.60	100.65	1.80	414.580
	9-3	103.80	103.95	2.00	99.50	99.65	2.15	411.020
4	6-4	98.10	98.25	1.30	94.00	94.05	1.40	387.030
	9-4	97.40	97.65	2.00	93.35	93.45	2.15	385.915

TABLE 6

COMPARISON OF BIASED ERRORS
(For 12-Unit Configuration)

(Mean Propellant Flow Rate After 200,000 sec.)
All Propellant Flow Values in (Kg/sec) x 10^6

System	Run	Bias Error *	Random Error **	Total System Propellant Flow Rate
1	100-1	0%	5%	*** 51.575
	101-1	1%		*** 75.834
	102-1	5%		*** 121.110
3	100-3	0		12.485
	101-3	1%		16.430
	102-3	5%		194.925
4	100-4	0		7.500
	101-4	1%		12.435
	102-4	5%		203.030

* Maximum thrust level bias error

** 3-Sigma Value for $\epsilon_{(\,)\,(\,)\,12}$

*** These propellant flow rates have not completely settled out to steady state values.

TABLE 7

ATTITUDE CONTROL PROGRAM
TABLE GROUP #2 - ENGINE FIRING TORQUE TABLES

Table Group No. (3)	
	2

Configuration (6 or 12) (4)	
	6

RANDOM ERRORS - NOMINAL
THRUST BIAS ERRORS - NOMINAL

Engine No.			K (max value of ϵ)		β			L	
6 Eng.	12 Eng.	Error	(2) 1	(14) 2	(26) 1	(38) 3	(50) 5	Mom Arm	(62)
53	13	1	.03	.01	.005	.01	-.005	1	17.2
		2	.05	.015	.005	.01	-.005	2	3.55
54	14	1	.03	.01	-.005	.015	.005	1	17.2
		2	.05	.015	-.005	.015	.005	2	3.55
55	15	1	.03	.01	.005	.005	-.01	1	17.2
		2	.05	.015	.005	.005	-.01	2	3.55
63	16	1	.03	.01	.005	.01	-.005	1	17.2
		2	.05	.015	.005	.01	-.005	2	3.55
64	23	1	.03	.01	-.005	-.015	.005	1	17.2
		2	.05	.015	-.005	-.015	.005	2	3.55
66	24	1	.03	.01	-.005	.005	.01	1	17.2
		2	.05	.015	-.005	.005	.01	2	3.55
	25	1						1	
		2						2	
	26	1						1	
		2						2	
	35	1						1	
		2						2	
	36	1						1	
		2						2	
	45	1						1	
		2						2	
	46	1						1	
		2						2	

J (KG-M^2)		
(2) Pitch	(14) Roll	(26) Yaw
4.905×10^6	1.668×10^5	4.905×10^6

TABLE 8

ATTITUDE CONTROL PROGRAM

TABLE GROUP #2 - ENGINE FIRING TORQUE TABLES

Table Group No. (3)	
	2

RANDOM ERRORS - NOMINAL

THRUST BIAS ERRORS - LARGE

Configuration (6 or 12) (1)	
	6

Engine No.			K (max value of ϵ)		β			L	
6 Eng.	12 Eng.	Error	(2) 1	(14) 2	(26) 1	(38) 3	(50) 5	Mom Arm	(62)
53	13	1	.03	.01	.01	.02	-.01	1	17.2
		2	.05	.015	.01	.04	-.01	2	3.55
54	14	1	.03	.01	-.01	.055	.01	1	17.2
		2	.05	.015	-.01	.11	.01	2	3.55
55	15	1	.03	.01	.01	-.01	-.02	1	17.2
		2	.05	.015	.01	-.01	-.04	2	3.55
63	16	1	.03	.01	.01	.065	-.01	1	17.2
		2	.05	.015	.01	.13	-.01	2	3.55
64	23	1	.03	.01	-.01	-.025	.01	1	17.2
		2	.05	.015	-.01	-.05	.01	2	3.55
66	24	1	.03	.01	-.01	.01	.0	1	17.2
		2	.05	.015	-.01	.01	.0	2	3.55
	25	1						1	
		2						2	
	26	1						1	
		2						2	
	35	1						1	
		2						2	
	36	1						1	
		2						2	
	45	1						1	
		2						2	
	46	1						1	
		2						2	

J ($KG-M^2$)		
(2) Pitch	(14) Roll	(26) Yaw
4.905×10^6	1.668×10^5	4.905×10^6

TABLE 9

ATTITUDE CONTROL PROGRAM

TABLE GROUP #2 - ENGINE FIRING TORQUE TABLES

Table Group No.	3
	2

RANDOM ERRORS - LARGE

THRUST BIAS ERRORS - VERY LARGE

Configuration (6 or 12)	2
	6

Engine No.			K (max value of ϵ)		β			L	
6 Eng.	12 Eng.	Error	2 1	14 2	26 1	38 3	50 5	Mom Arm	62
53	13	1	.10	.03	.03	.06	-.03	1	17.2
		2	.15	.045	.03	.12	-.03	2	3.55
54	14	1	.10	.03	-.03	.165	.03	1	17.2
		2	.15	.045	-.03	.33	.03	2	3.55
55	15	1	.10	.03	.03	-.03	.06	1	17.2
		2	.15	.045	.03	-.03	.12	2	3.55
63	16	1	.10	.03	.03	.195	-.03	1	17.2
		2	.15	.045	.03	.39	-.03	2	3.55
64	23	1	.10	.03	-.03	-.075	.03	1	17.2
		2	.15	.045	-.03	-.150	.03	2	3.55
66	24	1	.10	.03	-.03	.01	.0	1	17.2
		2	.15	.045	-.03	.01	.0	2	3.55
	25	1						1	
		2						2	
	26	1						1	
		2						2	
	35	1						1	
		2						2	
	36	1						1	
		2						2	
	45	1						1	
		2						2	
	46	1						1	
		2						2	

J ($KG\text{-}M^2$)		
2 Pitch	14 Roll	26 Yaw
4.905×10^6	1.668×10^5	4.905×10^6

TABLE 10

ATTITUDE CONTROL PROGRAM
TABLE GROUP #2 - ENGINE FIRING TORQUE TABLES

Table Group No. (3)	
	2

Configuration (6 or 12) (4)	
	6

RANDOM ERRORS - SMALL
THRUST BIAS ERRORS - ZERO

Engine No.			K (max value of ϵ)		β			L	
6 Eng.	12 Eng.	Error	(2) 1	(14) 2	(26) 1	(38) 3	(50) 5	Mom Arm	(62)
53	13	1	.01	.01	.005	.0	-.005	1	17.2
		2	.015	.015	.005	.0	-.005	2	3.55
54	14	1	.01	.01	-.005	.0	.005	1	17.2
		2	.015	.015	-.005	.0	.005	2	3.55
55	15	1	.01	.01	.005	.005	.0	1	17.2
		2	.015	.015	.005	.005	.0	2	3.55
63	16	1	.01	.01	.005	.0	-.005	1	17.2
		2	.015	.015	.005	.0	-.005	2	3.55
64	23	1	.01	.01	-.005	.0	.005	1	17.2
		2	.015	.015	-.005	.0	.005	2	3.55
66	24	1	.01	.01	-.005	.005	.0	1	17.2
		2	.015	.015	-.005	.005	.0	2	3.55
	25	1						1	
		2						2	
	26	1						1	
		2						2	
	35	1						1	
		2						2	
	36	1						1	
		2						2	
	45	1						1	
		2						2	
	46	1						1	
		2						2	

J ($KG-M^2$)		
(2) Pitch	(14) Roll	(26) Yaw
4.905×10^6	1.668×10^5	4.905×10^6

TABLE 11

LIMIT CYCLE OPERATIONAL PHILOSOPHY NO. 1
SIMPLE LIMIT CYCLE

Pulse No.	Firing Criteria	Magnitude of Commanded Pulse		Which Engine(s) Fired					
				Configuration 6			Configuration 12		
		Config. 6	Config. 12	Axis	+ Error	- Error	Axis	+ Error	- Error
1	$\lvert\theta\rvert \geq \Delta\theta$	I_o	I_o	Pitch	55	66	Pitch	16, 25	15, 26
				Roll	63, 54	64, 53	Roll	35, 46	36, 45
				Yaw	64, 54	63, 53	Yaw	13, 24	14, 23
2	Same philosophy as above			Pitch			Pitch		
				Roll			Roll		
				Yaw			Yaw		

TABLE 12

LIMIT CYCLE OPERATIONAL PHILOSOPHY NO. 12
"DIAMOND" LIMIT CYCLE

Pulse No.	Firing Criteria	Magnitude of Commanded Pulse: Config. 6	Magnitude of Commanded Pulse: Config. 12	Configuration 6: Axis	Configuration 6: + Error	Configuration 6: - Error	Configuration 12: Axis	Configuration 12: + Error	Configuration 12: - Error
1	$\lvert\lambda_1\rvert \geq \Delta\theta$	I_o	N.A.	Pitch	55	66	Pitch	Not Applicable to this configuration	
	See Below			Roll	See Below		Roll		
				Yaw			Yaw		
2	Same philosophy as above			Pitch			Pitch		
				Roll			Roll		
				Yaw			Yaw		

$$\lambda_1 = a_1 \theta_P + b_1 \dot{\theta}_P$$

$$\lambda_2 = a_2 \theta_R + b_2 \dot{\theta}_R$$

$$\lambda_3 = a_3 \theta_Y + b_3 \dot{\theta}_Y$$

For roll and yaw axes, firing occurs whenever

$$\lvert\lambda_2\rvert + \lvert\lambda_3\rvert \geq \Delta\theta,$$

in accordance with the table below

Sign Of λ_2	Sign Of λ_3	Engine Fired
+	+	54
+	-	63
-	-	53
-	+	64

TABLE 12 (continued)

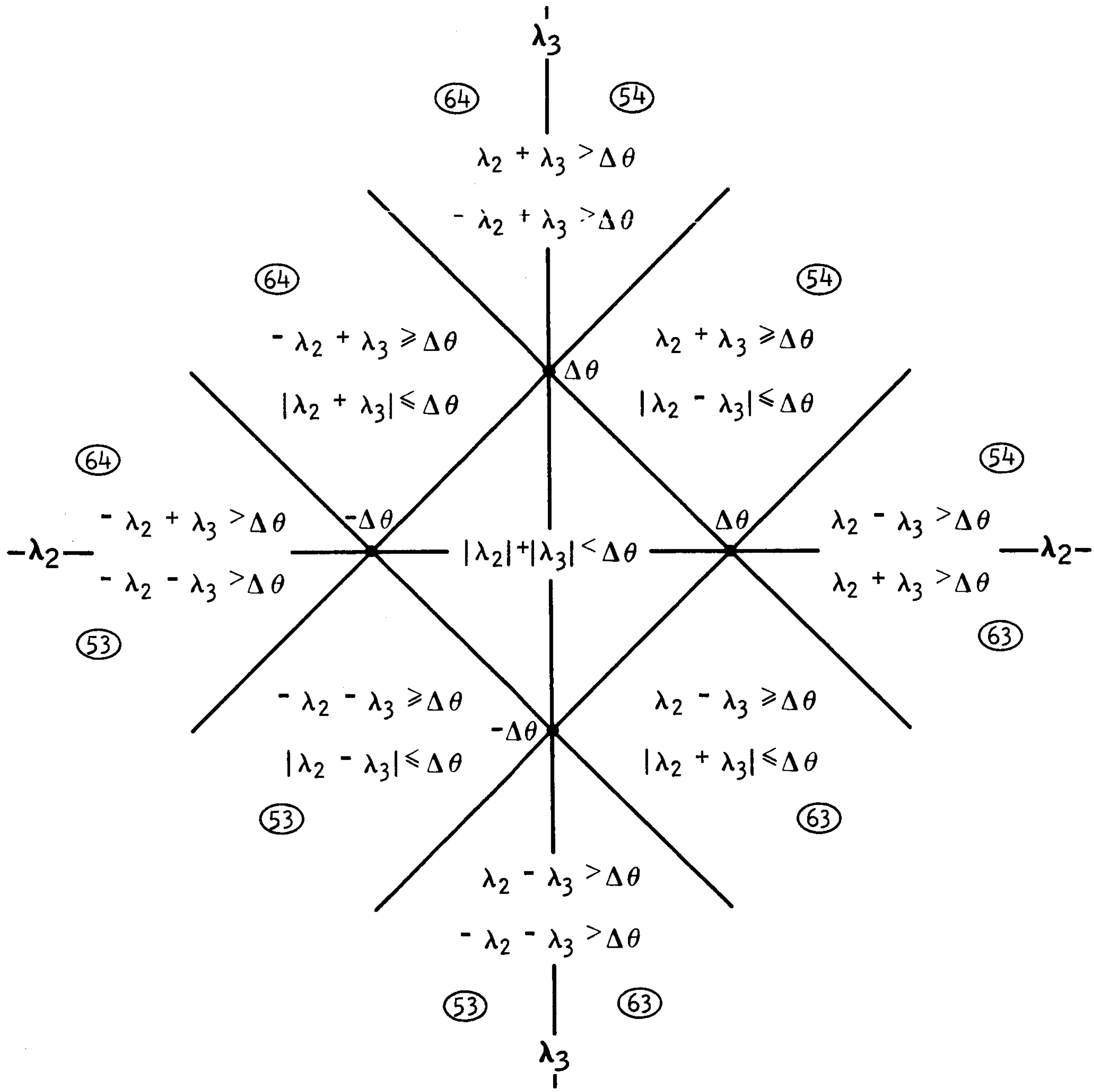

TABLE 12 (continued)

CONTROL PHILOSOPHY NO 2
("DIAMOND" ERROR DISPLAY)

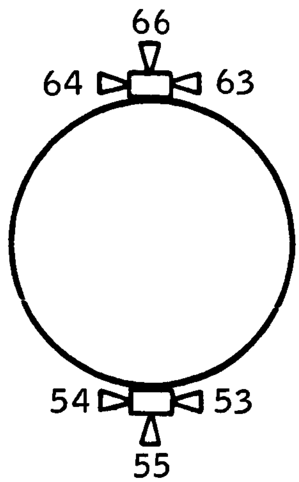

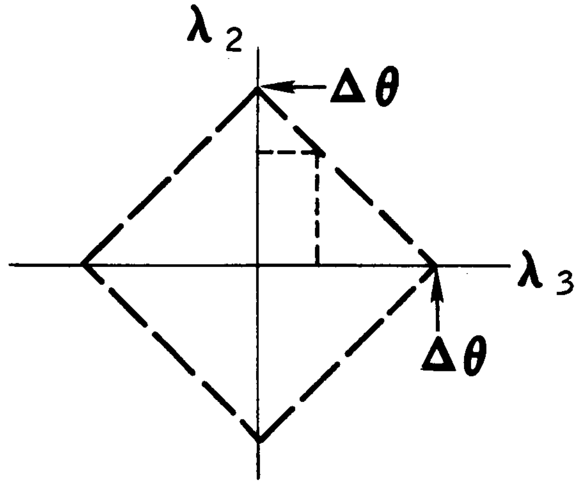

$|\lambda_2| + |\lambda_3| = \Delta\theta$ AT TIME OF FIRING

W_T = TOTAL PROPELLANT EXPENDED AT PULSE FIRING

W_R = PORTION OF W_T ASSIGNED TO ROLL AXIS

W_Y = PORTION OF W_T ASSIGNED TO YAW AXIS

$$W_R = \frac{|\lambda_2|}{\Delta\theta} W_T \; ; \quad W_Y = \frac{|\lambda_3|}{\Delta\theta} W_T$$

TABLE 13

LIMIT CYCLE OPERATIONAL PHILOSOPHY NO. 3
ADVANCED LIMIT CYCLE WITH POSITION
CUTOFF

Pulse No.	Firing Criteria	Magnitude of Commanded Pulse		Which Engine(s) Fired					
		Config. 6	Config. 12	Configuration 6			Configuration 12		
				Axis	+ Error	- Error	Axis	+ Error	- Error
1	$\lvert\theta\rvert \geq \Delta\theta$	$I_o + J_{11} \lvert\dot{\theta}\rvert / L_1$	$I_o + J_{12} \lvert\dot{\theta}\rvert / L_3$	Pitch	55	63	Pitch	16, 25	15, 26
		$I_o + J_{21} \lvert\theta\rvert / L_2$	$I_o + J_{22} \lvert\dot{\theta}\rvert / L_4$	Roll	63, 54	64, 53	Roll	35, 46	36, 45
		$I_o + J_{31} \lvert\theta\rvert / L_o$	$I_o + J_{32} \lvert\dot{\theta}\rvert / L_5$	Yaw	64, 54	63, 53	Yaw	13. 24	14, 23
2	See Note Below	I_o	I_o	Pitch	66	55	Pitch	15, 26	16, 25
				Roll	64, 53	63, 54	Roll	36, 45	35, 46
				Yaw	63, 53	64, 54	Yaw	14, 23	13, 24

J_1 = Moment of Inertia about Pitch Axis

J_2 = Moment of Inertia about Roll Axis

J_3 = Moment of Inertia about Yaw Axis

Note: The second pulse of the sequence is fired following a time delay of τ after the first pulse.

Axis	τ	
	Config. 6	Config. 12
Pitch	$\Delta\theta J_{11}/I_o L_1$	$\Delta\theta J_{12}/I_o L_3$
Roll	$\Delta\theta J_{21}/I_o L_2$	$\Delta\theta J_{22}/I_o L_4$
Yaw	$\Delta\theta J_{31}/I_o L_o$	$\Delta\theta J_{32}/I_o L_5$

TABLE 13 (continued)

Moment Arms

$L_o = 1/2\ (L_{153} + L_{154} + L_{163} + L_{164})$

$L_1 = 1/2\ (L_{155} + L_{166})$

$L_2 = 1/2\ (L_{253} + L_{254} + L_{263} + L_{264})$

$L_3 = 1/2\ (L_{315} + L_{316} + L_{325} + L_{326})$

$L_4 = 1/2\ (L_{435} + L_{436} + L_{445} + L_{446})$

$L_5 = 1/2\ (L_{313} + L_{314} + L_{323} + L_{324})$

These L_i appear in Control Philosophy No. 3 and No. 4.

Inside the program, the indexing of these paramenters is changed as follows:

L_o, $\bar{L}(3,1)$	L_3, $\bar{L}(1,2)$
L_1, $\bar{L}(1,1)$	L_4, $\bar{L}(2,2)$
L_2, $\bar{L}(2,1)$	L_5, $\bar{L}(3,2)$

TABLE 14

LIMIT CYCLE OPERATIONAL PHILOSOPHY NO. 4
ADVANCED LIMIT CYCLE WITH RATE CUTOFF

Pulse No.	Firing Criteria	Magnitude of Commanded Pulse		Which Engine(s) Fired					
				Configuration 6			Configuration 12		
		Config. 6	Config. 12	Axis	+ Error	- Error	Axis	+ Error	- Error
1	$\lvert\lambda_1\rvert \geq \Delta\theta$	$I_o + J_{11} \lvert\dot{\theta}\rvert / L_1$	$I_o + J_{12} \lvert\dot{\theta}\rvert / L_3$	Pitch	55	66	Pitch	16, 25	15, 26
	$\lvert\lambda_2\rvert \geq \Delta\theta$	$I_o + J_{21} \lvert\dot{\theta}\rvert / L_2$	$I_o + J_{22} \lvert\dot{\theta}\rvert / L_4$	Roll	63, 54	64, 53	Roll	35, 46	36, 45
	$\lvert\lambda_3\rvert \geq \Delta\theta$	$I_o + J_{31} \lvert\dot{\theta}\rvert / L_o$	$I_o + J_{32} \lvert\dot{\theta}\rvert / L_5$	Yaw	64, 54	63, 53	Yaw	13, 24	14, 23
2	$\theta = 0$	$J_{11} \lvert\dot{\theta}\rvert / L_1$	$J_{12} \lvert\dot{\theta}\rvert / L_3$	Pitch	66	55	Pitch	15, 26	16, 25
		$J_{21} \lvert\dot{\theta}\rvert / L_2$	$J_{22} \lvert\dot{\theta}\rvert / L_4$	Roll	64, 53	63, 54	Roll	36, 45	35, 46
		$J_{31} \lvert\dot{\theta}\rvert / L_o$	$J_{32} \lvert\dot{\theta}\rvert / L_5$	Yaw	63, 53	64, 54	Yaw	14, 23	13, 24

$\lambda_1 = a_1 \theta_P + b_1 \theta_P$ $\qquad J_1$ = Moment of Inertia about Pitch Axis

$\lambda_2 = a_2 \theta_R + b_2 \theta_R$ $\qquad J_2$ = Moment of Inertia about Roll Axis

$\lambda_3 = a_3 \theta_Y + b_3 \theta_Y$ $\qquad J_3$ = Moment of Inertia about Yaw Axis

TABLE 15

TOTAL IMPULSE DELIVERED AT EACH ENGINE FIRING

ENGINE FIRED	IMPULSE EXPENDED
13	$I_T (1 + \epsilon_{1311} + \beta_{1331}) + I_o (\epsilon_{1312} + \beta_{1332})$
14	$I_T (1 + \epsilon_{1411} + \beta_{1441}) + I_o (\epsilon_{1412} + \beta_{1442})$
15	$I_T (1 + \epsilon_{1511} + \beta_{1551}) + I_o (\epsilon_{1512} + \beta_{1552})$
16	$I_T (1 + \epsilon_{1611} + \beta_{1661}) + I_o (\epsilon_{1612} + \beta_{1662})$
23	$I_T (1 + \epsilon_{2311} + \beta_{2331}) + I_o (\epsilon_{2312} + \beta_{2332})$
24	$I_T (1 + \epsilon_{2411} + \beta_{2441}) + I_o (\epsilon_{2412} + \beta_{2442})$
25	$I_T (1 + \epsilon_{2511} + \beta_{2551}) + I_o (\epsilon_{2512} + \beta_{2552})$
26	$I_T (1 + \epsilon_{2611} + \beta_{2661}) + I_o (\epsilon_{2612} + \beta_{2662})$
35	$I_T (1 + \epsilon_{3511} + \beta_{3551}) + I_o (\epsilon_{3512} + \beta_{3552})$
36	$I_T (1 + \epsilon_{3611} + \beta_{3661}) + I_o (\epsilon_{3612} + \beta_{3662})$
45	$I_T (1 + \epsilon_{4511} + \beta_{4551}) + I_o (\epsilon_{4512} + \beta_{4552})$
46	$I_T (1 + \epsilon_{4611} + \beta_{4661}) + I_o (\epsilon_{4612} + \beta_{4662})$
53	$I_T (1 + \epsilon_{5311} + \beta_{5331}) + I_o (\epsilon_{5312} + \beta_{5332})$
54	$I_T (1 + \epsilon_{5411} + \beta_{5441}) + I_o (\epsilon_{5412} + \beta_{5442})$
55	$I_T (1 + \epsilon_{5511} + \beta_{5551}) + I_o (\epsilon_{5512} + \beta_{5552})$
63	$I_T (1 + \epsilon_{6311} + \beta_{6331}) + I_o (\epsilon_{6312} + \beta_{6332})$
64	$I_T (1 + \epsilon_{6411} + \beta_{6441}) + I_o (\epsilon_{6412} + \beta_{6442})$
66	$I_T (1 + \epsilon_{6611} + \beta_{6661}) + I_o (\epsilon_{6612} + \beta_{6662})$

TABLE 16

Engine Fired	Axis Affected	Change in $\dot{\theta}$
53	Pitch	$-L_{153}/J_{11}\,[I_T(\epsilon_{5321}+\beta_{5351})+I_o(\epsilon_{5322}+\beta_{5352})]-L_{253}/J_{11}\,[I_T(\epsilon_{\underline{5321}}+\beta_{5311})+I_o(\epsilon_{\underline{5322}}+\beta_{5312})]$
	Roll	$L_{253}/J_{21}\,[I_T(1+\epsilon_{5311}+\beta_{5331})+I_o(\epsilon_{5312}+\beta_{5332})]$
	Yaw	$L_{153}/J_{31}\,[I_T(1+\epsilon_{5311}+\beta_{5331})+I_o(\epsilon_{5312}+\beta_{5332})]$
54	Pitch	$-L_{154}/J_{11}\,[I_T(\epsilon_{5421}+\beta_{5451})+I_o(\epsilon_{5422}+\beta_{5452})]-L_{254}/J_{11}\,[I_T(\epsilon_{\underline{5421}}+\beta_{5411})+I_o(\epsilon_{\underline{5422}}+\beta_{5412})]$
	Roll	$-L_{254}/J_{21}\,[I_T(1+\epsilon_{5411}+\beta_{5441})+I_o(\epsilon_{5412}+\beta_{5442})]$
	Yaw	$-L_{154}/J_{31}\,[I_T(1+\epsilon_{5411}+\beta_{5441})+I_o(\epsilon_{5412}+\beta_{5442})]$
55	Pitch	$-L_{155}/J_{11}\,[I_T(1+\epsilon_{5511}+\beta_{5551})+I_o(\epsilon_{5512}+\beta_{5552})]-L_{253}/J_{11}\,[I_T(\epsilon_{\underline{5521}}+\beta_{5511})+I_o(\epsilon_{\underline{5522}}+\beta_{5512})]$
	Roll	$L_{255}/J_{21}\,[I_T(\epsilon_{5521}+\beta_{5531})+I_o(\epsilon_{5522}+\beta_{5532})]$
	Yaw	$L_{155}/J_{31}\,[I_T(\epsilon_{5521}+\beta_{5531})+I_o(\epsilon_{5522}+\beta_{5532})]$
63	Pitch	$-L_{163}/J_{11}\,[I_T(\epsilon_{6321}+\beta_{6351})+I_o(\epsilon_{6322}+\beta_{6352})]+L_{263}/J_{11}\,[I_T(\epsilon_{\underline{6321}}+\beta_{6311})+I_o(\epsilon_{\underline{6322}}+\beta_{6312})]$
	Roll	$-L_{263}/J_{21}\,[I_T(1+\epsilon_{6311}+\beta_{6331})+I_o(\epsilon_{6312}+\beta_{6332})]$
	Yaw	$L_{163}/J_{31}\,[I_T(1+\epsilon_{6311}+\beta_{6331})+I_o(\epsilon_{6312}+\beta_{6332})]$
64	Pitch	$-L_{164}/J_{11}\,[I_T(\epsilon_{6421}+\beta_{6451})+I_o(\epsilon_{6422}+\beta_{6452})]+L_{264}/J_{11}\,[I_T(\epsilon_{\underline{6421}}+\beta_{6411})+I_o(\epsilon_{\underline{6422}}+\beta_{6412})]$
	Roll	$L_{264}/J_{21}\,[I_T(1+\epsilon_{6411}+\beta_{6441})+I_o(\epsilon_{6412}+\beta_{6442})]$
	Yaw	$-L_{164}/J_{31}\,[I_T(1+\epsilon_{6411}+\beta_{6441})+I_o(\epsilon_{6412}+\beta_{6442})]$
66	Pitch	$L_{166}/J_{11}\,[I_T(1+\epsilon_{6611}+\beta_{6661})+I_o(\epsilon_{6612}+\beta_{6662})]+L_{266}/J_{11}\,[I_T(\epsilon_{\underline{6621}}+\beta_{6611})+I_o(\epsilon_{\underline{6622}}+\beta_{6612})]$
	Roll	$-L_{266}/J_{21}\,[I_T(\epsilon_{6621}+\beta_{6631})+I_o(\epsilon_{6622}+\beta_{6632})]$
	Yaw	$L_{166}/J_{31}\,[I_T(\epsilon_{6621}+\beta_{6631})+I_o(\epsilon_{6622}+\beta_{6632})]$

After the values of the ϵ's for any given box have been used, they are not retained for future calculations.
Underlined ϵ's are different in numerical value from non-underlined ϵ's, even though they bear the same subscripts.

TABLE 17

Engine Fired	Axis Affected	Change in $\dot{\theta}$
	Pitch	$L_{313}/J_{12}\,[I_T(\epsilon_{1321} + \beta_{1351}) + I_o(\epsilon_{1322} + \beta_{1352})]$
13	Roll	0
	Yaw	$-L_{313}/J_{32}\,[I_T(1 + \epsilon_{1311} + \beta_{1331}) + I_o(\epsilon_{1312} + \beta_{1332})]$
	Pitch	$L_{314}/J_{12}\,[I_T(\epsilon_{1421} + \beta_{1451}) + I_o(\epsilon_{1422} + \beta_{1452})]$
14	Roll	0
	Yaw	$L_{314}/J_{32}\,[I_T(1 + \epsilon_{1411} + \beta_{1441}) + I_o(\epsilon_{1412} + \beta_{1442})]$
	Pitch	$L_{315}/J_{12}\,[I_T(1 + \epsilon_{1511} + \beta_{1551}) + I_o(\epsilon_{1512} + \beta_{1552})]$
15	Roll	0
	Yaw	$-L_{315}/J_{32}\,[I_T(\epsilon_{1521} + \beta_{1531}) + I_o(\epsilon_{1522} + \beta_{1532})]$
	Pitch	$-L_{316}/J_{12}\,[I_T(1 + \epsilon_{1611} + \beta_{1661}) + I_o(\epsilon_{1612} + \beta_{1662})]$
16	Roll	0
	Yaw	$-L_{316}/J_{32}\,[I_T(\epsilon_{1621} + \beta_{1631}) + I_o(\epsilon_{1622} + \beta_{1632})]$
	Pitch	$-L_{323}/J_{12}\,[I_T(\epsilon_{2321} + \beta_{2351}) + I_o(\epsilon_{2322} + \beta_{2352})]$
23	Roll	0
	Yaw	$L_{323}/J_{32}\,[I_T(1 + \epsilon_{2311} + \beta_{2331}) + I_o(\epsilon_{2312} + \beta_{2352})]$
	Pitch	$-L_{324}/J_{12}\,[I_T(\epsilon_{2421} + \beta_{2451}) + I_o(\epsilon_{2422} + \beta_{2452})]$
24	Roll	0
	Yaw	$-L_{324}/J_{32}\,[I_T(1 + \epsilon_{2411} + \beta_{2441}) + I_o(\epsilon_{2412} + \beta_{2442})]$

TABLE 17 (continued)

Engine Fired	Axis Affected	Change in $\dot{\theta}$
	Pitch	$-L_{325}/J_{12}\ [I_T\ (1 + \epsilon_{2511} + \beta_{2551}) + I_o\ (\epsilon_{2512} + \beta_{2552})$
25	Roll	0
	Yaw	$L_{325}/J_{32}\ [I_T\ (\epsilon_{2521} + \beta_{2531}) + I_o\ (\epsilon_{2522} + \beta_{2532})]$
	Pitch	$L_{326}/J_{12}\ [I_T\ (1 + \epsilon_{2611} + \beta_{2661}) + I_o\ (\epsilon_{2612} + \beta_{2662})]$
26	Roll	0
	Yaw	$L_{326}/J_{32}\ [I_T\ (\epsilon_{2621} + \beta_{2631}) + I_o\ (\epsilon_{2622} + \beta_{2632})]$
	Pitch	0
35	Roll	$-L_{435}/J_{22}\ [I_T\ (1 + \epsilon_{3511} + \beta_{3551}) + I_o\ (\epsilon_{3512} + \beta_{3552})]$
	Yaw	$L_{435}/J_{32}\ [I_T\ (\epsilon_{3521} + \beta_{3511}) + I_o\ (\epsilon_{3522} + \beta_{3512})]$
	Pitch	0
36	Roll	$L_{435}/J_{22}\ [I_T\ (1 + \epsilon_{3611} + \beta_{3661}) + I_o\ (\epsilon_{3612} + \beta_{3662})]$
	Yaw	$L_{435}/J_{32}\ [I_T\ (\epsilon_{3621} + \beta_{3611}) + I_o\ (\epsilon_{3622} + \beta_{3612})]$
	Pitch	0
45	Roll	$L_{445}/J_{22}\ [I_T\ (1 + \epsilon_{4511} + \beta_{4551}) + I_o\ (\epsilon_{4512} + \beta_{4552})]$
	Yaw	$-L_{445}/J_{32}\ [I_T\ (\epsilon_{4521} + \beta_{4511}) + I_o\ (\epsilon_{4522} + \beta_{4512})]$
	Pitch	0
46	Roll	$-L_{446}/J_{22}\ [I_T\ (1 + \epsilon_{4611} + \beta_{4661}) + I_o\ (\epsilon_{4612} + \beta_{4662})]$
	Yaw	$-L_{446}/J_{32}\ [I_T\ (\epsilon_{4621} + \beta_{4611}) + I_o\ (\epsilon_{4622} + \beta_{4612})]$

ADVANCED LIMIT CYCLE STUDY

SAMPLE- HOLD CIRCUIT FOR OBTAINING RANDOM ERRORS

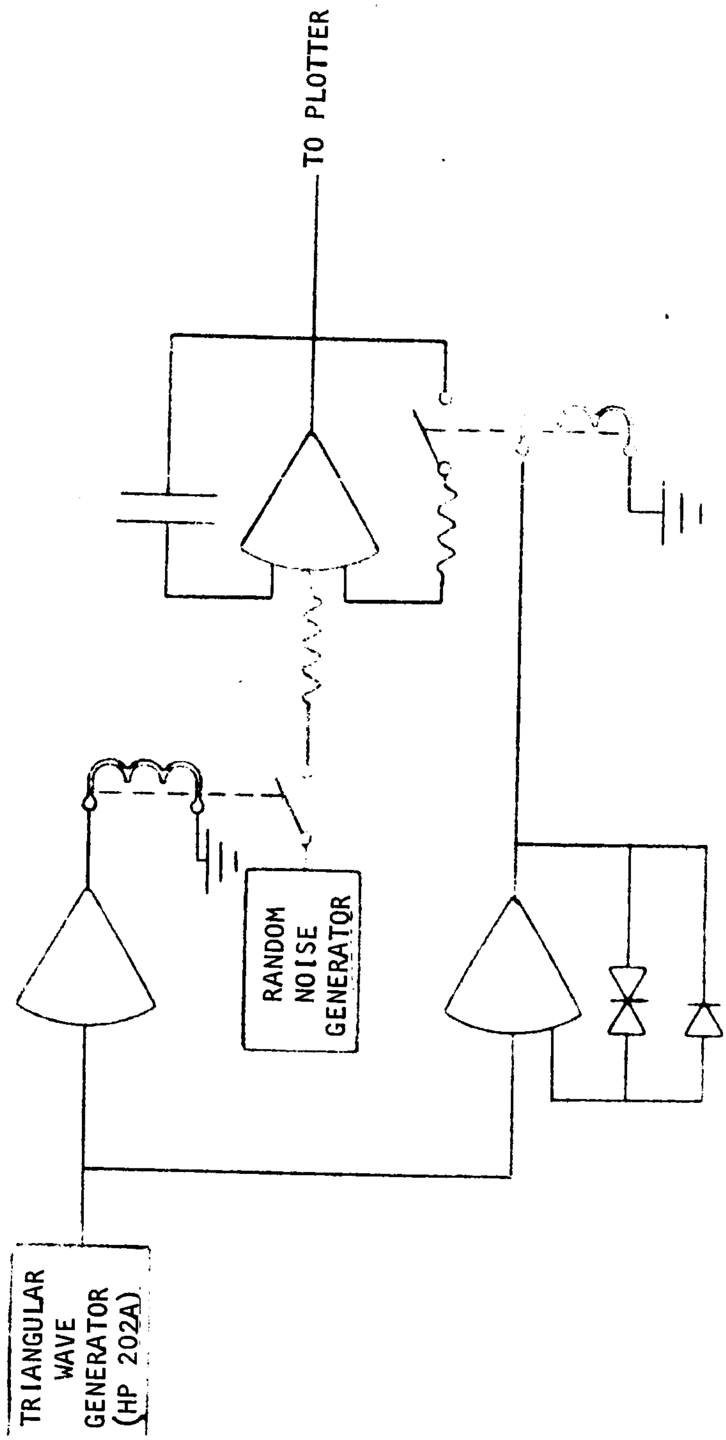

Figure 1

THRUST AND ATTITUDE ANGLE SIMULATION

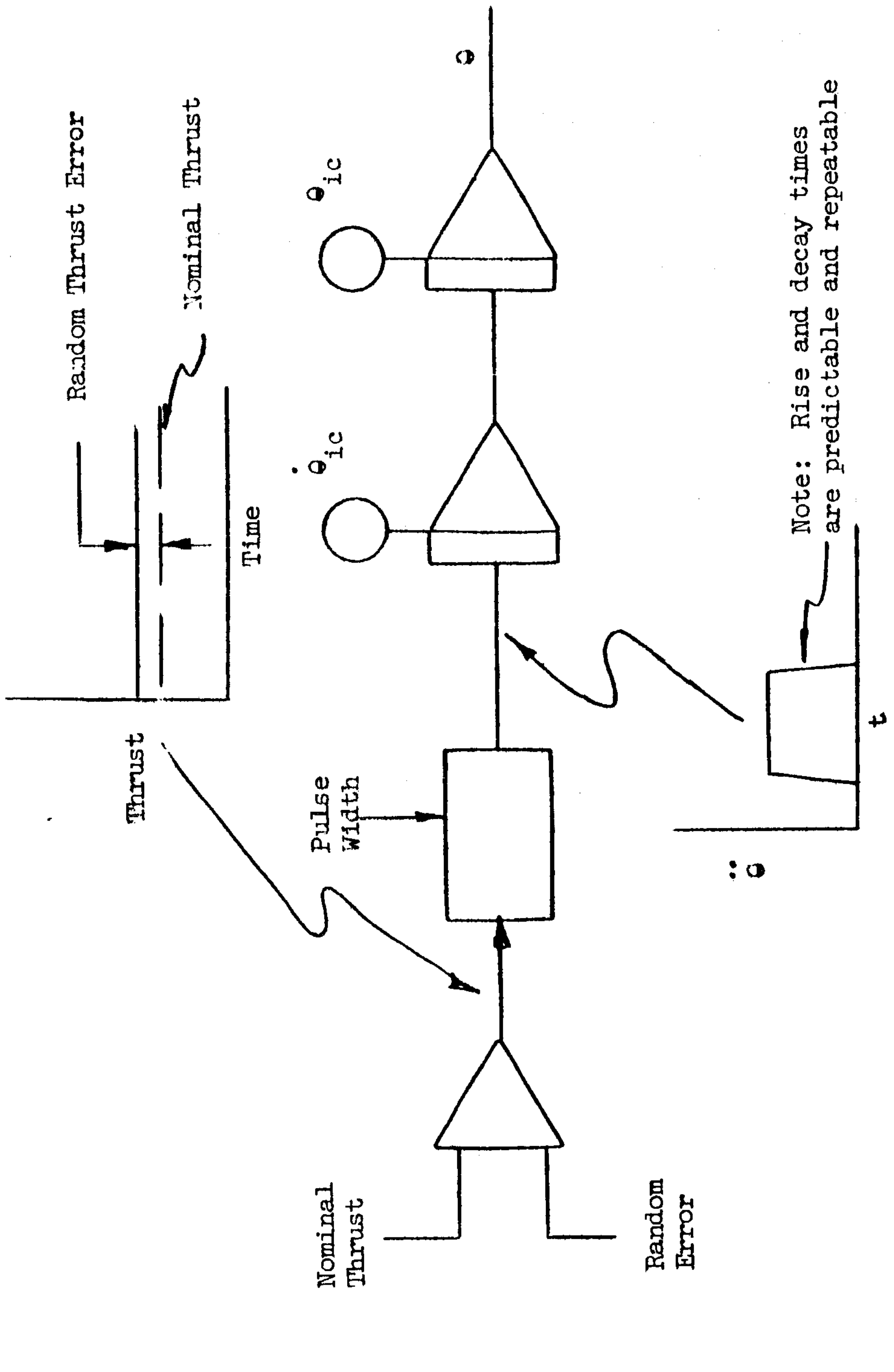

Figure 2

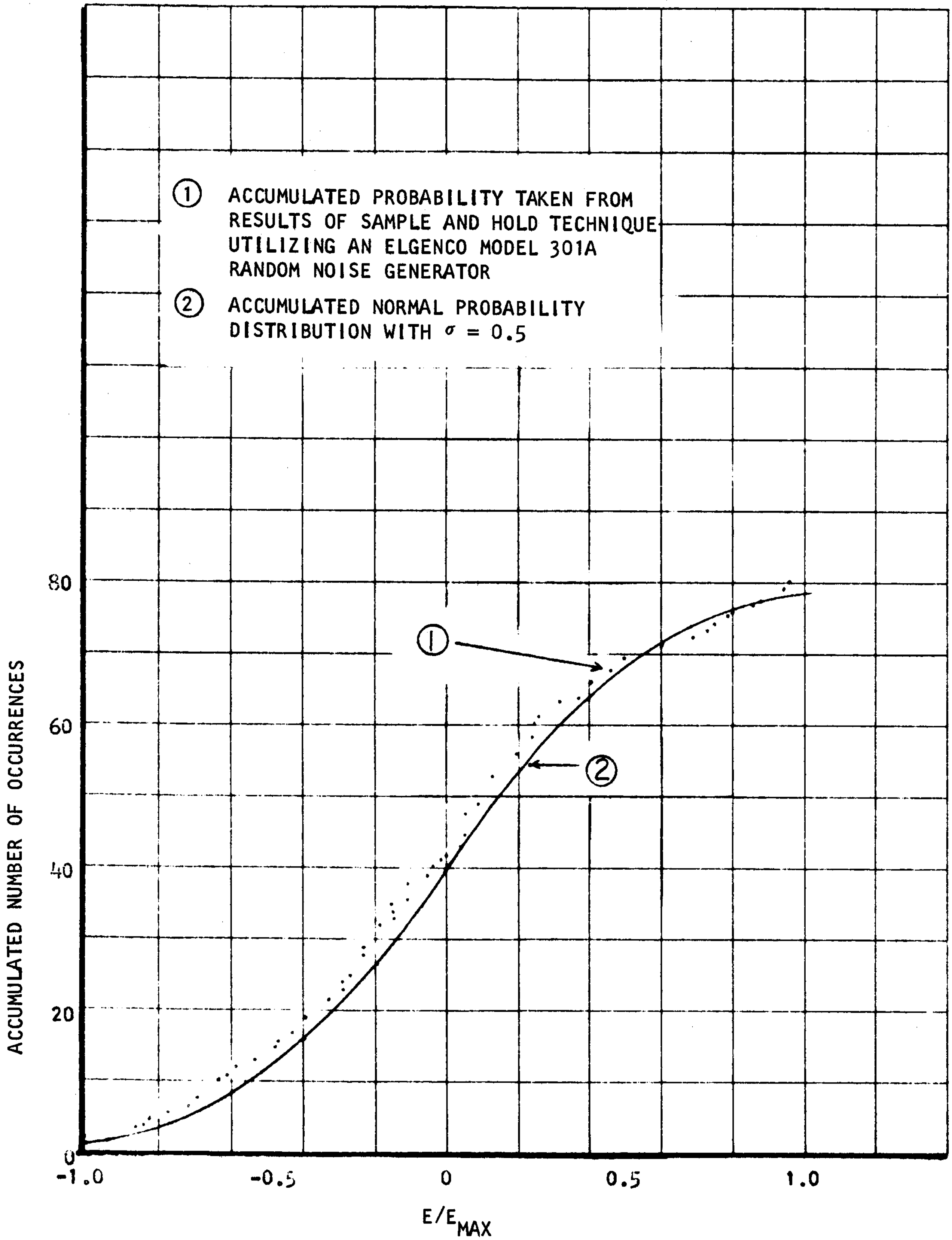
① ACCUMULATED PROBABILITY TAKEN FROM RESULTS OF SAMPLE AND HOLD TECHNIQUE UTILIZING AN ELGENCO MODEL 301A RANDOM NOISE GENERATOR
② ACCUMULATED NORMAL PROBABILITY DISTRIBUTION WITH σ = 0.5
ACCUMULATED NUMBER OF OCCURRENCES
0
20
40
60
80
①
②
-1.0
-0.5
0
0.5
1.0
E/E_MAX

Figure 3

ADVANCED LIMIT CYCLE STUDY

DRIFT VOLTAGES VS TIME FOR SELECTED INTEGRATORS

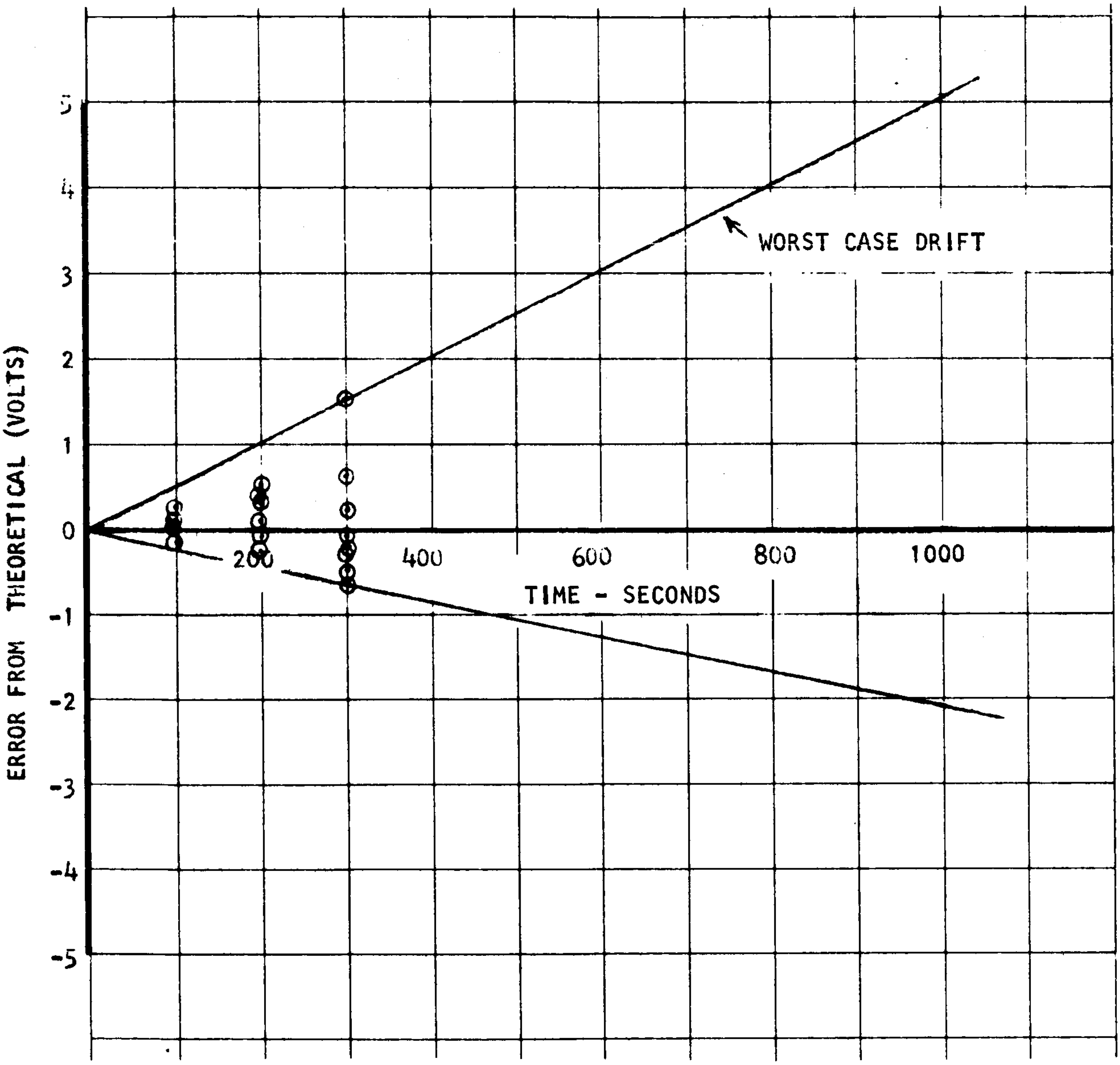

Figure 4

ENGINE PULSE FIRING DISTRIBUTION

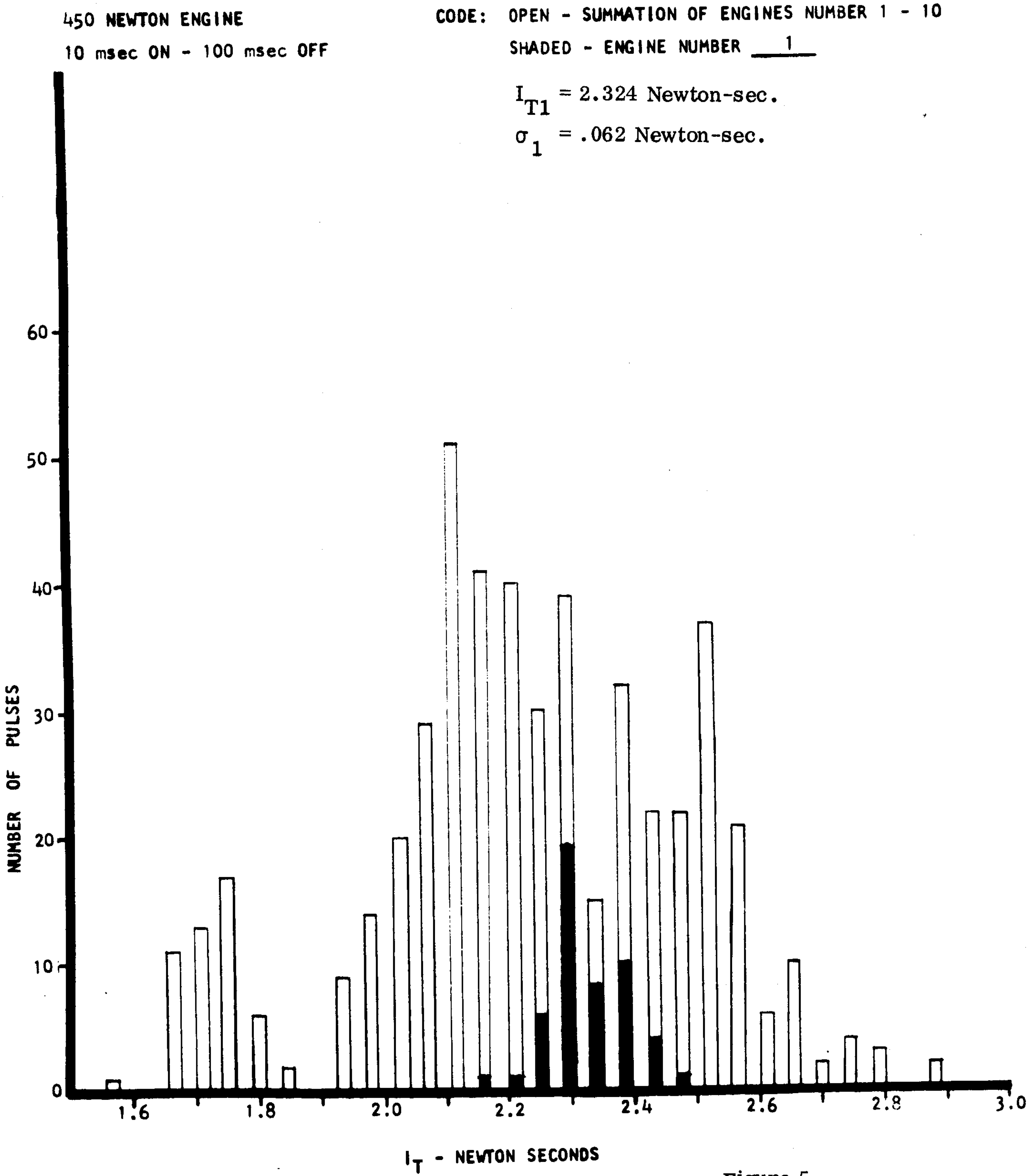

Figure 5

ENGINE PULSE FIRING DISTRIBUTION

450 NEWTON ENGINE

10 msec ON - 100 msec OFF

CODE: OPEN - SUMMATION OF ENGINES NUMBER 1 - 10

SHADED - ENGINE NUMBER 2

I_{T2} = 2.534 Newton-sec.

σ_2 = .123 Newton-sec.

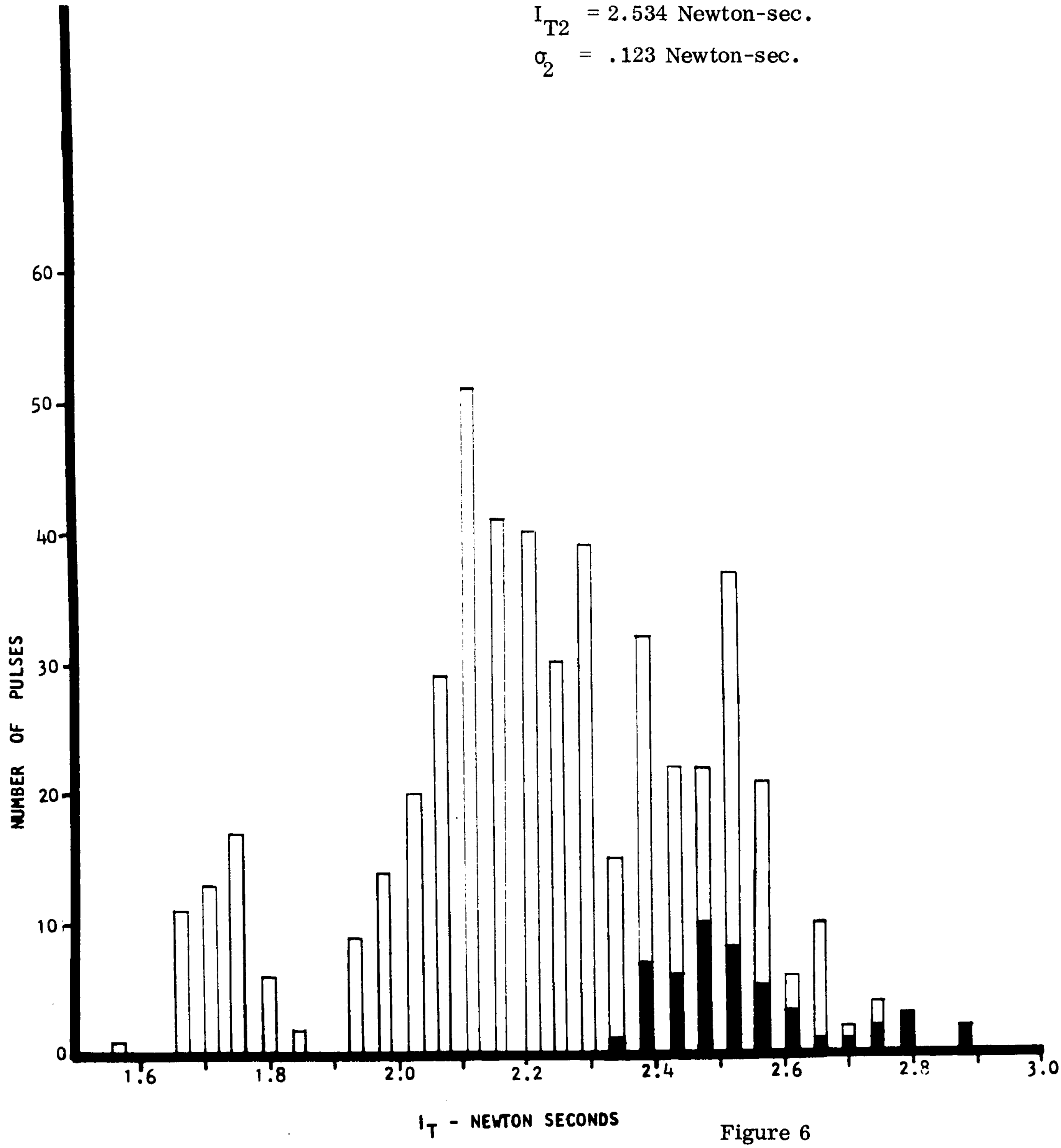

Figure 6

ENGINE PULSE FIRING DISTRIBUTION

450 NEWTON ENGINE

10 msec ON - 100 msec OFF

CODE: OPEN - SUMMATION OF ENGINES NUMBER 1 - 10

SHADED - ENGINE NUMBER 3

I_{T3} = 1.729 Newton-sec.

σ_3 = .053 Newton-sec.

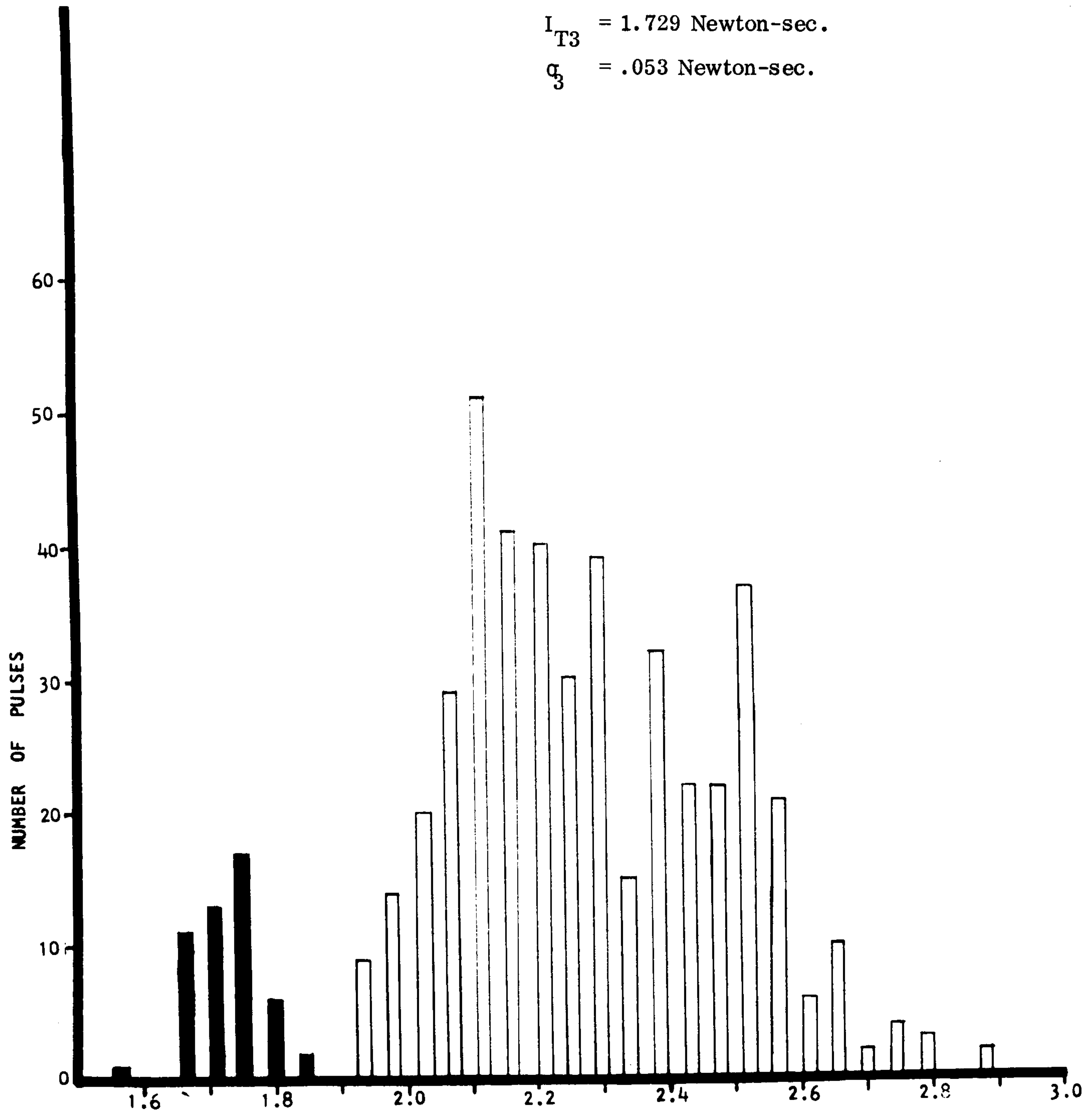

Figure 7

ENGINE PULSE FIRING DISTRIBUTION

450 NEWTON ENGINE

10 msec ON - 100 msec OFF

CODE: OPEN - SUMMATION OF ENGINES NUMBER 1 - 10

SHADED - ENGINE NUMBER 4

I_{T4} = 2.155 Newton-sec.

σ_4 = .090 Newton-sec.

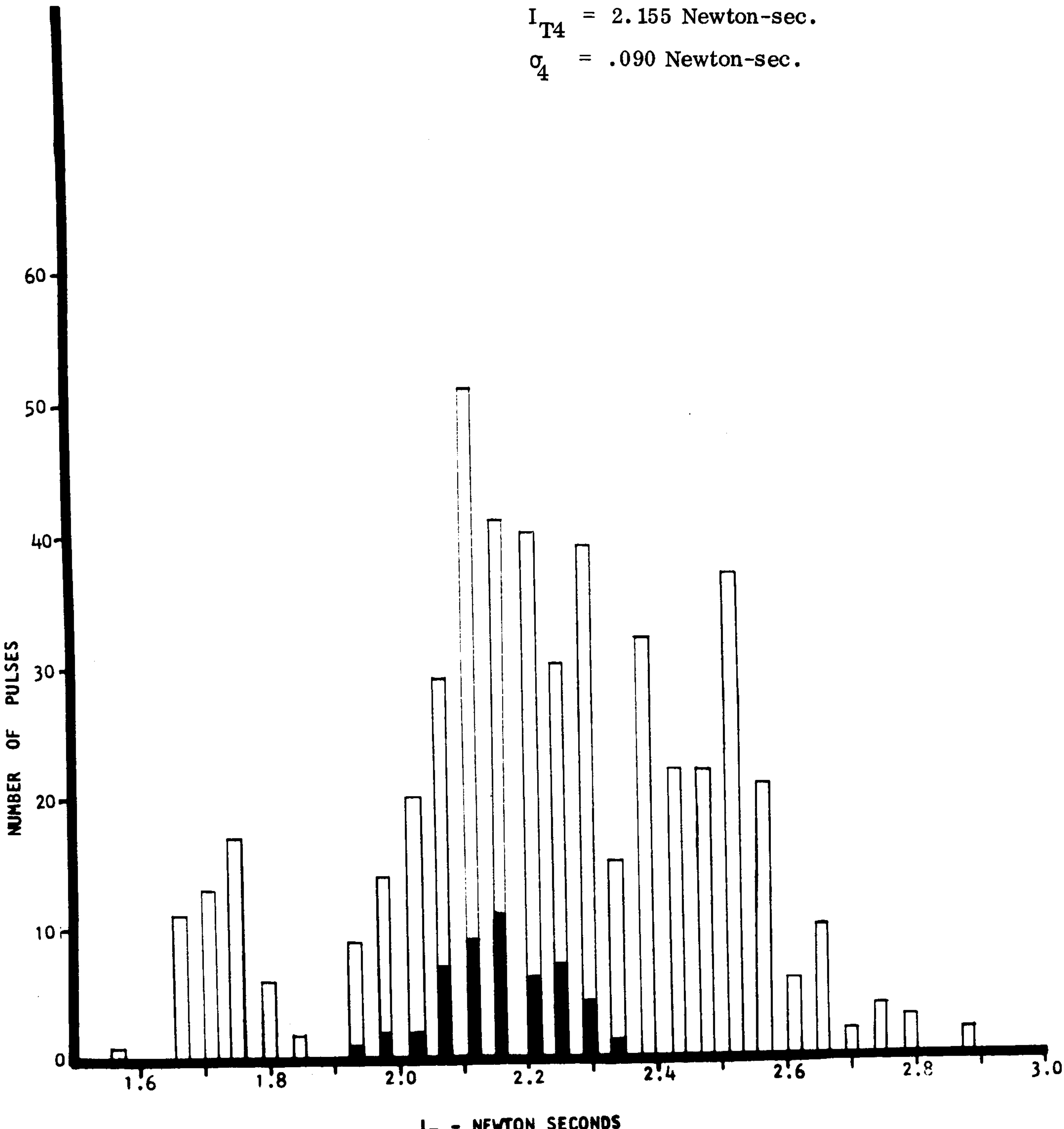

Figure 8

ENGINE PULSE FIRING DISTRIBUTION

450 NEWTON ENGINE
10 msec ON - 100 msec OFF

CODE: OPEN - SUMMATION OF ENGINES NUMBER 1 - 10
SHADED - ENGINE NUMBER 5
I_{T5} = 2.521 Newton-sec.
σ_5 = .090 Newton-sec.

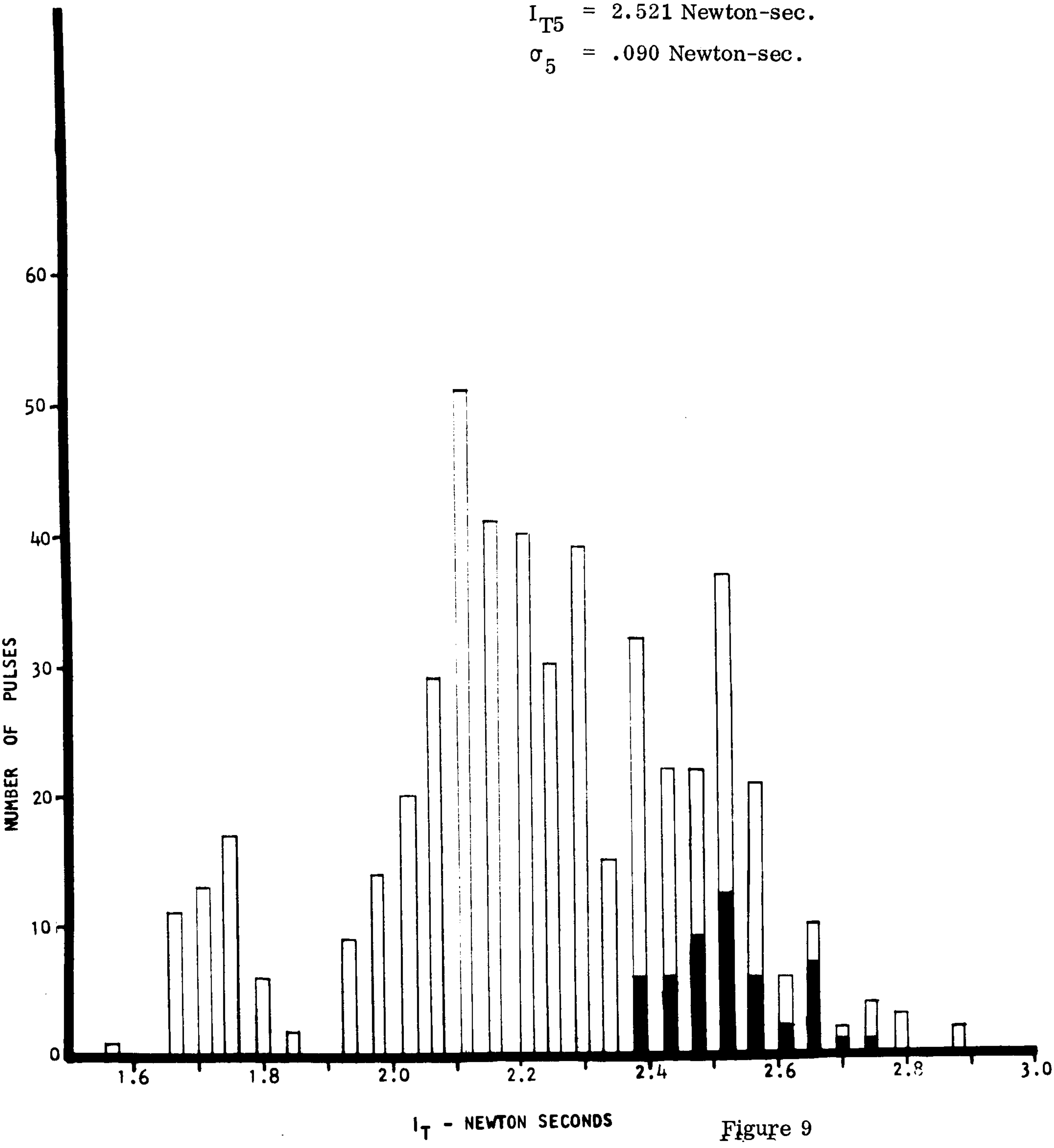

Figure 9

ENGINE PULSE FIRING DISTRIBUTION

450 NEWTON ENGINE

10 msec ON - 100 msec OFF

CODE: OPEN - SUMMATION OF ENGINES NUMBER 1 - 10

SHADED - ENGINE NUMBER 6

I_{T6} = 2.137 Newton-sec.

σ_6 = .092 Newton-sec.

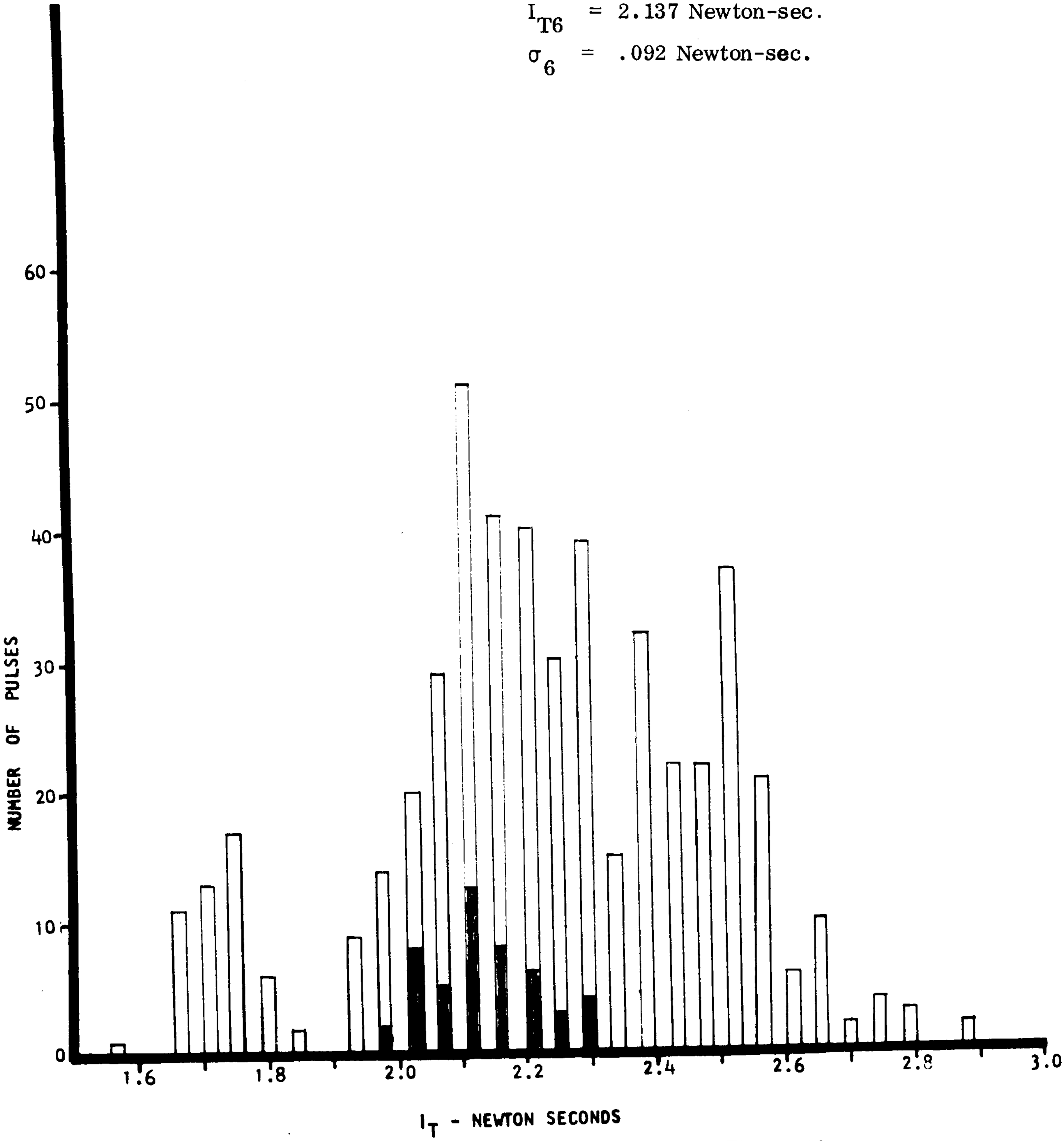

Figure 10

ENGINE PULSE FIRING DISTRIBUTION

450 NEWTON ENGINE
10 msec ON - 100 msec OFF

CODE: OPEN - SUMMATION OF ENGINES NUMBER 1 - 10
SHADED - ENGINE NUMBER 7

I_{T7} = 2.037 Newton-sec.

σ_7 = .069 Newton-sec.

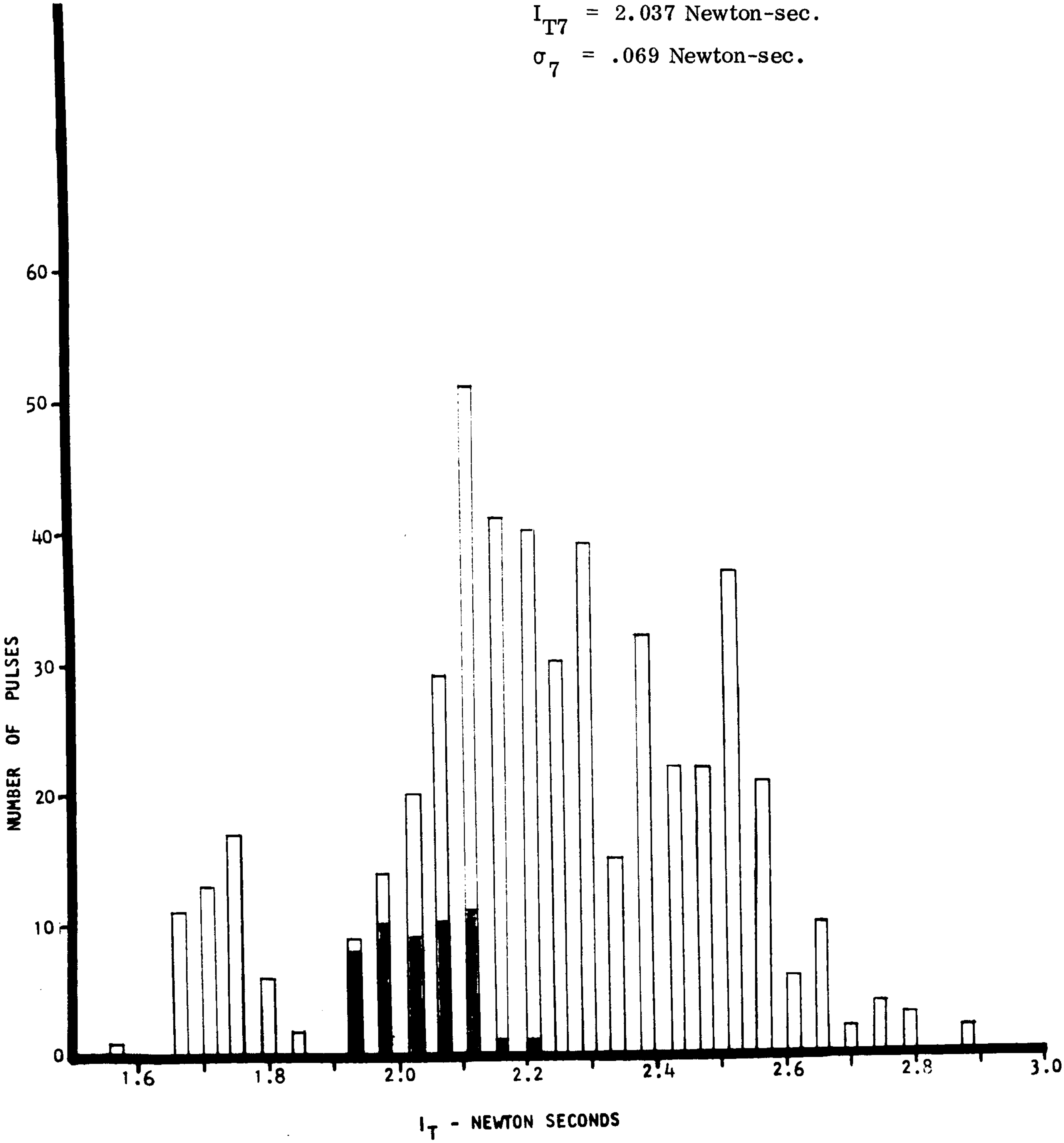

Figure 11

ENGINE PULSE FIRING DISTRIBUTION

450 NEWTON ENGINE

10 msec ON - 100 msec OFF

CODE: OPEN - SUMMATION OF ENGINES NUMBER 1 - 10

SHADED - ENGINE NUMBER 8

I_{T8} = 2.228 Newton-sec.

σ_8 = .071 Newton-sec.

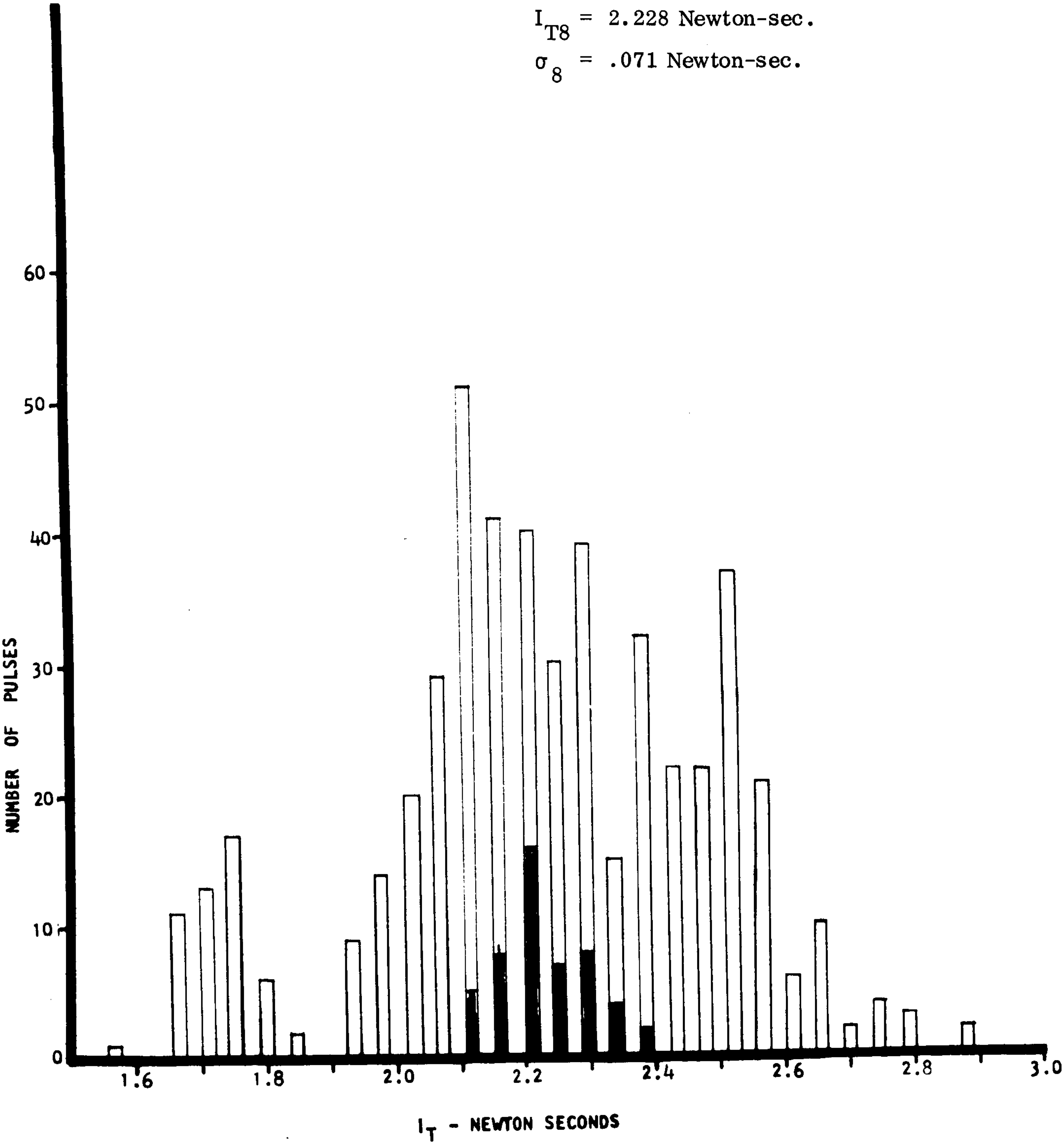

Figure 12

ENGINE PULSE FIRING DISTRIBUTION

450 NEWTON ENGINE

10 msec ON - 100 msec OFF

CODE: OPEN - SUMMATION OF ENGINES NUMBER 1 - 10

SHADED - ENGINE NUMBER 9

I_{T9} = 2.162 Newton-sec.

σ_9 = .075 Newton-sec.

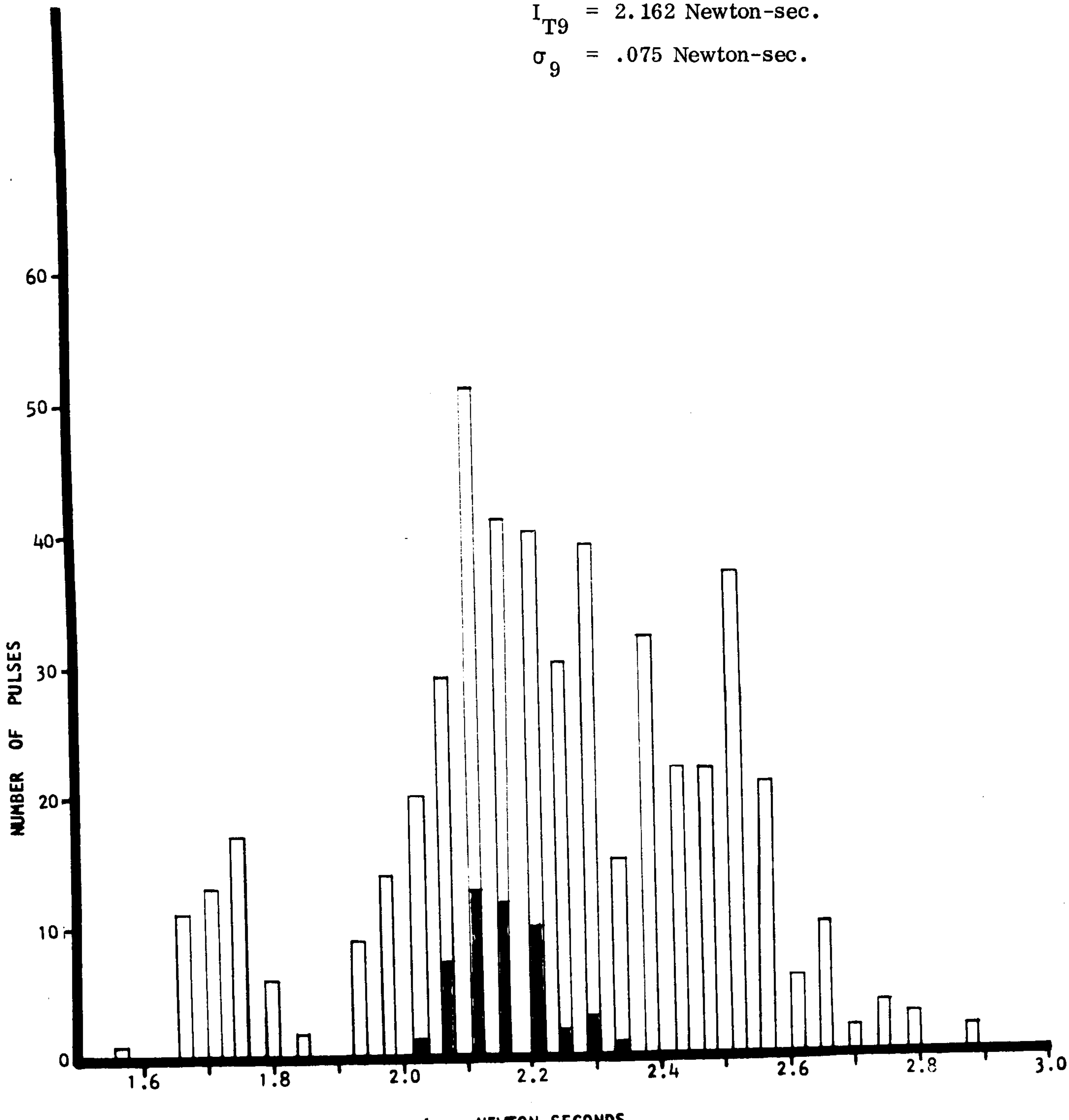

Figure 13

ENGINE PULSE FIRING DISTRIBUTION

450 NEWTON ENGINE

10 msec ON - 100 msec OFF

CODE: OPEN - SUMMATION OF ENGINES NUMBER 1 - 10

SHADED - ENGINE NUMBER 10

I_{T10} = 2.483 Newton-sec.

σ_{10} = .110 Newton-sec.

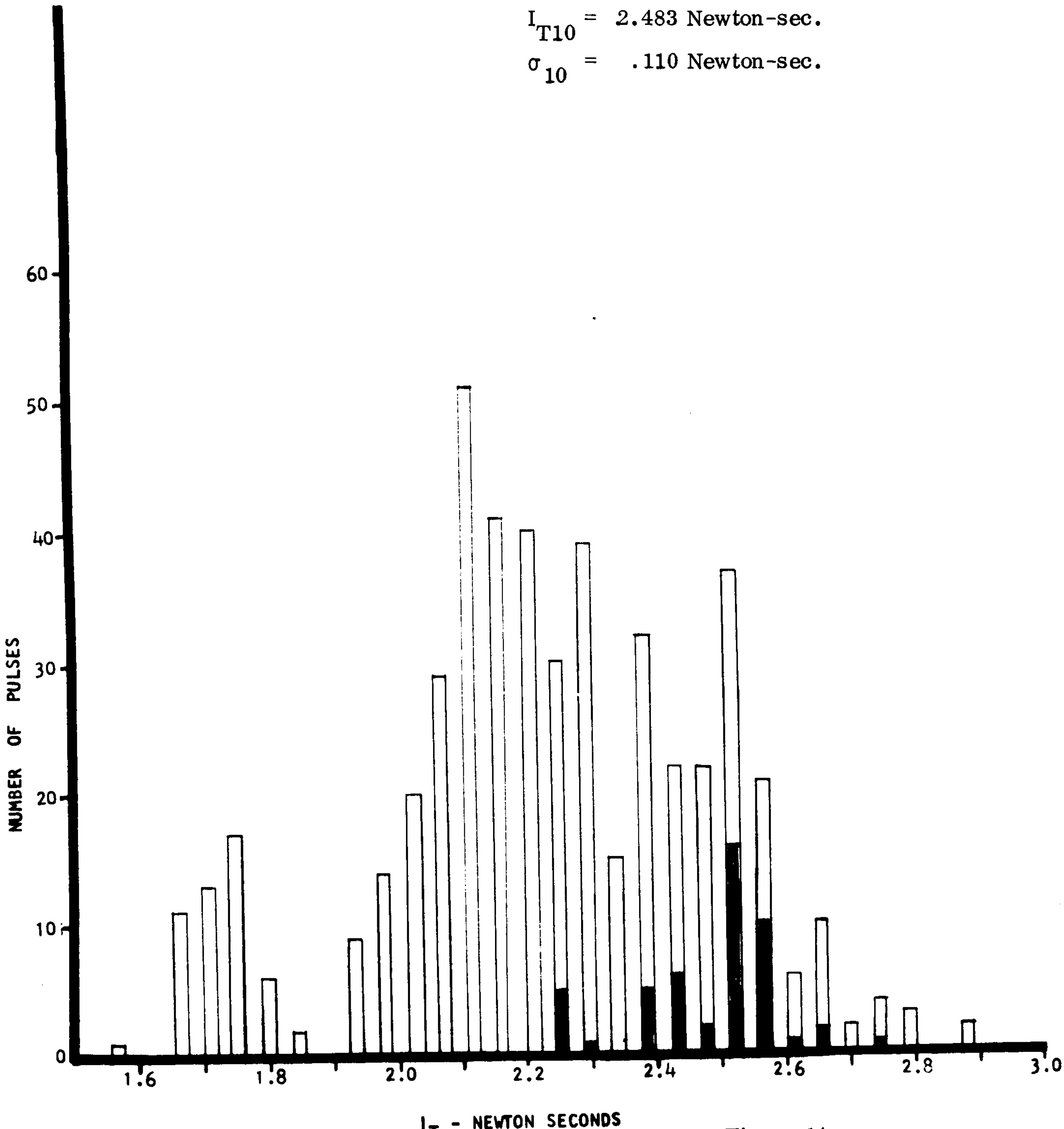

Figure 14

PROPELLANT CONSUMED PER PULSE VS TOTAL IMPULSE PER PULSE

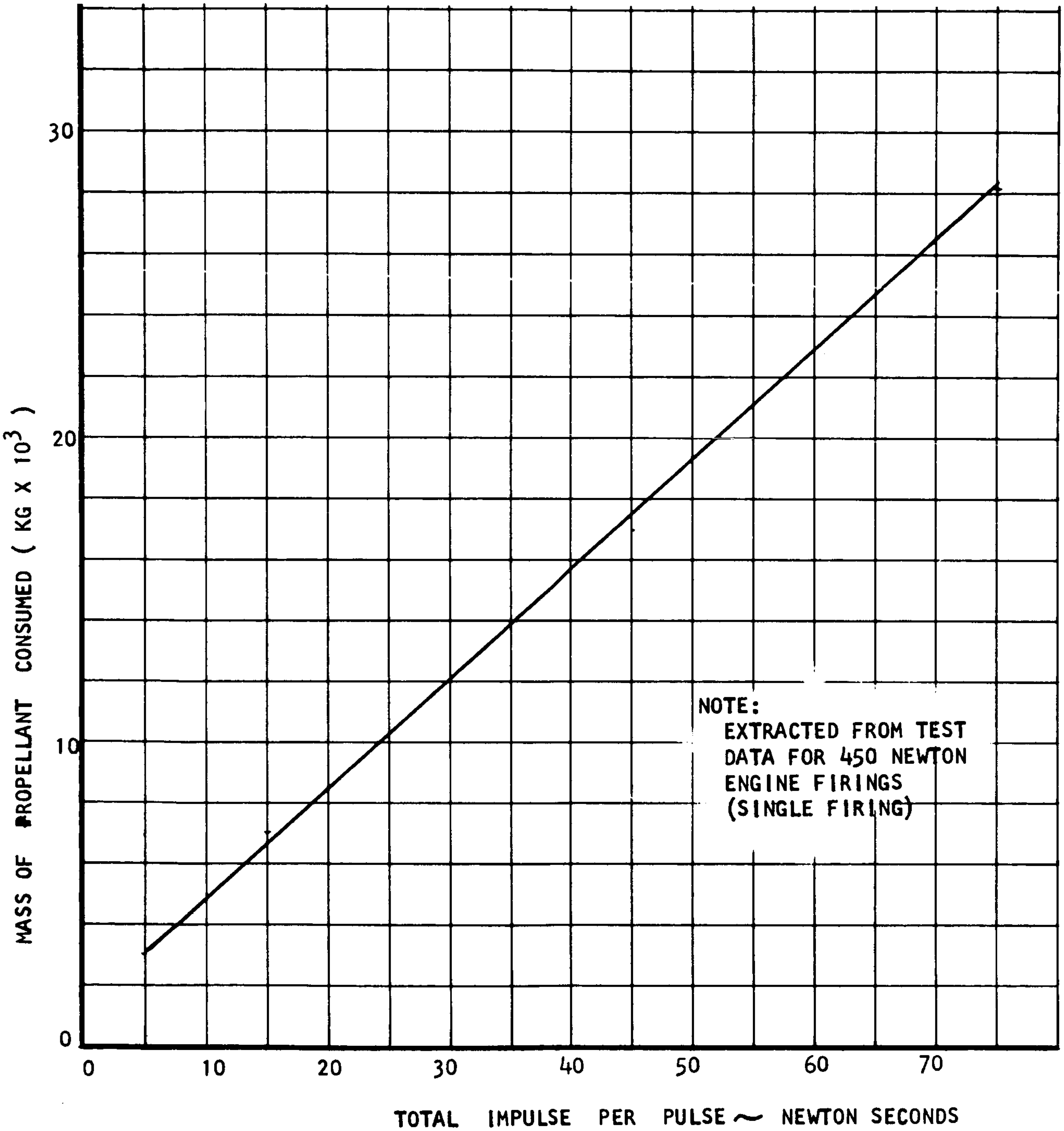

Figure 15

SIMPLE BOX LIMIT CYCLE OPERATION

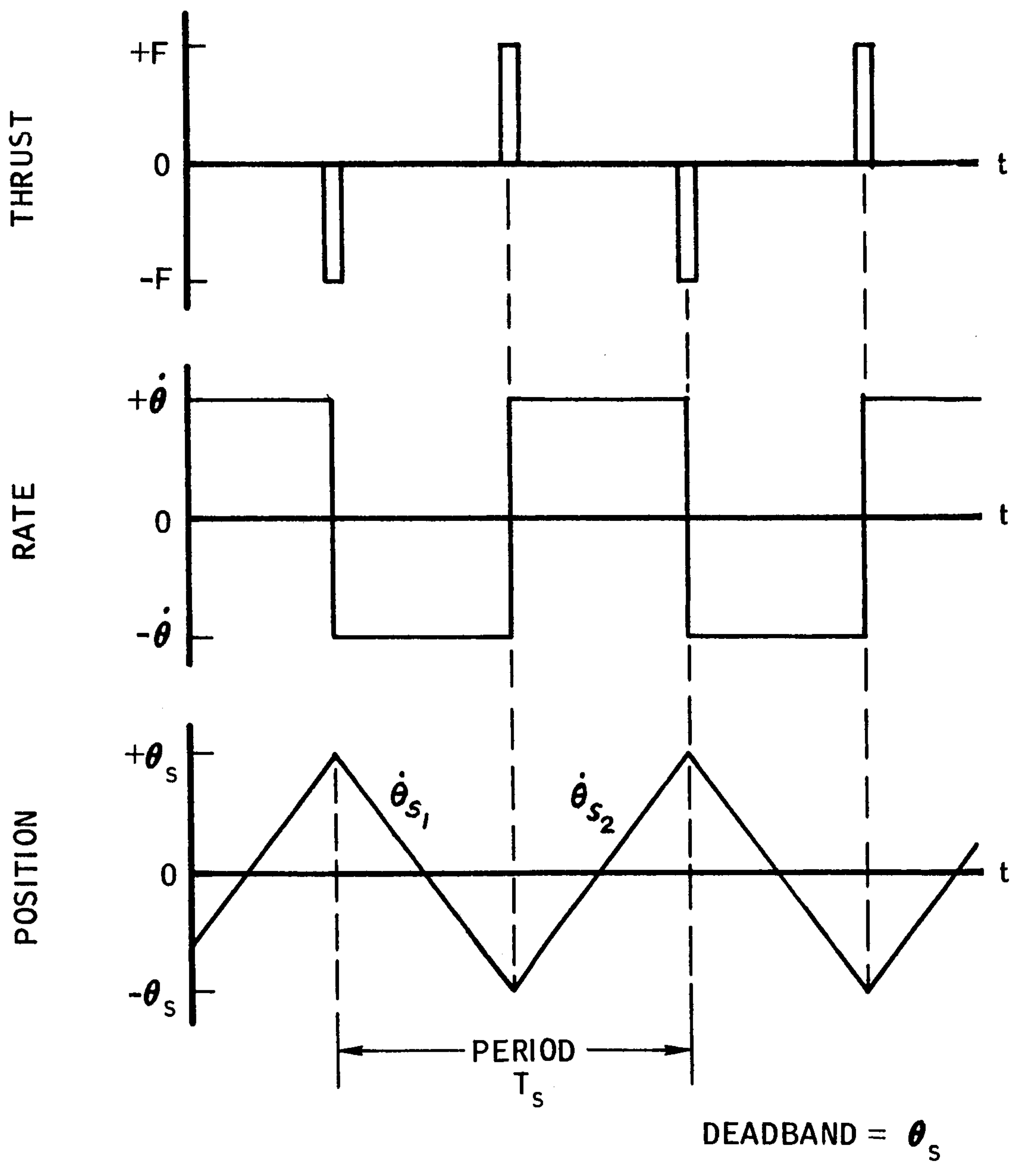

Figure 16

VARIATION OF OSCILLATION FREQUENCY WITH INITIAL ANGULAR RATE

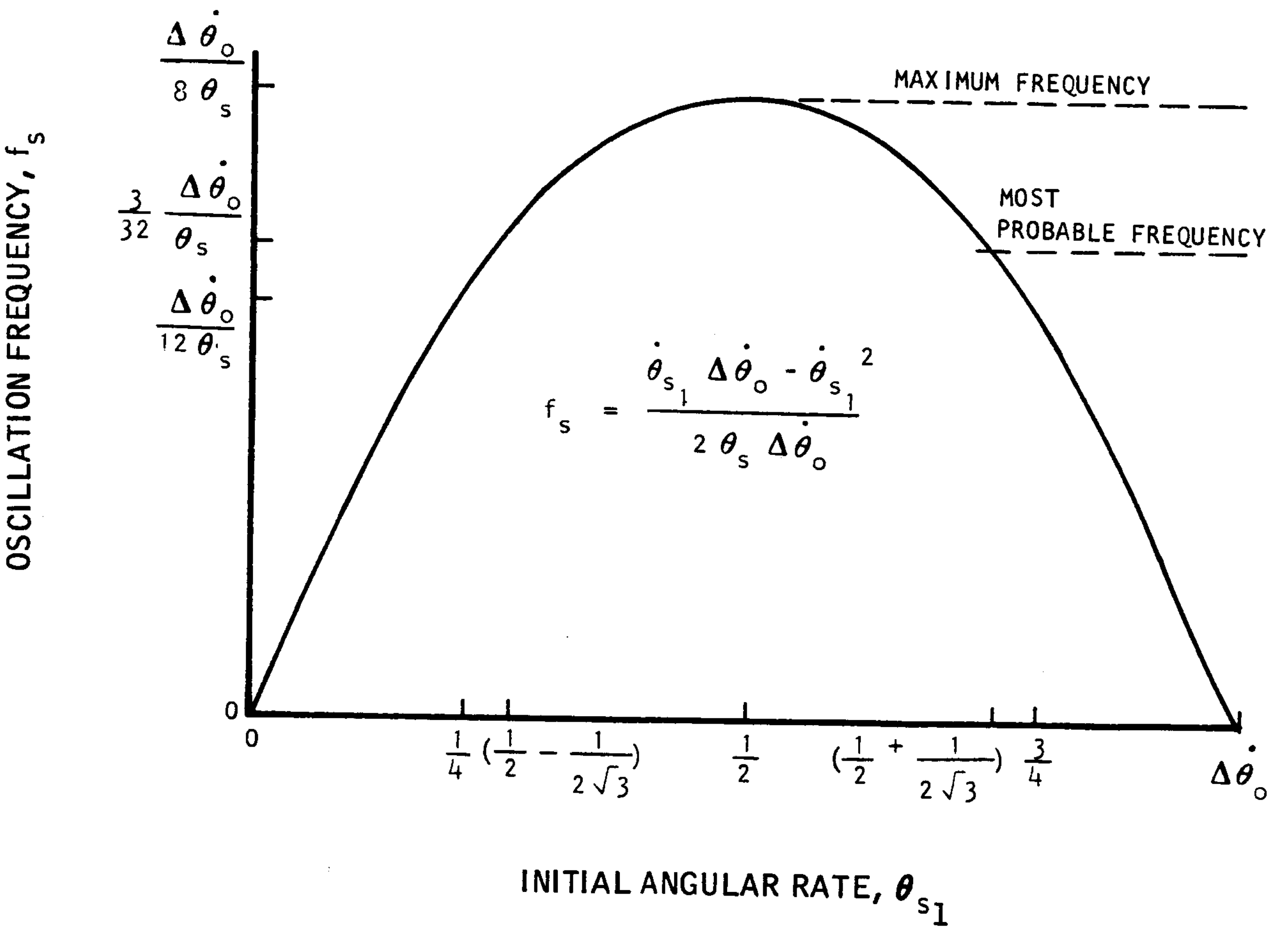

Figure 17

6 ENGINE CONFIGURATION

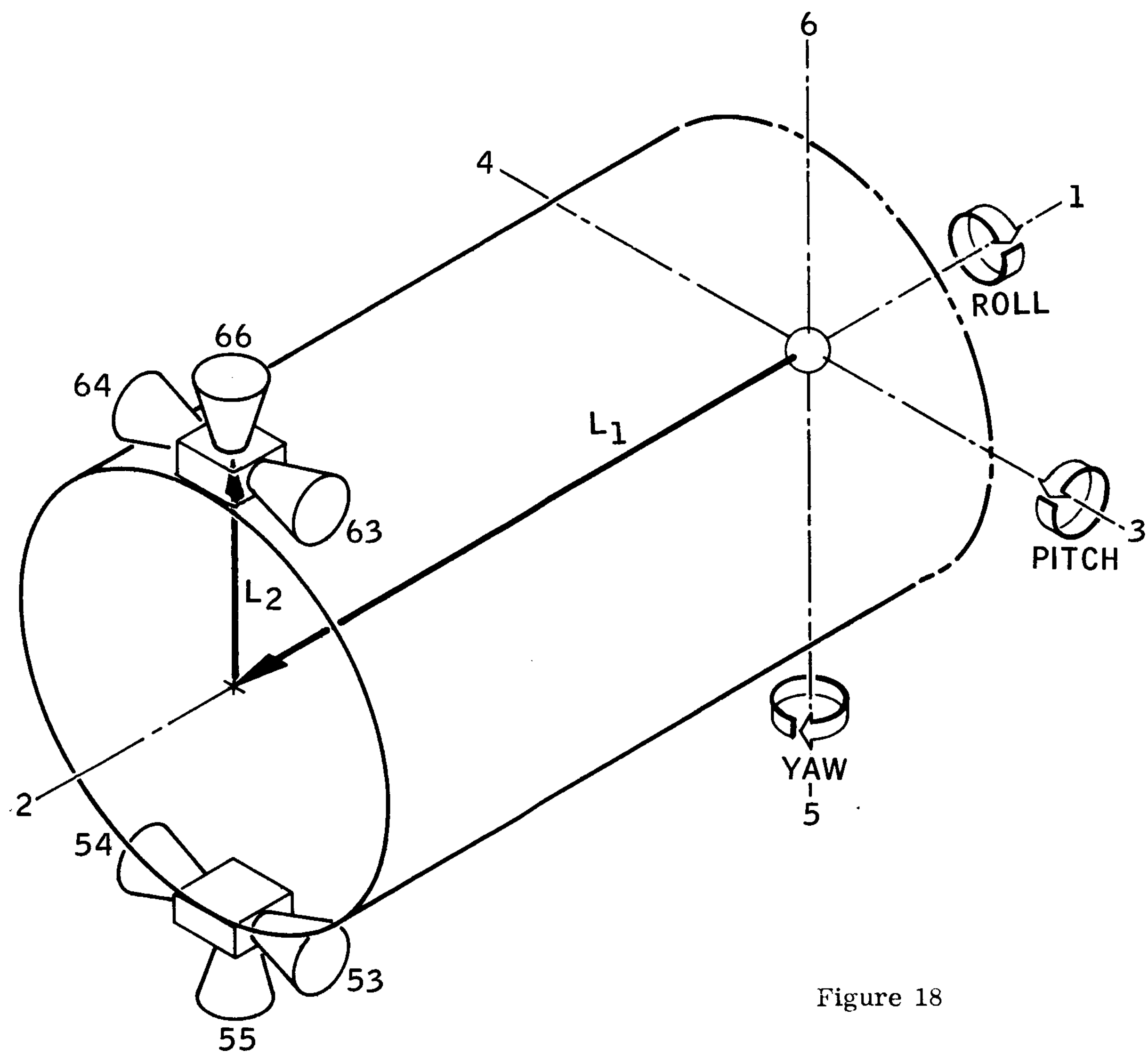

Figure 18

12 ENGINE CONFIGURATION

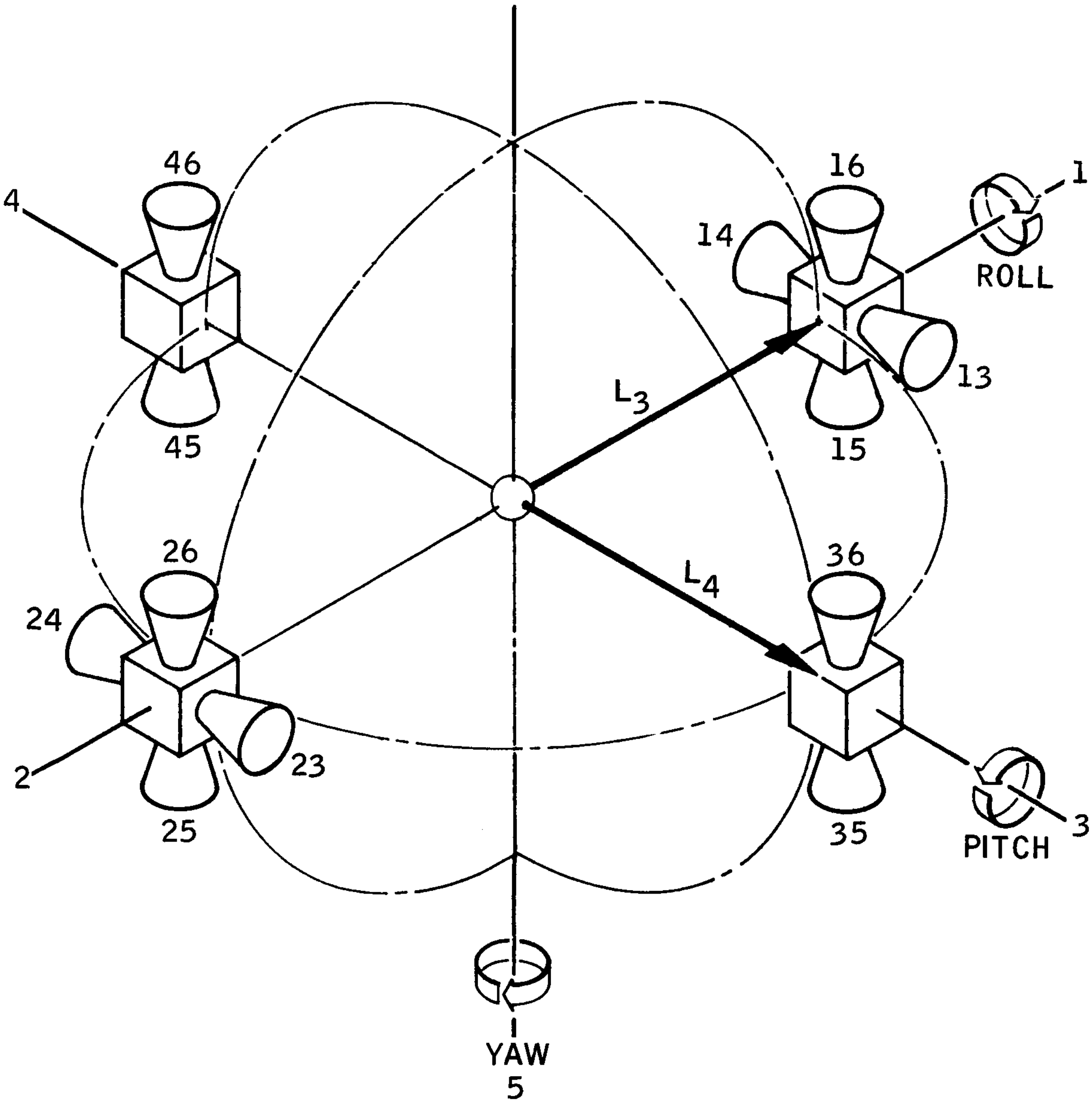

Figure 19

COORDINATE CONVENTION

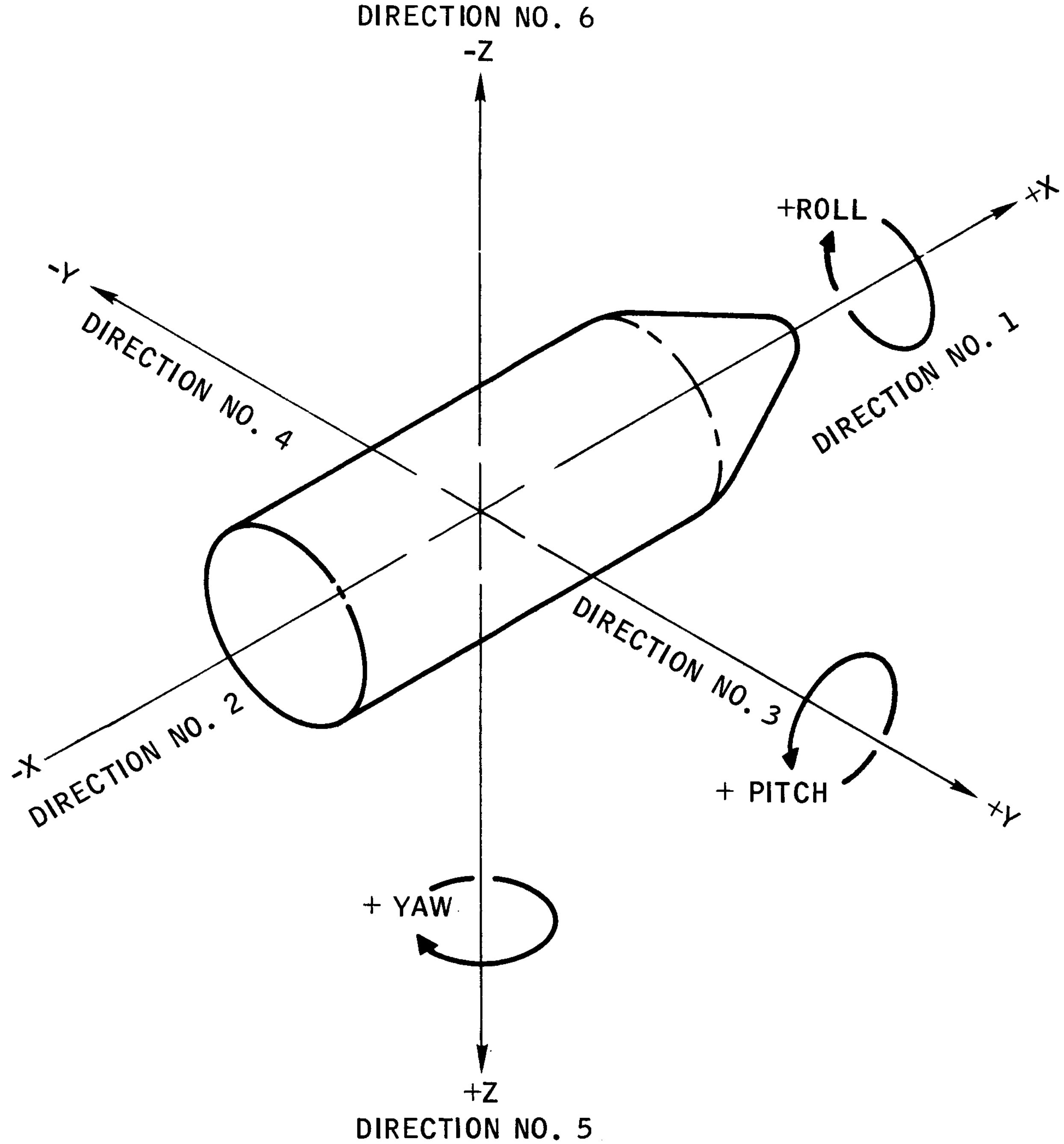

Figure 20

CONTROL PHILOSOPHY #1

θ(i) VS TIME

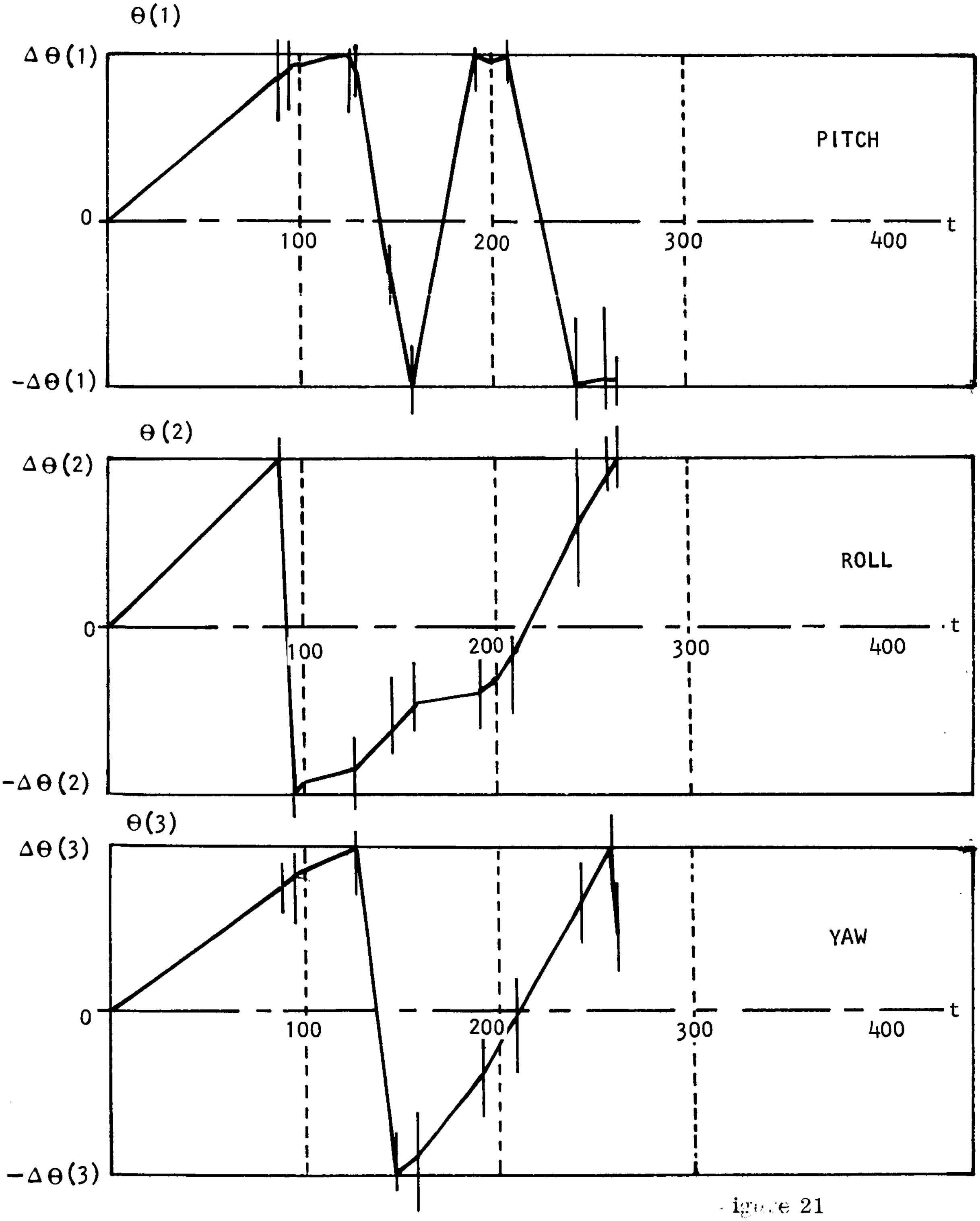

Figure 21

------GRID TIME

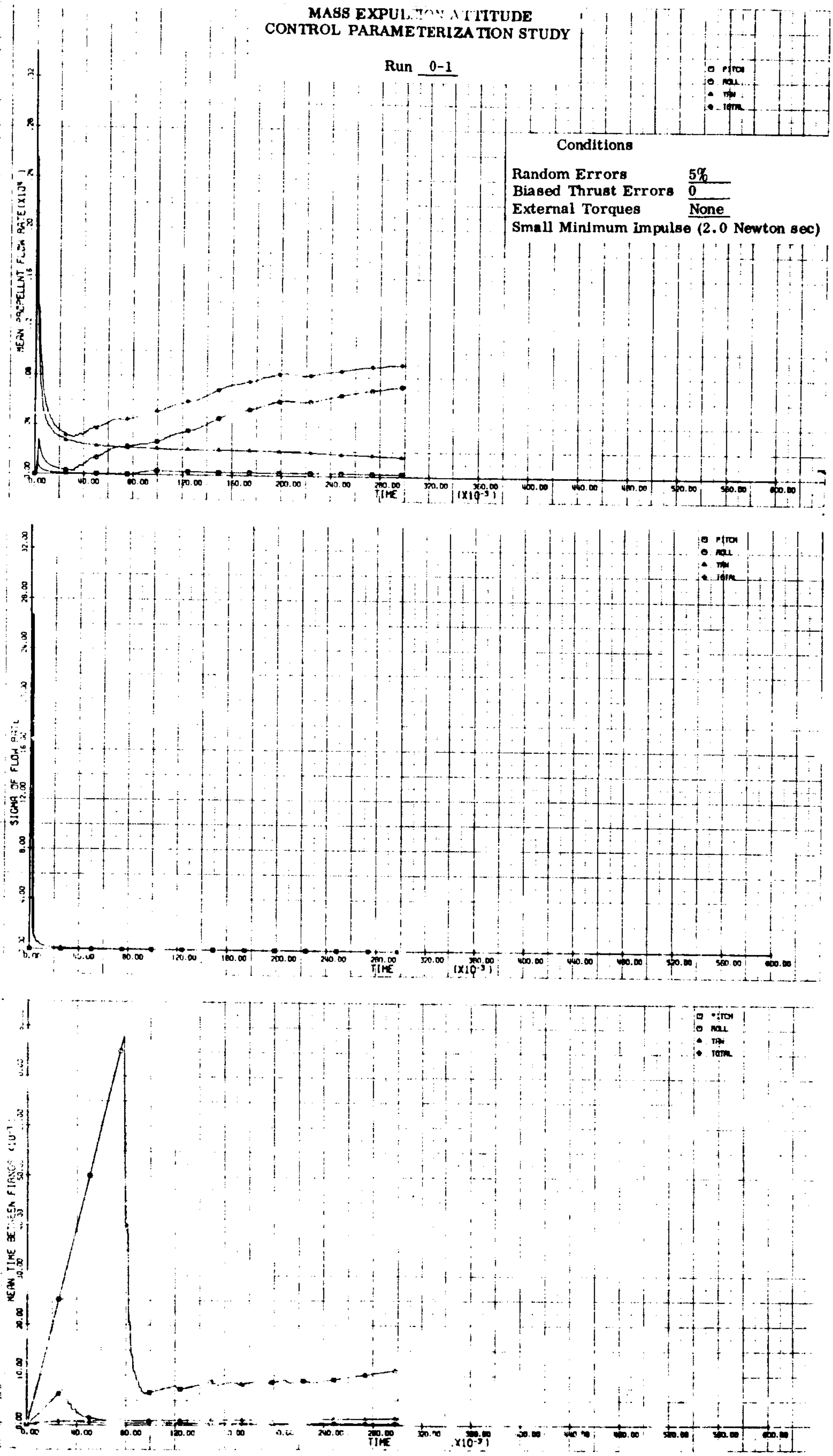
MASS EXPULSION ATTITUDE
CONTROL PARAMETERIZATION STUDY
Run 0-1
PITCH
ROLL
YAW
TOTAL
Conditions
Random Errors 5%
Biased Thrust Errors 0
External Torques None
Small Minimum Impulse (2.0 Newton sec)
MEAN PROPELLANT FLOW RATE
TIME
SIGMA OF FLOW RATE
MEAN TIME BETWEEN FIRINGS

Figure 22

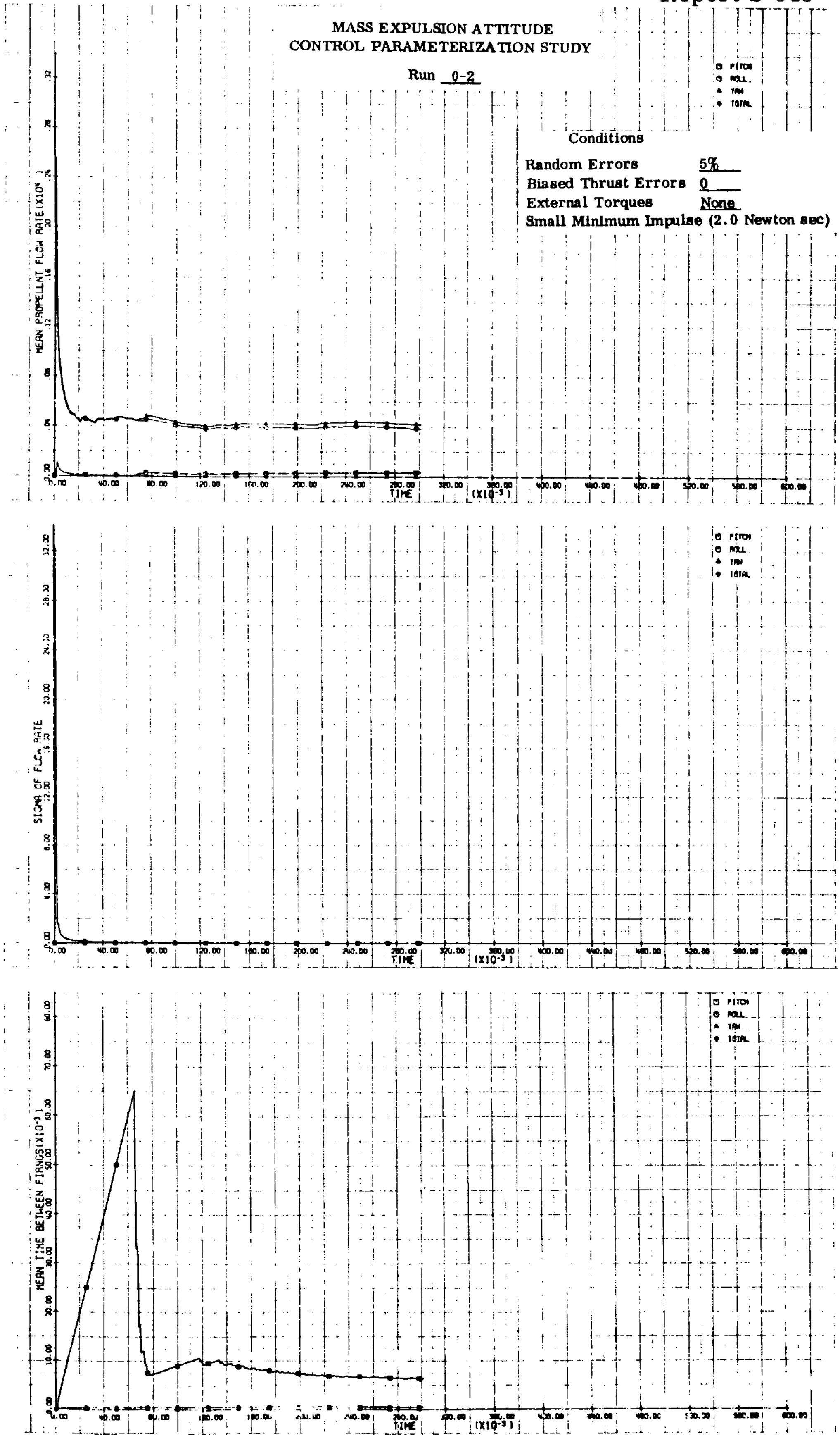
MASS EXPULSION ATTITUDE
CONTROL PARAMETERIZATION STUDY
Run 0-2
Conditions
Random Errors 5%
Biased Thrust Errors 0
External Torques None
Small Minimum Impulse (2.0 Newton sec)
PITCH
ROLL
YAW
TOTAL
MEAN PROPELLANT FLOW RATE (X10⁴)
SIGMA OF FLOW RATE
MEAN TIME BETWEEN FIRINGS (X10⁻³)
TIME (X10⁻³)

Figure 23

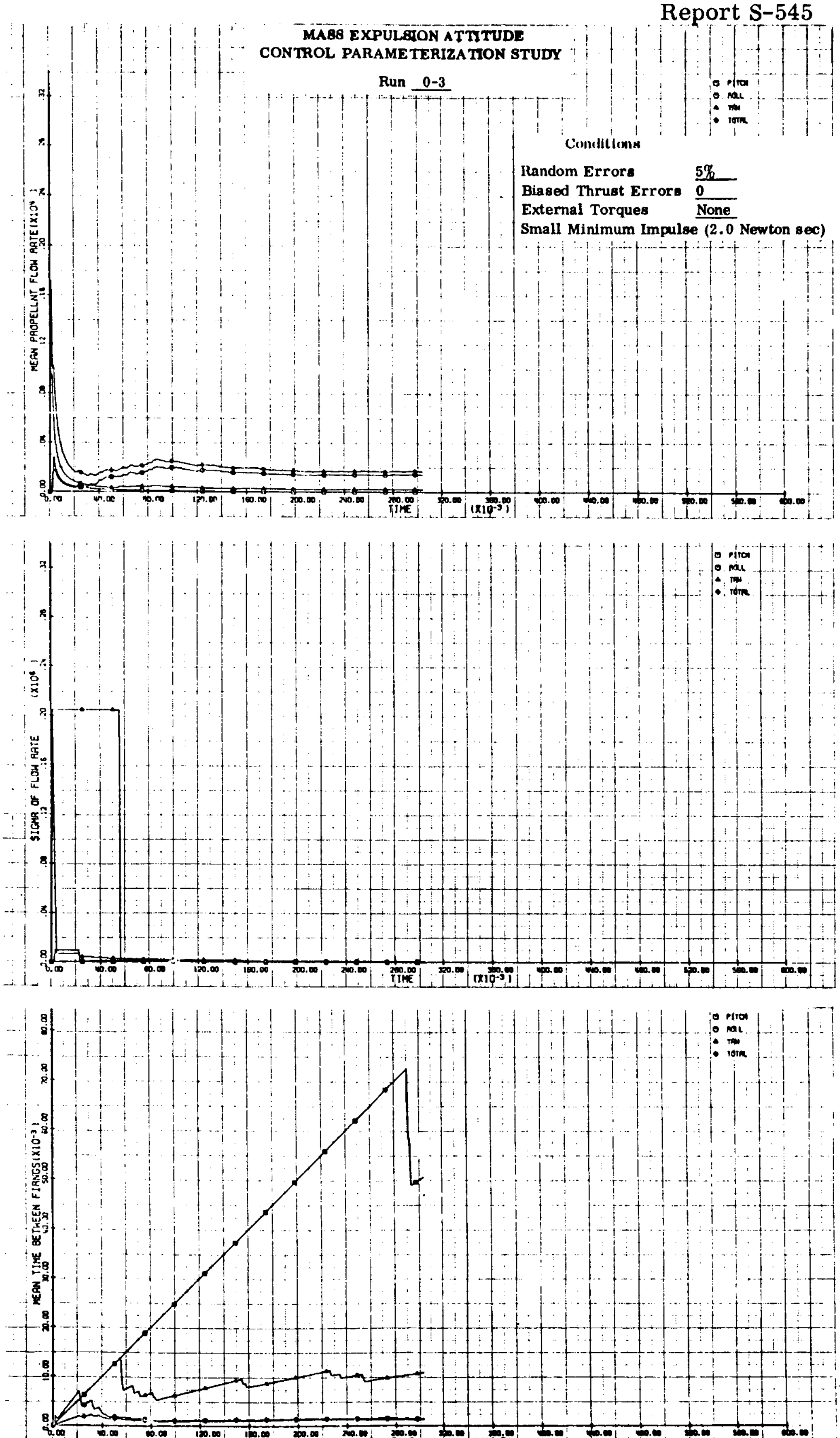
MASS EXPULSION ATTITUDE
CONTROL PARAMETERIZATION STUDY
Run 0-3
Conditions
Random Errors 5%
Biased Thrust Errors 0
External Torques None
Small Minimum Impulse (2.0 Newton sec)
MEAN PROPELLANT FLOW RATE
SIGMA OF FLOW RATE
MEAN TIME BETWEEN FIRINGS
TIME
PITCH
ROLL
YAW
TOTAL

Figure 24

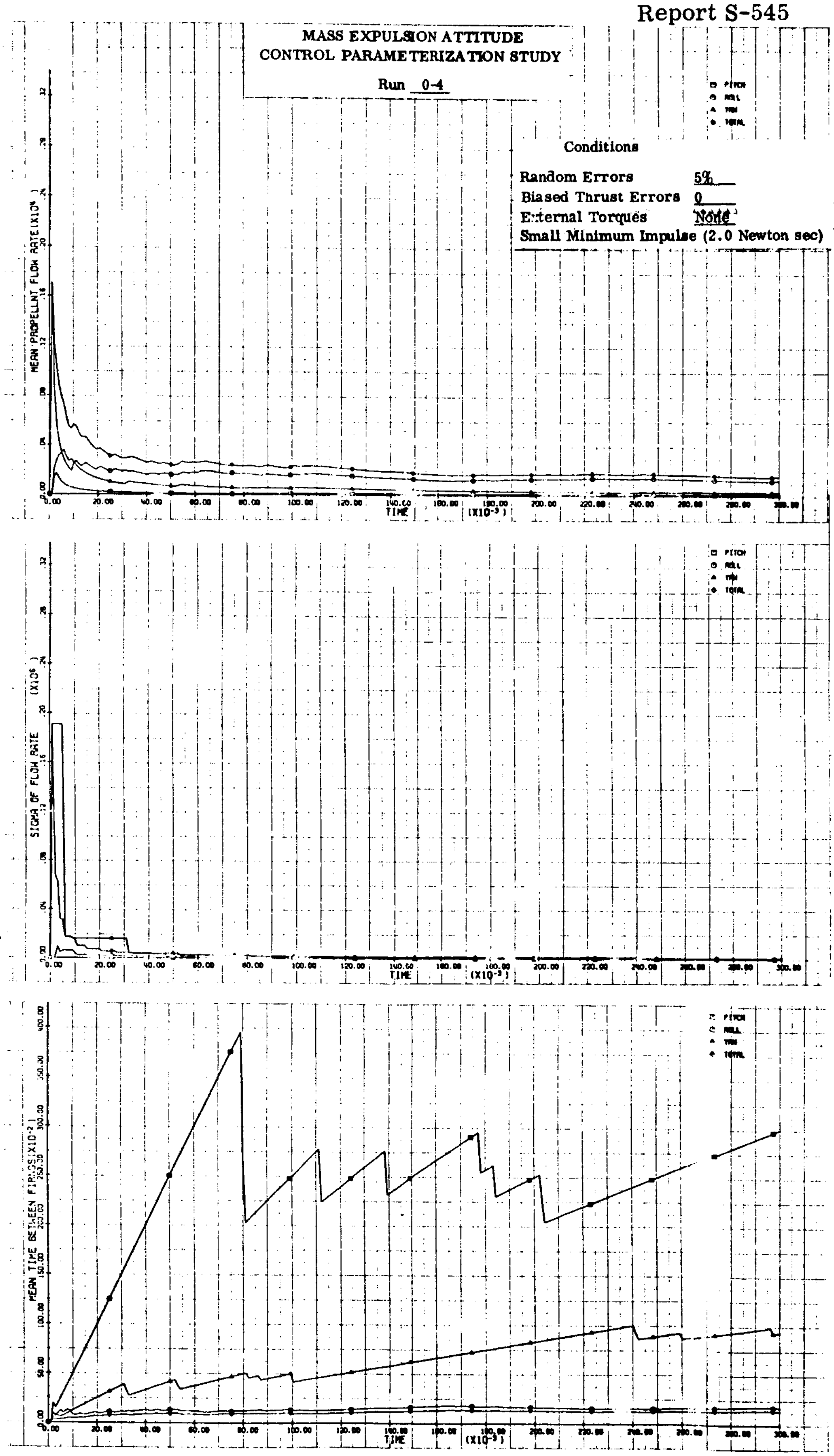
MASS EXPULSION ATTITUDE
CONTROL PARAMETERIZATION STUDY
Run 0-4
Conditions
Random Errors 5%
Biased Thrust Errors 0
External Torques None
Small Minimum Impulse (2.0 Newton sec)
PITCH
ROLL
YAW
TOTAL
MEAN PROPELLANT FLOW RATE
SIGMA OF FLOW RATE
MEAN TIME BETWEEN FIRINGS
TIME

Figure 25

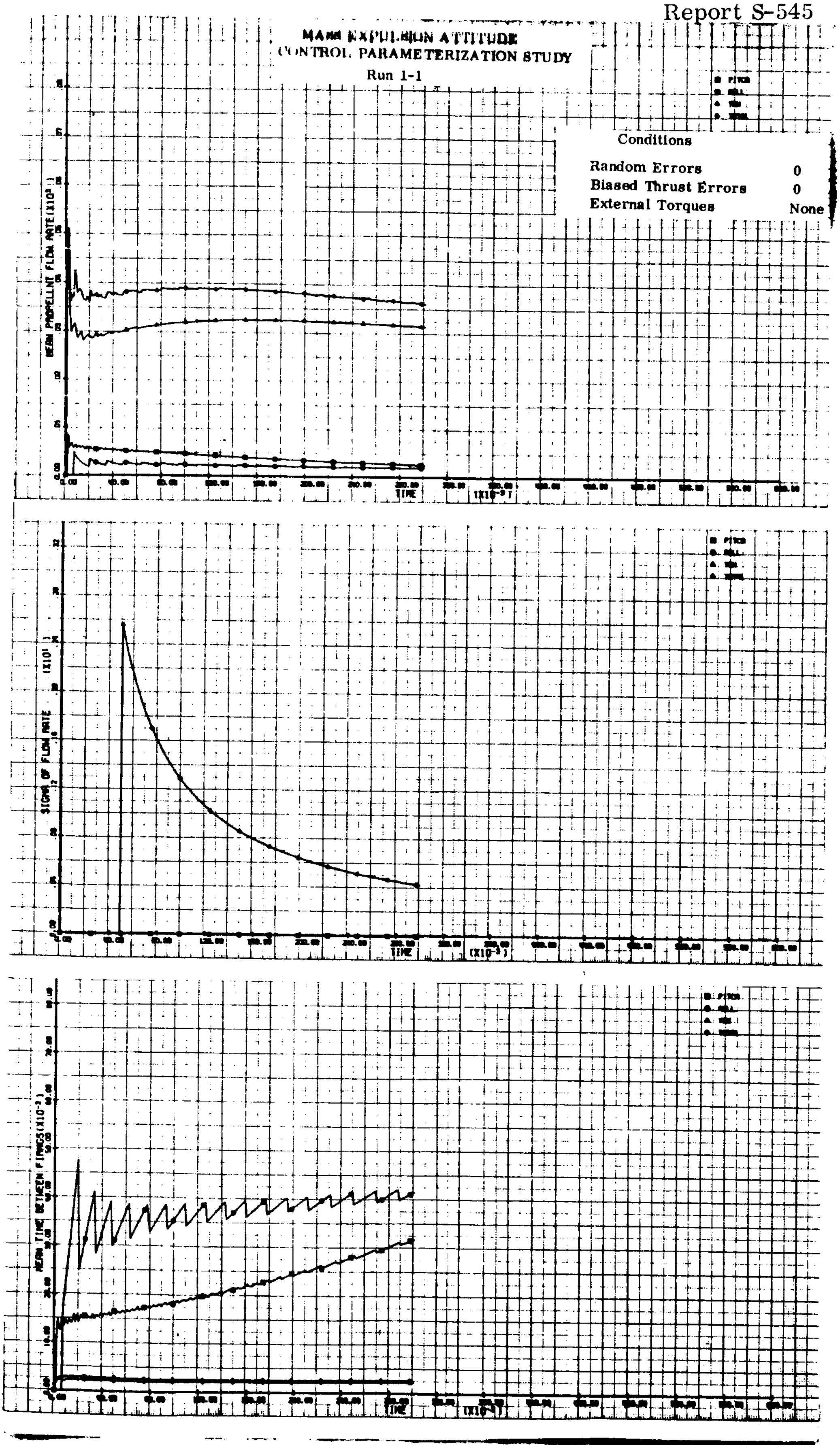
MASS EXPULSION ATTITUDE
CONTROL PARAMETERIZATION STUDY
Run 1-1
Conditions
Random Errors 0
Biased Thrust Errors 0
External Torques None
TIME
TIME
TIME

Figure 26

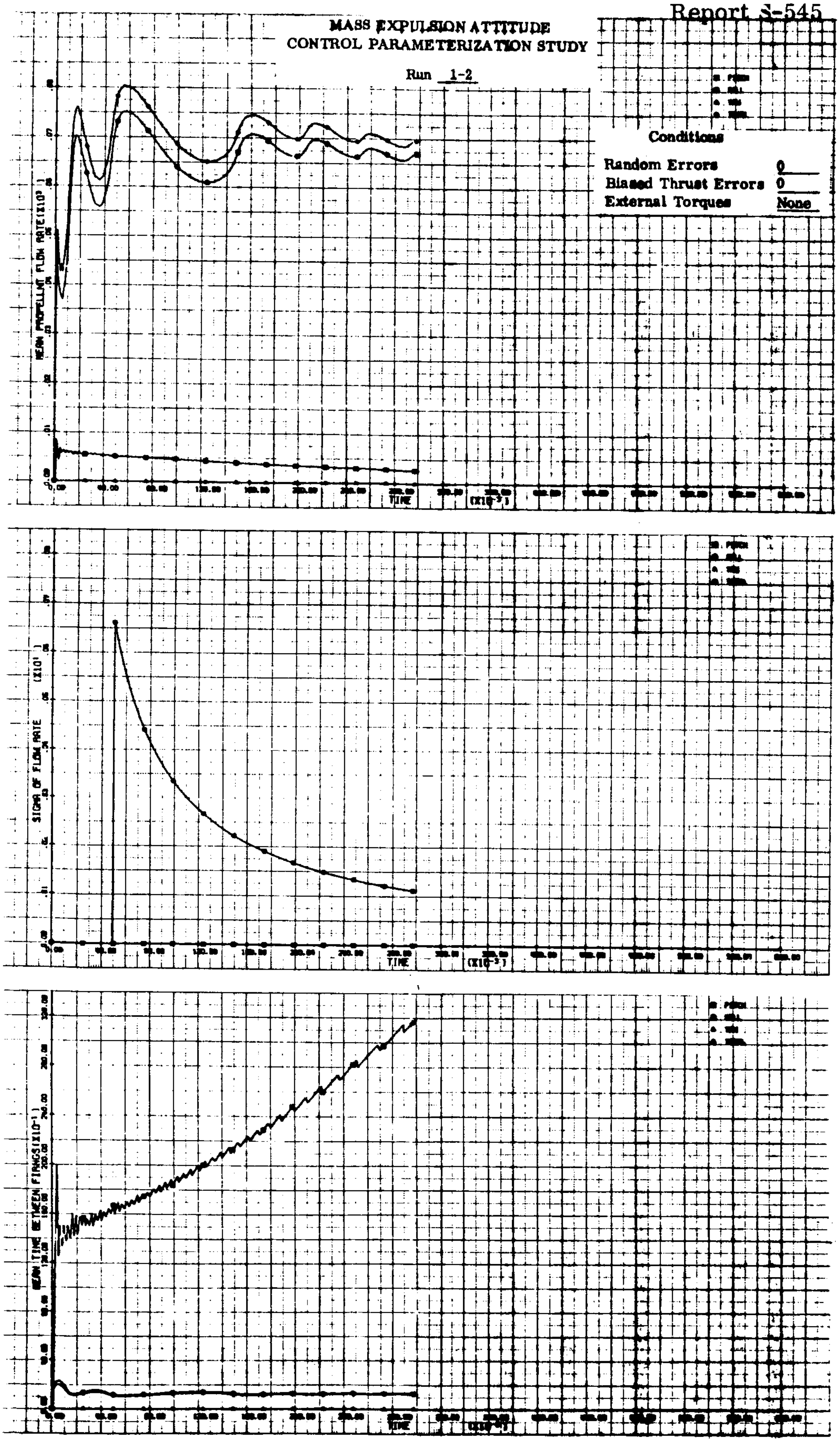
MASS EXPULSION ATTITUDE
CONTROL PARAMETERIZATION STUDY
Run 1-2
Conditions
Random Errors 0
Biased Thrust Errors 0
External Torques None
MEAN PROPELLANT FLOW RATE (X10³)
SIGMA OF FLOW RATE (X10¹)
MEAN TIME BETWEEN FIRINGS (X10⁻¹)
TIME (X10⁻³)

Figure 27

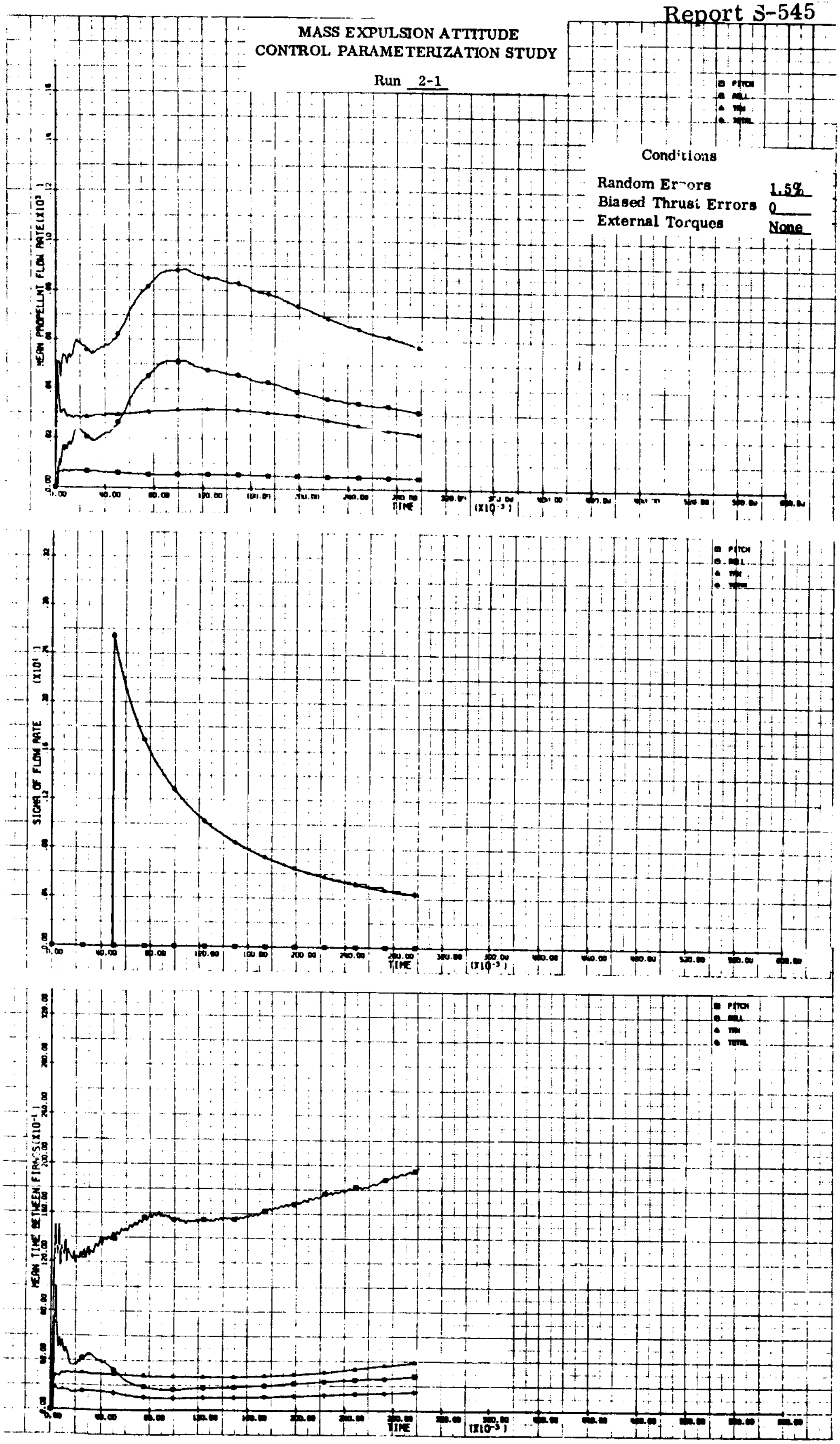
MASS EXPULSION ATTITUDE
CONTROL PARAMETERIZATION STUDY
Run 2-1
Conditions
Random Errors 1.5%
Biased Thrust Errors 0
External Torques None
TIME

Figure 28

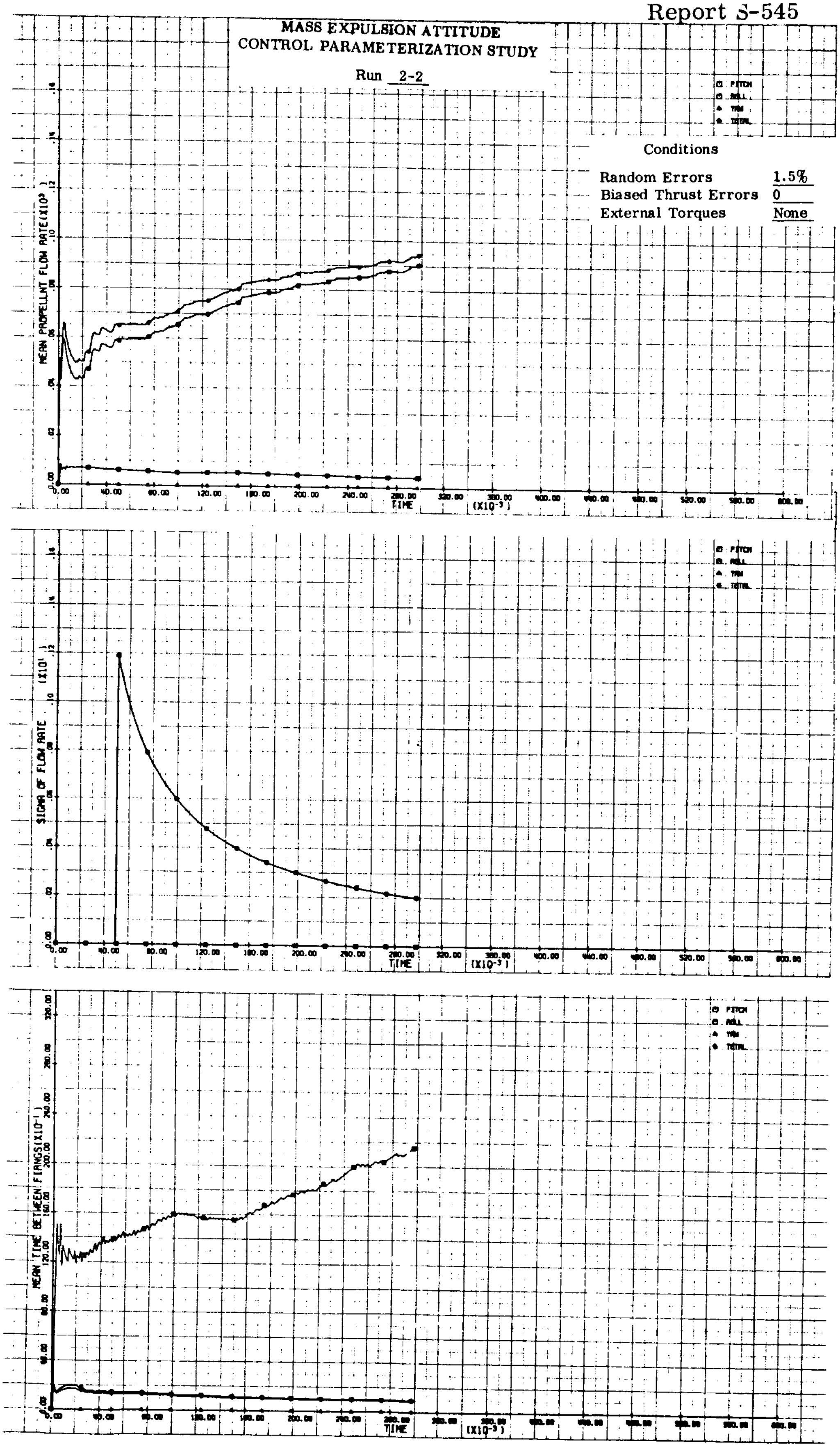
MASS EXPULSION ATTITUDE
CONTROL PARAMETERIZATION STUDY
Run 2-2
PITCH
ROLL
YAW
TOTAL
Conditions
Random Errors 1.5%
Biased Thrust Errors 0
External Torques None
MEAN PROPELLANT FLOW RATE
SIGMA OF FLOW RATE
MEAN TIME BETWEEN FIRNGS
TIME
(X10⁻³)

Figure 29

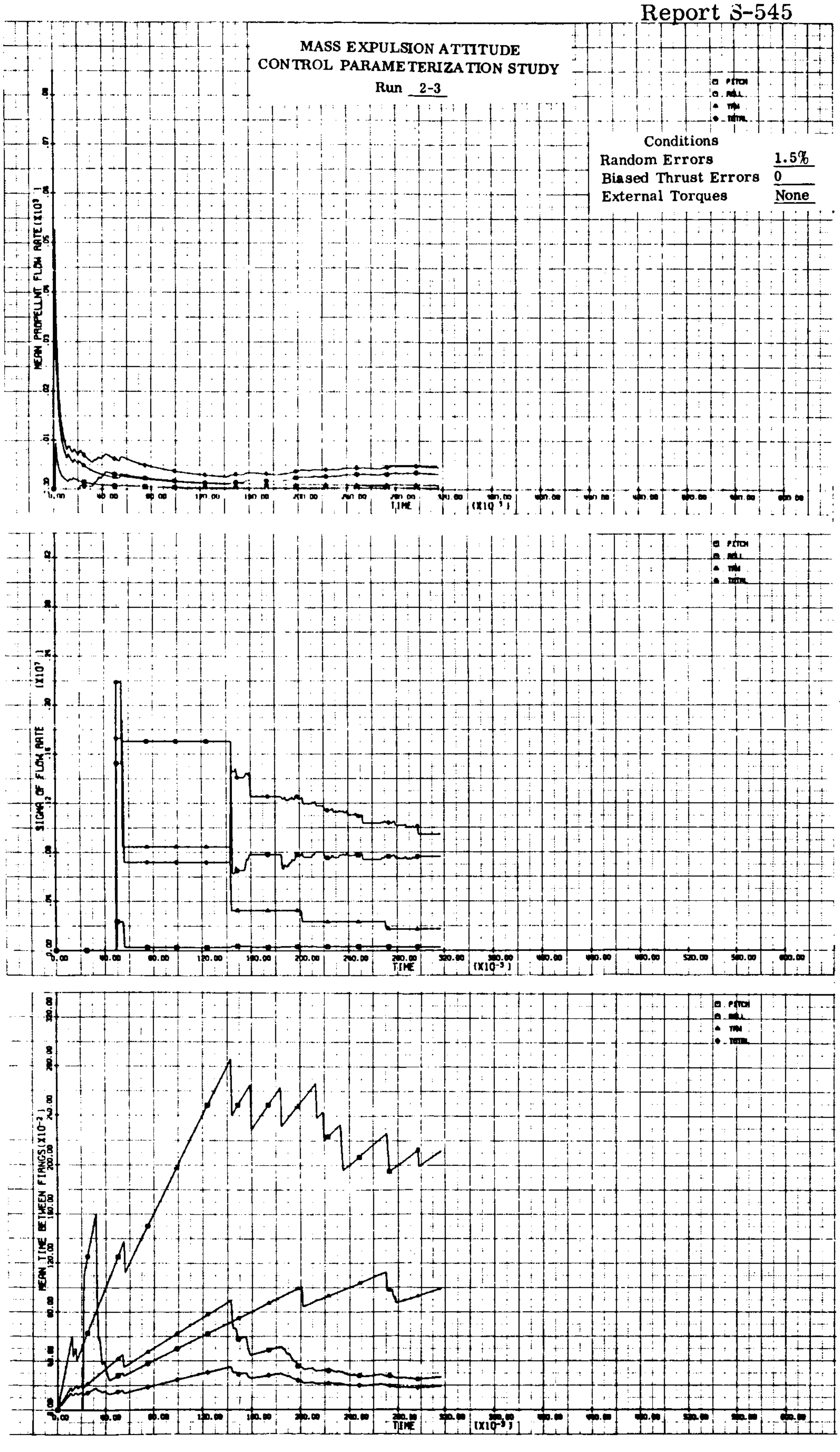
MASS EXPULSION ATTITUDE CONTROL PARAMETERIZATION STUDY
Run 2-3
Conditions
Random Errors 1.5%
Biased Thrust Errors 0
External Torques None
PITCH
ROLL
YAW
TOTAL
MEAN PROPELLANT FLOW RATE (X10²)
SIGMA OF FLOW RATE (X10²)
MEAN TIME BETWEEN FIRINGS (X10⁻¹)
TIME (X10⁻³)

Figure 30

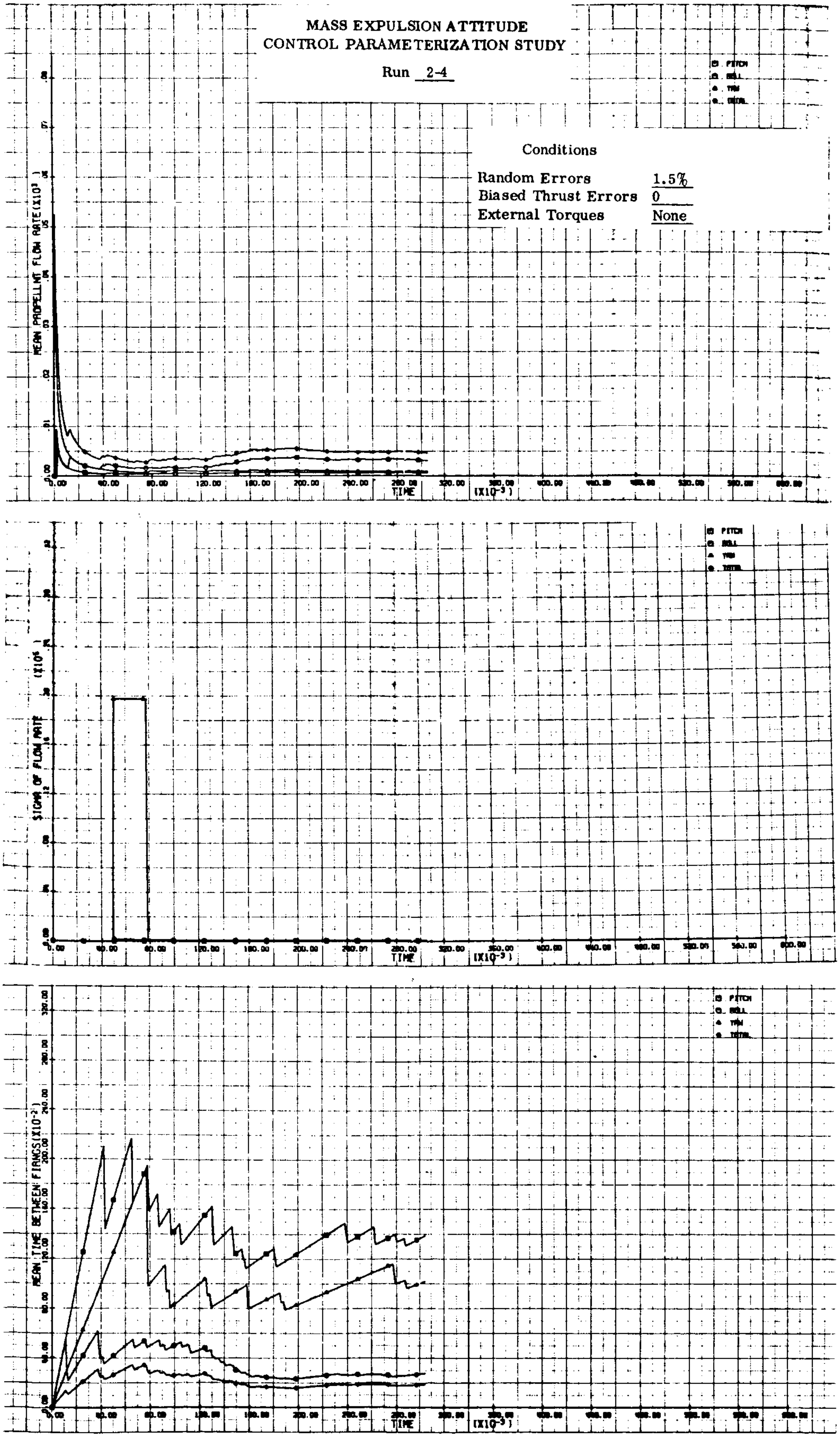
MASS EXPULSION ATTITUDE
CONTROL PARAMETERIZATION STUDY
Run 2-4
Conditions
Random Errors 1.5%
Biased Thrust Errors 0
External Torques None
MEAN PROPELLANT FLOW RATE (X10³)
SIGMA OF FLOW RATE (X10⁶)
MEAN TIME BETWEEN FIRINGS (X10⁻²)
TIME (X10⁻³)

Figure 31

MASS EXPULSION ATTITUDE
CONTROL PARAMETERIZATION STUDY

Run 4-1

Conditions

Random Errors 5%
Biased Thrust Errors 0
External Torques None

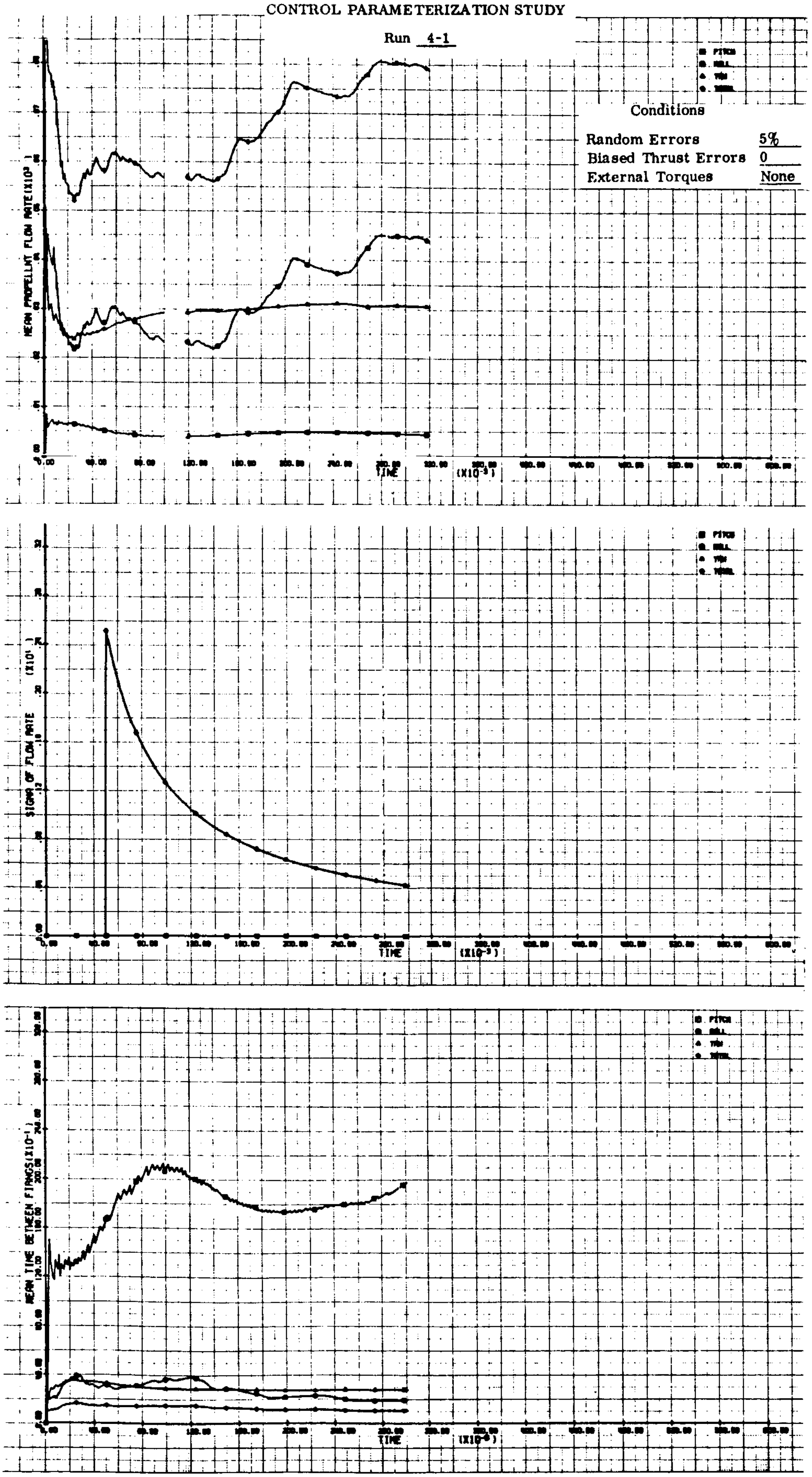

Figure 32

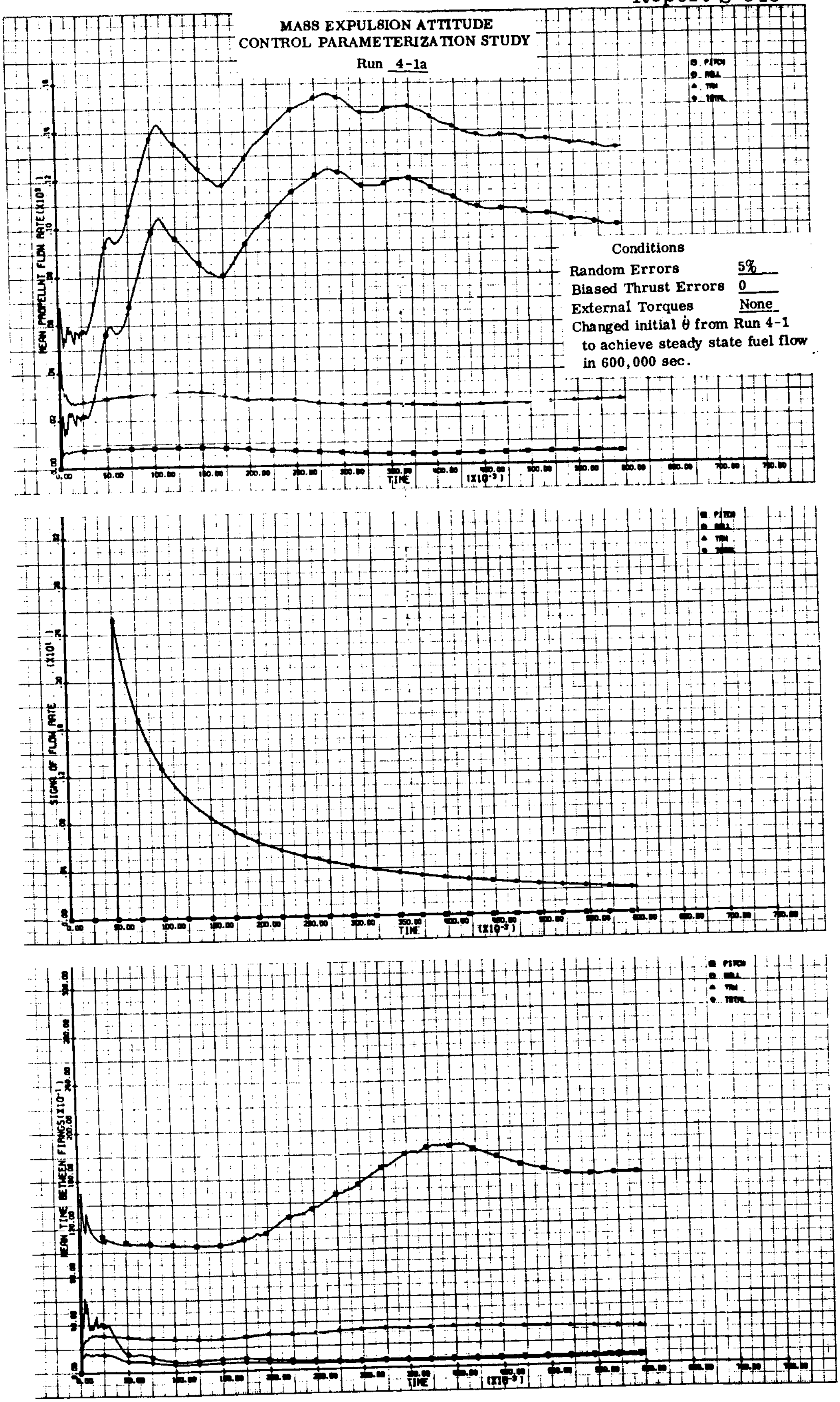
MASS EXPULSION ATTITUDE
CONTROL PARAMETERIZATION STUDY
Run 4-1a
Conditions
Random Errors 5%
Biased Thrust Errors 0
External Torques None
Changed initial $\dot{\theta}$ from Run 4-1
to achieve steady state fuel flow
in 600,000 sec.
MEAN PROPELLANT FLOW RATE (X10^3)
SIGMA OF FLOW RATE (X10^1)
MEAN TIME BETWEEN FIRINGS (X10^{-1})
TIME (X10^{-3})
PITCH
ROLL
YAW
TOTAL

Figure 33

MASS EXPULSION ATTITUDE
CONTROL PARAMETERIZATION STUDY

Run 4-2

Conditions

Random Errors	5%
Biased Thrust Errors	0
External Torques	None

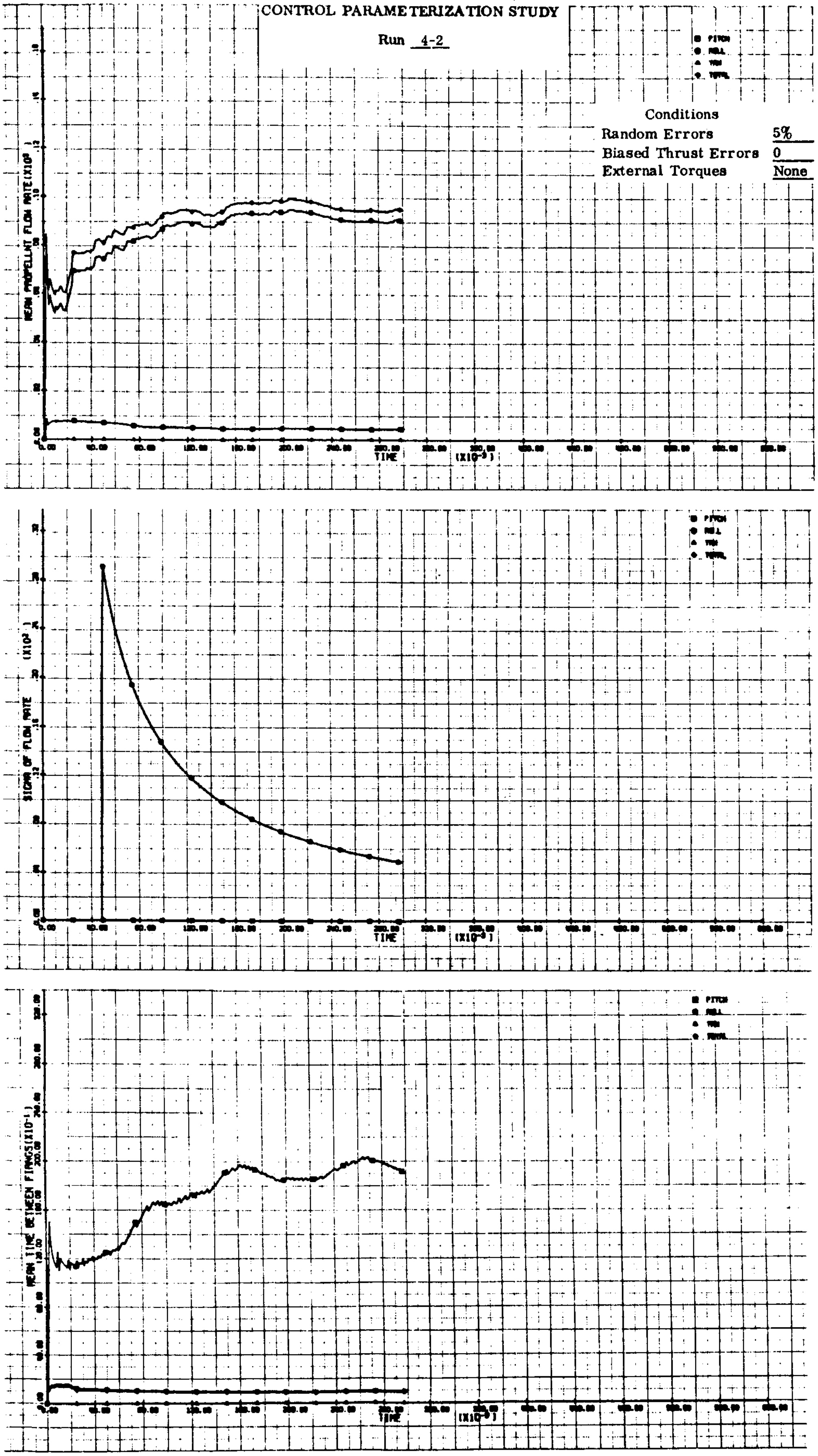

Figure 34

MASS EXPULSION ATTITUDE CONTROL PARAMETERIZATION STUDY

Run 4-3

Conditions

Random Errors	5%
Biased Thrust Errors	0
External Torques	None

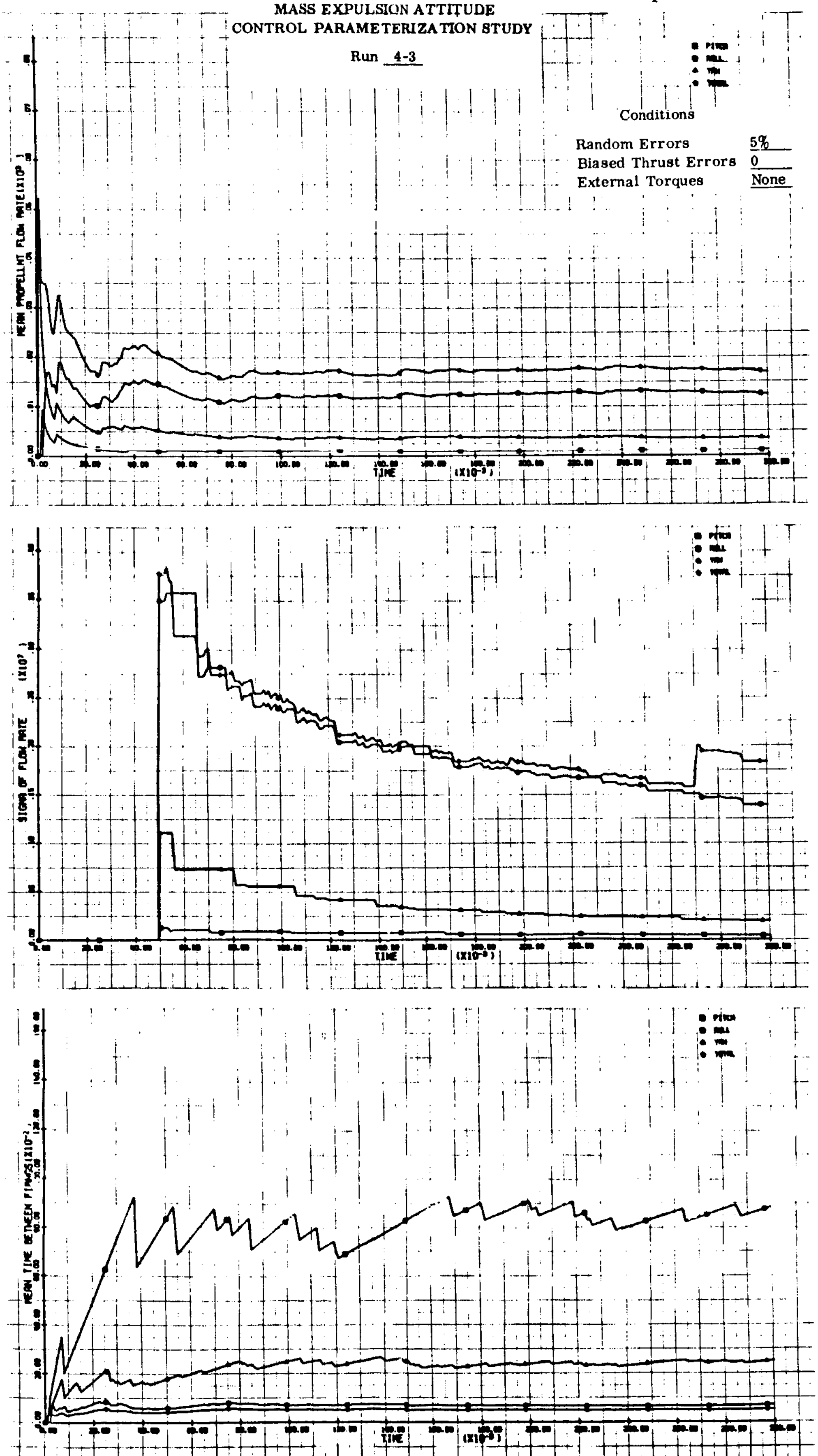

Figure 35

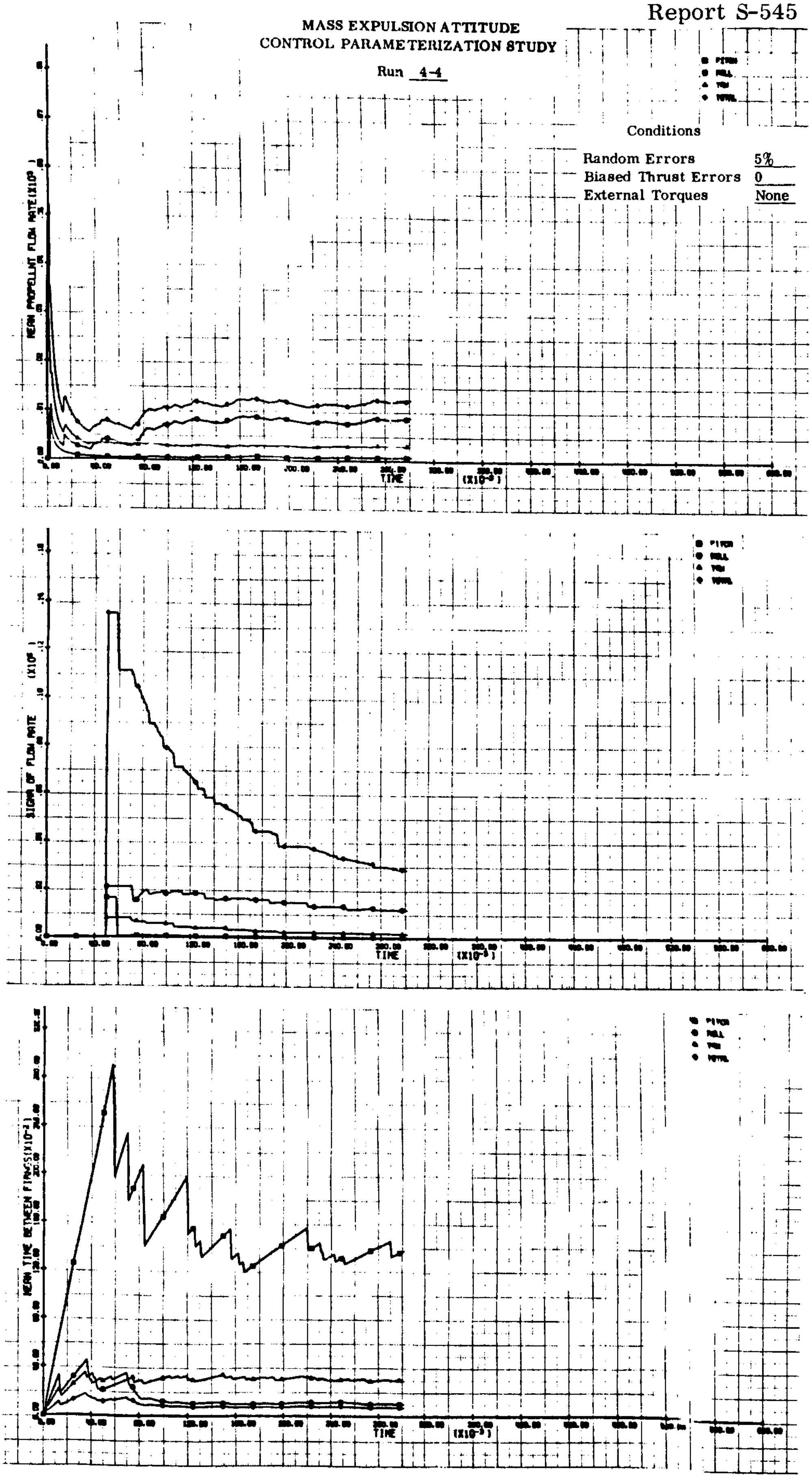
MASS EXPULSION ATTITUDE
CONTROL PARAMETERIZATION STUDY
Run 4-4
Conditions
Random Errors 5%
Biased Thrust Errors 0
External Torques None
MEAN PROPELLANT FLOW RATE (X10^3)
SIGMA OF FLOW RATE (X10^2)
MEAN TIME BETWEEN FIRINGS (X10^-2)
TIME
PITCH
ROLL
YAW
TOTAL

Figure 36

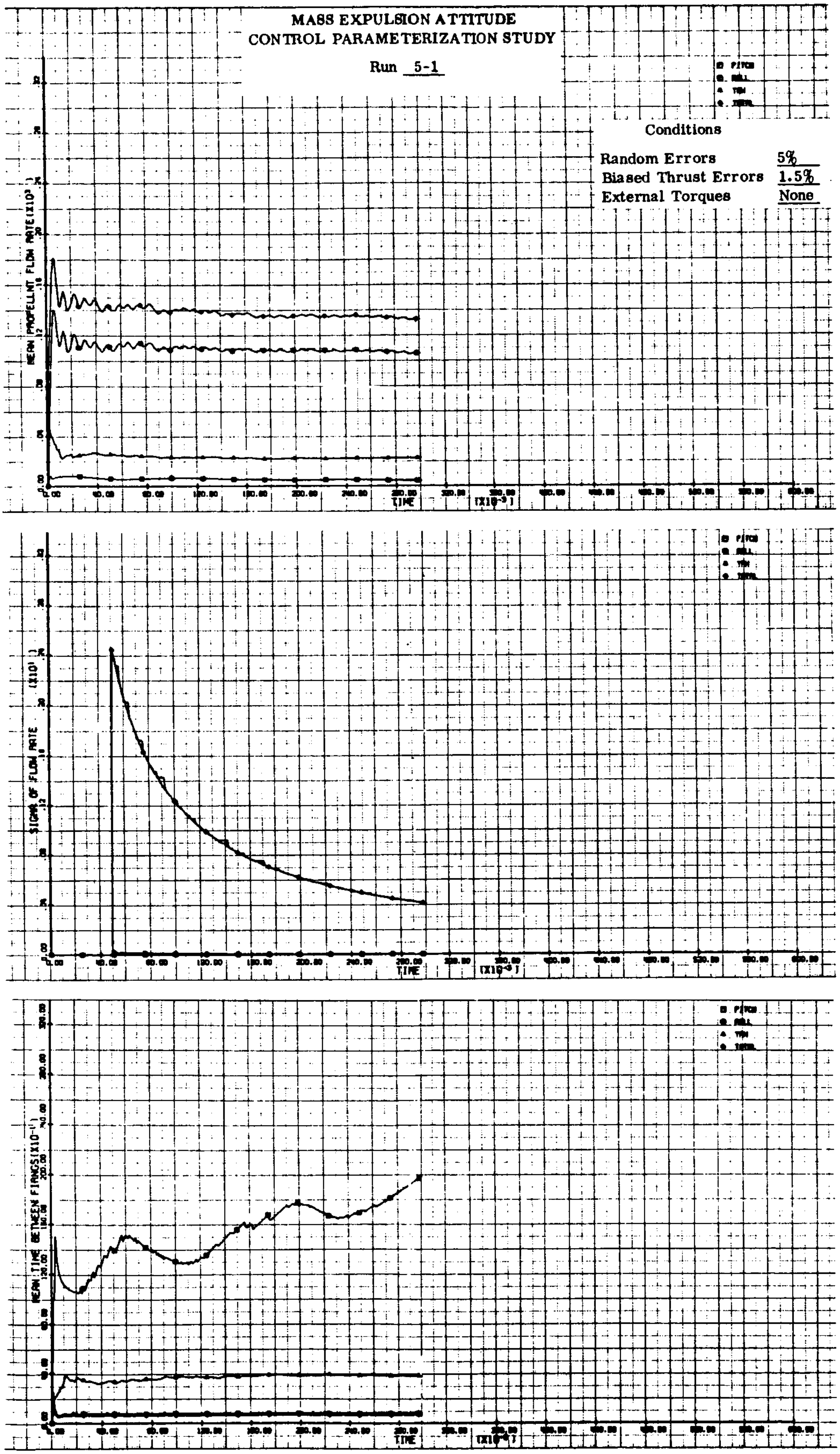
MASS EXPULSION ATTITUDE
CONTROL PARAMETERIZATION STUDY
Run 5-1
Conditions
Random Errors 5%
Biased Thrust Errors 1.5%
External Torques None
MEAN PROPELLANT FLOW RATE
SIGMA OF FLOW RATE
MEAN TIME BETWEEN FIRINGS
TIME

Figure 37

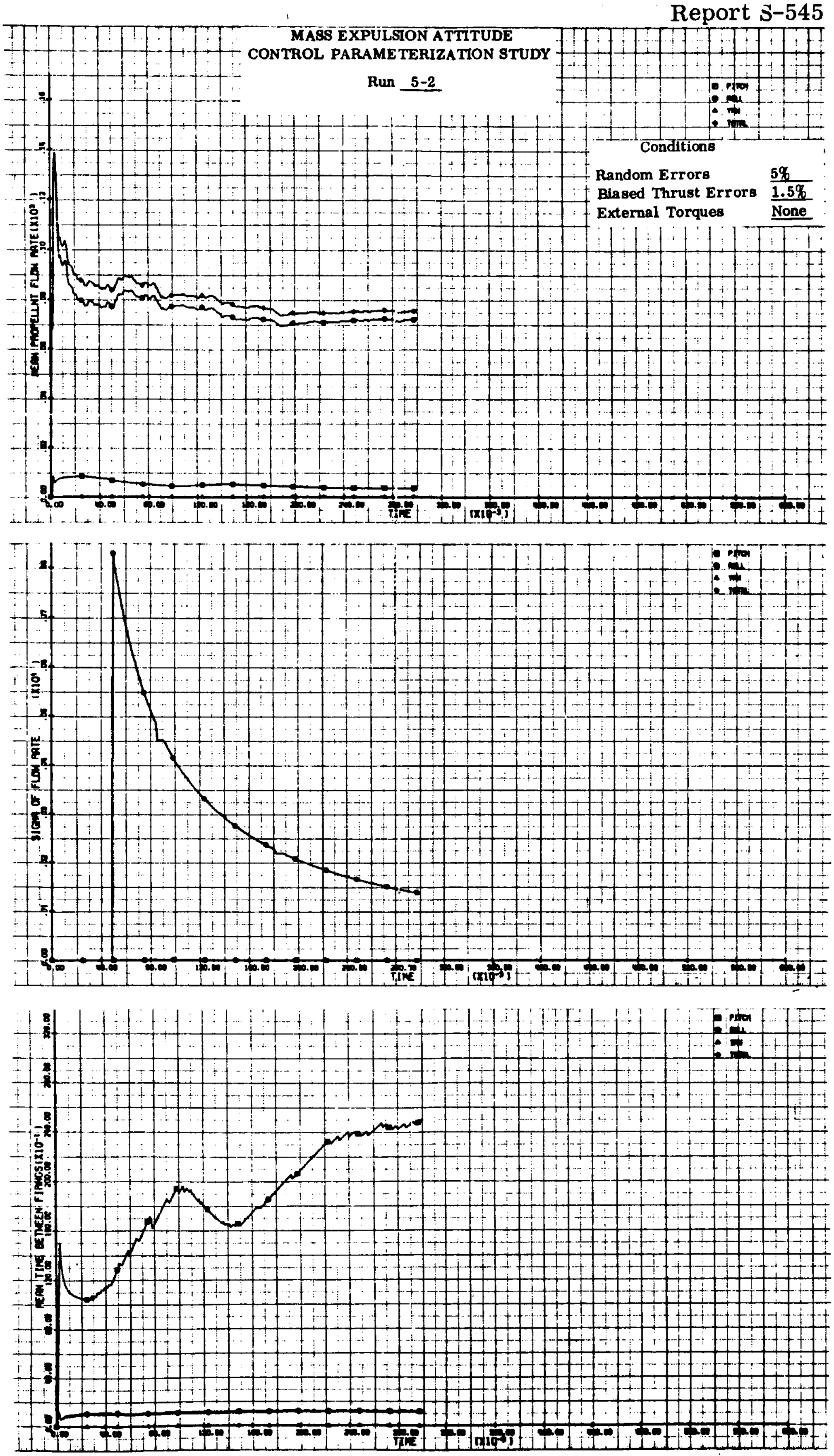
MASS EXPULSION ATTITUDE
CONTROL PARAMETERIZATION STUDY
Run 5-2
Conditions
Random Errors 5%
Biased Thrust Errors 1.5%
External Torques None
TIME
TIME
TIME

Figure 38

MASS EXPULSION ATTITUDE CONTROL PARAMETERIZATION STUDY

Run 5-3

Conditions

Random Errors	5%
Biased Thrust Errors	1.5%
External Torques	None

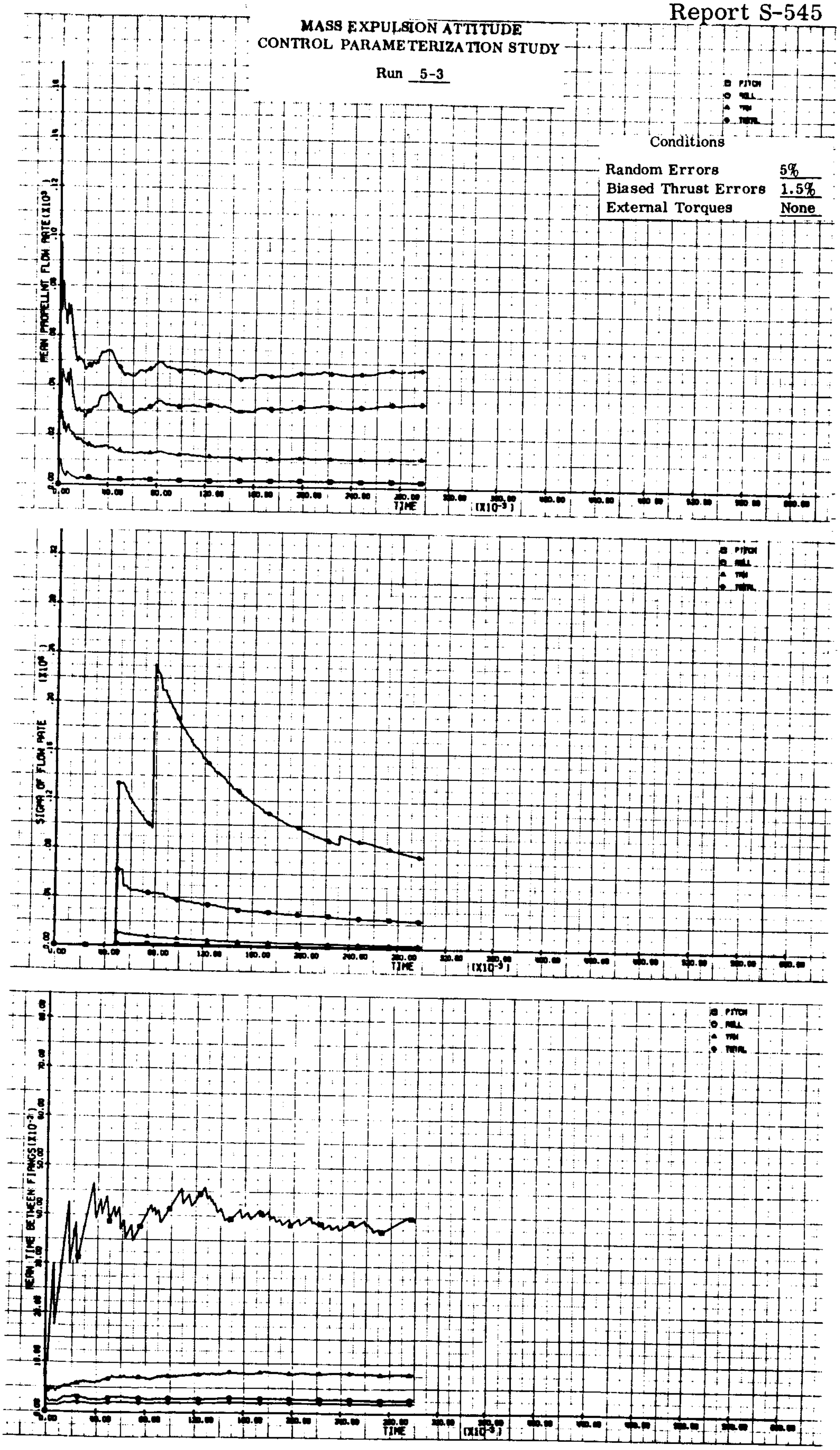

Figure 39

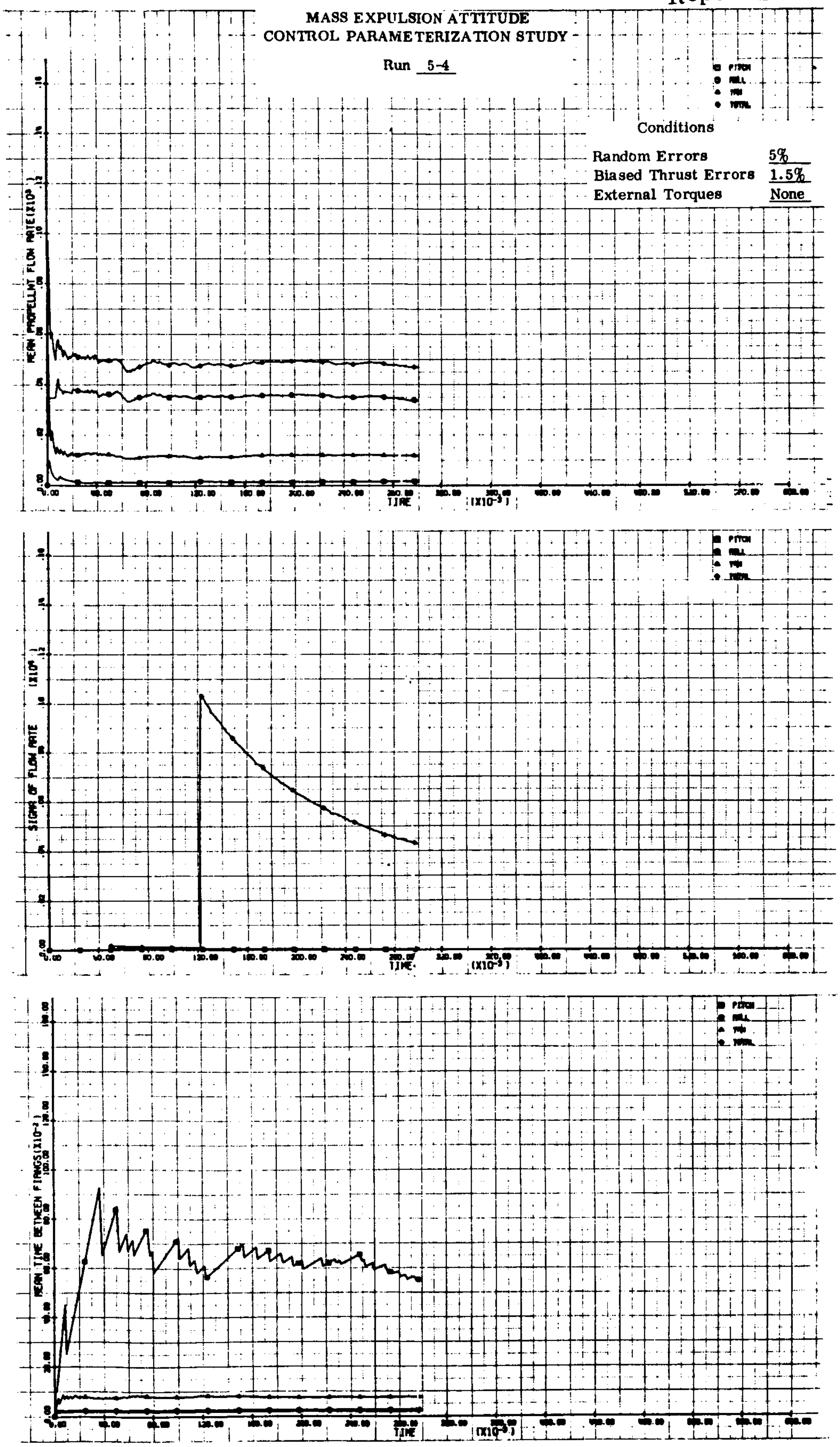
MASS EXPULSION ATTITUDE
CONTROL PARAMETERIZATION STUDY
Run 5-4
Conditions
Random Errors 5%
Biased Thrust Errors 1.5%
External Torques None
TIME
TIME
TIME

Figure 40

MASS EXPULSION ATTITUDE CONTROL PARAMETERIZATION STUDY

Run 6-1

Conditions

Random Errors	5%
Biased Thrust Errors	6.5%
External Torques	None

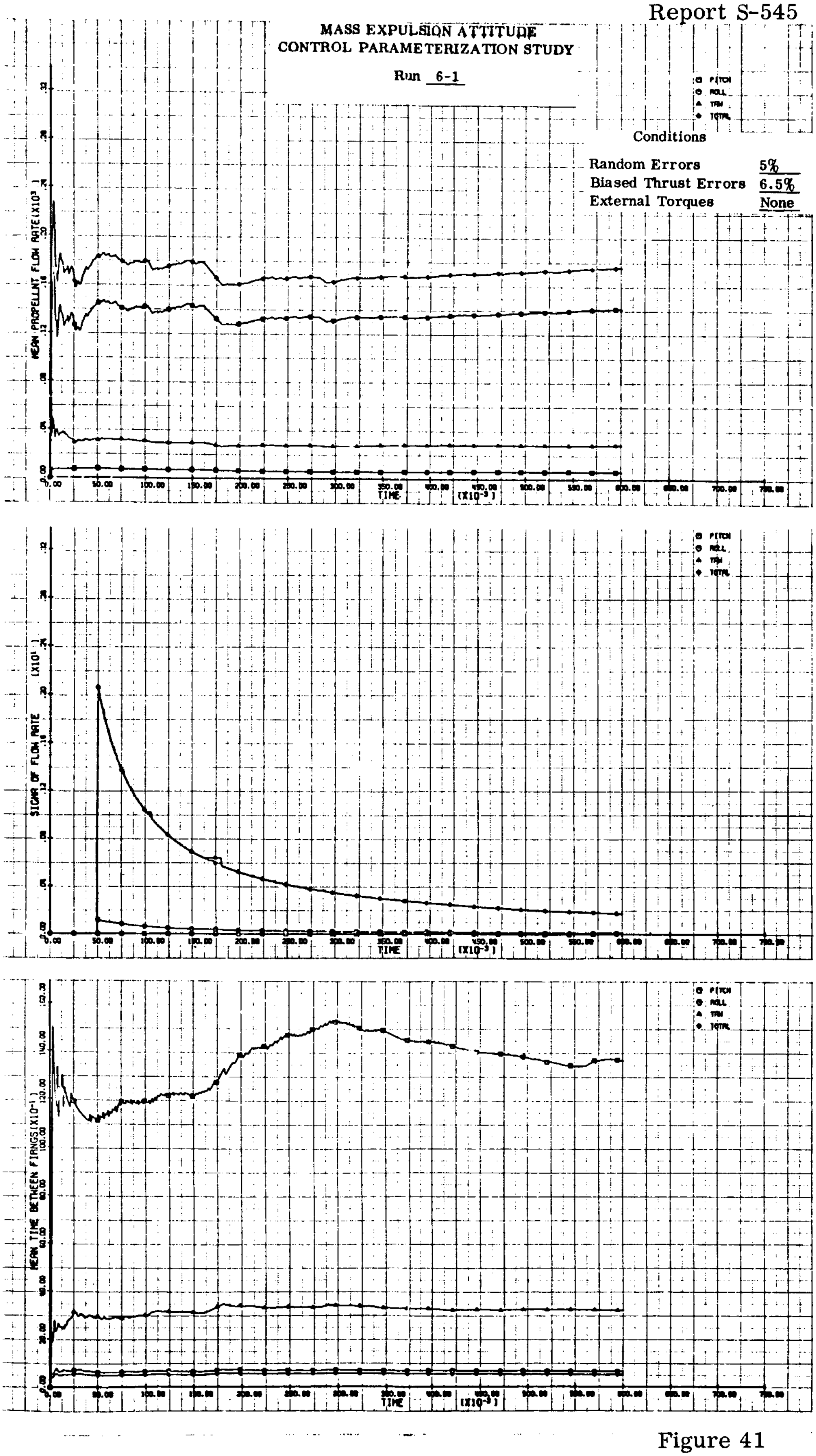

Figure 41

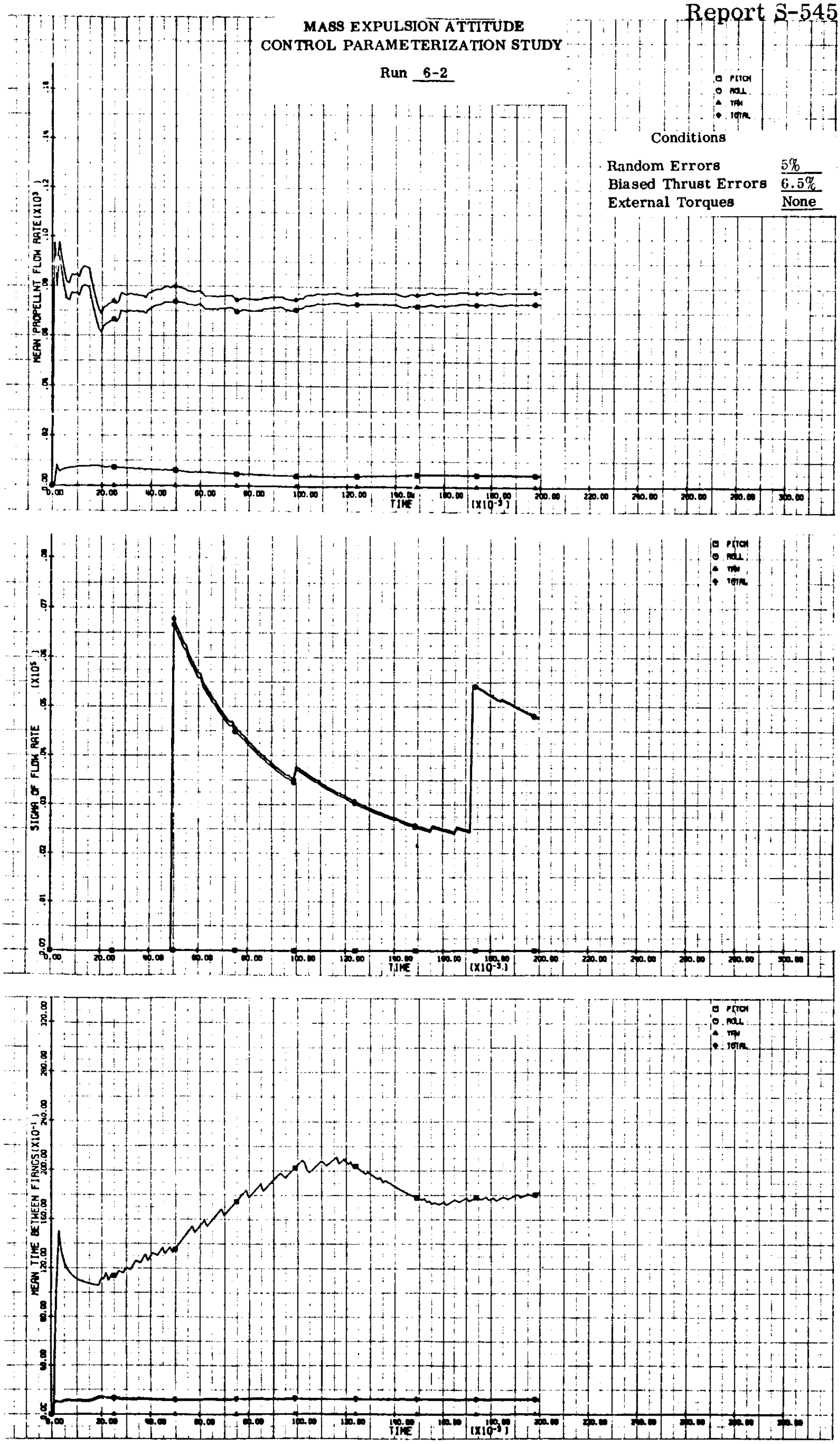
MASS EXPULSION ATTITUDE
CONTROL PARAMETERIZATION STUDY
Run 6-2
PITCH
ROLL
YAW
TOTAL
Conditions
Random Errors 5%
Biased Thrust Errors 6.5%
External Torques None
MEAN PROPELLANT FLOW RATE (X10³)
SIGMA OF FLOW RATE (X10⁵)
MEAN TIME BETWEEN FIRINGS (X10⁻¹)
TIME (X10⁻³)

Figure 42

MASS EXPULSION ATTITUDE
CONTROL PARAMETERIZATION STUDY

Run 6-3

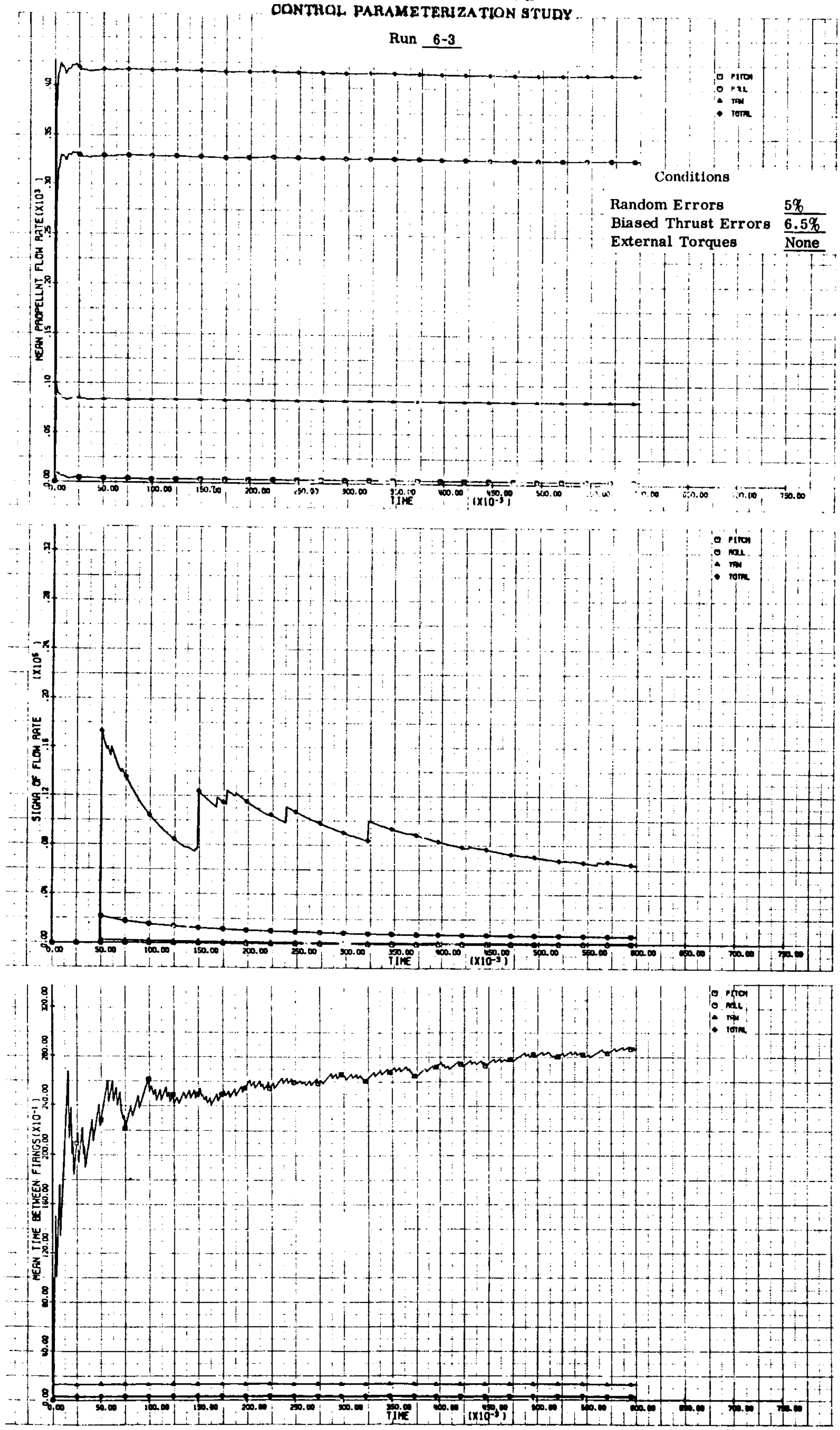

Figure 43

MASS EXPULSION ATTITUDE CONTROL PARAMETERIZATION STUDY

Run 6-4

Conditions

Random Errors	5%
Biased Thrust Errors	6.5%
External Torques	None

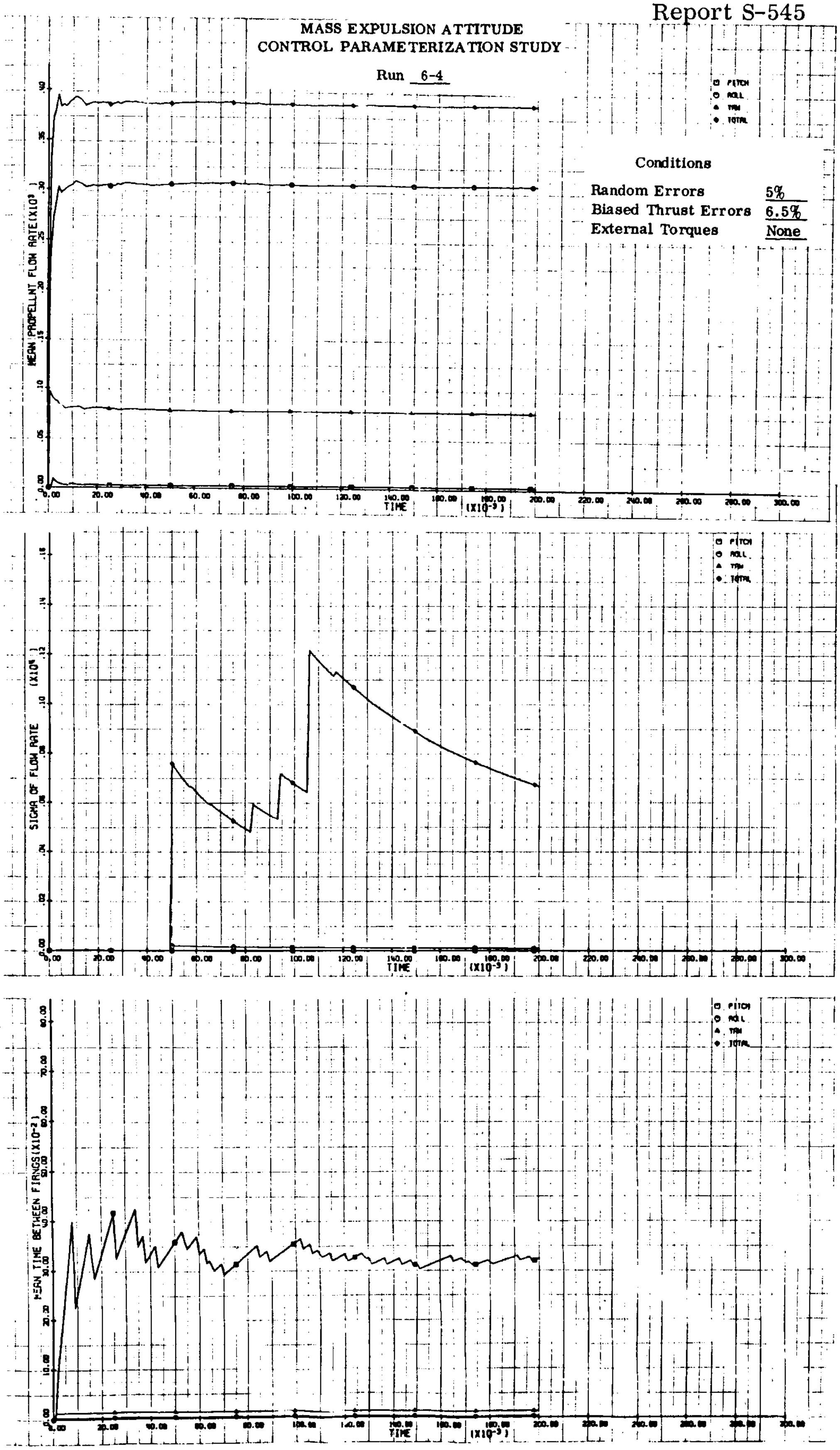

Figure 44

MASS EXPULSION ATTITUDE CONTROL PARAMETERIZATION STUDY

Run 7-1

Conditions

Random Errors	15%
Biased Thrust Errors	6.5%
External Torques	None

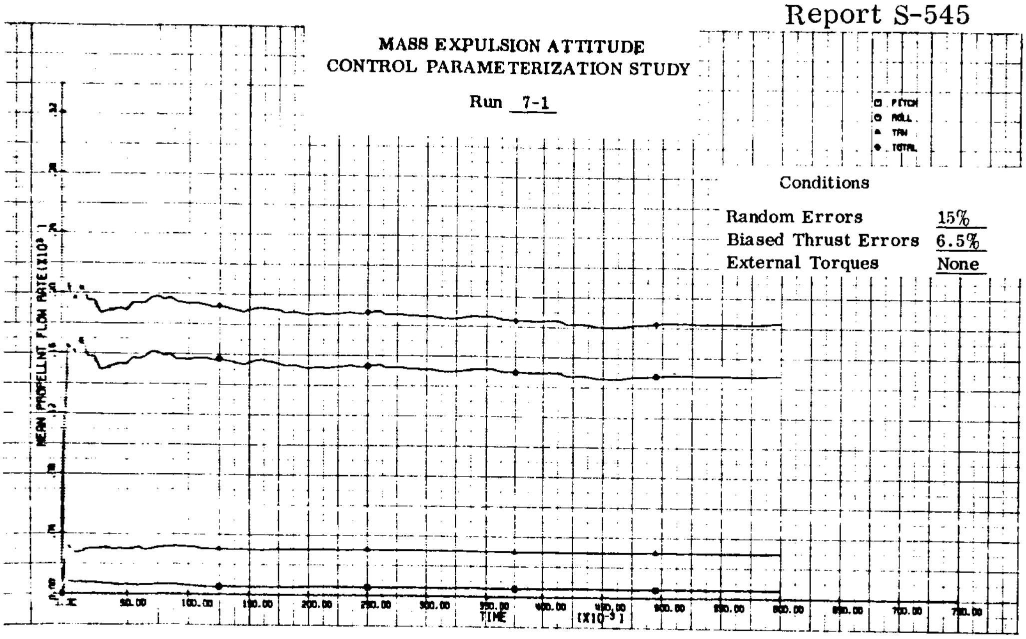

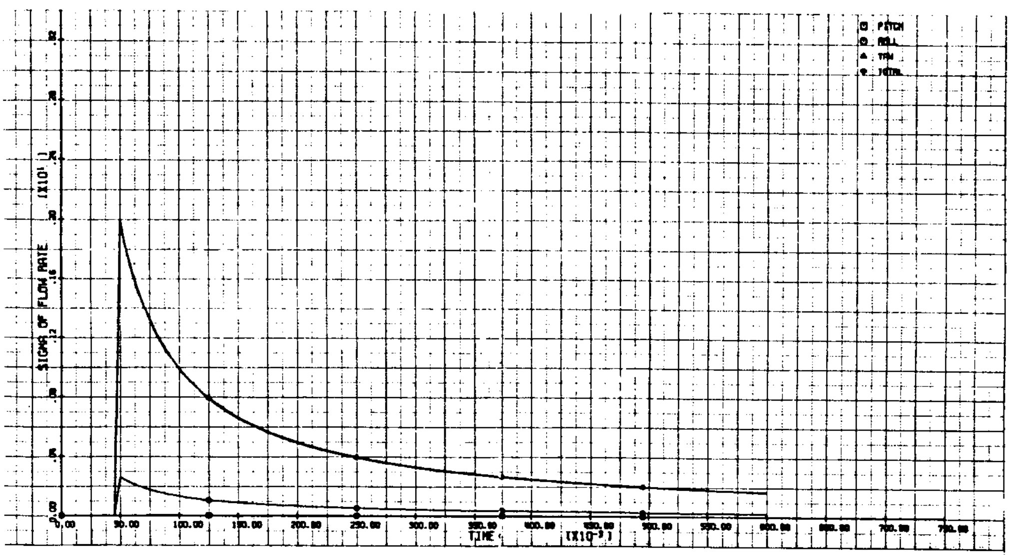

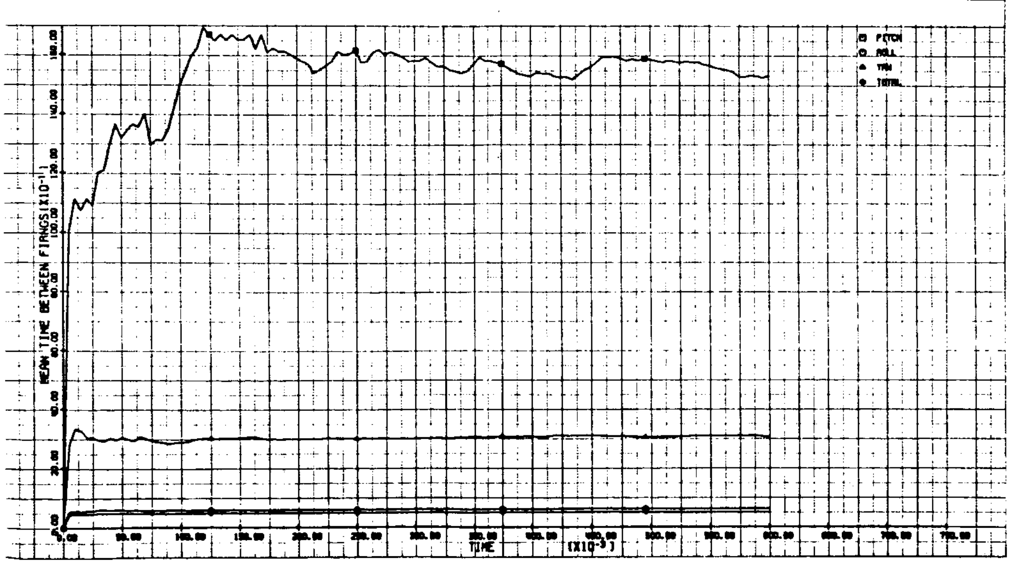

Figure 45

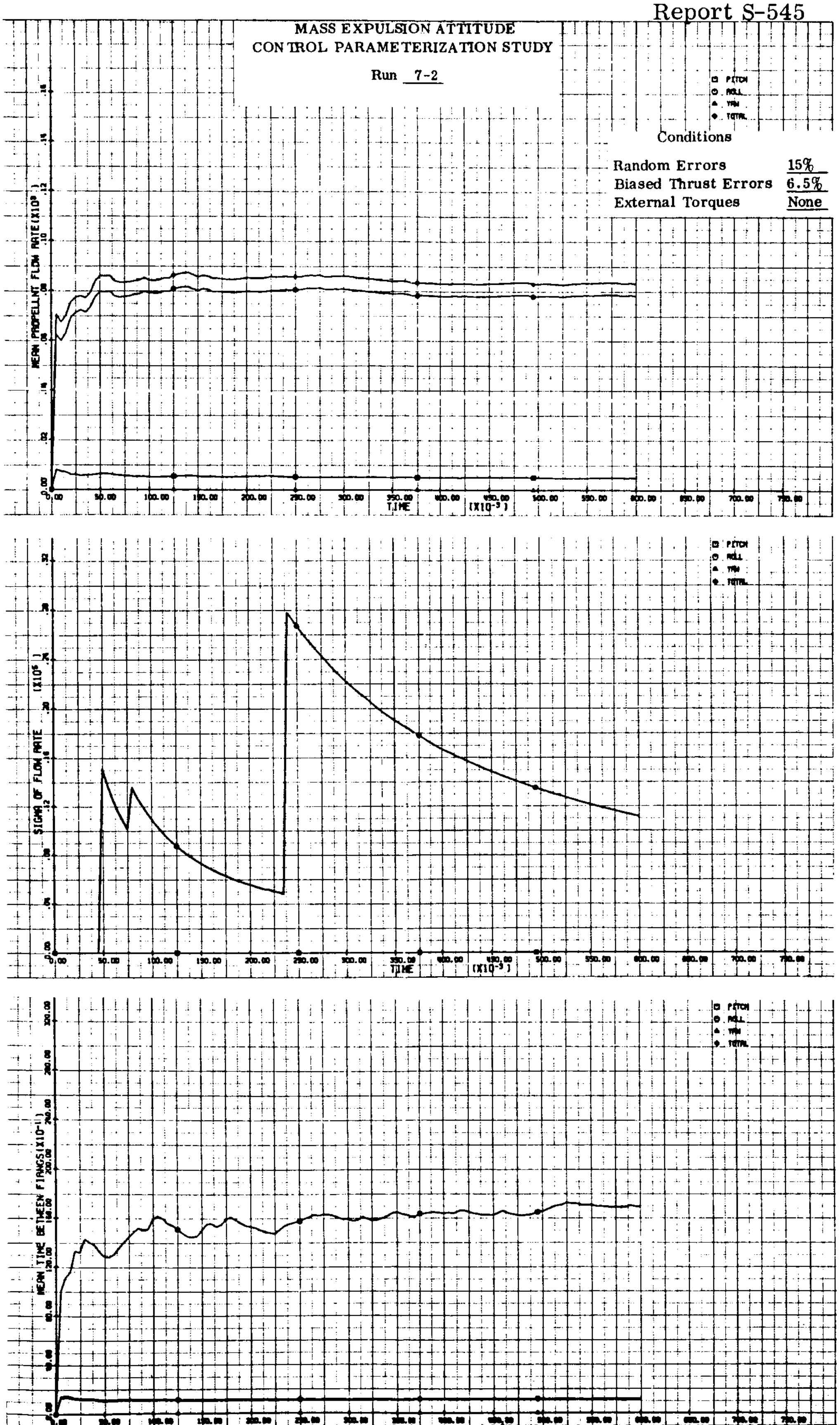
MASS EXPULSION ATTITUDE
CONTROL PARAMETERIZATION STUDY
Run 7-2
Conditions
Random Errors 15%
Biased Thrust Errors 6.5%
External Torques None
PITCH
ROLL
YAW
TOTAL
MEAN PROPELLNT FLOW RATE
SIGMA OF FLOW RATE
MEAN TIME BETWEEN FIRINGS
TIME

Figure 46

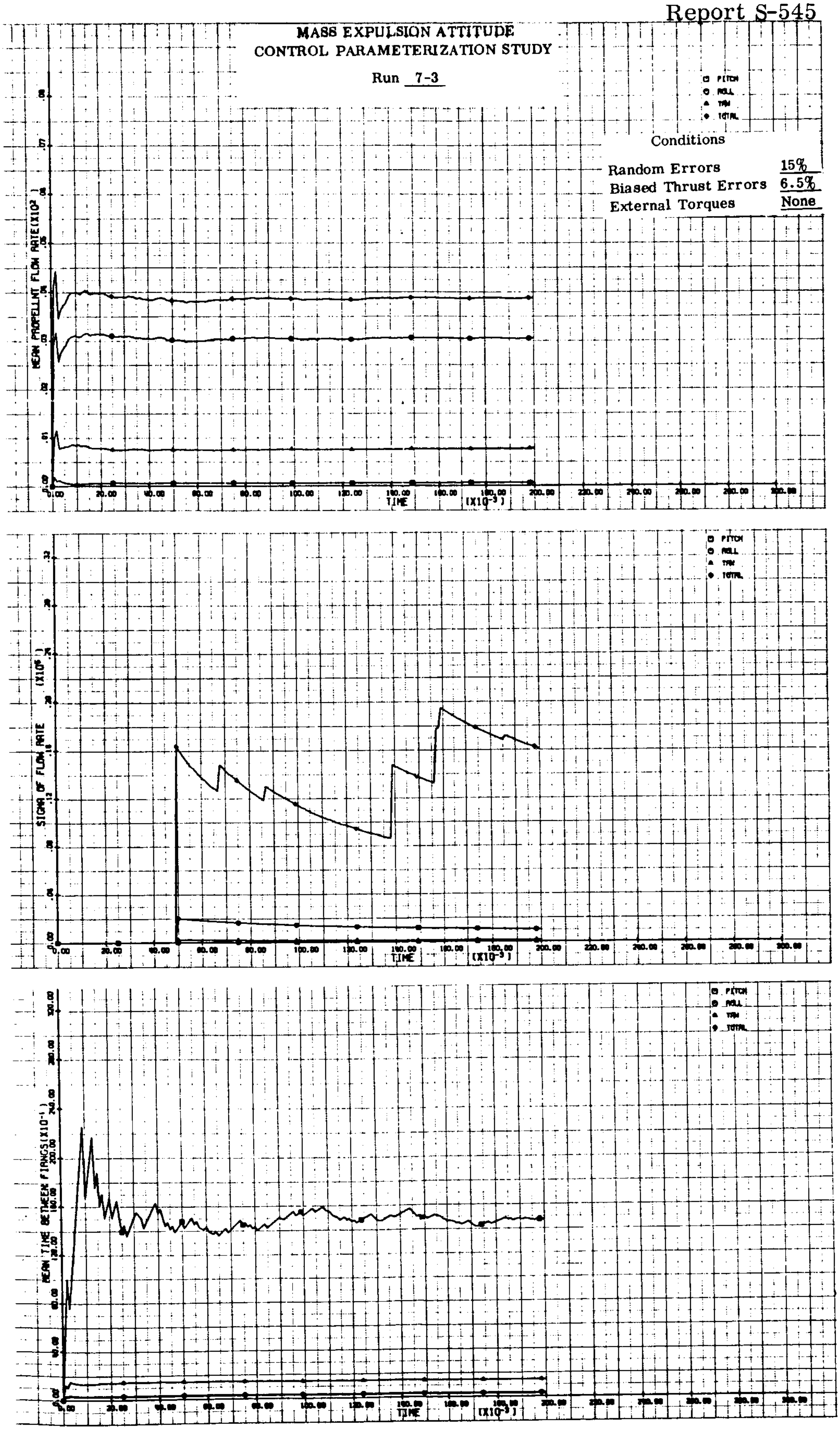
MASS EXPULSION ATTITUDE
CONTROL PARAMETERIZATION STUDY
Run 7-3
PITCH
ROLL
YAW
TOTAL
Conditions
Random Errors 15%
Biased Thrust Errors 6.5%
External Torques None
MEAN PROPELLANT FLOW RATE
TIME
SIGMA OF FLOW RATE
MEAN TIME BETWEEN FIRINGS

Figure 47

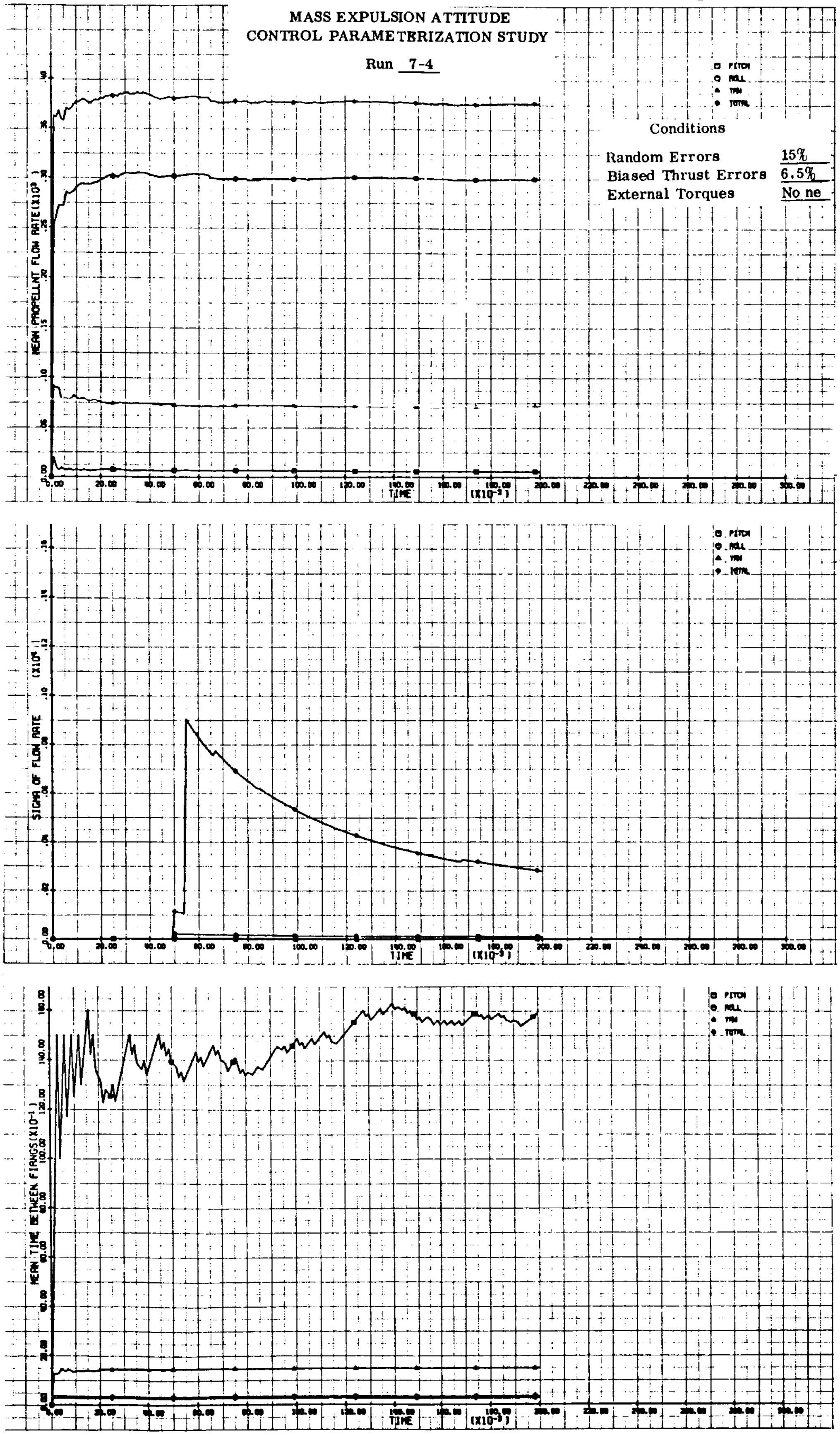
MASS EXPULSION ATTITUDE
CONTROL PARAMETERIZATION STUDY
Run 7-4
PITCH
ROLL
YAW
TOTAL
Conditions
Random Errors 15%
Biased Thrust Errors 6.5%
External Torques None
MEAN PROPELLANT FLOW RATE (X10^3)
SIGMA OF FLOW RATE
MEAN TIME BETWEEN FIRINGS (X10^-1)
TIME
(X10^-3)

Figure 48

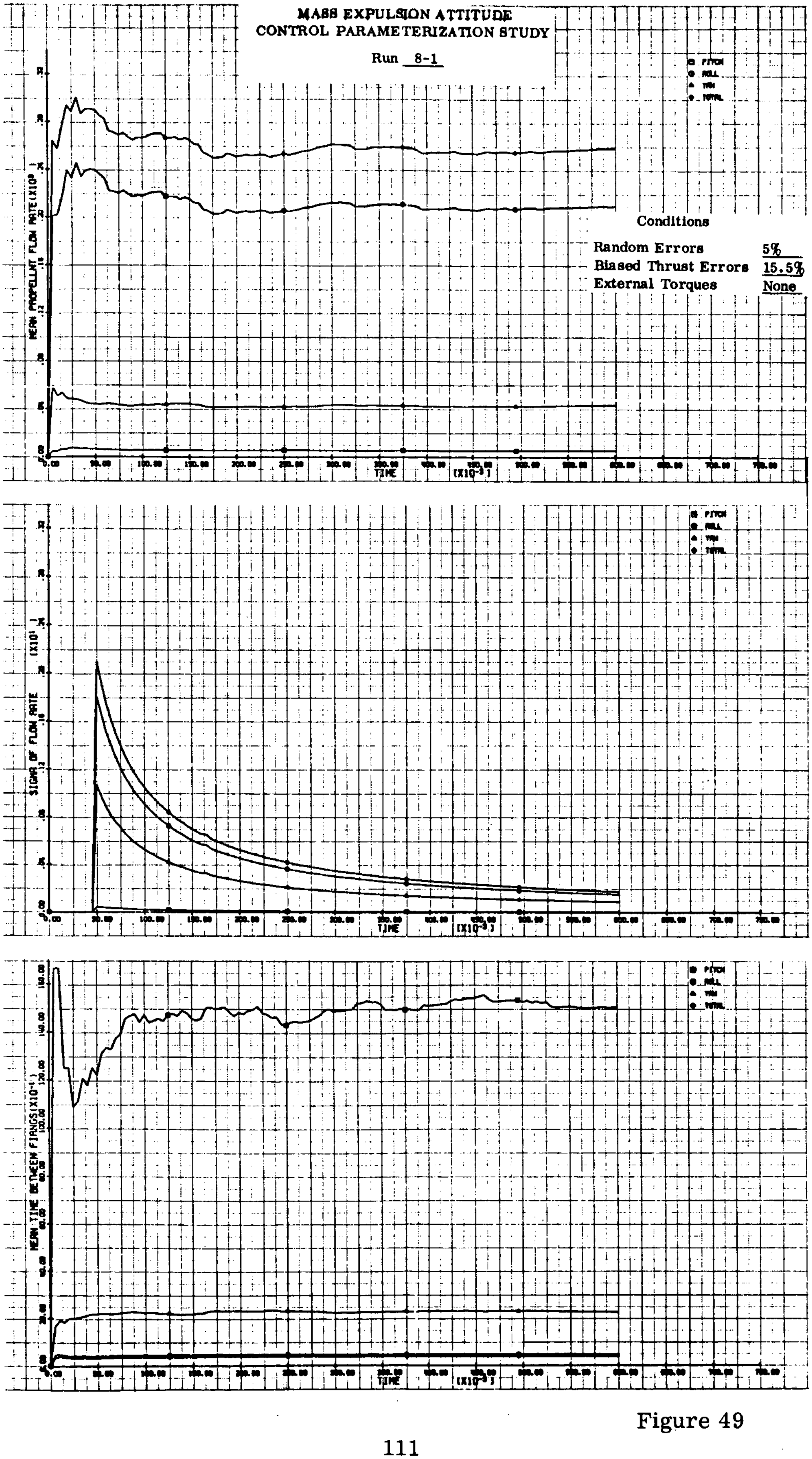
MASS EXPULSION ATTITUDE
CONTROL PARAMETERIZATION STUDY
Run 8-1
Conditions
Random Errors 5%
Biased Thrust Errors 15.5%
External Torques None
PITCH
ROLL
YAW
TOTAL
MEAN PROPELLANT FLOW RATE (X10^-3)
SIGMA OF FLOW RATE (X10^-1)
MEAN TIME BETWEEN FIRINGS (X10^-1)
TIME (X10^-3)

Figure 49

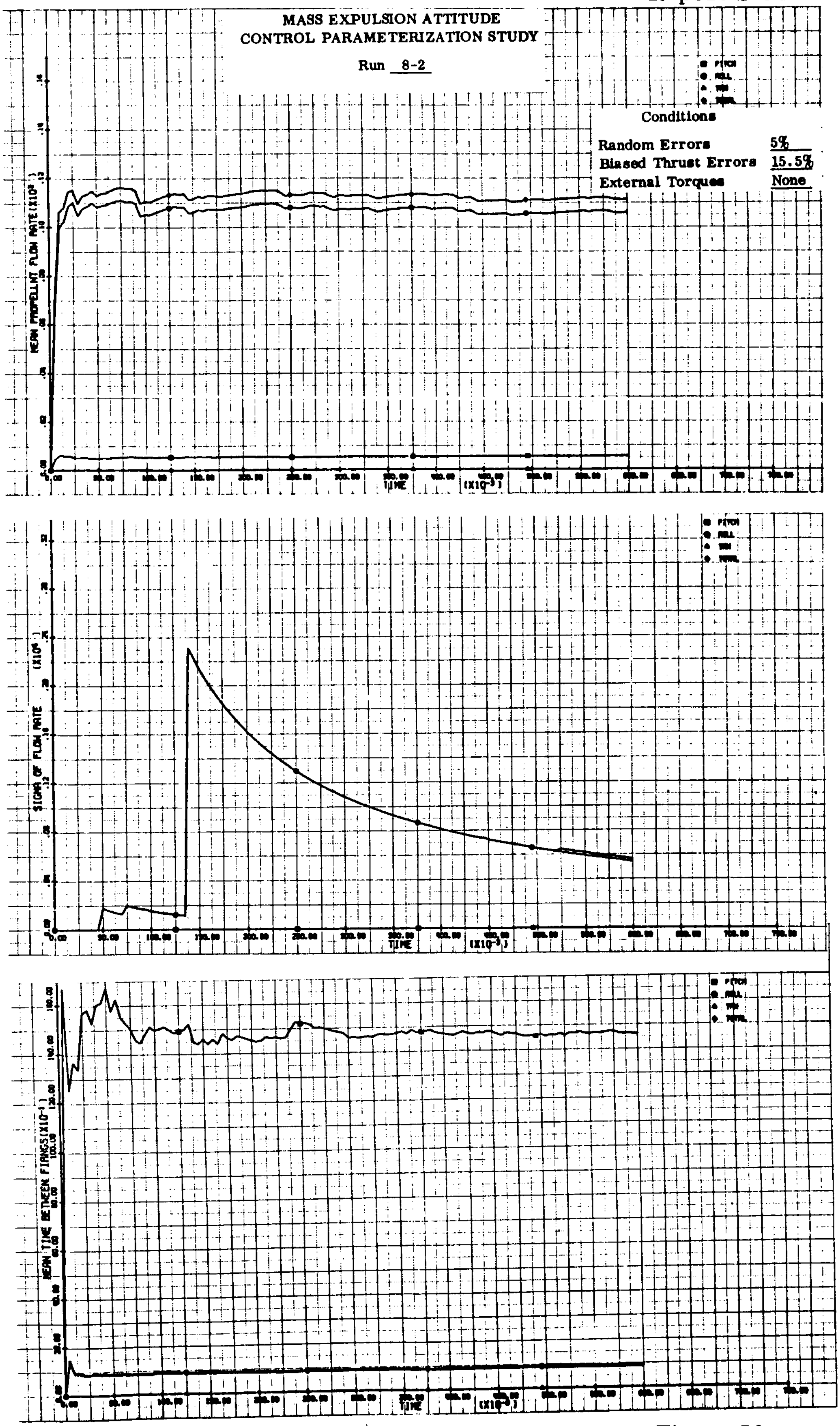
MASS EXPULSION ATTITUDE
CONTROL PARAMETERIZATION STUDY
Run 8-2
Conditions
Random Errors 5%
Biased Thrust Errors 15.5%
External Torques None
MEAN PROPELLANT FLOW RATE
SIGMA OF FLOW RATE
MEAN TIME BETWEEN FIRINGS
TIME

Figure 50

MASS EXPULSION ATTITUDE
CONTROL PARAMETERIZATION STUDY

Run 8-3

Conditions

Random Errors	5%
Biased Thrust Errors	15.5%
External Torques	None

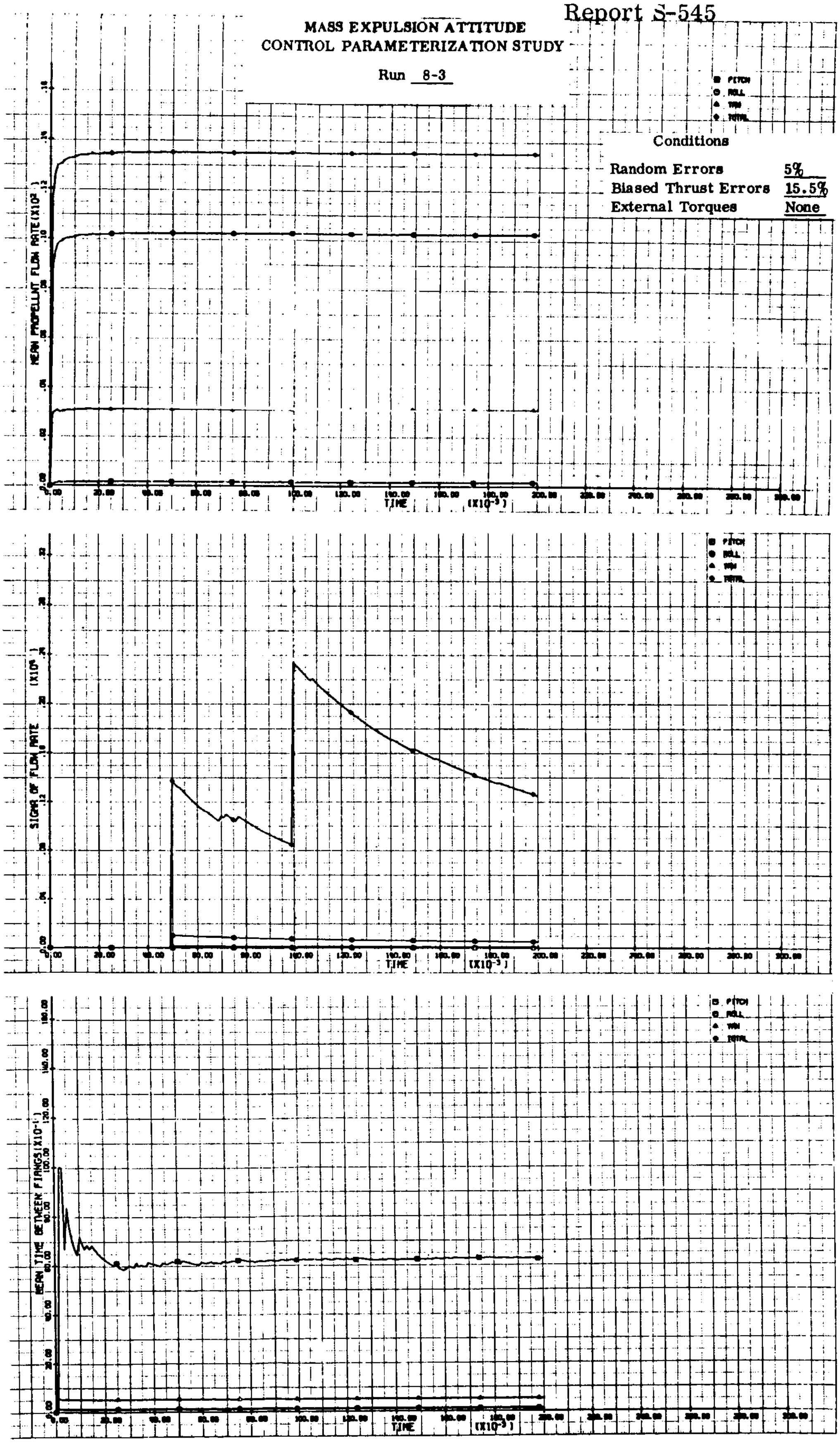

Figure 51

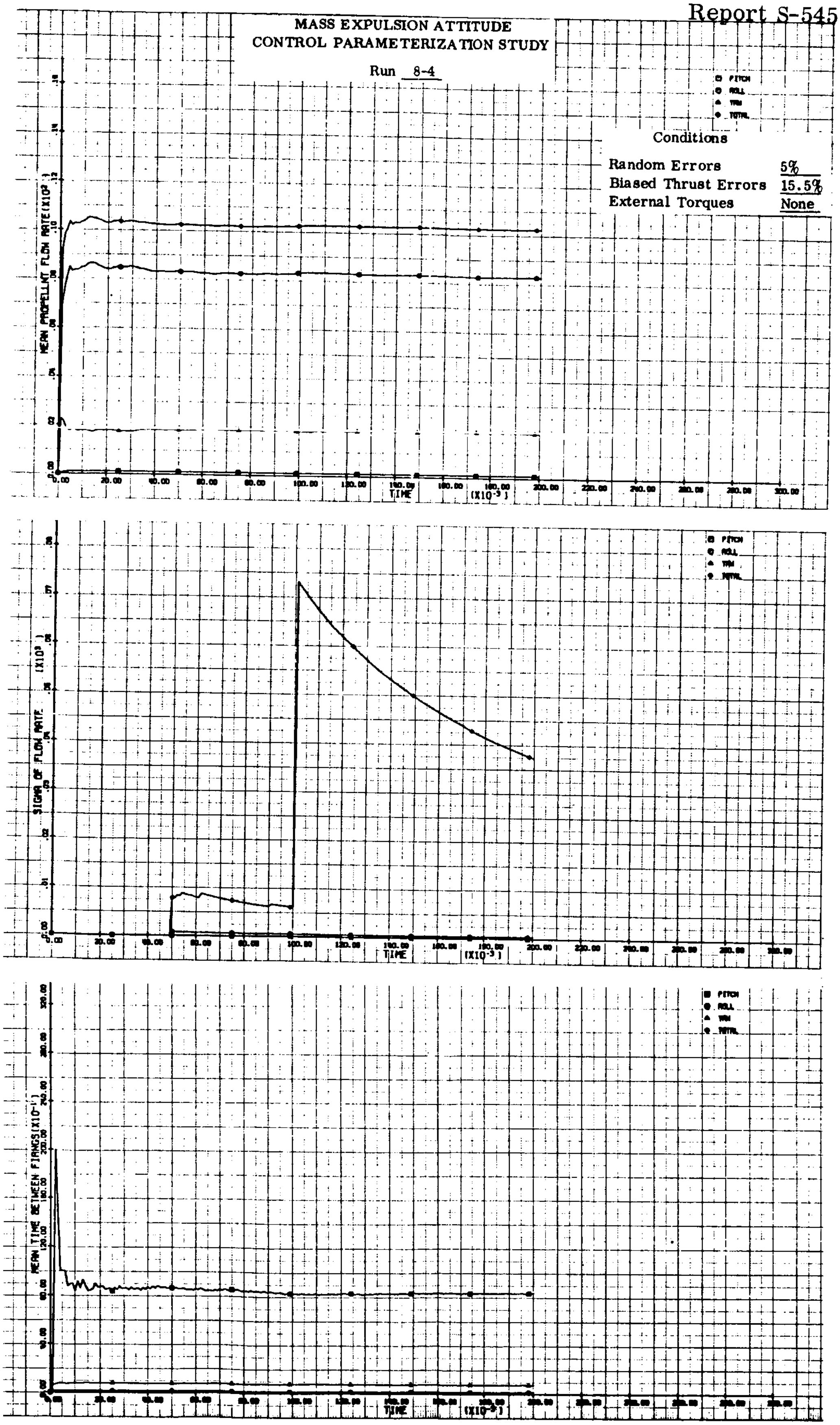
MASS EXPULSION ATTITUDE
CONTROL PARAMETERIZATION STUDY
Run 8-4
Conditions
Random Errors 5%
Biased Thrust Errors 15.5%
External Torques None
PITCH
ROLL
YAW
TOTAL
MEAN PROPELLANT FLOW RATE (X10^2)
TIME
(X10^-3)
SIGMA OF FLOW RATE (X10^3)
MEAN TIME BETWEEN FIRINGS (X10^-1)

Figure 52

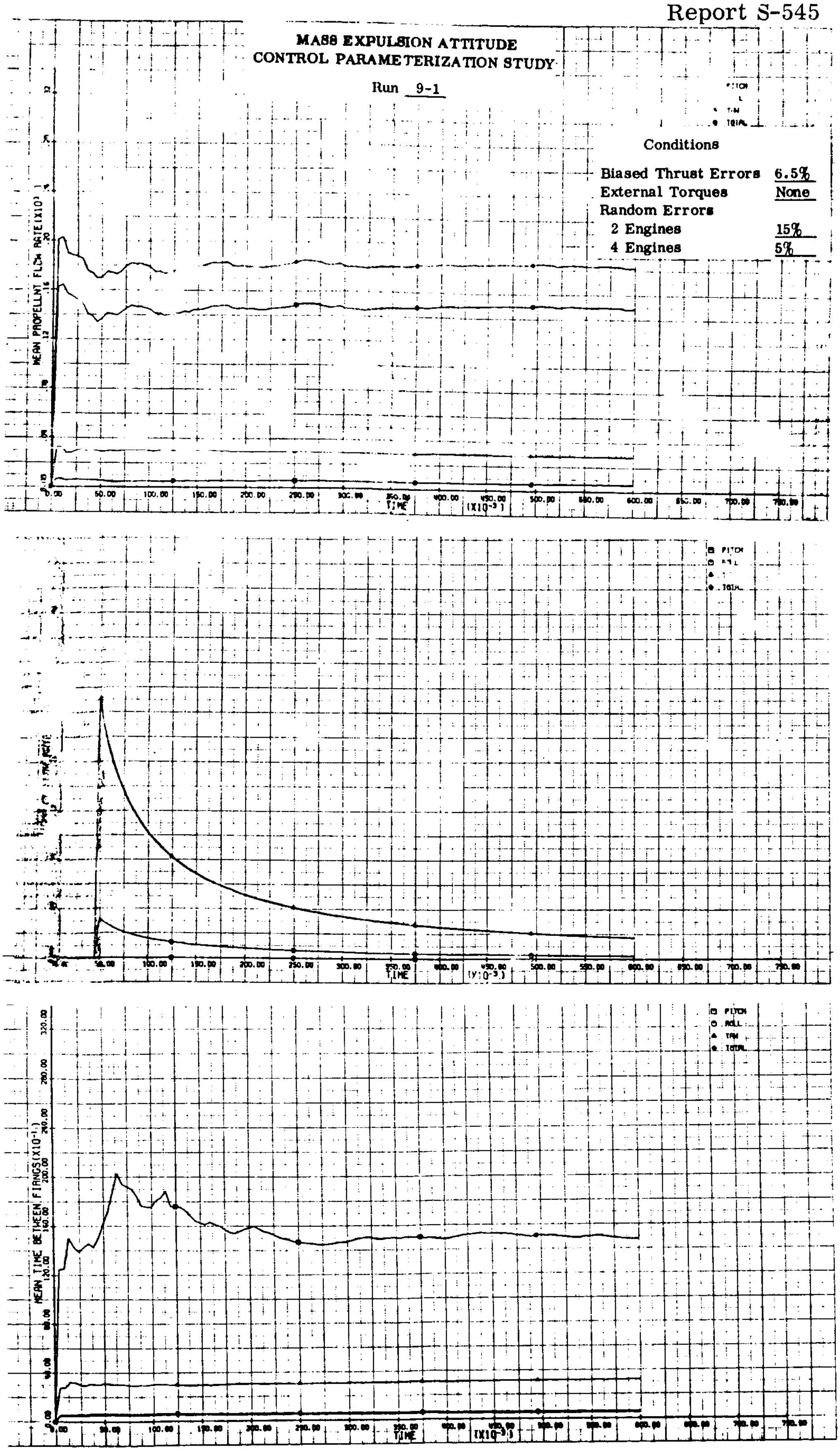
MASS EXPULSION ATTITUDE
CONTROL PARAMETERIZATION STUDY
Run 9-1
Conditions
Biased Thrust Errors 6.5%
External Torques None
Random Errors
2 Engines 15%
4 Engines 5%
MEAN PROPELLANT FLOW RATE (X10^{-1})
TIME (X10^{-3})
MEAN TIME BETWEEN FIRINGS (X10^{-1})
PITCH
ROLL
YAW
TOTAL

Figure 53

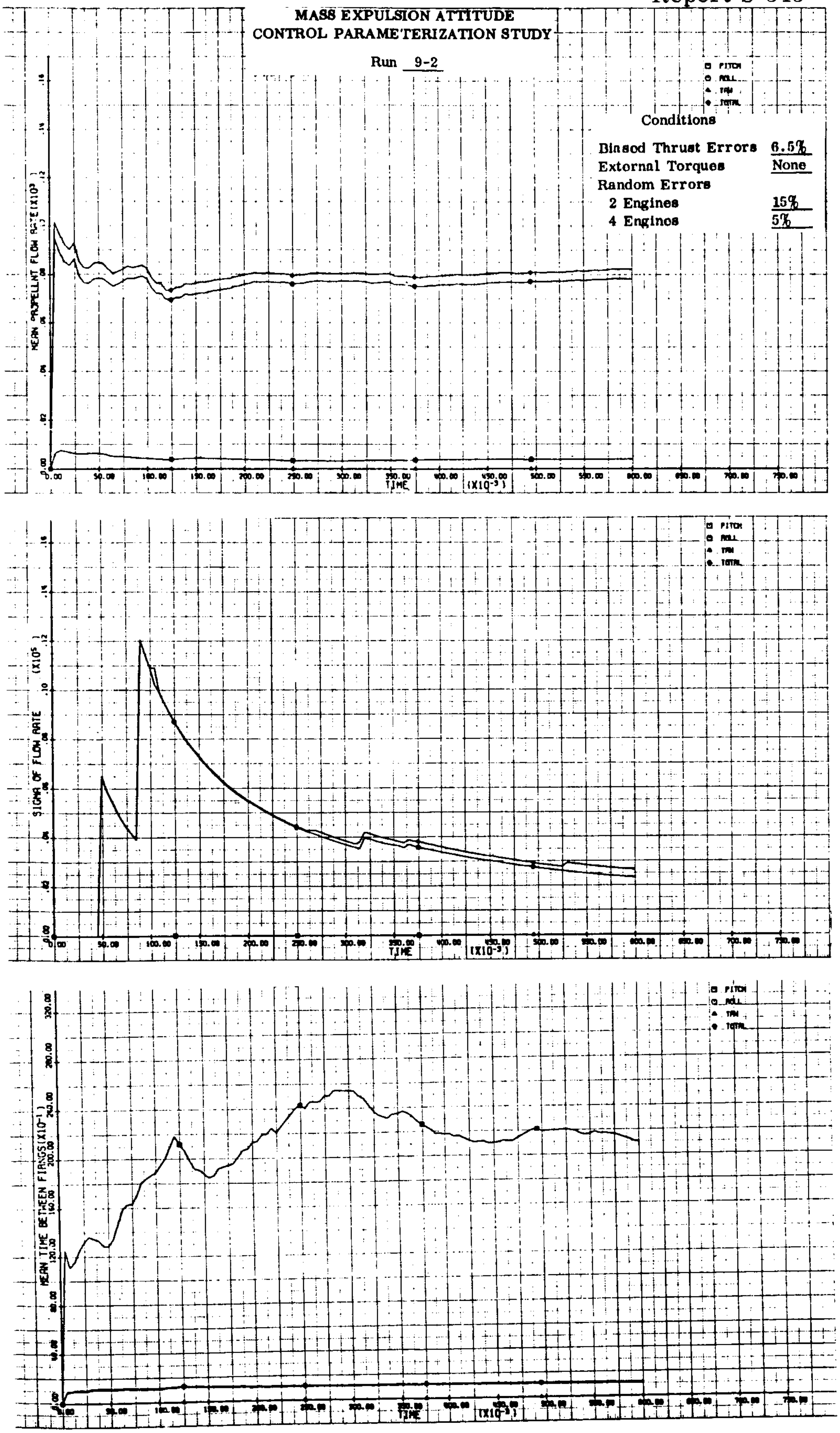
MASS EXPULSION ATTITUDE
CONTROL PARAMETERIZATION STUDY
Run 9-2
Conditions
Biased Thrust Errors 6.5%
External Torques None
Random Errors
2 Engines 15%
4 Engines 5%
MEAN PROPELLANT FLOW RATE (X10³)
SIGMA OF FLOW RATE (X10⁵)
MEAN TIME BETWEEN FIRINGS (X10⁻¹)
TIME (X10⁻³)
PITCH
ROLL
YAW
TOTAL

Figure 54

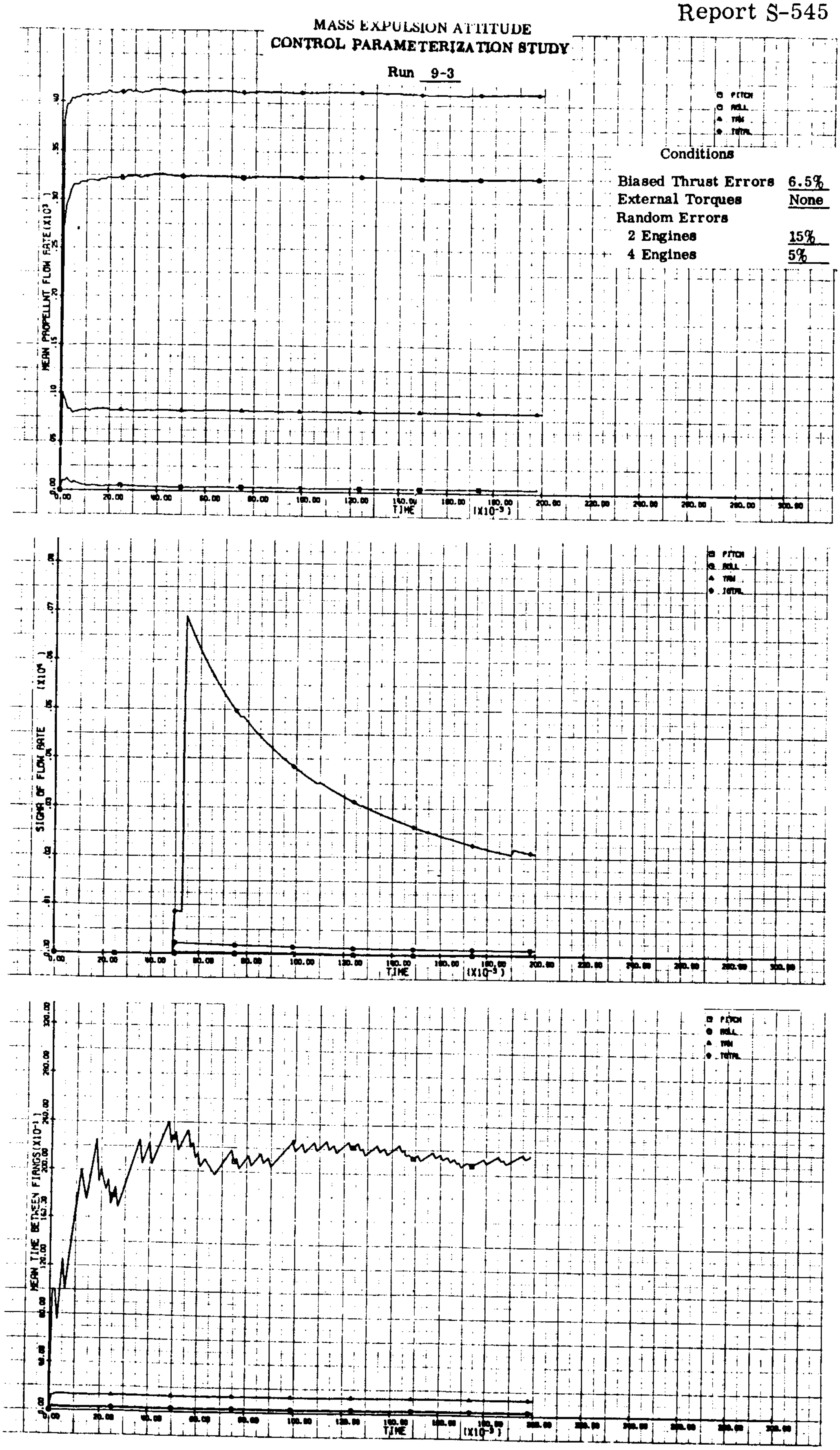
MASS EXPULSION ATTITUDE
CONTROL PARAMETERIZATION STUDY
Run 9-3
PITCH
ROLL
YAW
TOTAL
Conditions
Biased Thrust Errors 6.5%
External Torques None
Random Errors
2 Engines 15%
4 Engines 5%
MEAN PROPELLANT FLOW RATE (X10³)
TIME (X10⁻³)
SIGMA OF FLOW RATE (X10⁴)
TIME (X10⁻³)
MEAN TIME BETWEEN FIRINGS (X10⁻¹)
TIME (X10⁻³)

Figure 55

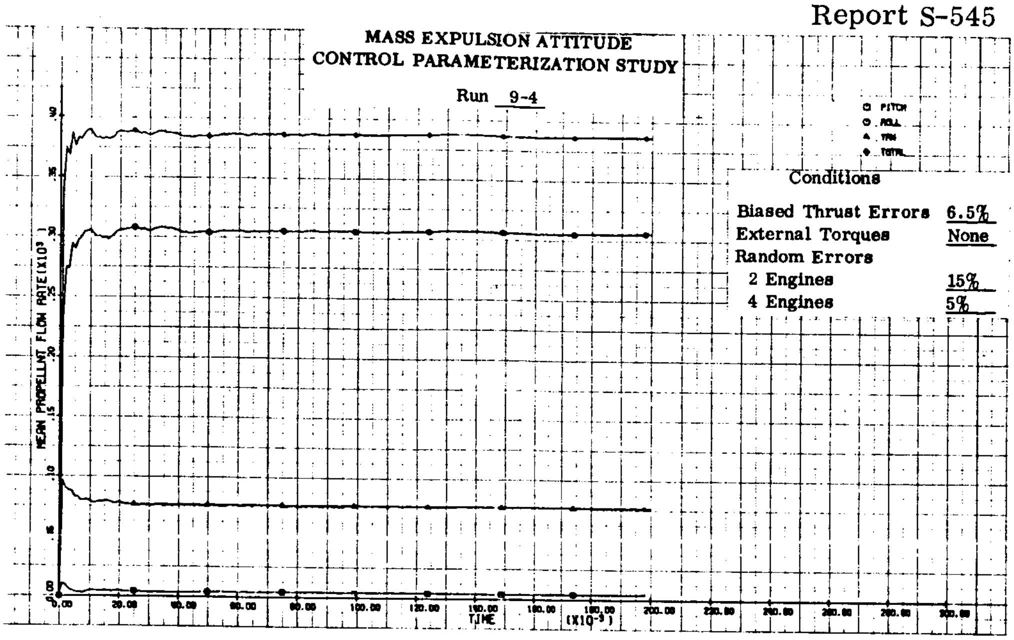
MASS EXPULSION ATTITUDE
CONTROL PARAMETERIZATION STUDY
Run 9-4
Conditions
Biased Thrust Errors 6.5%
External Torques None
Random Errors
2 Engines 15%
4 Engines 5%
PITCH
ROLL
YAW
TOTAL
MEAN PROPELLANT FLOW RATE
TIME

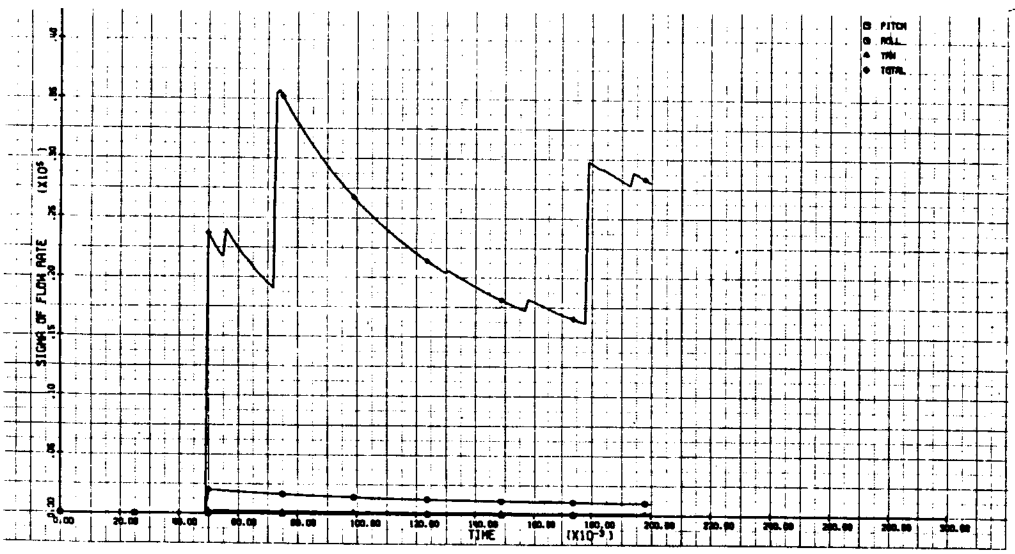
PITCH
ROLL
YAW
TOTAL
SIGMA OF FLOW RATE
TIME

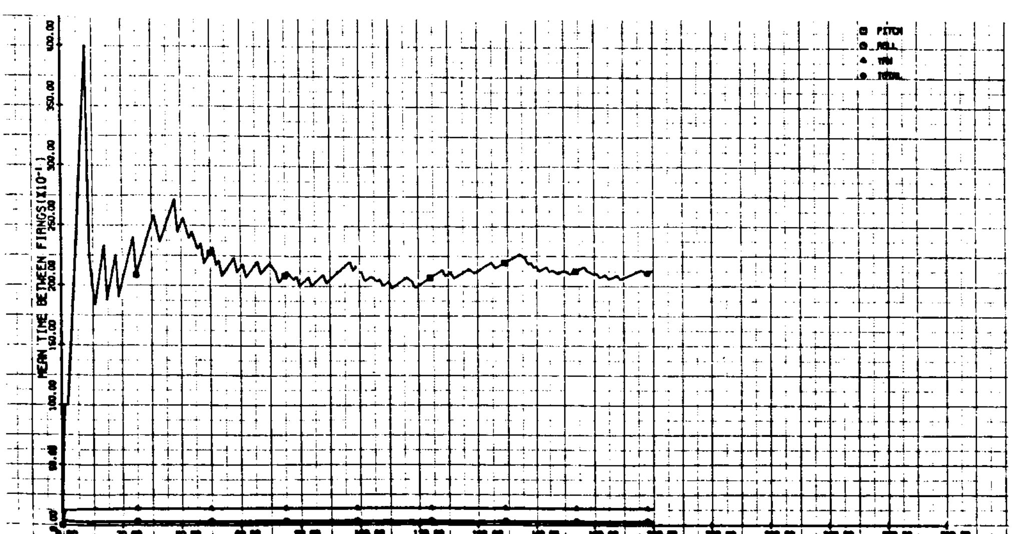
PITCH
ROLL
YAW
TOTAL
MEAN TIME BETWEEN FIRINGS
TIME

Figure 56

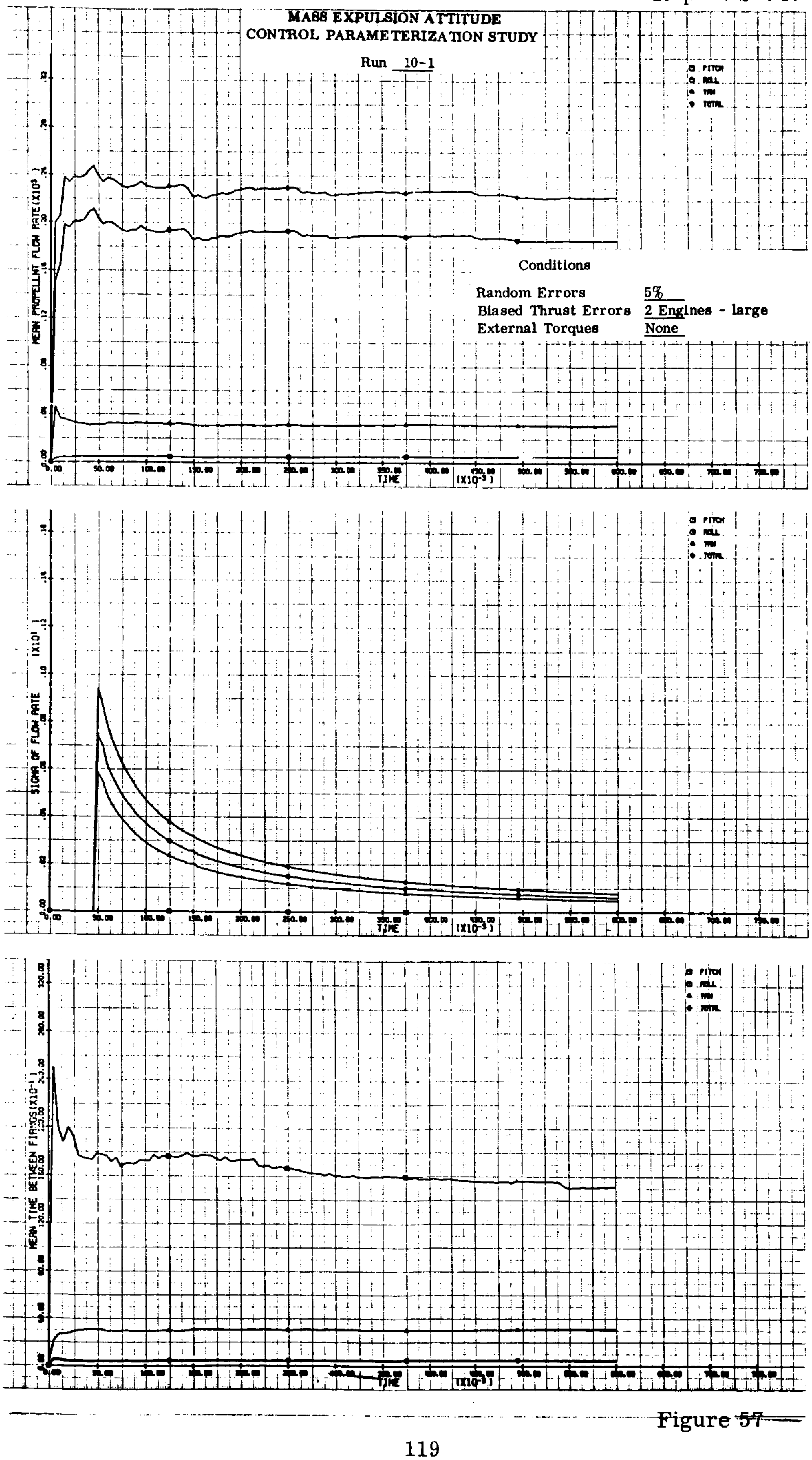
MASS EXPULSION ATTITUDE
CONTROL PARAMETERIZATION STUDY
Run 10-1
Conditions
Random Errors 5%
Biased Thrust Errors 2 Engines - large
External Torques None
MEAN PROPELLANT FLOW RATE (X10³)
SIGMA OF FLOW RATE (X10¹)
MEAN TIME BETWEEN FIRINGS (X10⁻¹)
TIME (X10⁻³)
PITCH
ROLL
YAW
TOTAL

Figure 57

MASS EXPULSION ATTITUDE CONTROL PARAMETERIZATION STUDY

Run 10-2

Conditions

Random Errors	5%
Biased Thrust Errors	2 Engines - large
External Torques	None

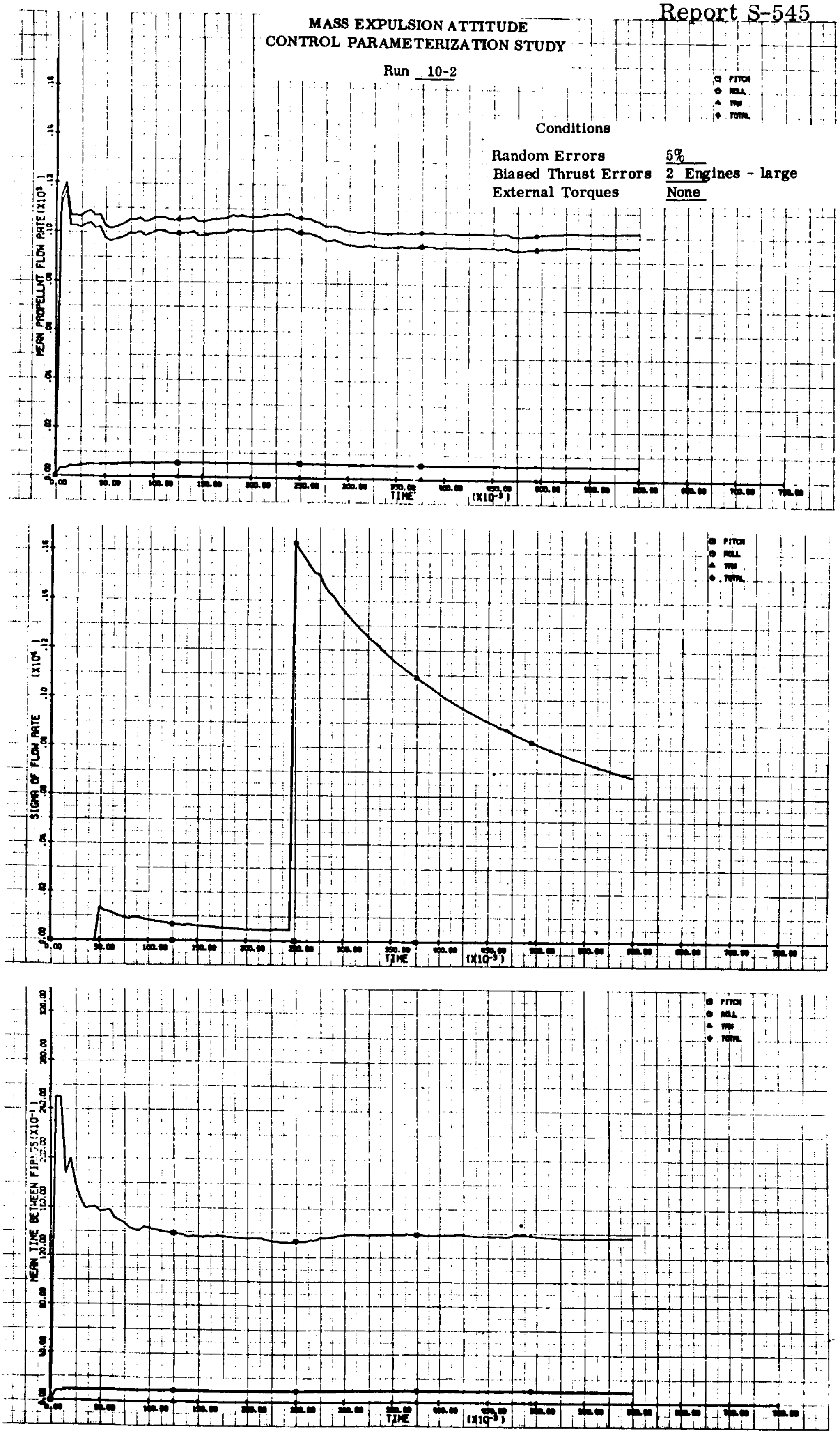

Figure 58

MASS EXPULSION ATTITUDE
CONTROL PARAMETERIZATION STUDY

Run 10-3

Conditions

Random Errors 5%
Biased Thrust Errors 2 Engines - large
External Torques None

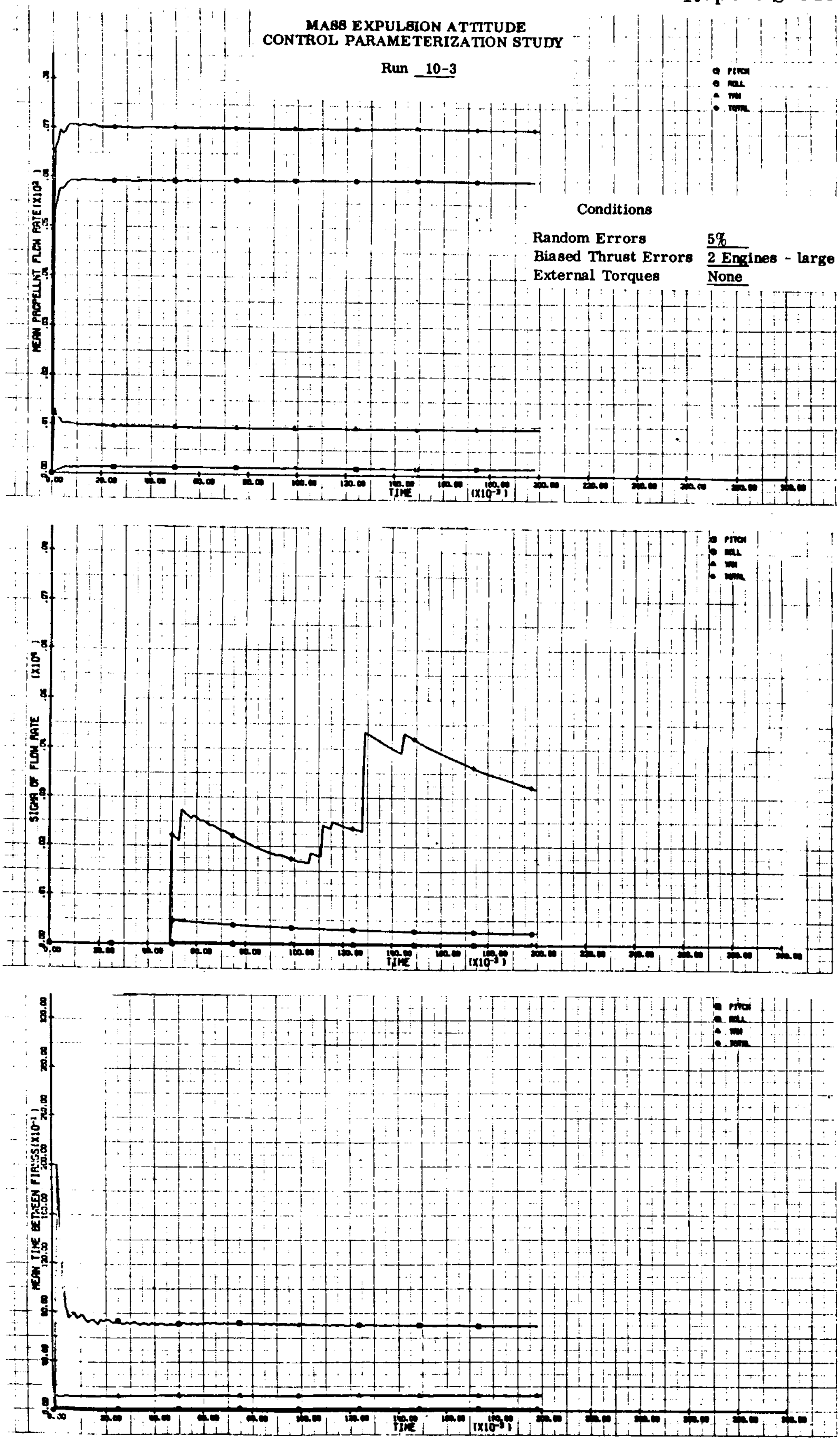

Figure 59

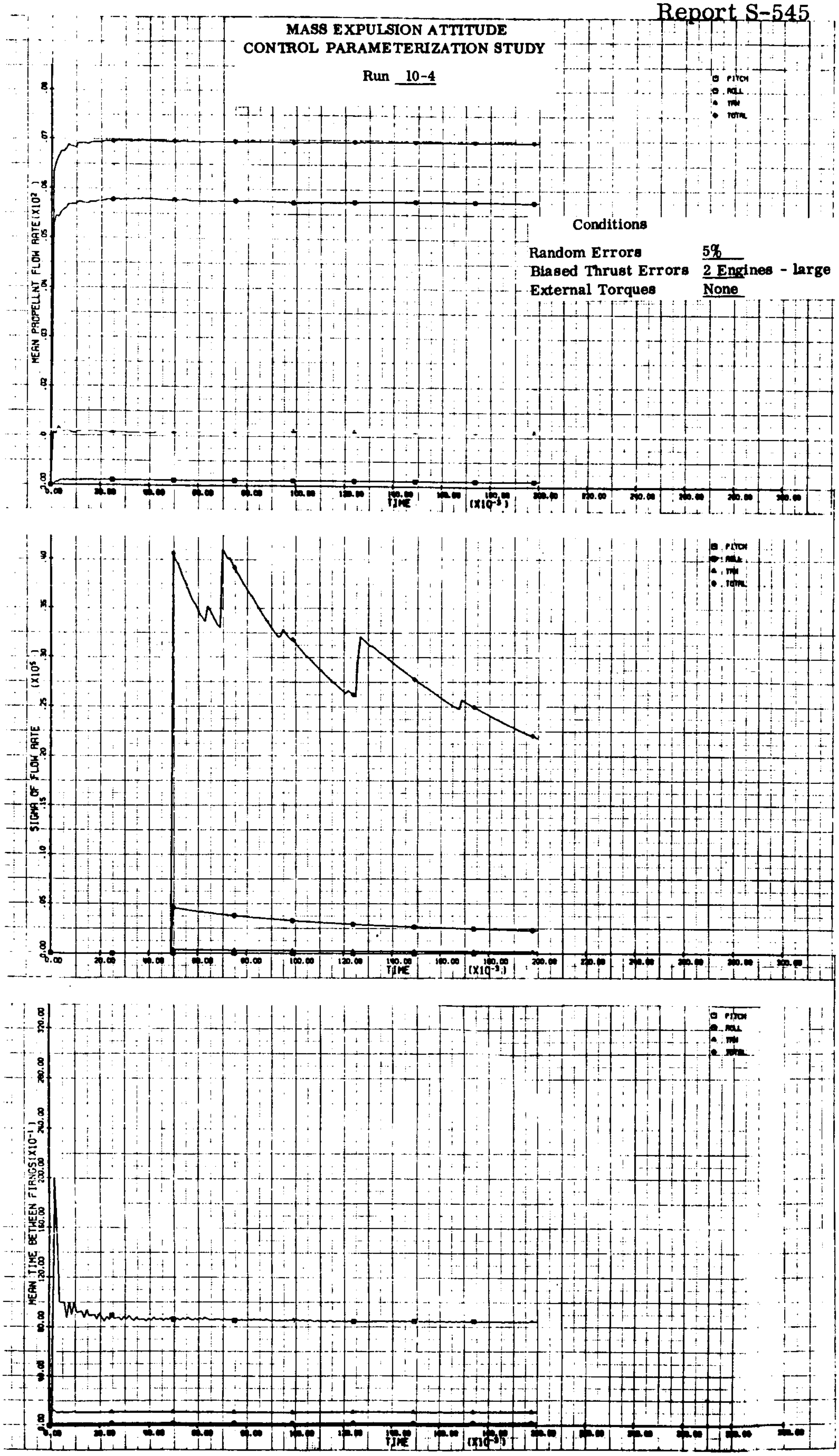
MASS EXPULSION ATTITUDE
CONTROL PARAMETERIZATION STUDY
Run 10-4
Conditions
Random Errors 5%
Biased Thrust Errors 2 Engines - large
External Torques None
MEAN PROPELLANT FLOW RATE (X10^2)
SIGMA OF FLOW RATE (X10^5)
MEAN TIME BETWEEN FIRINGS (X10^-1)
TIME (X10^-3)
PITCH
ROLL
YAW
TOTAL

Figure 60

MASS EXPULSION ATTITUDE CONTROL PARAMETERIZATION STUDY

Run 11-1

Conditions

Random Errors	5%
Biased Thrust Errors	0
External Torques	Light

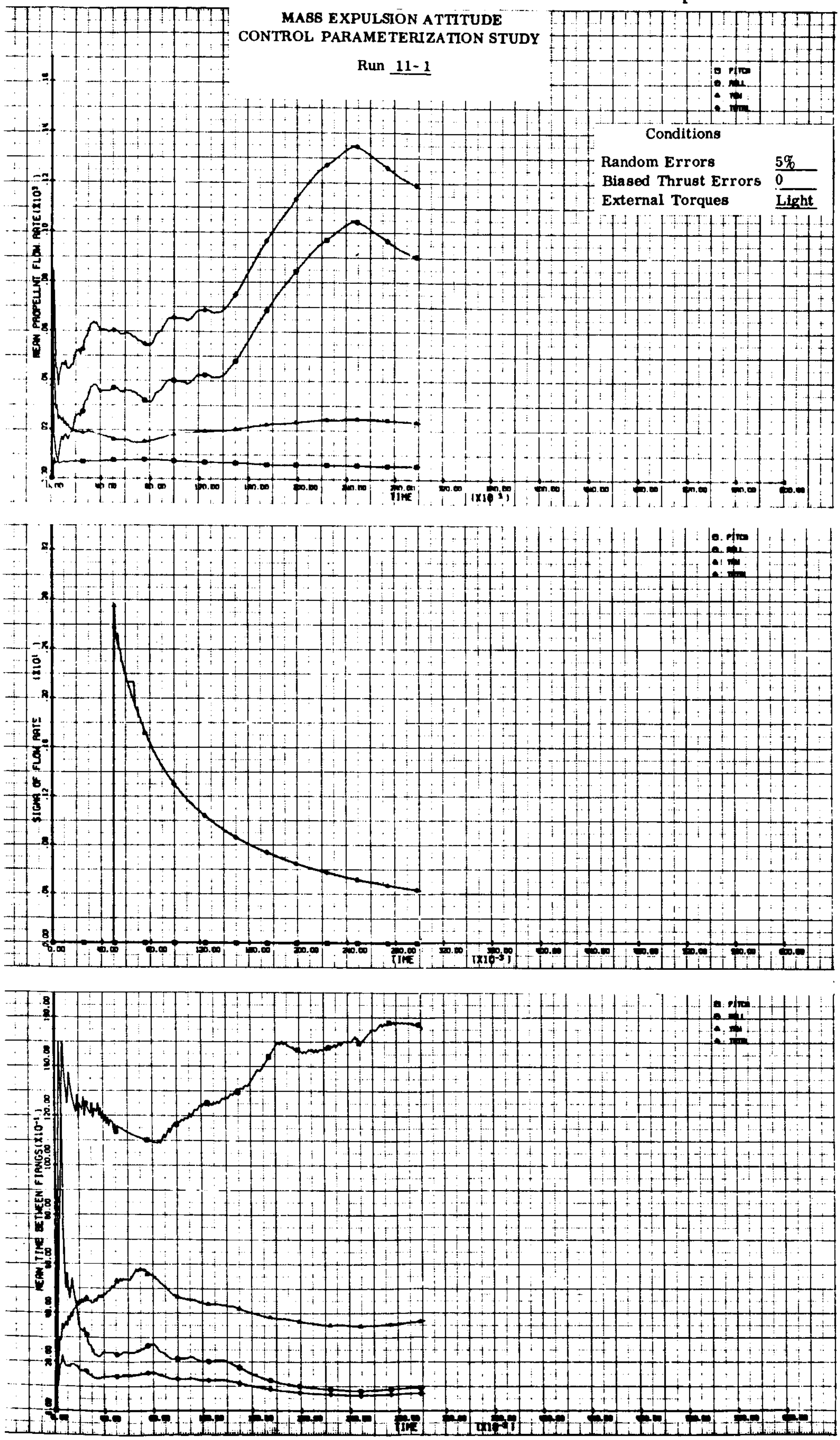

Figure 61

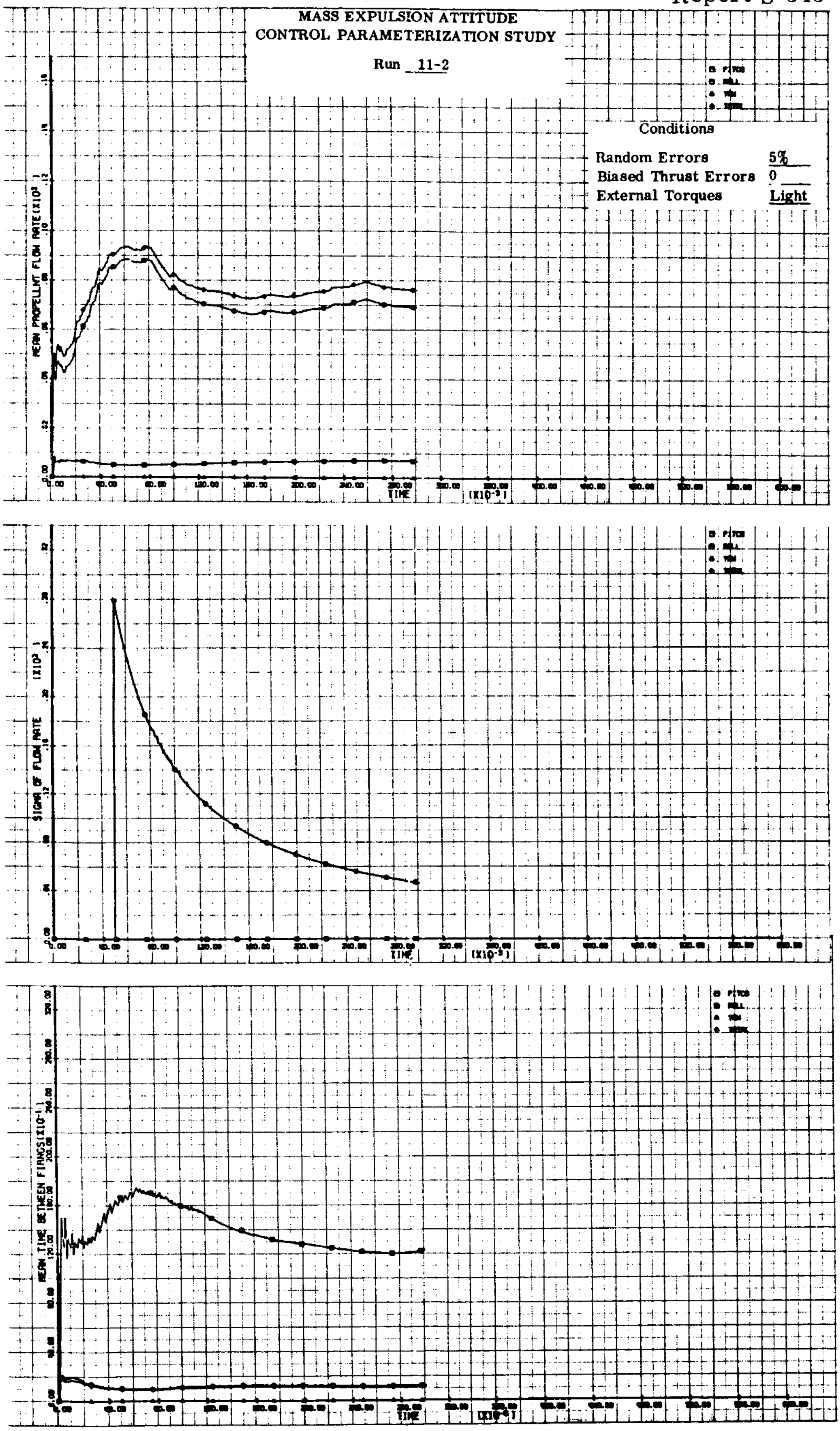
MASS EXPULSION ATTITUDE
CONTROL PARAMETERIZATION STUDY
Run 11-2
Conditions
Random Errors 5%
Biased Thrust Errors 0
External Torques Light
MEAN PROPELLANT FLOW RATE (X10²)
TIME
SIGMA OF FLOW RATE (X10²)
TIME
MEAN TIME BETWEEN FIRINGS (X10⁻¹)
TIME

Figure 62

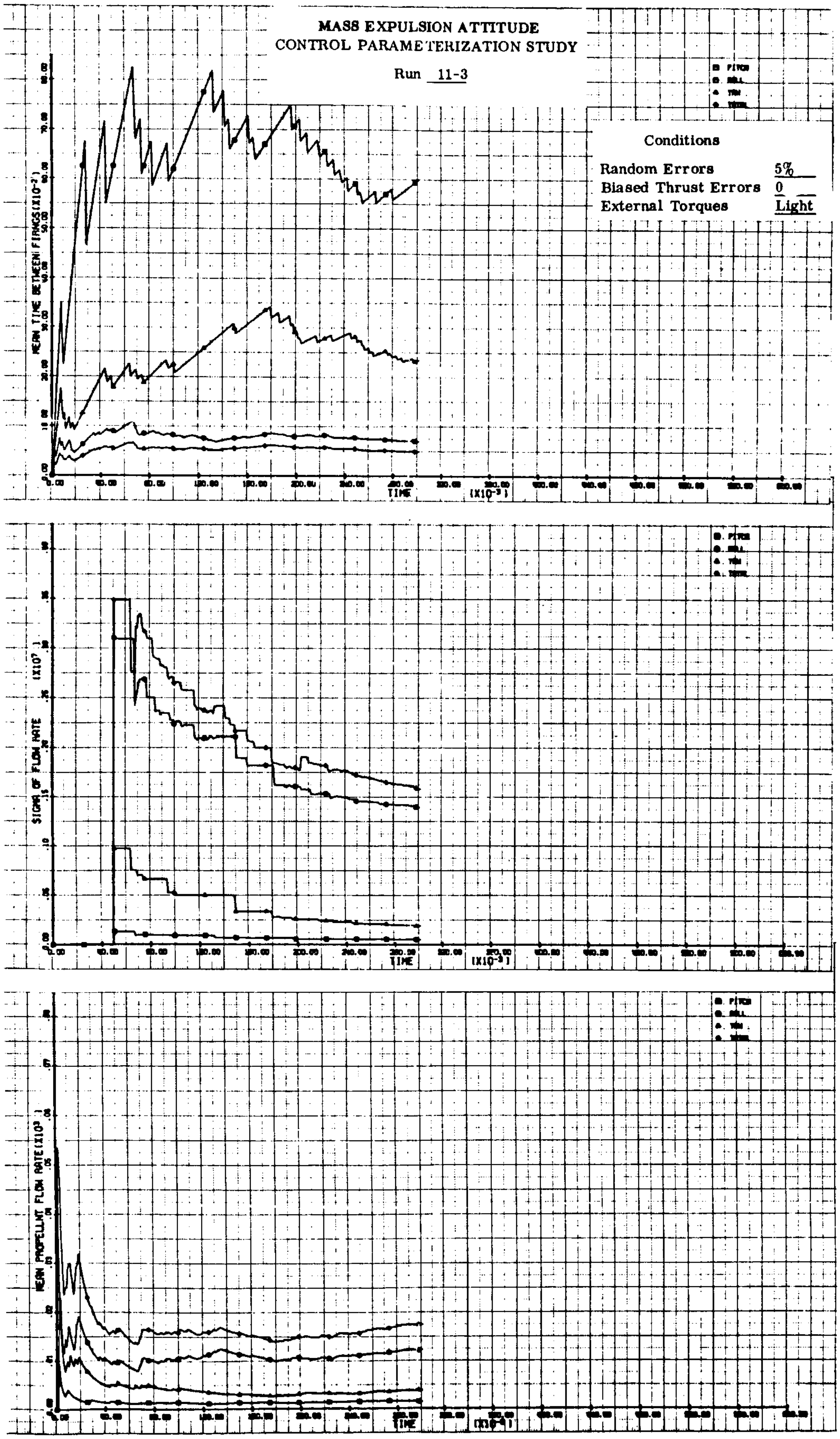
MASS EXPULSION ATTITUDE
CONTROL PARAMETERIZATION STUDY
Run 11-3
Conditions
Random Errors 5%
Biased Thrust Errors 0
External Torques Light
TIME

Figure 63

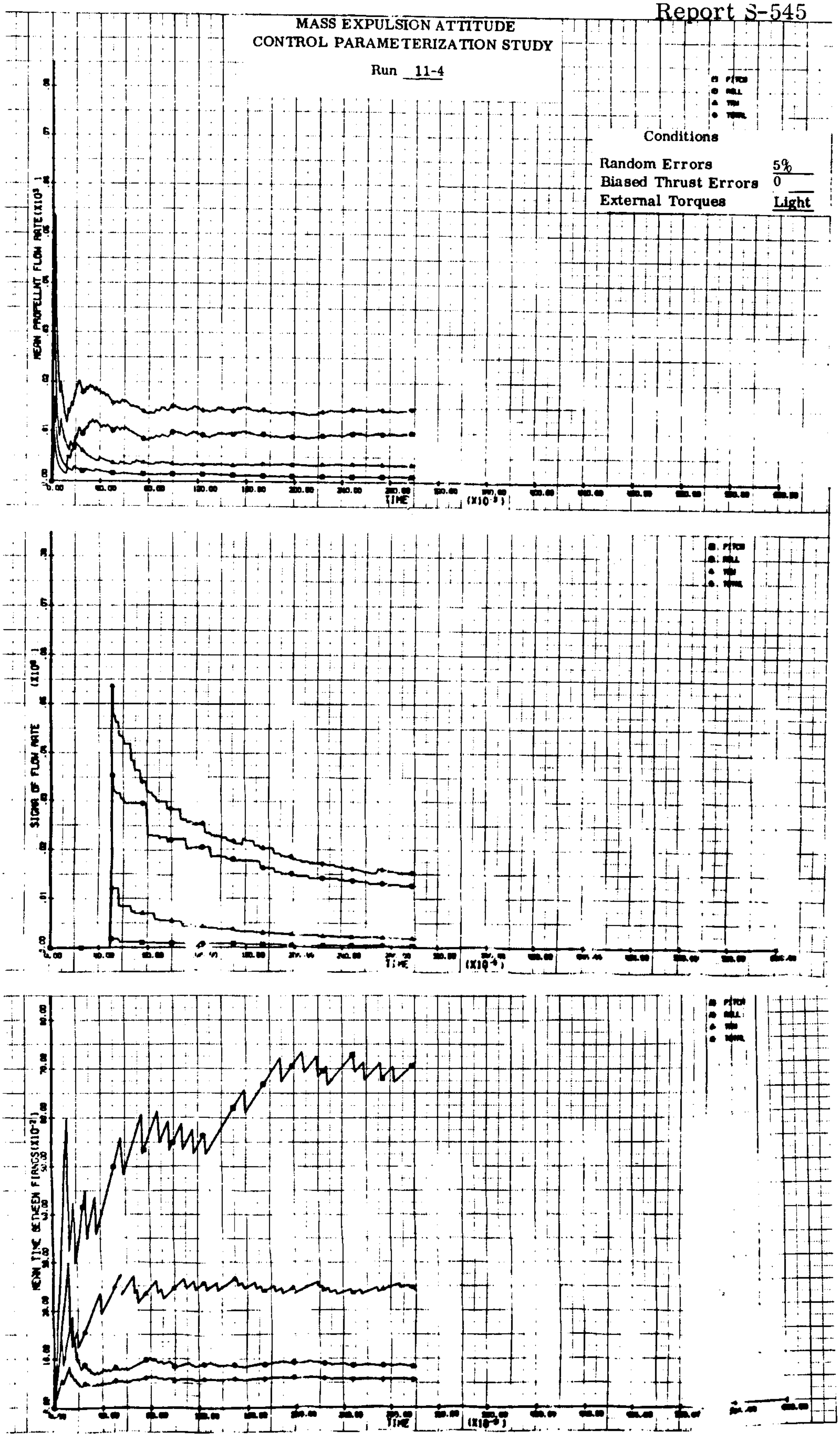
MASS EXPULSION ATTITUDE
CONTROL PARAMETERIZATION STUDY
Run 11-4
Conditions
Random Errors 5%
Biased Thrust Errors 0
External Torques Light
MEAN PROPELLANT FLOW RATE (X10³)
SIGMA OF FLOW RATE (X10³)
MEAN TIME BETWEEN FIRINGS (X10⁻¹)
TIME
(X10⁻³)

Figure 64

MASS EXPULSION ATTITUDE CONTROL PARAMETERIZATION STUDY

Run 12-1

Conditions

Random Errors 5%
Biased Thrust Errors 0
External Torques Heavy

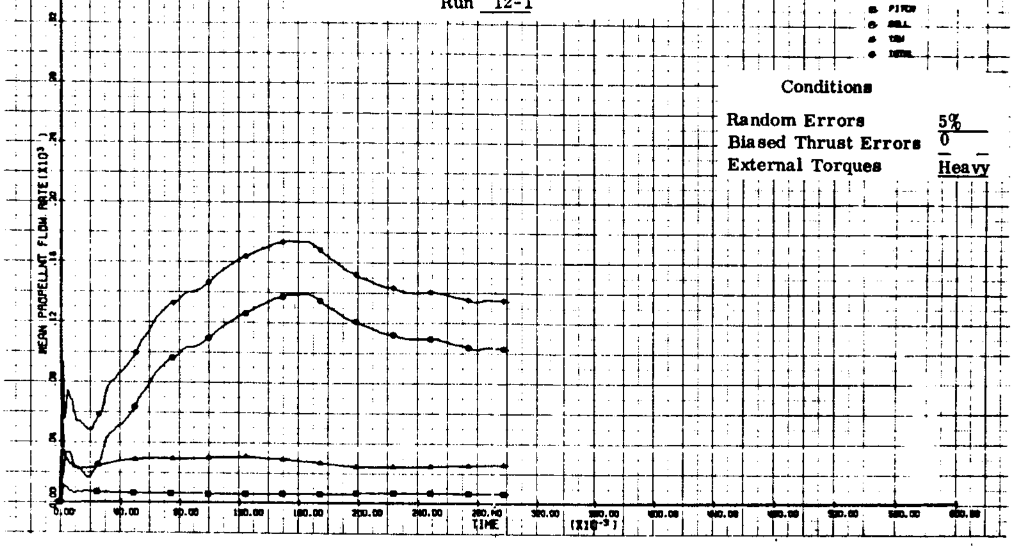

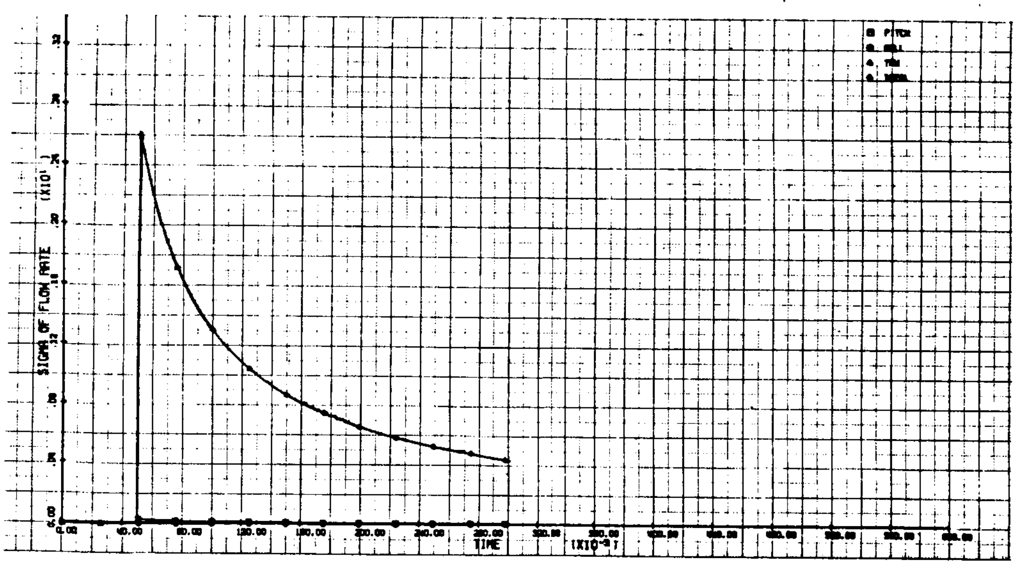

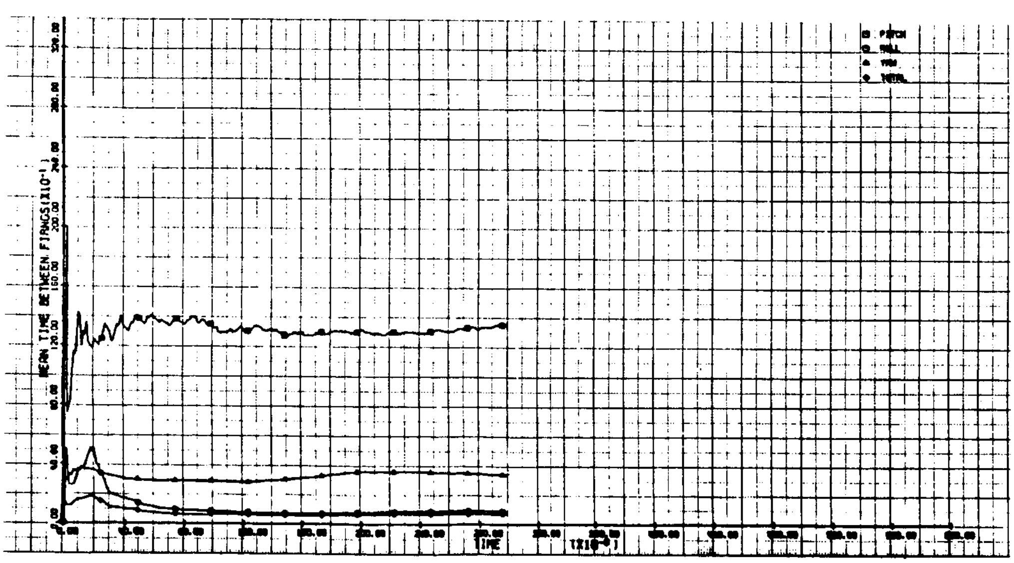

Figure 65

MASS EXPULSION STUDY
CONTROL PARAMETERIZATION STUDY

Run 12-2

Conditions

Random Errors	5%
Biased Thrust Errors	0
External Torques	Heavy

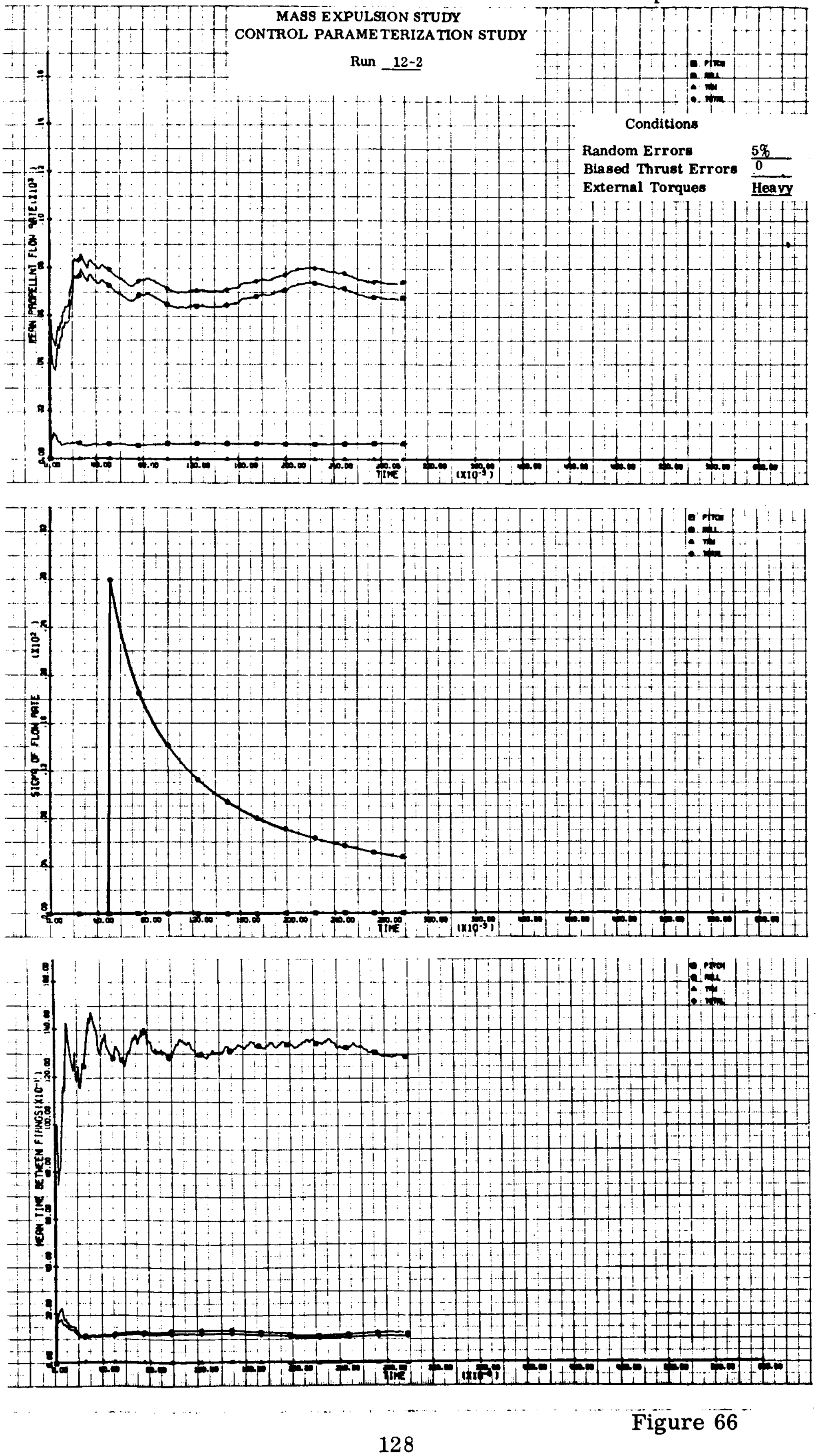

Figure 66

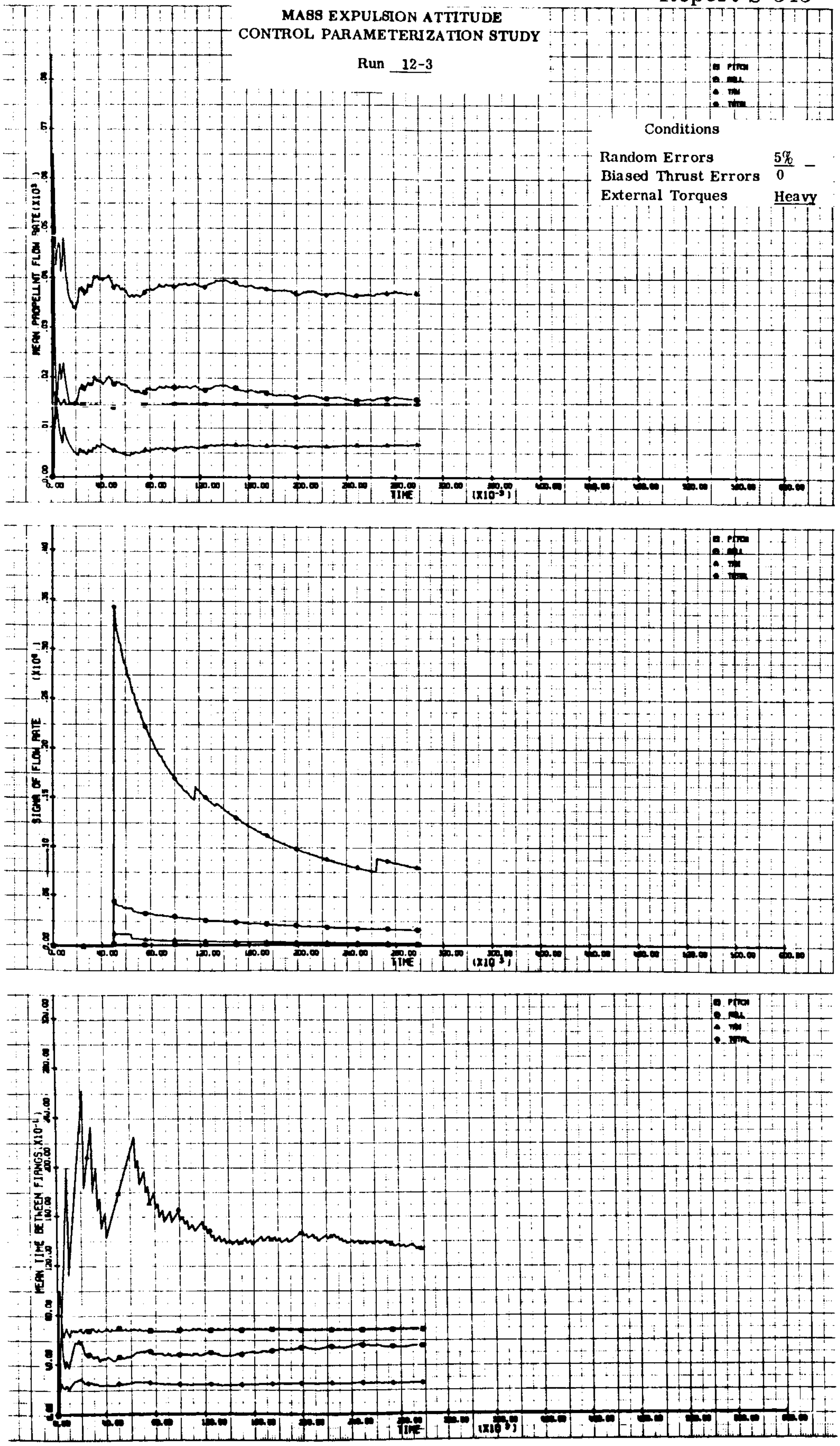
MASS EXPULSION ATTITUDE
CONTROL PARAMETERIZATION STUDY
Run 12-3
Conditions
Random Errors 5%
Biased Thrust Errors 0
External Torques Heavy
MEAN PROPELLANT FLOW RATE
SIGMA OF FLOW RATE
MEAN TIME BETWEEN FIRINGS
TIME

Figure 67

MASS EXPULSION ATTITUDE CONTROL PARAMETERIZATION STUDY

Run 12-4

Conditions

Random Errors	5%
Biased Thrust Errors	0
External Torques	Heavy

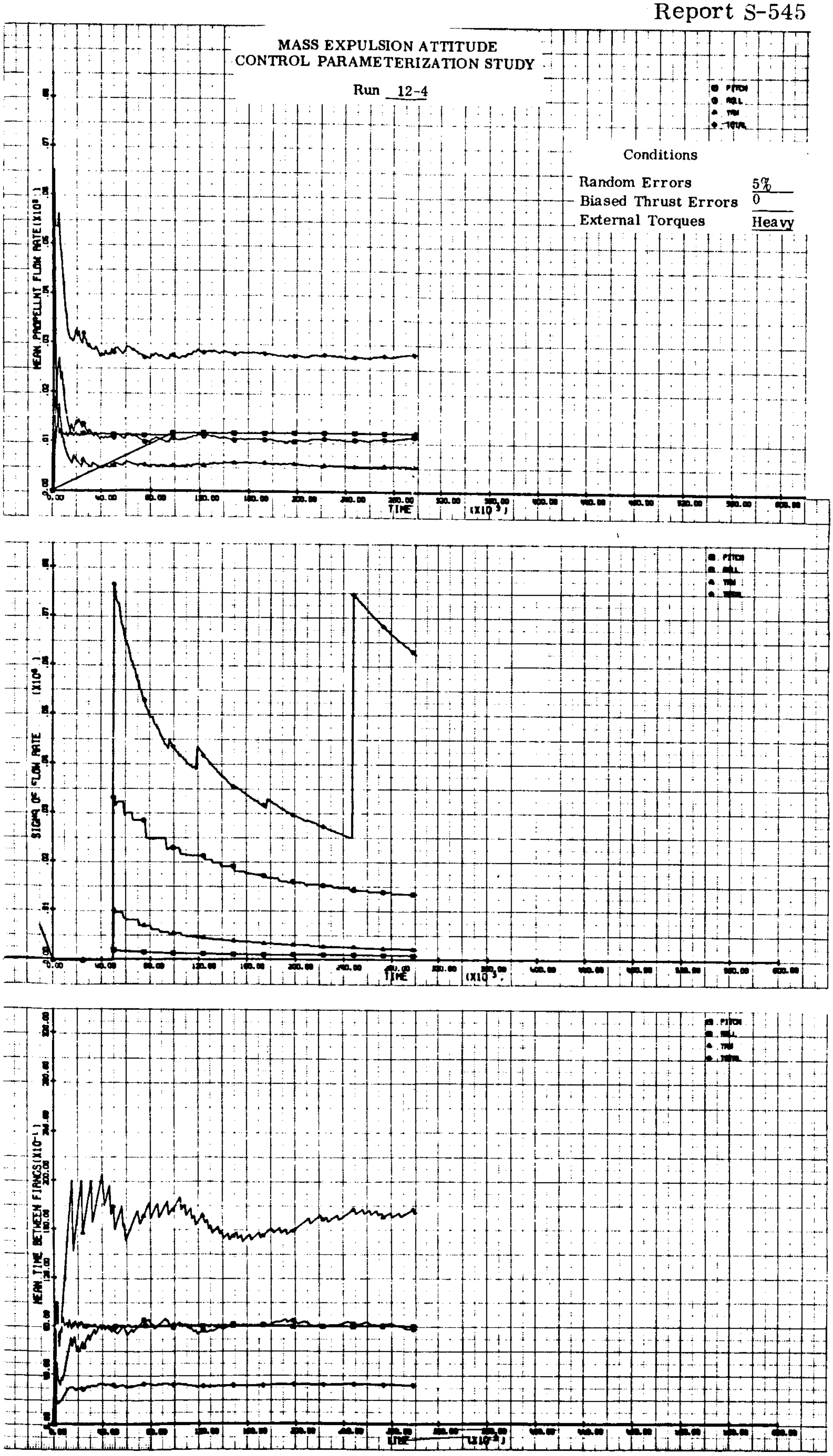

Figure 68

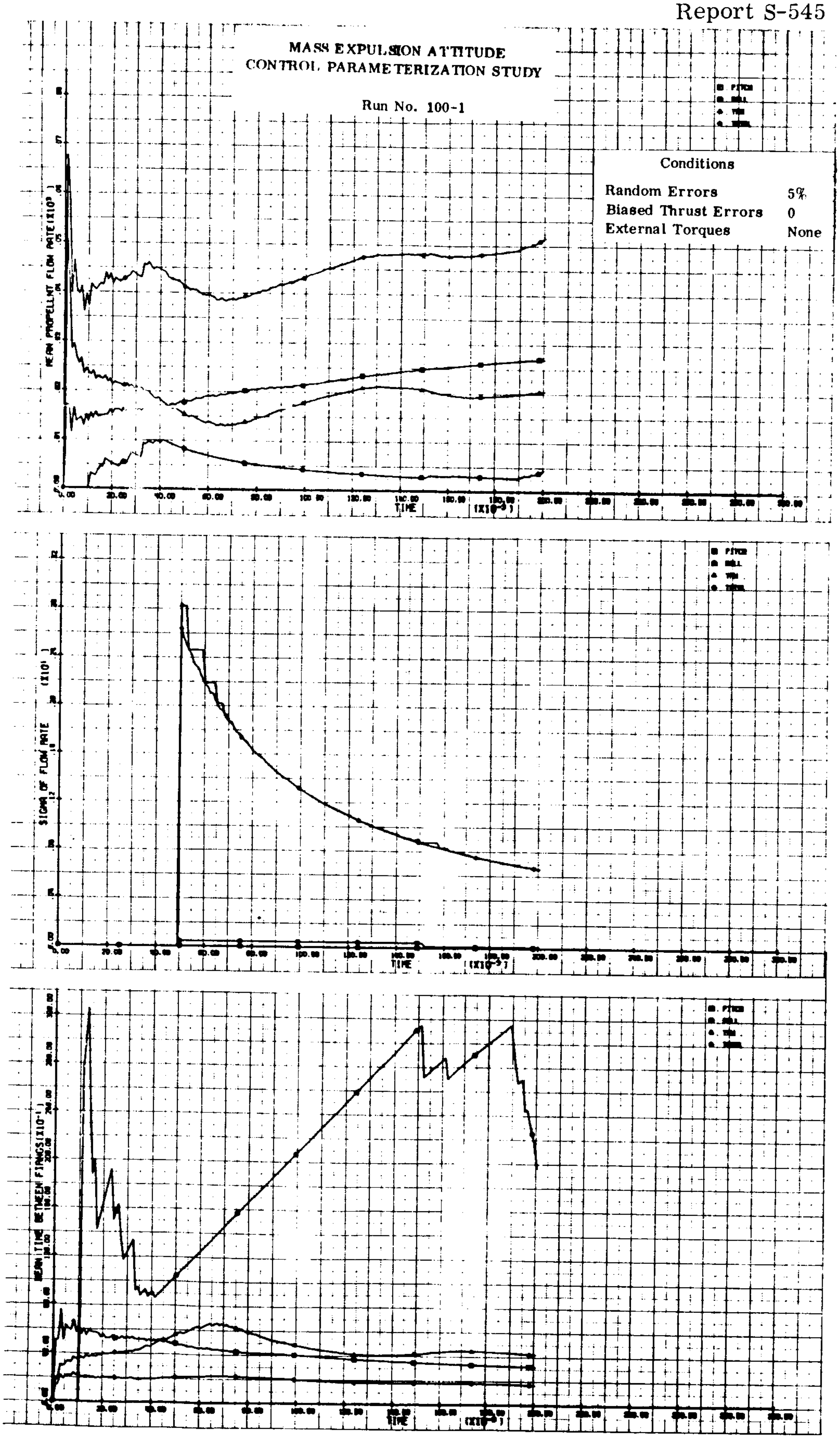
MASS EXPULSION ATTITUDE CONTROL PARAMETERIZATION STUDY
Run No. 100-1
Conditions
Random Errors 5%
Biased Thrust Errors 0
External Torques None
PITCH
ROLL
YAW
TOTAL
MEAN PROPELLANT FLOW RATE (X10^3)
TIME (X10^-3)
SIGMA OF FLOW RATE (X10^1)
MEAN (TIME BETWEEN FIRINGS)(X10^-1)

Figure 69

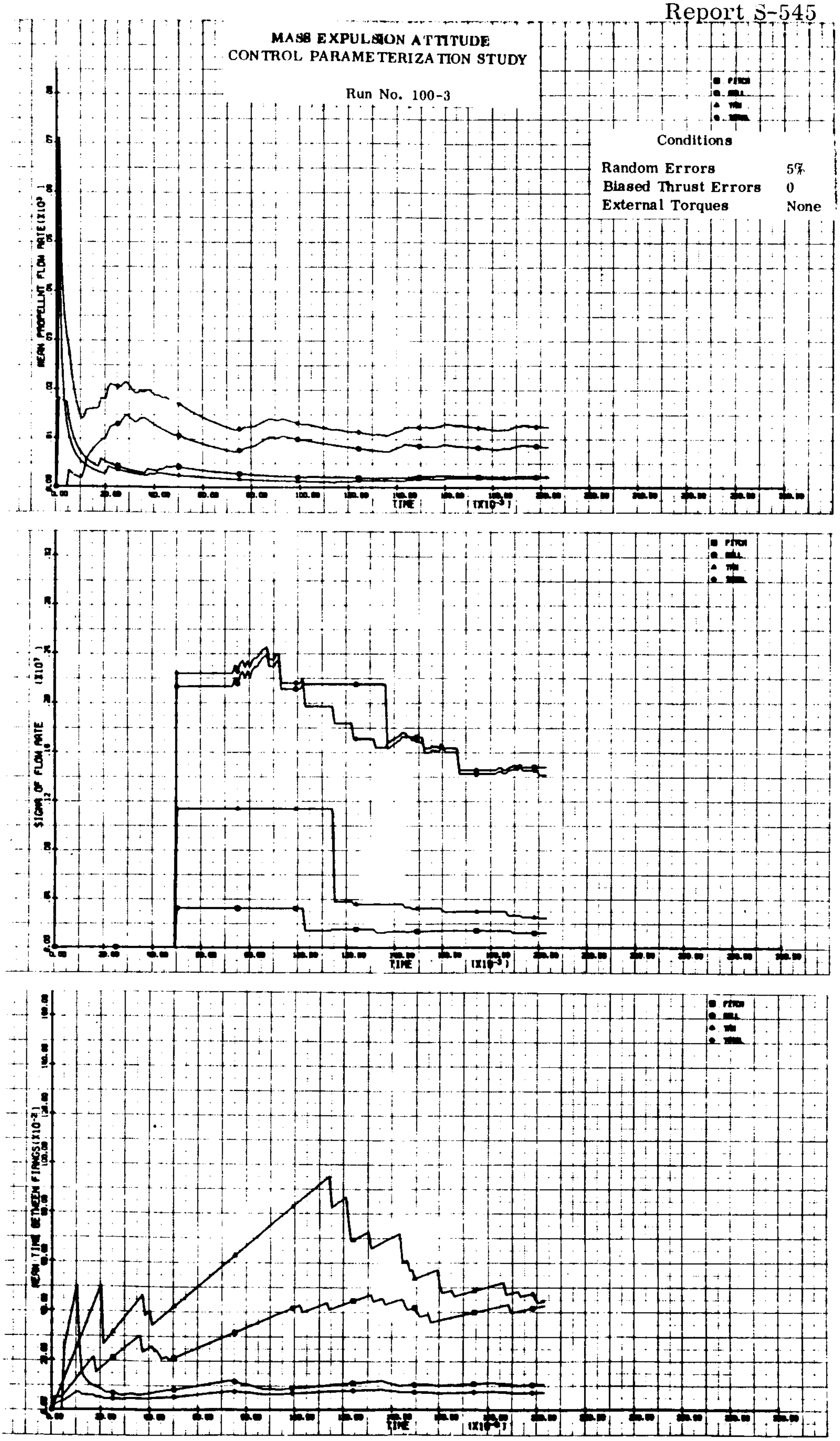
MASS EXPULSION ATTITUDE
CONTROL PARAMETERIZATION STUDY
Run No. 100-3
Conditions
Random Errors 5%
Biased Thrust Errors 0
External Torques None
MEAN PROPELLANT FLOW RATE
TIME
SIGMA OF FLOW RATE
TIME
MEAN TIME BETWEEN FIRINGS
TIME

Figure 70

MASS EXPULSION ATTITUDE CONTROL PARAMETERIZATION STUDY

Run No. 100-4

Conditions	
Random Errors	5%
Biased Thrust Errors	0
External Torques	None

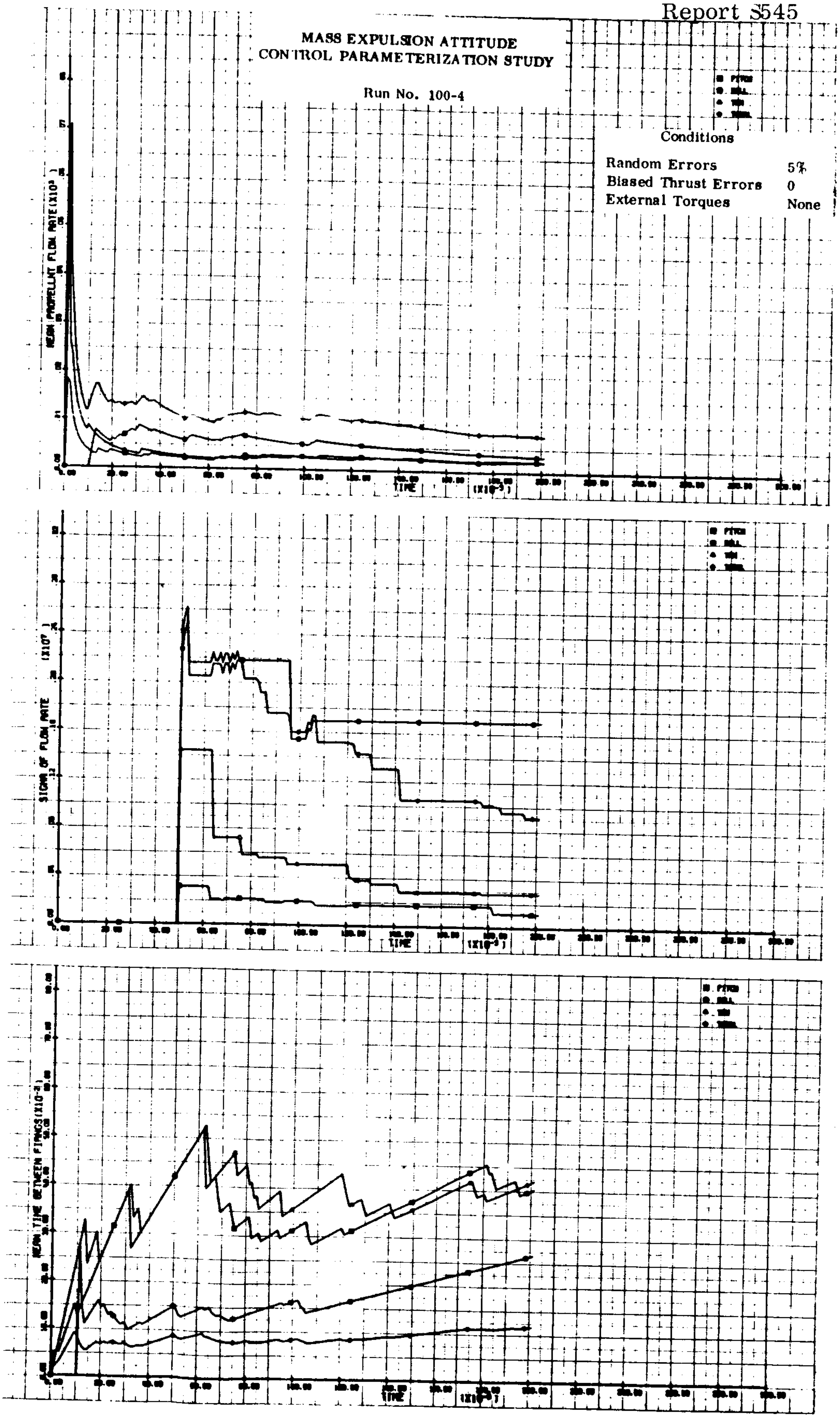

Figure 71

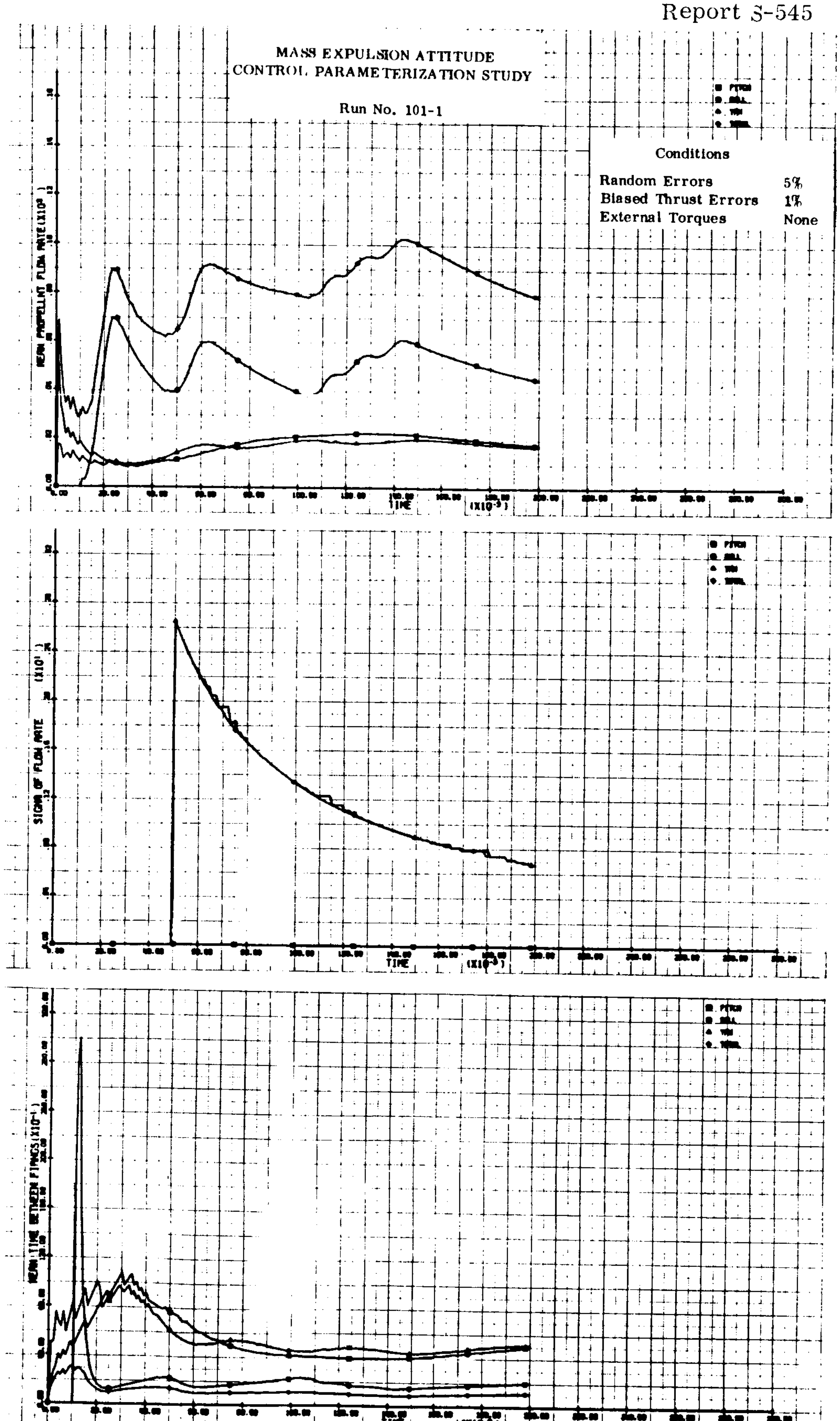
MASS EXPULSION ATTITUDE
CONTROL PARAMETERIZATION STUDY
Run No. 101-1
Conditions
Random Errors 5%
Biased Thrust Errors 1%
External Torques None
TIME
TIME
TIME

Figure 72

MASS EXPULSION ATTITUDE
CONTROL PARAMETERIZATION STUDY

Run No. 101-3

Conditions

Random Errors	5%
Biased Thrust Errors	1%
External Torques	None

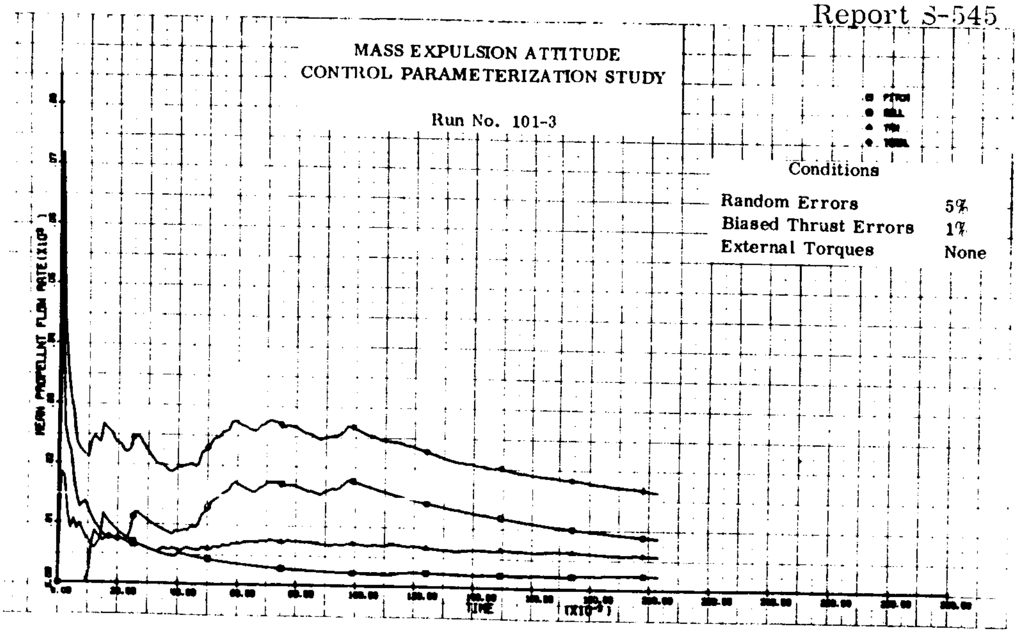

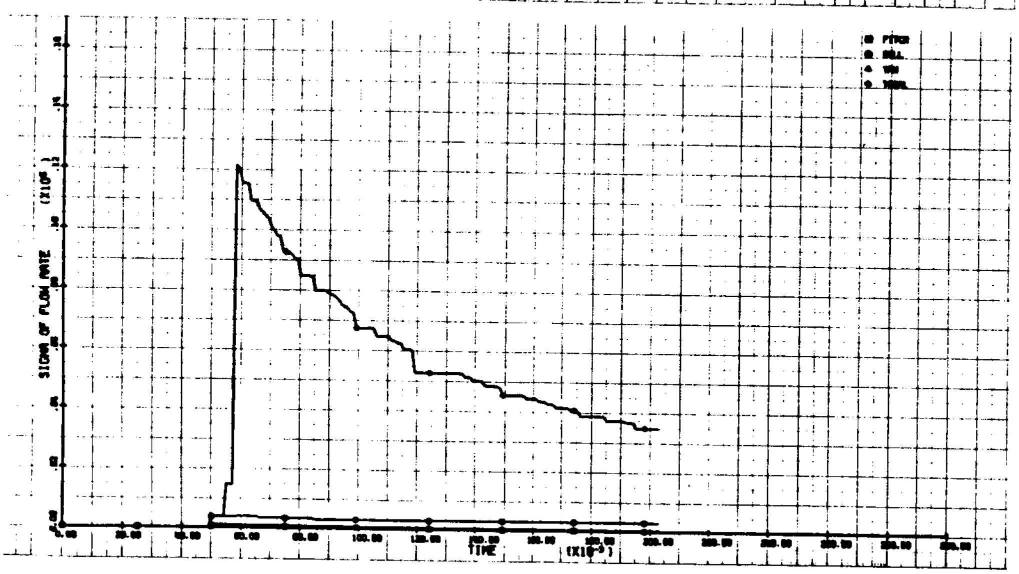

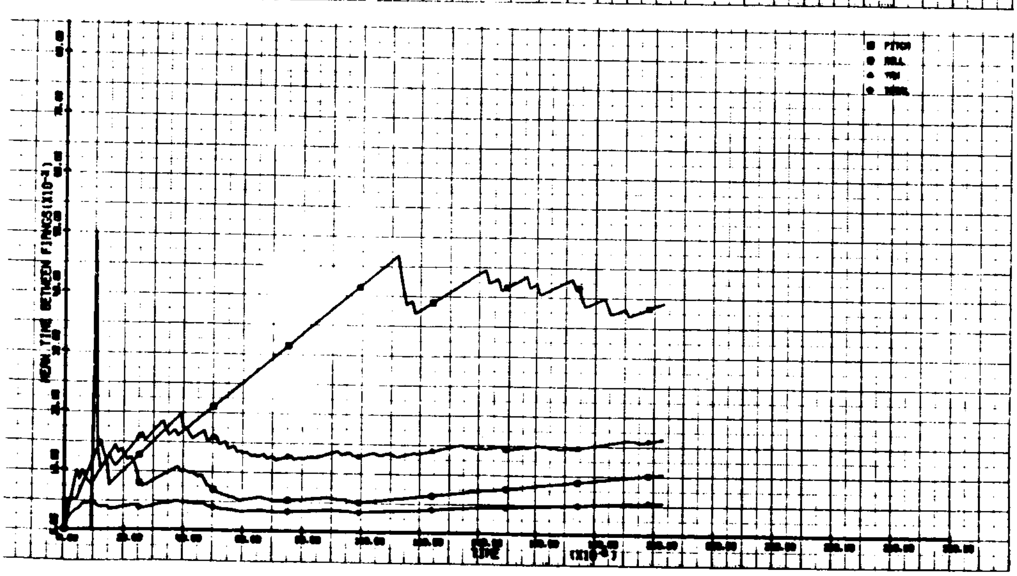

Figure 73

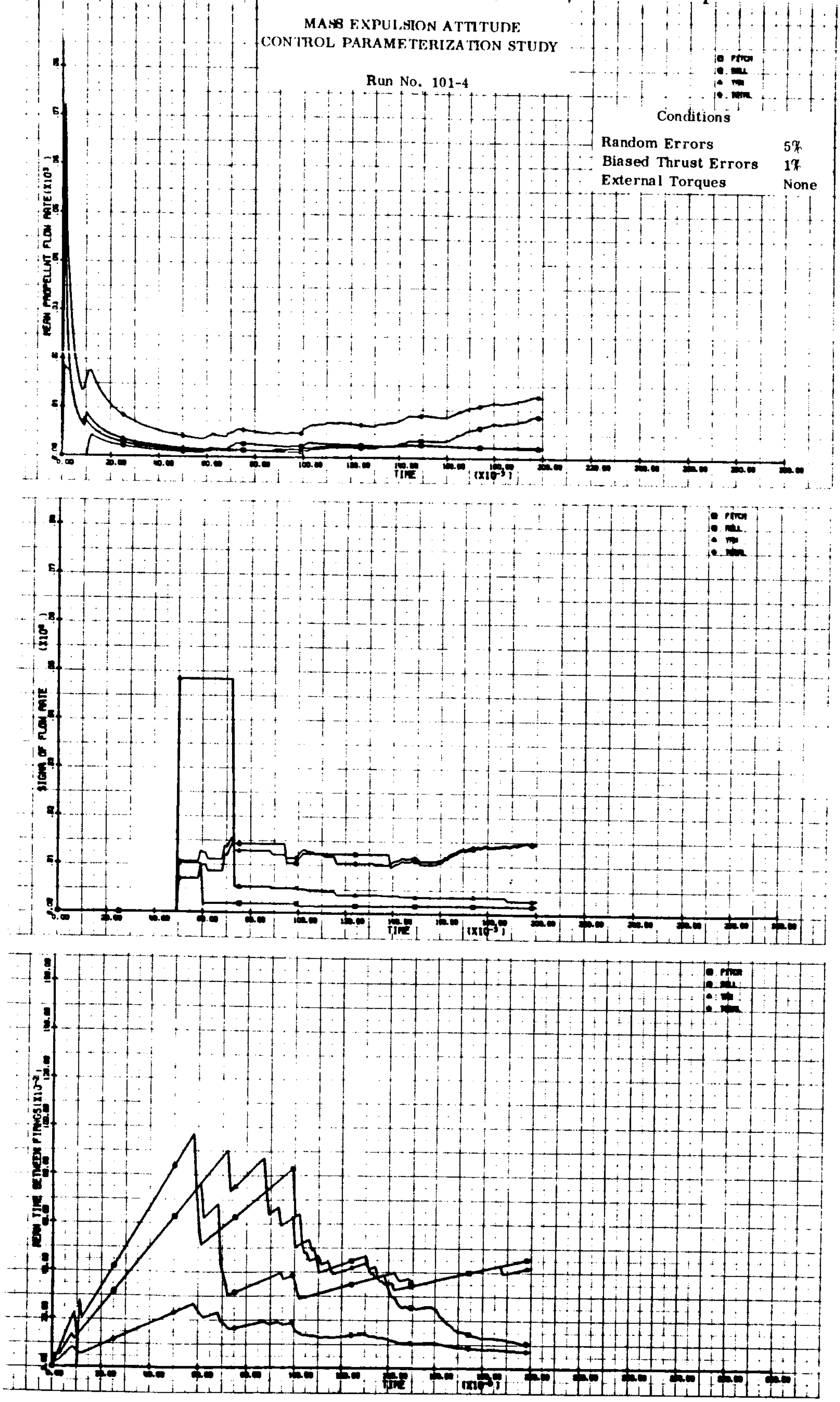
MASS EXPULSION ATTITUDE
CONTROL PARAMETERIZATION STUDY
Run No. 101-4
Conditions
Random Errors 5%
Biased Thrust Errors 1%
External Torques None
PITCH
ROLL
YAW
TOTAL
MEAN PROPELLANT FLOW RATE (X10³)
SIGMA OF FLOW RATE (X10³)
MEAN TIME BETWEEN FIRINGS (X10⁻²)
TIME (X10⁻³)

Figure 74

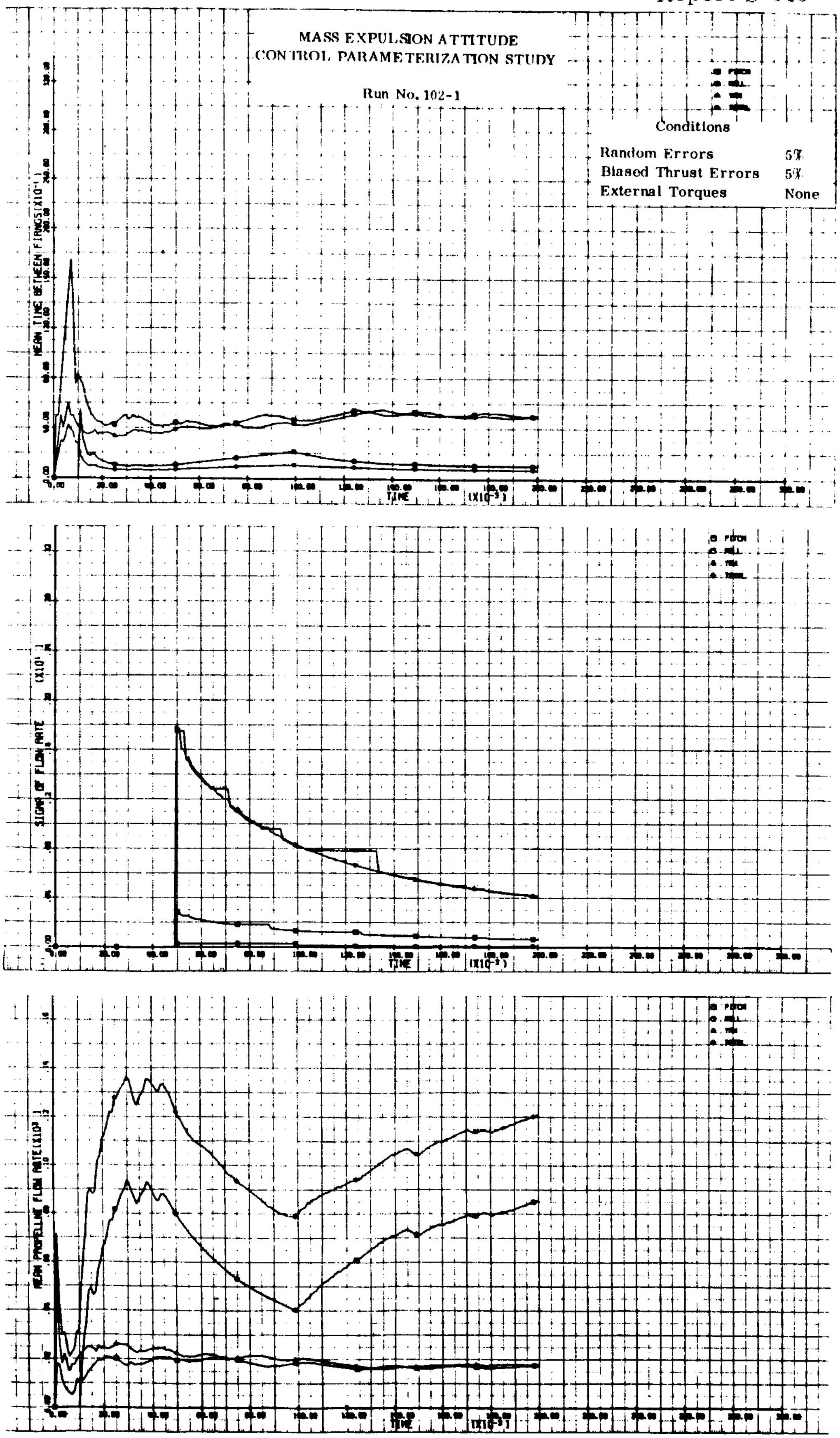
MASS EXPULSION ATTITUDE
CONTROL PARAMETERIZATION STUDY
Run No. 102-1
Conditions
Random Errors 5%
Biased Thrust Errors 5%
External Torques None
MEAN TIME BETWEEN FIRINGS(X10⁻¹)
SIGMA OF FLOW RATE (X10⁻)
MEAN PROPELLANT FLOW RATE(X10⁻)
TIME (X10⁻³)

Figure 75

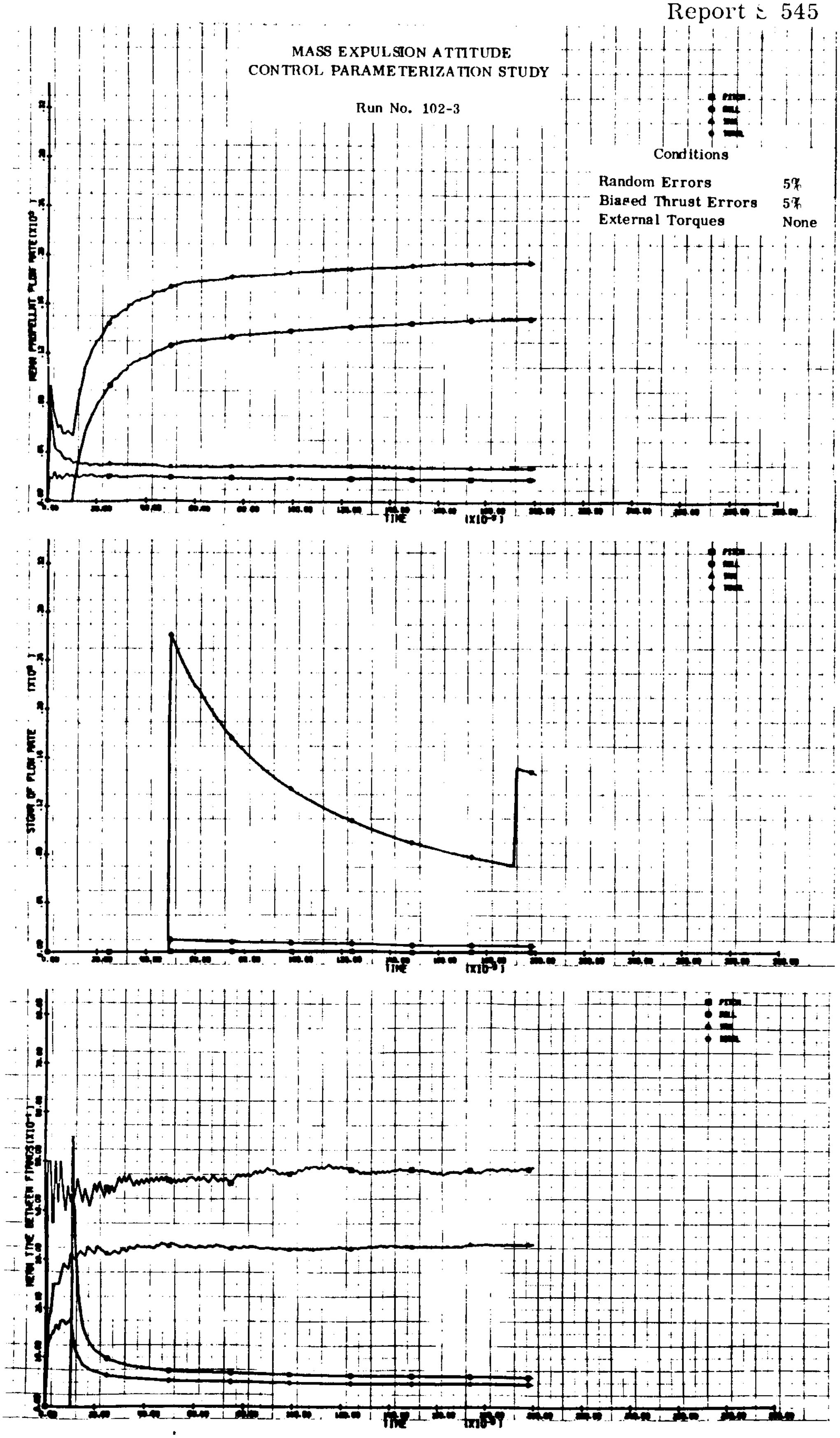
MASS EXPULSION ATTITUDE
CONTROL PARAMETERIZATION STUDY
Run No. 102-3
Conditions
Random Errors 5%
Biased Thrust Errors 5%
External Torques None
TIME
TIME
TIME

Figure 76

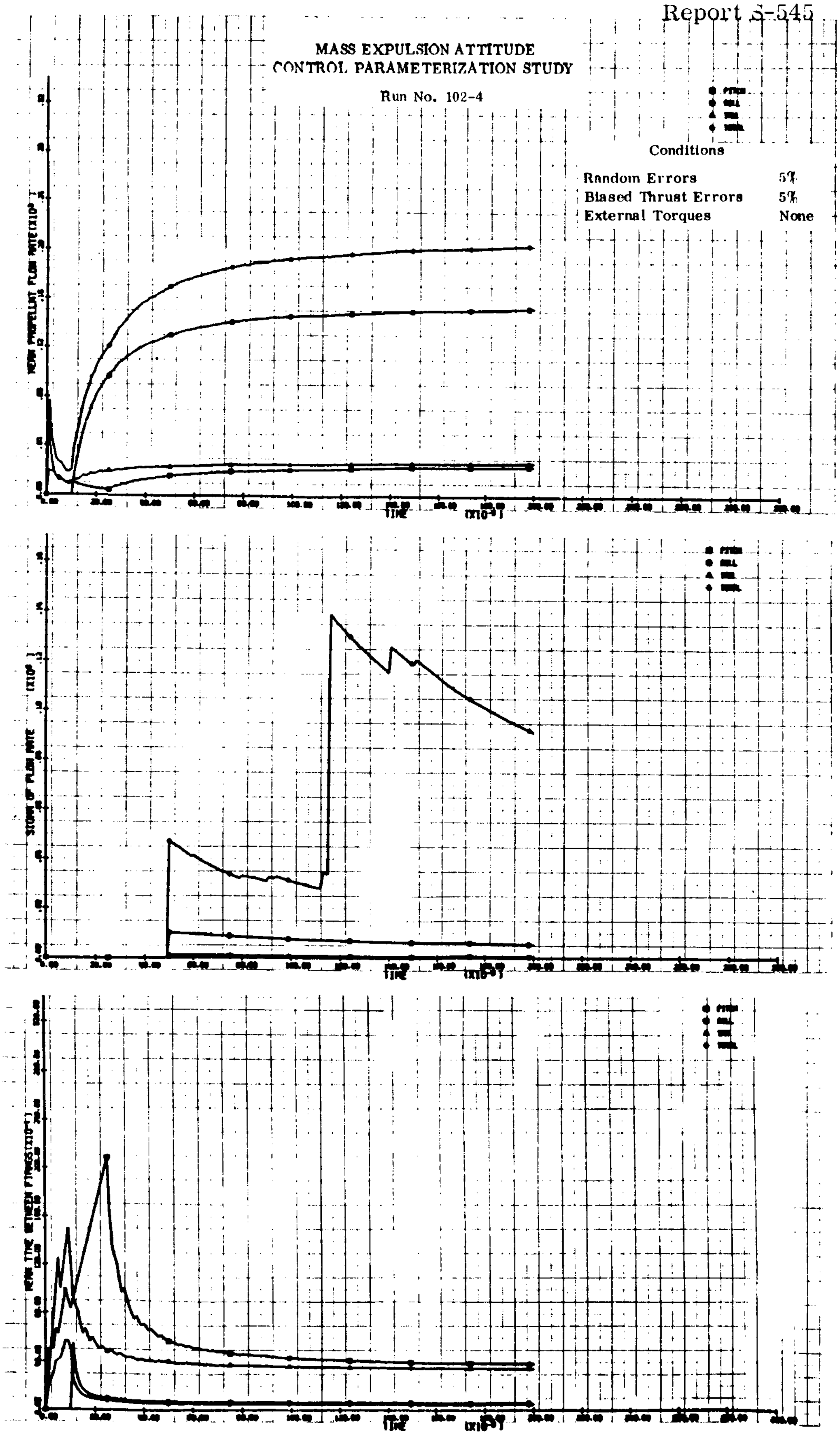
MASS EXPULSION ATTITUDE
CONTROL PARAMETERIZATION STUDY
Run No. 102-4
Conditions
Random Errors 5%
Biased Thrust Errors 5%
External Torques None

Figure 77

APPENDIX 1

DIGITAL COMPUTER PROGRAM

APPENDIX 1

IDENTIFICATION

A. 3261 - Mass Expulsion Attitude Control

B. FORTRAN IV

C. D. H. Sampson, February 1966

ABSTRACT

This program evaluates the performance of certain attitude control systems. Four different control cycle philosophies are dealt with. In each cycle small rocket engines, located at appropriate points on the vehicle, apply an impulse to acquire and maintain an angular position between acceptable dead-band limits. Either a six-engine or a twelve-engine configuration may be considered.

Angular position of the vehicle, with respect to its pitch, roll, and yaw axis, is computed as a function of time. The effect of external disturbances is taken into account. The time grid interval over which the external torque is numerically integrated is constant within each run, and is an input to the program. Both fixed and random factors are looked at when computing the increment in angular velocity brought about by engine pulses and external forces.

Whenever a control engine is fired, the time and expended impulse are printed. At specified time intervals, the accumulated number of engine pulses and mass of propellant burned are printed, along with the mean time between firings and the standard deviation, σ, of the mean time between firings. These cumulative results are tabulated for each engine, each axis, and for the total system.

Each run is terminated by a specified cut off time, number of pulses, or mass of propellant burned.

Appendix 1 (continued)

PROGRAM RESTRICTIONS

Submittal of Data

The input data for any number of runs may be stacked one behind another provided applicable tabular data or changes thereto are inserted in front of the appropriate beginning run. Maximum nunber of items per table is limited to spaces shown on input forms.

No test is made by the program as to the accuracy or arrangement of data.

No error returns have been built into the program to cover possible inconsistancies due to the nature of the problem. Excessive machine time usage can usually be controlled by the input of proper cutoff criteria.

INPUT FORM

Pages A1-13 thru A1-16 are tabular data required by the program. Each page is a table-group of related tabular data. A complete set of table-groups must precede the first run. Thereafter, changes may be introduced before any run by submitting new data for only the table groups affected.

Table Group 1 - WP Consumed vs. Impulse

1st Card:	Table Group No. Enter '1'
2nd Card:	No. of Tabular Values. Enter number of values in each of the following two tables.
Next card(s):	Impulse (Independent variable expressed in Newton/sec). Enter in decimal form.
Next card(s):	Mass of Propellant Consumed (dependent variable in kilograms). Enter in decimal form.

Appendix 1 (continued)

Table Group 2 - Engine Firing Torque Tables

1st Card: Table Group No. Enter '2'

2nd Card: Engine Configuration. Enter '6' or '12'

Next card(s): (1) For each engine, enter the following in decimal form:

Error 1: K_{a1}, K_{a2}, β_1, β_3, β_5; $L_{\text{moment arm 1}}$

Error 2: K_{a1}, K_{a2}, β_1, β_3, β_5; $L_{\text{moment arm 2}}$

Where:

K = maximum value ϵ may assume

β= Fixed impulse

L = Length of moment arm, in meters (see program analysis for definition of subscripts)

Next card: (2) J .. Moment of inertia in KG per meter^2

Table Group 3 - External Disturbance Torque Tables

1st Card: Table Group No. Enter '3'

2nd Card: No. of Tabular Values. Enter number of values in each of the following two sets of tables:

Next card(s): T, H_{pitch}, H_{roll}, H_{yaw}. Enter in decimal form.

Where:

T = Independent variable "time" in seconds, a periodic table where last item entered reflects the period end.

H = Dependent variable, in Newton-meters.

Next card(s): N, F_{pitch}, F_{roll}, F_{yaw}, F_{ϵ}. Enter in decimal form.

Appendix 1 (continued)

Where:

N = Table of numbers in ascending order including the range -0.5 thru +0.5 (independent variable)

F = Dependent variable used in grid computations, nondimensional

F_{ϵ} = Dependent variable used in computation of ϵ at engine firing time

Next card: $\text{Sigma}_{\text{pitch}}$, $\text{Sigma}_{\text{roll}}$, $\text{Sigma}_{\text{yaw}}$, Sigma_{ϵ}. Enter in decimal form.

Where:

Sigma = Standard deviation, nondimensional, as used in grid computations

Sigma_{ϵ} = Standard deviation, nondimensional, as used in computation of ϵ at engine firing time.

Next card: K_{pitch}, K_{roll}, K_{yaw}. In Newton-meter units. Enter in decimal form.

Table Group 4 - Control Philosophy

1st Card: Table Group No. Enter '4'

2nd Card: Control Philosophy. Enter '1', '2', '3', or '4' (see program analysis for description).

3rd Card: Lambda Coefficients. Enter in decimal form only if Control Philosophy No. 2 or No. 4; otherwise leave blank:

A_1, A_2, A_3, B_1, B_2, B_3

(A_1, A_2, A_3 are nondimensional; B_1, B_2, B_3 are expressed in seconds).

Appendix 1 (continued)

Individual Run Parameters

Pages A1-17 and A1-18 of input forms provide for entires of all run parameters required for up to 10 runs.

Sequencing

By submitting additional pages, up to 100 runs may be submitted at one time provided '0' is entered in the tens position of Run No. for the first 10 runs, '1' is entered for the second 10 runs, etc. All cards for Run Parameters must be hand sorted or machine-sorted to card number order within each run before submittal.

Card No. 1: Title. Alpha-numeric description of seconds for run. Enter no more than 66 characters, including blanks.

Card No. 2: Grid Time Interval. Enter number of seconds for which each set of computed external forces shall remain applicable.

Print Time Interval. Enter time in seconds between printout of mean time between firings, sigma (mass of propellant consumed), number of pulses, and mass of propellant consumed. (These same values will also be printed at the end of each run).

I_o. Minimum Impulse. Enter in Newton-seconds.

Random Number Starter. Enter any integer 1 thru 9. Use of a different random number starter for otherwise identical runs will vary results significantly.

Plot Option. Enter '1' to plot, otherwise leave blank.

Appendix 1 (continued)

Card No. 3: End of Run Criteria (leave blank if not applicable).

1. No. of Pulses. Enter a number such that if number of firings $\geq$ number of pulses, run will be concluded. Decimal point must be omitted.

2. T Final. Enter time in seconds, in decimal form, when run shall be concluded.

3. Total Fuel Expended. Enter total consumption of fuel, in kilograms per pound-mass, wherein run shall be concluded. Enter in decimal form.

Card No. 4: Angle Theta .. Position angle. Enter θ_{pitch}, θ_{roll}, and θ_{yaw} in degrees, decimal form.

Theta Dot .. Angular Velocity. Enter $\dot{\theta}_{pitch}$, $\dot{\theta}_{roll}$, and $\dot{\theta}_{yaw}$ in degrees, decimal form.

Delta Theta .. Deadband Limits. Enter $\Delta\theta_{pitch}$, $\Delta\theta_{roll}$, and $\Delta\theta_{yaw}$ in degrees, decimal form.

GLOSSARY OF SOME FORTRAN NAMES AND THEIR CORRESPONDING NAMES IN THE PROGRAM ANALYSIS

Program Name	Analysis Name
CØNFIG	Engine configuration (Figures 18 and 19)
DTBAR	Input value of $\Delta\ \theta$ (i) (Appendix 6)
DIDØT	Name of subroutine used in computation of $\Delta\ \dot{\theta}$ (i)
DTHDØT	$\Delta\ \dot{\theta}$ (i) (Page 23)
DTHETA	$\pm\ \Delta\ \theta$ (i) (Page 23)
DTZBAR	$\overline{\overline{\Delta\ \theta}}$ (i) change in $\dot{\theta}$ (Tables and)
EK	$K_{ijk\alpha}$ (Appendix 7)
ENTRP	Name of Interpolative subroutine
EPS	Name of subroutine returning value of $\epsilon_{ijk\alpha}$ and $\bar{\epsilon}_{ijk\alpha}$
EPSBAR	$\epsilon_{ijk\alpha}$ (Appendix 7)
EPSI	$\epsilon_{ijk\alpha}$ (Appendix 7)
FIR1ST	Minimum T (i) (Page 24)
FTAB	f_i (N) (Appendix 2) and F (Appendix 3)
GRID	Name of subroutine calculating random outside disturbances.
HTAB	h_i (t) (Appendix 2)
IMP	Delivered impulse, per engine
IMPTAB	$\tilde{I}$ (Appendix 4)
IØ	I_o (Appendix 6)
IQUØT	Intermediate value used in applying Time (Appendix 6)
IT	Commanded pulse (Tables 11, 12, 13, and 14)
KENG	Engines fired per configuration, axis, error (Tables 11, 12, 13, and 14)

Program Name	Analysis Name
KG	k_i (Appendix 2)
LAM1, -2, -3	L (t)
LAMB1, -2, -3	λ_i
LBAR	$\bar{L}$ . . L_0, L_1, L_2, L_3, L_4, L_5 (Table 3)
LTIME	L (t) where t = TIME (Page 26)
LTIMEA	L (t) where t = a (Page 26 Sketch 4)
LTIMEB	L (t) where t = b (Page 26 Sketch 4)
LTIMED	L (t) where t = d = some time later than b (Page 26)
MGRID	M (Appendix 3)
MTBF	$\bar{T}$, mean time between firings/engine (Page 25)
MTBFAX	mean time between firings/axis (Page 25)
MTBFTØ	mean time between firings/total (Page 25)
NAXIS	Axis number see i of θ_i (Appendix 7)
NCØNFG	Engine configuration number see j of J_{ij} (Appendix 7)
NCYCLE	Control Philosophy (= Cycle) (Tables 11, 12, 13 and 14)
NENGIN	Engine no. of engine being fired j, K of L_{ijk} (Appendix 7)
NEXFIR	2nd pulse of Control Philosophy No. 3 (Table 13)
NGRIDT	No. of items on tables h_i (t) and f_i (N) (Appendix 2)
NIMPT	No. of items on table F ($\tilde{I}$) (Appendix 4)
NPEND	Cutoff point determined by number of pulses (Page 25)
NPULSE	No. of firings per engine
NRAND	Name of subroutine which generates random numbers

Program Name	Analysis Name
NRUN1	Program flag to indicate 1st of a batch of runs
NSEQ	Pulse No. (1 or 2) (Tables 13 and 14)
NSIGN	Sign indication; 1 = +, 2 = -
NTAB	N (Appendix 2)
PRØBUR	W T . . mass of propellant expended (also Table 12)
PULSAX	No. of firings per axis
PULSTO	No. of firings total
RAND	N_1 (Appendix 2)
SIG	σ (N) per engine (Appendix 5)
SIGAX	σ (N) per axis (Appendix 5)
SIGNSV	Record of NSIGN of 1st pulse for examination at 2nd pulse (Table 14)
SIGTØ	σ (N) total (Appendix 5)
SIGMAG	σ_1, σ_2, σ_3 (Appendix 2)
T	T (i) (Page 24)
TDIFF	Z (N) per engine (Appendix 5)
TDIFAX	Z (N) per axis (Appendix 5)
TDIFTØ	Z (N) total (Appendix 5)
TFINAL	Cut off point determined by time (Page 25)
TGINCR	Δ t (grid) (Page 25)
TGNEXT	Next grid time (Page 25)
THDØT	$\dot{\theta}$ (Appendix 6)

Program Name	Analysis Name
THETA	θ (Appendix 6)
TIME	time
TIMFIR	time of 1st pulse of Control Philosophy No. 3 (Table 13)
TIMZER	2nd pulse of control philosophy No. 4 (Table 14)
TMØDUL	time remainder . . time modulus T (periodic) (Appendix 6)
TPRVAX	time of previous firing, per axis
TPRVEN	time of previous firing, per engine
TPRVTØ	time of previous firing, total
TTAB	T (periodic) (Appendix 6)
UNFIRD	Program flag to record that no firing was imminent
WP	Mass of propellant expended, per engine
WPAX	Mass of propellant expended, per axis
WPTØT	Mass of propellant expended, total
WPEND	Cut off point determined by propellant expended (Page 25)

OPERATIONS

Program is written in FORTRAN IV and is intended to run under the IBM IBSYS system. The program requires no tape drives other than the normal I/o units used by the operating system.

The control cards required are the usual $JØB, $IBJØB and the $IBFTC cards as well as those which are pertinent to each installation.

The deck setup is illustrated below.

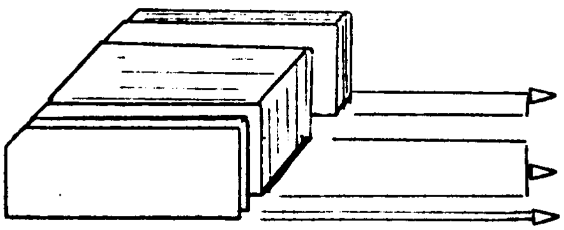

ATTITUDE CONTROL PROGRAM

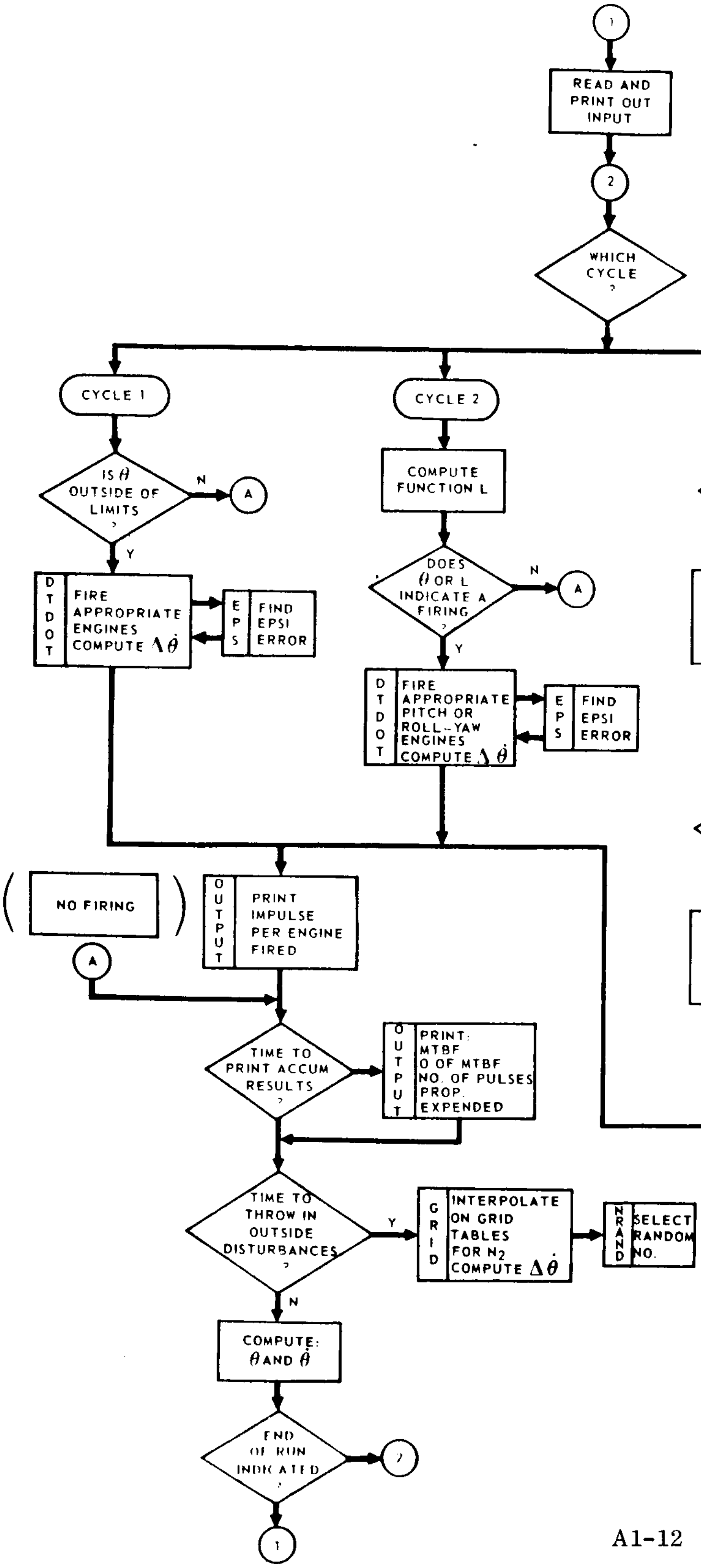

Figure A-1

ATTITUDE CONTROL PROGRAM JOB 3261

ENGINEER	DATE

A complete set of Table-Groups must precede the 1st run. Thereafter, tabular data will be available for all runs, or changes may be introduced before any run by submitting new data for only the table-groups affected.

TABLE GROUP #1 TABLE OF WP VS. IMPULSE

TABLE GROUP NO. 3

NO. OF TABULAR VALUES 12

IMPULSE (NEWTON - SEC)

2 decimal form

2	14	26	38	50	62

MASS OF PROPELLANT CONSUMED (KILOGRAMS)

2	14	26	38	50	62

Table Group No. 3	
	2

Configuration (6 or 12) 12	
	6

ATTITUDE CONTROL PROGRAM
TABLE GROUP #2 - ENGINE FIRING TORQUE TABLES

Engine No.			K (max value of ϵ)		β			L	
6 Eng.	12 Eng.	Error	2 1	14 2	26 1	38 3	50 5	Mom Arm	62
53	13	1						1	
		2						2	
54	14	1						1	
		2						2	
55	15	1						1	
		2						2	
63	16	1						1	
		2						2	
64	23	1						1	
		2						2	
66	24	1						1	
		2						2	
	25	1						1	
		2						2	
	26	1						1	
		2						2	
	35	1						1	
		2						2	
	36	1						1	
		2						2	
	45	1						1	
		2						2	
	46	1						1	
		2						2	

J ($KG-M^2$)		
2 Pitch	14 Roll	26 Yaw

ATTITUDE CONTROL PROGRAM

TABLE GROUP #3 EXTERNAL DISTURBANCE TORQUE TABLES

Table Group No. (3)

NO. OF TABULAR VALUES (12)

decimal

(2) T-(PERIODIC, LAST ITEM ENTERED MUST REFLECT END OF PERIOD)	H (14) PITCH	(26) ROLL	(38) YAW

(2) N	F (14) PITCH	(26) ROLL	(38) YAW

(50) F_ϵ

SIGMA (2) PITCH	(14) ROLL	(26) YAW

(38) $SIGMA_\epsilon$

K (N.M.) (2) PITCH	(14) ROLL	(26) YAW

ATTITUDE CONTROL PROGRAM

TABLE GROUP # 4 - CONTROL PHILOSOPHY

Table Group No.	3

CONTROL PHILOSOPHY	#12

ENTER FOLLOWING ONLY IF CONTROL PHILOSOPHY #2 OR #4....OTHERWISE LEAVE BLANK

2 A_1	14 A_2	26 A_3	38 B_1	50 B_2	62 B_3

ATTITUDE CONTROL PROGRAM

INDIVIDUAL RUN PARAMETERS - CARD 1

	TITLE (6)	SEQUENCE RUN NO. (77)	SEQUENCE CARD
		0	01
		1	01
		2	01
		3	01
		4	01
		5	01
		6	01
		7	01
		8	01
		9	01

INDIVIDUAL RUN PARAMETERS - CARD 2

GRID TIME INTERVAL (SEC) (2)	PRINT TIME INTERVAL (SEC) (14)	I_o (IN.SEC) (26)	RANDOM NO STARTER (ANY INTEGER) (48)	PLOT OPTION (ENTER '1' TO PLOT, OTHERWISE LEAVE BLANK) (60)		SEQUENCE RUN NO. (77)	SEQUENCE CARD
						0	02
						1	02
						2	02
						3	02
						4	02
						5	02
						6	02
						7	02
						8	02
						9	02

ATTITUDE CONTROL PROGRAM

(ANGLES EXPRESSED IN DEGREES)

INDIVIDUAL RUN PARAMETERS - CARD 3

END OF RUN CRITERIA "LEAVE BLANK WHERE APPLICABLE"			θ			SEQUENCE	
NO. OF PULSES (OMIT DECIMAL PT.) 12	14 T FINAL (SEC)	26 TOTAL FUEL EXPENDED(KG)	38 PITCH	50 ROLL	62 YAW	RUN NO. 77	CARD
						0	03
						1	03
						2	03
						3	03
						4	03
						5	03
						6	03
						7	03
						8	03
						9	03

INDIVIDUAL RUN PARAMETERS - CARD 4

$\dot{\theta}$			Δθ (LIMITS)			SEQUENCE	
2 PITCH	14 ROLL	26 YAW	38 PITCH	50 ROLL	62 YAW	RUN NO. 77	CARD
						0	04
						1	04
						2	04
						3	04
						4	04
						5	04
						6	04
						7	04
						8	04
						9	04

APPENDIX 2

OUTSIDE DISTURBANCE TORQUES

APPENDIX 2

OUTSIDE DISTURBANCE TORQUES

(Normally Distributed Random Portion)

$$J_{ij} \left[\dot{\theta}_i (t) - \dot{\theta}_i (t - \Delta t) \right] = \Delta t \left\{ h_i (t) + \frac{k_i}{\sigma_i} f_i \left(2M_i \left[N - 1/2 \right]\right)\right\}$$

Subscripts:	i	=	1 ~ Pitch Axis
			2 ~ Roll Axis
			3 ~ Yaw Axis
	j	=	1 ~ 6 Engine Configuration
			2 ~ 12 Engine Configuration
	Δt	=	Integration interval (specified as input)
	$h_i (t)$	=	Predictable disturbance - probably cyclic with period, T
	k_i	=	Maximum magnitude of random disturbance
	σ_i	=	Number of standard deviations included
	M_i	=	Defined by $f_i (M_i) = \sigma_i$
	N	=	Random number ($0 \leq N \leq 1$, uniformly distributed)

Input Functions	Input Constants
$h_1 (t)$, $f_1 (N)$	σ_1 , k_1
$h_2 (t)$, $f_2 (N)$	σ_2 , K_2
$h_3 (t)$, $f_3 (N)$	σ_3 , K_3

APPENDIX 3

GENERATION OF $\epsilon_{ijk\alpha}$

APPENDIX 3

GENERATION OF $\epsilon_{ijk\alpha}$

Given the following inputs:

$K_{ijk\alpha}$	$\lvert K_{ijk\alpha}\rvert < 1$
σ	$0 < \sigma \leq 3$
$f(x)$	A monotone function defined for $-1/2 \leq x \leq 1/2$, where $-3 \leq f(x) \leq 3$

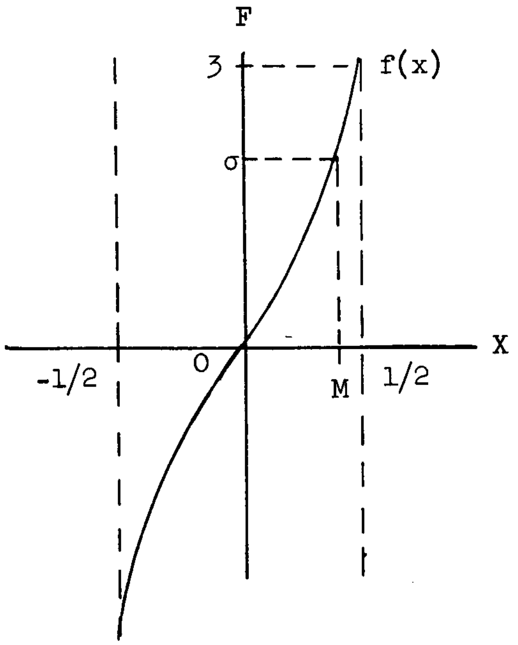

M is defined by the relation $\sigma = f(M)$

Appendix 3 (continued)

Define: N_1 = Output of random number generator

$O \le N_1 \le 1$ and is uniformly distributed in the interval

$N_2 = 2 (N_1 - 1/2) \qquad -1 \le N_2 \le 1$

$N_3 = M N_2 \qquad - 1/2 \le N_3 \le 1/2$

$N_4 = 1/\sigma \; f(N_3)$

$\epsilon_{ijk\alpha} = K_{ijk\alpha} N_4$

APPENDIX 3 (continued)

108 Combinations

$\beta_{\underbrace{i\;j}_{\text{18 engines}}\;\underbrace{k}_{\text{3 directions}}\;\underbrace{\alpha}_{\text{two types}}}$

Engine	Error Types	Pointing Direction*		
		1	3	5
13	1	0.027	0.003	0.056
	2	0.010	0.105	0.075
14	1			
	2			
15	1			
	2			
16	1			
	2			

etc

β_{1351} in this space, for example

β_{1442} in this space - would be accompanied by 1432 except for deviation explained below.

* Whenever j is even and k = j-1, then k is changed to be equal to j. This is done to keep the error in the direction of the engine pointing positive in that direction. For example, see the space for β_{1432}.

APPENDIX 3 (Continued)

Combination Display of Inputs Pertinent to Both ϵ and β Values

Engine (18 Total)	Error Type	Maximum Values of ϵ		Values of β		
		Direction		Direction		
		Primary (1)	Secondary (2)	1(X)	3(Y)	5(Z)
13	1	K_{1311}	K_{1321}	β_{1311}	β_{1331}	β_{1351}
	2	K_{1312}	K_{1322}	β_{1312}	β_{1332}	β_{1352}
14	1	etc.				
	2					
15	1					
	2					
63	1					
	2					
64	1					
	2					
66	1					
	2					

$K_{ijk\alpha}$ corresponds to the maximum value of the random number, $\epsilon_{ijk\alpha}$, may assume

APPENDIX 4

PROPELLANT CONSUMED PER PULSE

APPENDIX 4

PROPELLANT CONSUMED PER PULSE

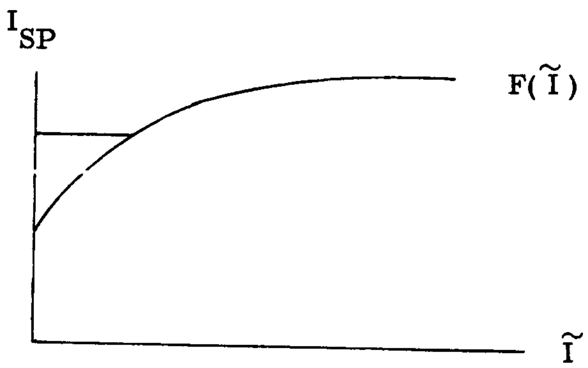

$\tilde{I}$ = Impulse expended

W_T = Weight of propellant consumed

W_T = $\tilde{I} / I_{SP}$ $\qquad I_{SP} = F(\tilde{I})$

W_T = $\tilde{I} / F(\tilde{I})$

APPENDIX 5

CALCULATION OF SIGMA (W_p)

APPENDIX 5

CALCULATION OF SIGMA (W_p)

$$\sigma = \frac{1}{t_i} \sqrt{Z_n}$$

where

$$Z_n = \sum_{i=1}^{n} \left(\frac{W_{p_i} - W_{p_{(i-1)}}}{t_i \quad t_{(i-1)}} - \frac{W_{p_i}}{t_i} \right)^2$$

t_i = Time at last firing before print out

$t_{(i-1)}$ = Time at second to last firing before print out

W_p = Mass of propellant

APPENDIX 6

INPUT PARAMETERS

APPENDIX 6

INPUT PARAMETERS

Constants

σ_o, σ_1, σ_2, σ_3		Standard Deviations Included in Random Errors
$K_{ijk\alpha}$	ARRAY	Max. Magnitude of Thrust Errors
Δt		Integration Interval
k_1, k_2, k_3		Max. Magnitude of Outside Disturbances
$\Delta\theta$		$\pm$ Deadband Limits, 3 Values
a_1, a_2, a_3		Coefficient of Angular Error (See Cycle 2, Cycle 4)
b_1, b_2, b_3		Coefficient of Angular Rate (See Cycle 2, Cycle 4)
J_{ij}	ARRAY	Moments of Inertia
L_{ijk}	ARRAY	Lever Arms of Rockets
I_o		Nominal Minimum Impulse

Functions

f_o (N), f_1 (N), f_2 (N), f_3 (N)	Distribution of Random Errors
h_1 (t), h_2 (t), h_3 (t)	Predictable Portion of Outside Torque
$F(\ddot{I})$	I_{sp} vs Impulse

See Cycle 2, Cycle 4

APPENDIX 6 (Continued)

Constants

$\dot{\theta}_1$, $\dot{\theta}_2$, $\dot{\theta}_3$ — Initial Values $(\dot{\theta}_i\ (t=o) = o)$

$\beta_{ijk\alpha}$ ARRAY — Fixed (Bias) Errors

(Selection of Engine Configurations and Control Philosophy)

T — Cyclic Period of $h_i\ (t)$

APPENDIX 7

NOMENCLATURE

APPENDIX 7

NOMENCLATURE

ENGINE:		Designated by two numbers (i j). The number, i, represents the axis on which the engine is situated, and j represents the axis along which the engine points. See Figures 18 &19 for clarification.
RANDOM IMPULSE ERROR OF ENGINE:	$\epsilon_{ijk\alpha}$	ij represents the engine with which the error is associated. k represents the directional category of the thrust error. k = 1 designates an error in line with the engine pointing while k = 2 designates an error perpendicular to engine pointing. α represents the type of error. $\alpha = 1$ designates an error in thrust level while $\alpha = 2$ designates an error associated with startup and shutdown transients.
MAGNITUDE OF RANDOM IMPULSE ERROR:	$K_{ijk\alpha}$	is the maximum value which $\epsilon_{ijk\alpha}$ may assume.
FIXED IMPULSE ERROR:	$\beta_{ijk\alpha}$	ij represents the engine with which the error is associated. k represents the direction in which the positive direction of the error component points. Except in the case where the error component is in-line with an engine pointing in the negative direction of one of the coordinate axes, k will be either i, 3, or 5. Otherwise k and j will be the same number (2, 4 or 6). This is done to keep the direction of positive error the same as the pointing direction of the engine.

APPENDIX 7 (continued)

MOMENT ARM OF ENGINE:	L_{ijk}	i represents the engine cluster position relative to the appropriate axis (see Figures 18, 19). jk represents the particular engine in question.
MOMENT OF INERTIA:	J_{ij}	i represents the axis in question (1, 2, 3 denote pitch, roll, yaw) j represents the engine configuration in question (j = 1 denotes the six unit and j = 2 denotes the twelve unit configuration)
ANGULAR DISPLACEMENT:	θ_i	i represents the axis about which rotation takes place (1, 2, 3 denote pitch, roll, yaw)